1957

A plastic load analysis of continuous circular stiffening frames, M.S. thesis, 1957

Charles Edwin Stuhlman

"A PLASTIC LOAD ANALYSIS OF CONTINUOUS CIRCULAR STIFFENING FRAMES"

by

Charles Edwin Stuhlman

A Thesis

Presented to the Graduate Faculty

of Lehigh University

in Candidacy for the Degree of

Master of Science

Lehigh University

1957

This Thesis is

Dedicated to

My Wife

Norma Lea

ACKNOWLEDGMENTS

The author is sincerely indebted to Dr. R. L. Ketter, professor of Civil Engineering, Lehigh University. Without his expert supervision, this thesis would not have been possible in its entirety. His advice and suggestions are deeply appreciated.

The author whishes to recognize the efforts of his wife, Norma Lea, who typed the manuscript, performed many of the calculations, and assisted in arranging the pages for binding. Thanks are also expressed to Mrs. Veronica Olanvich, who ran off the masters on multilith.

PREFACE

Before entering into the main text of the subject of circular ring analysis, it is felt that one point should be clarified. The analysis of this thesis as it stands is a plastic load analysis. That is, it is an analysis based on the ultimate carrying capacity of the structure as a whole.

Plastic stress analysis is nothing comparatively new. Various fields of engineering have been employing plastic stress solutions for quite a few years. In fact, J.A. Van den Broek published his well known paper "Theory of Limit Design" in 1939. Aircraft engineers have been taking advantage of the plastic properties of the materials they employ in their design for years. However, the manner in which they determined their loads was derived from elastic strength assumptions.

The criterion advanced in the text of this treatise is based upon plastic load or strength assumptions in conjunction with plastic stress assumptions. It is believed that this pursuit is a much, much more rational approach to the subject of the theory of strength.

TABLE OF CONTENTS

Table of Contents (con'd.)

ABSTRACT

Two plausible conditions complement the theory of strength. The first supposition, the condition of equilibrium, is primary, whereas the second supposition, the condition of continuity, is subordinate. To supplement the assumption of equilibrium, two theories are advanced, the theory of elasticity and the theory of plasticity. The former of these theories presumes an elastic or linear stress distribution and compatibility of strains. The latter of these theories presupposes a ductile or semi-ductile stress distribution and compatibility of deformations. Accordingly, the emphasis is shifted from permissable limiting stresses in the case of elasticity to permissable safe deformations in the case of plasticity.

It has only been in recent years that the structural analyst has given any really serious consideration to the advantages of designing structures consistent with an ultimate collapse load. Yet for a long time this same class of engineers have been fully aware that continuous beams and rigid frames can carry loads considerably in excess of those which just reach the elastic limit of the material. Regardless of how rational elastic methods may appear otherwise, an elastic design based on an allowable stress value is incapable of predicting structural failure which means that the real margin of safety is not defined or computed. The purpose of plastic or limit design, on the other hand, is to proportion the structure in such a manner that it will just fail when subjected to a limit load multiplied by some

arbitrary factor of safety. Consequently, in a plastic design, the term factor of safety assumes a definite meaning contrasted to an elastic solution where the analyst has no idea of whether the structure is on the verge of collapse or if it is capable of carrying considerable additional loading.

Aircraft Engineers have attempted to compensate for this "Reserve in Strength Beyond the Elastic Limit" by first performing an elastic analysis on a structure, and then designing the maximum bending sections employing a plastic section modulus. Moreover, under certain conditions, they may even attempt to design to a negative margin of safety in order to account for simplifying assumptions and for the difference between the elastic and plastic strength of the complex structure. Obviously, this procedure is inconsistent and erroneous. It is like shuffling cards with elastic and plastic analyses with no regard for compatible structural behavior. In order to be consistent, the structural designer must seek a new method of attacking the problem by means of simple plastic hypotheses, and then follow up his plastic analysis by designing the structural components with a plastic section modulus. That is exactly what is attempted in this dissertation.

It was while working in the aircraft industry that the writer first became acquainted with the problem of designing stiffening rings. In general, the methods of least work based on elastic assumptions were employed in solving these ring problems. Instead of further elucidating on the applications of least work to ring analysis, the following dissertation was

developed with the emphasis on limit analysis, suggested as a more rational procedure for analyzing continuous stiffening rings. More rational is the procedure because the objective of the theory is to develop simple and general methods for predicting the actual ultimate load-carrying capacity, rather than to base design on attainment of an allowable extreme fiber stress as in an elastic solution.

The subject of plastic analysis of rings is approached, first, by reviewing the basic assumptions of the simple plastic theory and then by illustrating the applications with a few examples. Essentially, the method contained in this treatise was derived from the methods of plastic analysis and design that have been used for structural steel rigid frames.*

*See Reference 5

SECTION 1.0.0

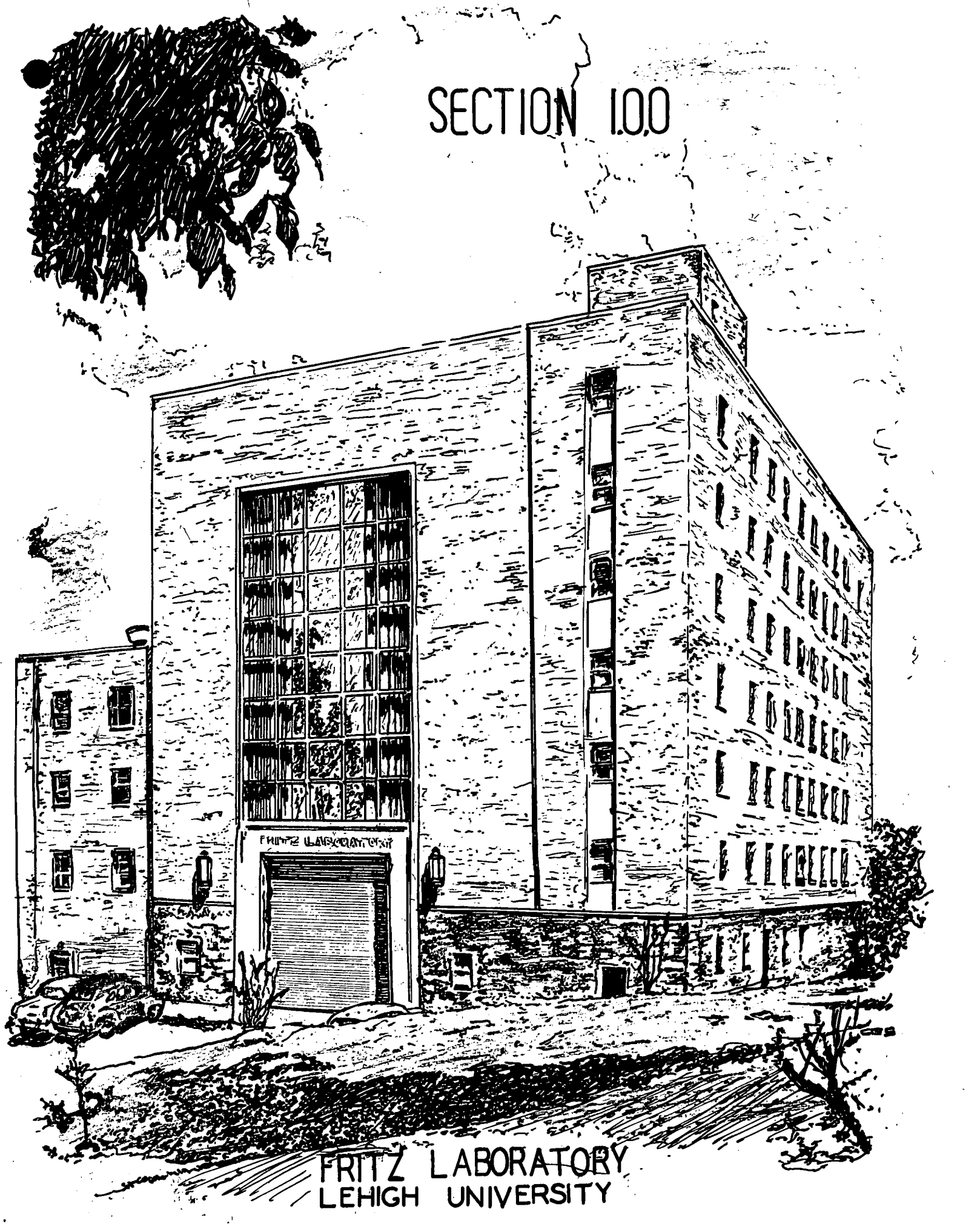

FRITZ LABORATORY
LEHIGH UNIVERSITY

1.0.0 INTRODUCTION

1.0.1 Historical Review

Just because elastic stress analysis has been so closely associated with the theory of strength for the past century and a half that they are practically considered one and the same, does not imply that it was the first contribution to the theory of strength. On the contrary, Euler's paper on the strength of columns (1757), was published even before the advent of stress analysis. "It was pure limit design, as all earlier efforts had been up to that time."* Indeed, theory of plasticity is not of recent origin.

It seems that modern theories of simple plastic bending are actually not a recent development, but date as far back as the turn of the twentieth century. Perhaps, the first person to advance the theory of plasticity as applied to structural bending behavior was Dr. Gabor Kazinczy. In 1913, Kazinczy performed a number of experiments with girders of a new type of roof structure. After he discovered that the actual ultimate load carrying capacity was considerably greater than was determined from his calculations, Kazinczy concluded that an elastic theory was not adaptable for the determination of the collapse load. He observed that the beams were bent at the supports where, according to his analysis, the stresses in the steel were suppose to be below the yield point. He suggested that the points of maximum moment could be imagined to be provided with "Yield Hinges." From these observations he concluded that calculations should be based on plastic deformations and thus, he became the originator

*See reference 7, preface

of limit (or plastic) design.

About the same time that Kazinczy published the results of his girder experiments, there must have been other men investigating the same phenomenon. Although Kazinczy did not mention his method of proportioning beams publicly until 1928, in 1917 Professor N. C. Kist chose limit design for the theme of his inaugural address at the Polytechnic Institute of Delf, Holland. It was at an International Congress in Vienna, in 1928, that Maier-Liebnitz of Stuttgart disclosed the results of experiments which he performed on the carrying capacity of continuous beams, and proved that they disagreed with elastic theory. This is when Kazinczy first advanced his method of proportioning beams in order to substantiate Maier-Liebnitz's declarations.

At first these new ideas were not received very gratifyingly. About the only place where Kazinczy's methods were accepted was in Budapest. In the early twenties, that city incorporated his beam proportioning method in their building code and made it a design requirement for determining the collapse load of any structure. Most of the skepticism of the new method apparently stemed from the problems of variable repeated loading and the lack of tests of large scale structural members and frames.

In the early stages of its development all of the ideas concerning plastic design were proposed by Europeans such as Girkmann (with portal frames), Bleich (shake down), Gruning, Maier-Liebnitz, Kist, and of course Kazinczy. In 1936 J. F. Baker revived the problem in England. It was Baker who initiated a research study on the subject of the ultimate strength behavior of structual

steel at Bristol University and later continued his experiments at Cambridge University with J. W. Roderick, M. R. Horne and B. G. Neal. As a result of these investigations England has incorporated a plastic design specification(*) in its building codes.

It took until 1939 before anyone in this country publicly recognized the worth of plastic design. At this time, J. A. Van Den Broek published his treatise entitled "Theory of Limit Design"(**) which was the subject of much controversy. According to Van Den Broek, the vagueness and "wishful thinking" of most elasticity reasoning is compensated for by the logic of limit analysis. Yet design procedures did not radically change as a result of Van Den Broek's premises. In fact very few of his contemporaries have advocated Van Den Broek's ideas. The more prominent of the investigations, carried out in this country, have been by W. Prager, P. S. Symonds and D. C. Drucker at Brown University. However, their approach to plastic analysis has been strictly from the mathematical viewpoint; in establishing the mathematical laws and proofs governing plastic analysis.

Since 1946, an investigation toward the application of plastic analysis to structural design has been under way at Lehigh University in Bethlehem, Pennsylvania. Under the sponsorship of the American Institute of Steel Construction, The Welding Research Council, the American Iron and Steel Institute, and the Navy Department, methods for the development of practical

*See reference 10

**See reference 7

plastic design procedures have been established which now makes it possible to extend these solutions to continuous ring analysis.

1.0.2 Foreword

Before delving into the basic concepts of plastic behavior, this is an opportune time to point out the specific approach of this treatise. Although the ideas contained herein may be directly applied to design techiniques, it is not the primary purpose of this discourse to approach the problem from this aspect. The purpose of the dissertation is to present a method of analysis based on simple plastic theory for the solution of continuous circular rings. However, it should be evident from the text that the methods are readily applicable to a design pursuit.

1.0.3 Fundamental Concepts

To begin the study of plastic analysis, the reader should focus his attention on the fundamental concepts of simple bending theory. Since plastic analysis is a first order theory it is based on the precepts of bending theory for a structure stabilized against buckling (buckling being a second order phenomenon). Therefore, the theories of local or lateral buckling are not to be construed as a portion of this study. As unconservative as this may appear at first, further consideration of the practical applications of circular rings should make it apparent that stiffening rings are inherently stable laterally. We can account for local buckling by determining the required rotation capacity of the plastic hinges and then proportioning the width to the thickness of uotstanding flanges accordingly. Consequently, this whole presentation is founded on those bending theories pertaining to the behavior of stabilized structures bent beyond the elastic limit.

Before discussing bending in the plastic range, first let us recapitulate on the subject of elastic theory. Primarily we are concerned with the relationship between applied moment and resulting curvature. Segregating a small segment of a bent structural component, the following Figure results.

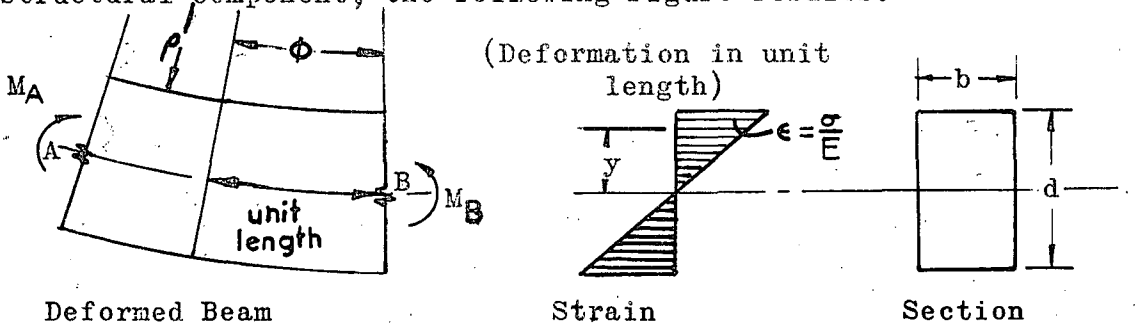

FIGURE 1.01 Segment of Deformed Beam

If it is assumed that plane sections remain plane and that Hooke's Law defines the relationship between stress and strain, it is apparent from Figure 1.01 that there is a linear variation between the applied bending moment and the resulting curvature. The parametric equations defining these quantities are

$$\phi = \frac{1}{\rho} = \frac{\epsilon}{y} = \frac{\sigma}{Ey} \qquad \text{.....(1.00)}$$

$$M = \int_{-d/2}^{+d/2} \sigma y \, dA \qquad \text{.....(1.01)}$$

where ϕ, ρ, ϵ, σ, E, M, and y are defined in section (V) page .

In order to formulate the relationship between moment and curvature in the plastic range, we must first stipulate our basic assumptions as we presumably did before deriving the elastic proposition.

Assumptions and Conditions

1. Plane sections remain plane after bending, that is, bending strains (but not necessarily stresses) are proportional to the distance from the neutral axis.

2. Idealized stress-strain relationship as in Figure 1.02.

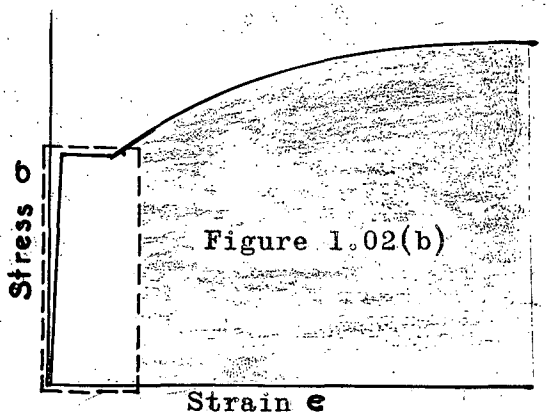

Figure 1.02(b)

FIGURE 1.02

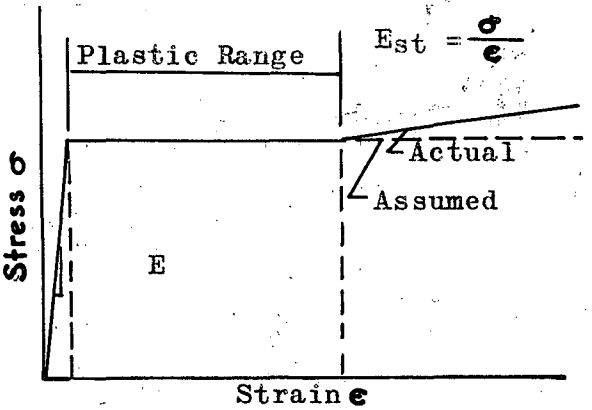

FIGURE 1.02(b)

a.) Properties in compression are the same as those in tension.

b.) Behavior of fibres in bending is the same as in tension.

3. Equilibrium exists between applied loads and moments and the resulting stress distribution pattern.

$$\text{Normal Force: } P = \int_A \sigma \, dA$$

$$\text{Moment : } M = \int_A \sigma \, y \, dA$$

4. Deformations are small such that

$$\tan \phi = \phi$$

For a rectangular cross section in bending, the following non dimensional $M-\phi$ curve is as shown in Figure 1.03.

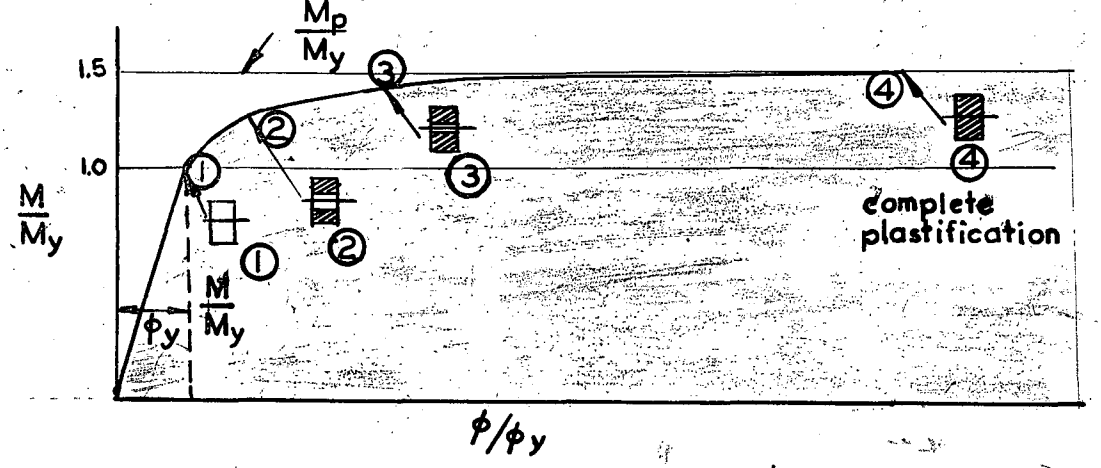

FIGURE 1.03 Non-Dimensional $M-\phi$ Curve

Strain Distributions:

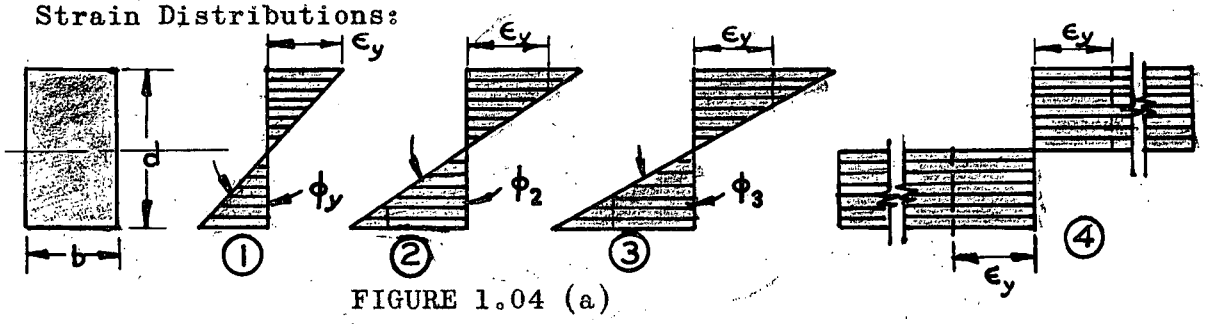

FIGURE 1.04 (a)

Resulting Stress Distributions: (Assumption No. 2)

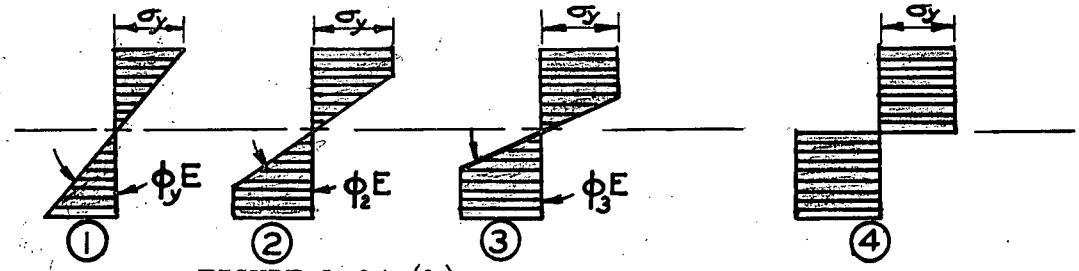

FIGURE 1.04 (b)

Stress Strain Distributions for a Rectangular Cross Section

From the yield distributions above and the M-ϕ curve of figure 1.03, it is noteworthy to observe that the curvature increases quite rapidly beyond the initial yield moment, M_y, and quickly approaches the full plastic moment value, M_p, assymptotically. The magnitude of the full plastic moment can be determined from Equation (1.01) by performing the indicated integration.

$$M = \int_A \sigma_y \, y \, dA \quad \ldots\ldots\ldots\ldots\ldots\ldots\ldots\ldots\ldots\ldots (1.01)$$

Therefore, if we wish to express the moment at any point, we first express the yield moment as

$$M_y = \sigma_y S \quad \ldots\ldots\ldots\ldots\ldots\ldots\ldots\ldots\ldots\ldots (1.03)$$

Where S=elastic section modulus.

Then, the moment at any other point between ① and ④ on the M-ϕ curve is expressed as

$$M = \sigma_y S_e + \sigma_y Z_p$$

Where S_e = section modulus of elastic part of cross section, and Z_p = section modulus of plastic part of cross section. Hence, the moment of resistance is made up of an elastic part $\sigma_y S_e$ and a plastic part $\sigma_y Z_p$. Then the full plastic moment can be expressed as(*)

$$M_p = Z \sigma_y \quad \text{.....(1.05)}$$

Now that the relation between moment and curvature has been established, it is possible to apply these observations to a structure. Consider one of the simplest structures, a simply supported beam with a concentrated load at mid-span as shown in Figure 1.05.

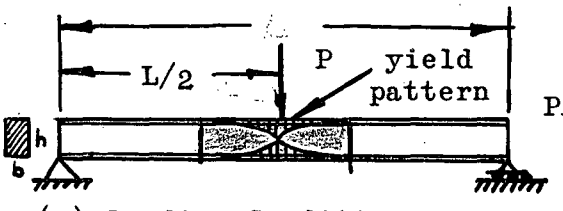

(a) Loading Condition

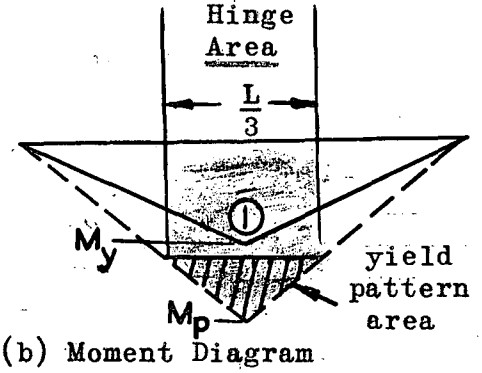

(b) Moment Diagram

Length of plastic hinge = L/3 for a rectangular cross section.

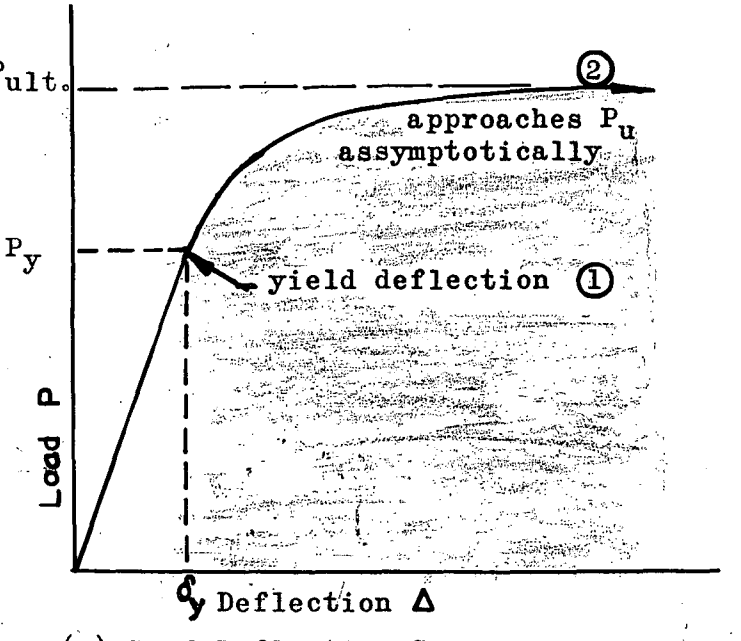

(c) Load Deflection Curve

FIGURE 1.05

As indicated there is a linear range of load versus deflection which corresponds to the linear range of the moment versus curvature relationship of Figure 1.03. Once the moment at mid-span exceeds the initial yield moment, the assumptions of elastic

behavior are violated and the relative bending stiffness (the increased moment associated with a unit increase in curvature) is appreciably reduced. The member becomes relatively weak with an increase in applied load and the beam deflects progressively at a faster and faster rate. As the load approaches its ultimate value the beam reacts to increases in load as if a hinge, (referred to as a "Plastic Hinge"), were formed at the point of maximum moment. That is, the member continues to deform under constant moment.

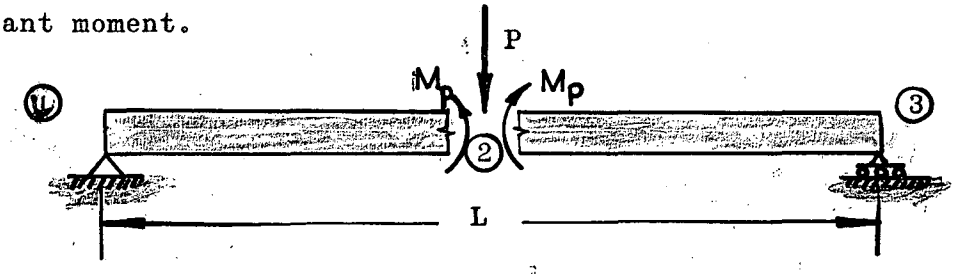

FIGURE 1.06-Simple Beam

Referring to Figure 1.05, failure occurs with the development of a kinematic mechanism: real hinges are present at the ends ① and ② and a "Plastic Hinge" forms at midpoint ②. The usefullness of the structure is exhausted at this point. If the structure were "built-in", however, (characteristic of statically redundant structures), a redistribution of moment could take place at this point of plastic hinge formation, and the structure would be capable of sustaining additional load.

At this point, perhaps it would be best to define two important fundamentals of plasticity concepts.

1. Plastic Hinge Concept

Contrary to what first comes to mind concerning a hinge, a plastic hinge is not a point of zero moment but rather the point of maximum moment. The reason for the connotation of the term

hinge to this form of mechanism is the marked ability of the structural component to rotate at this point.

2. Rotation Capacity

The rotation capacity of a member is its ability to rotate at near maximum moment. The rotation capacity is of ultimate importance because it is the characteristic of the structure which permits redistribution of moment. After the plastic moment is reached at a critical section, the moment remains constant and the section begins to rotate along the length of the hinge. Whereupon, moment is redistributed to other parts of the structure, thus permitting a gradual increase in applied load.

Now, that a plastic hinge concept has been established by the "simply supported beam" illustrated, another observation might be interjected that nothing is to be gained by analyzing structures of this nature by plastic analysis.

Focusing attention on the category of statically redundant structures, which comprises a multitude of practical applications, consider the structure shown in Figure 1.07.

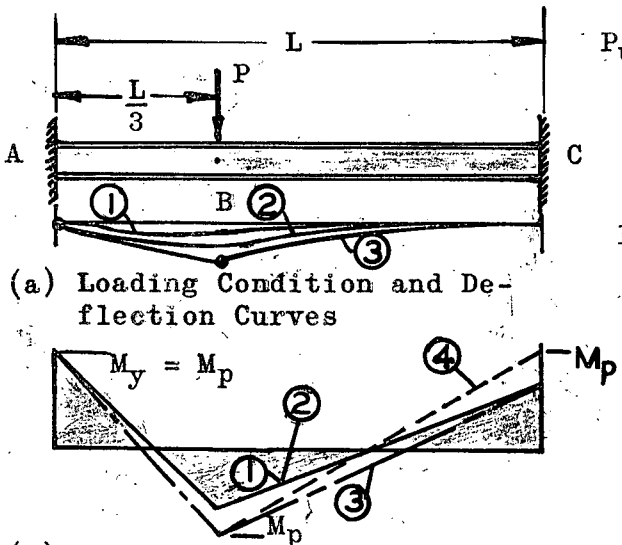

(a) Loading Condition and Deflection Curves

(b) Moment Diagram

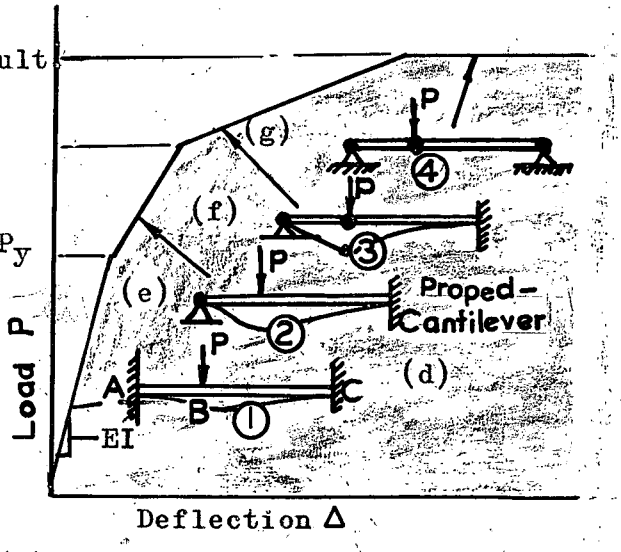

(c) Load Deflection Plot

FIGURE 1.07 Statically Indetermine Beam

As the load on this redundant structure is gradually increased from zero, the beam initially behaves elastically with the largest moment of the solution always at the end A . At some value of the applied load yielding will begin at A . The beam most certainly is capable of carrying additional load beyond this point, and as it is progressively further increased the beam responds as if it were a proped-cantilevered beam (see Figure 1.07(e)). As the load is further increased the beam yields under the applied load and there is observed another transition in the deflection curve (point e on Figure 1.07). Additional moments are again redistributed and another structure completely divorced in similarity to the former beam virtually forms. The load can be amplified very little beyond this point because the segment BC is required to support further load increments by cantilever action (Figure 1.07(f)). Eventually, the ultimate load carrying capacity of the structure is reached when yielding occurs also at C . As the final plastic hinge appears, the deflection curve becomes horizontal, or in other words a kinematic mechanism "ABC" is realized. Beyond this point the load carrying capacity is exhausted since small additional loads produce much larger deflection increments.

Since further examples add very little additional clarity, the previous illustrations will be considered sufficient.

1.04 Necessary and Sufficient Conditions for a Plastic Analysis Solution.

The purpose of stipulating necessary and sufficient plasticity conditions is two fold. The first reason is to establish the

conditions necessary to formulate plastic solutions. Secondly it affords an opportunity to compare the basic requirement of elastic and plastic analysis.

Referring to the previous examples, several observations will assist in defining the necessary conditions to verify or satisfy a complete plastic solution. If the reader will take particular note, in each of the cases discussed failure corresponded to the development of a mechanism. Another very important condition which must be fulfilled is that nowhere can the maximum moment in a member exceed its full plastic moment. A third condition, which obviously must also be attained, is equilibrium, since structural static equilibrium is the primary basic consideration of any "theory of strength." Therefore, summarizing these observations the conditions to be fulfilled for the attainment of a plastic analysis solution are as follows:

1. The structure must be in equilibrium with the applied loads.

2. A kinematic mechanism must be attained.

3. The maximum moment in any component can not exceed the full plastic moment of the section. (For ring solutions, the calculated moment anywhere in the ring can never exceed the calculated ultimate plastic moment (M_p)).

In contrast to the plastic conditions, the following are the conditions for an elastic solution:

1. The structure must be in equilibrium with the applied loads.

2. There must be compatibility or continuity wherever applicable.

3. Nowhere will the stress in a member exceed the initial yield stress. ($\sigma \leq \sigma_y$)

For purposes of comparison, table 1.0.0 has been constructed.

TABLE 1.0.0 Necessary Conditions for Plastic and Elastic Analysis. (*)

ELASTIC ANALYSIS	PLASTIC ANALYSIS
1. Equilibrium	1. Equilibrium
2. Continuity	2. Development of a Mechanism
3. $-\sigma_y \leq \sigma \leq +\sigma_y$	3. $-M_p \leq M \leq +M_p$

1.0.5 Method of Solution.

Plastic analysis is by no means confined to the application of one method of solution. In fact, several procedures have been advanced to supplement the methods of solution. The most prominent of the contemporary procedures are (a) The "Equilibrium" Method (b) The Mechanism Method (c) The Method of Inequalities and (d) The Moment Balancing Method. Rather than attempt to expound in great detail on each method individually, each procedure will be described briefly and the most appropriate method will be chosen to develop solutions of rings.

(a) "Equilibrium Method"**

The "Equilibrium Method" is essentially based on the lower bound theorem which states:

> "A load corresponding to an equilibrium configuration with arbitrarily assumed values for the redundants is smaller than or at best equal to the ultimate loading provided all $|M| \leq M_p$."

*See reference 5, page 3.8 or reference 13, page 13
**For more detail of this method see reference (10)

The method is most adaptable to continuous beams for which the procedure is straight forward. By constructing the composite moment diagram of the determinant and redundant moments it is possible to visualize the general pattern that the collapse moment diagram must take. A plastic solution could be realized by manipulating the magnitudes of redundant moments in the composite moment diagram always keeping $M \leq M_p$, and then checking to determine if there are sufficient plastic hinges to reduce the structure to a mechanism. Not only is the method adaptable to continuous beams but it is also an effective tool in solving simple frames where only one or two redundants or symmetrical loading are involved. On the other hand, more complex problems make this method quite inexpedient.

(b) Mechanism Method*

Conversely, just as the "Equilibrium Method" is based on the lower bound theorem, the Mechanism Method is based on the upper bound theorem, which states:**

> "A load computed on the basis of an assumed mechanism will always be greater than or at best equal to the ultimate load."

If it is possible to visualize the different modes in which the structure may fail, by investigating every possible combination of mechanisms, the systematic resolution of the corresponding critical loads will eventually engender the lowest or correct solution. Since this kind of procedure automatically presupposes an upper bound solution, it is mandatory to determine the lower bound in order to establish the correctness of the assumed answer. As mentioned before on page 16 this is accomplished by performing the plasticity check, whereby each of the three necessary con-

*Reference 5, Page 3.6
**See Reference 12

ditions will have been fulfilled. Because of its generality it lends itself readily to the solution of the more complex structures, and therefore it is the method selected in this text to solve continuous rings.

(c) Method of Inequalities*

This is a systematic mathematical process based on the premise that a member can sustain a moment at best equal to or less than its full postive or negative plastic strength. The procedure is to write a set of linear inequalities for each possible hinge specifying the limitation just mentioned. By manipulating these inequalities, such as combining and eliminating unknowns in simultaneous inequalities, eventually the process will result in the determination of a single unknown. This solution may be successively substituted into the previous simultaneous equations for a complete solution to the problem. Although this process is characterized by refinement, it is certainly not recommended for complex problems unless there is access to an electronic computer. Its elegance is offset by the necessity of solving tedious determinants.

(d) Moment Balancing**

This method is a sequel to the elastic method of moment distribution with the refinement of specifying the plasticity condition. Just as in the case of Cross's moment distribution, a procedure of successive relaxations of moments results in a moment diagram in equilibrium with the applied loads. The plastic method of moment balancing permits the analyst a much greater

*See reference 12
**For more details of this method see reference 11.

degree of freedom of analysis than the elastic method. The moment balancing method is adaptable to analysis of rectangular frame-works having members intersecting at right angles. Otherwise, its use is limited.

Consequently, because of the restrictions of simplicity and exclusiveness placed on the methods of equilibrium, inequalities, and moment balancing, the mechanism method is selected as the proposition for the solution of continuous circular rings.

Discussion of Mechanism Method and its Application to Rigid Frame Analysis

The purpose of this section is to present the mechanism method with all of its characteristic refinements by applying it to single span rigid frame analysis. Since the method of attack of the mechanism method is to presuppose a possible failure configuration, the second necessary condition for a plasticity solution is automatically fulfilled. The condition of equilibrium is sufficed by using the principle of virtual work. Thus, the only remaining condition is the one of a plasticity check, where the calculated moments in a member are confined to values less than or equal to the full plastic moment for their respective members.

Once the mechanism method has been applied to rigid frame analysis, it is only necessary to establish the same principles with respect to ring solutions considering the appropriate revisions. Hence, the single span fixed ended gable frame shown below in Figure 1.08 was selected to illustrate the applications of the mechanism method. It will be assumed that each of the members in the structure will deliver a certain resisting moment M_p.

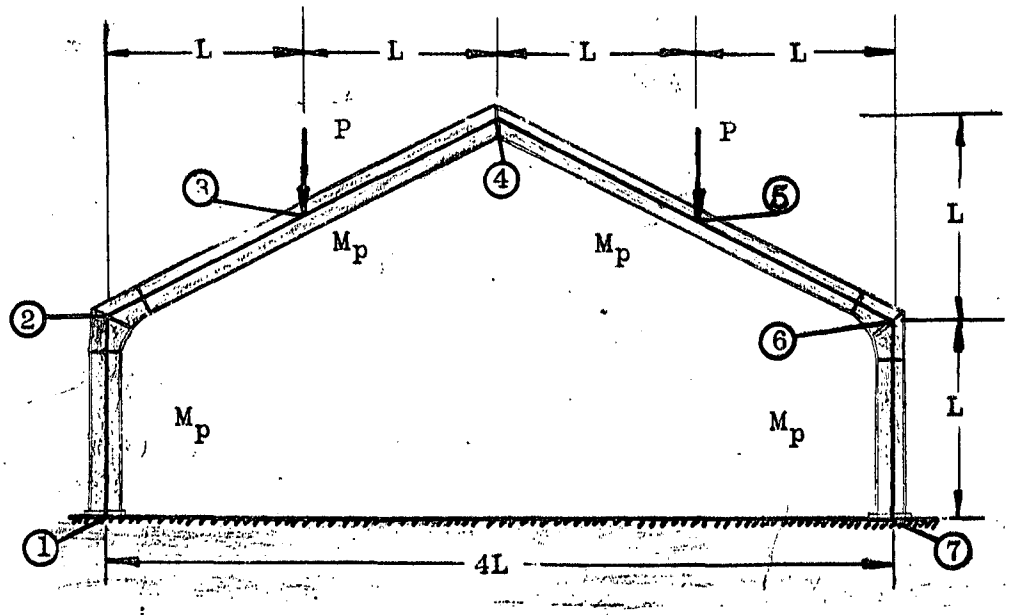

FIGURE 1.08 Single Span Fixed-Ended Gable Frame

Before beginning the analysis, reconsider the assumptions of simple plastic bending theory.

1. The structure will not become unstable prior to the attainment of the ultimate load.

2. The influence of normal and shearing forces on the plastic moment is neglected.

3. First order theory deformations are small such that the equilibrium equations can be formulated for the underformed structures.

4. Connections provide full continuity such that the full plastic moment can be transmitted.

5. Loads are proportional such that they increase in fixed proportions, one with respect to the other.

<u>The Procedure to Follow is as Stipulated</u>

1. Determine all locations of possible plastic hinges according to the following rules.

A hinge may possibly exist in a member at

I) A point of maximum moment (that is, zero shear)

II) A change in direction of a member (that is, at a joint)

2. Designate all possible mechanisms (elementary mechanisms and combinations therefrom)

3. Apply the principle of virtual displacements for each of the possible mechanisms by displacing the structure a virtual amount and compute the corresponding internal and external work.

4. Compute the critical load for each of these mechanisms and choose the lowest value obtained.

5. Perform a plasticity check.

Returning to the gable mechanism, according to the rules for determining all possible plastic hinges, it is obvious that there is no change in shear along the columns. Hence, plastic hinges can occur only at the ends of these members. Two other possibilities would be under the vertically applied loads. A seventh possible point of plastic hinge formation would be at the peak of the rafters, where the structure abruptly changes shape. These seven possible plastic hinges are numbered ① through ⑦ in Figure 1.08.

Any combination of these hinges resulting in the formation of a mechanism may result in a failure configuration. To expedite the determination of the number of failures modes, a simple rule has to be deduced to determine the number of independent mechansims. Since a statically determinate system requires but one plastic hinge to transform it into a mechanism; this structure will have as many independent mechanisms as there are plastic

hinge locations. On the other hand, statically indeterminate systems require an additional plastic hinge for each redundancy. Hence, to state the preceding in the form of a rule

If N = Number of possible plastic hinges

and X = Redundancies

N-X = Number of elementary mechanisms

The elementary mechanisms would correspond to independent static equations of equilibrium.

Applying this rule to the problem at hand, there are 7 possible hinges and 3 redundants. Hence, there should be (7-3) or 4 independent mechanisms, as shown below.

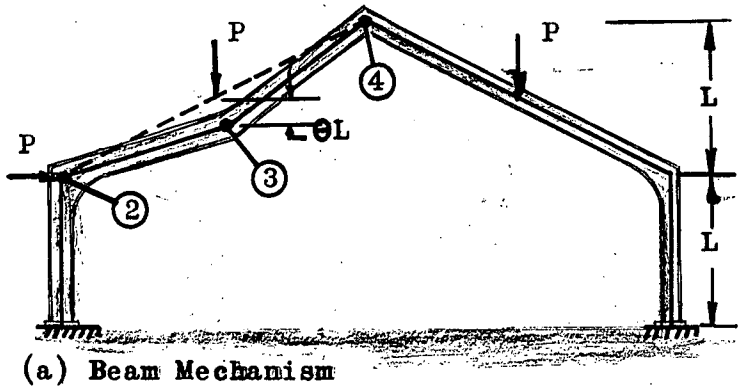

a.) Obviously rafter ② - ③ - ④ could fail as a beam mechanism

(a) Beam Mechanism

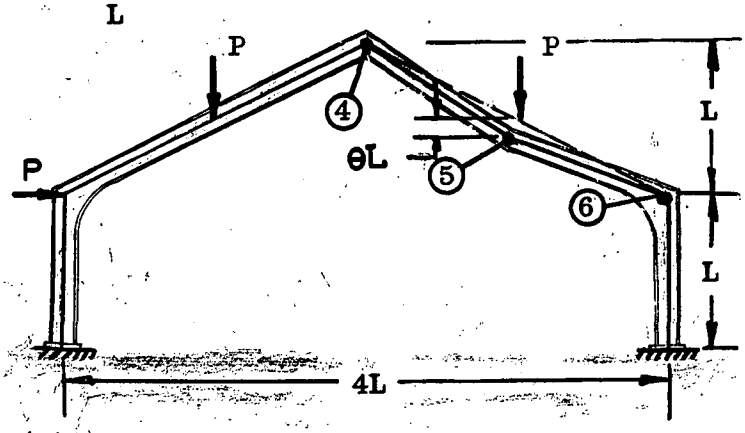

b.) Same as above for rafter ④ - ⑤ - ⑥

(b) Gable Mechanism

FIGURE 1.09

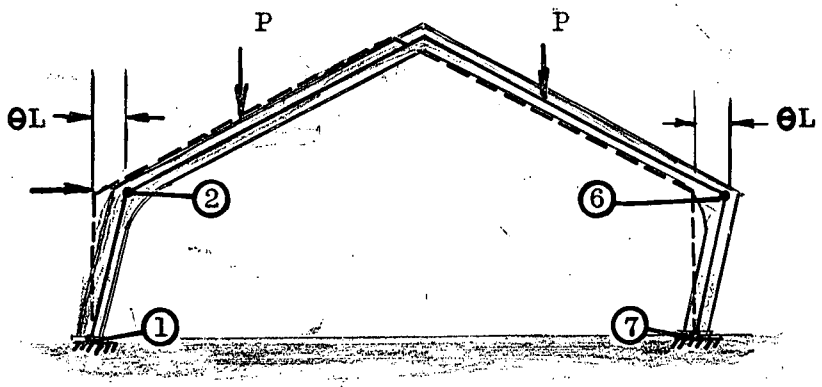

(c) Panel Mechanism

c.) Likewise, the total roof of the frame could remain rigid and the structure could sway as a panel. Figure 1.09(c)

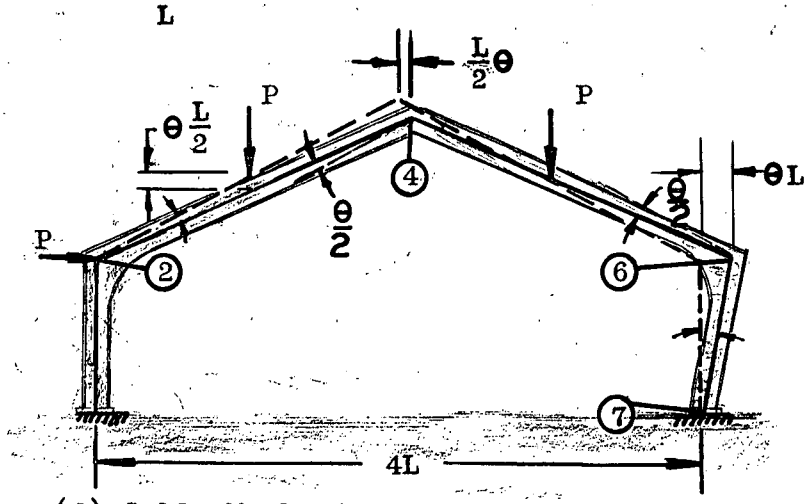

(d) Gable Mechanism

FIGURE 1.09

d.) Rafter ② - ④ and ④ - ⑥ could remain rigid in themselves as point ⑥ moves to the right point ④ would then move down while point ① remained fixed. The mechanism investigation is by no means finished at this point, because all combinations of these mechanisms must also be considered.

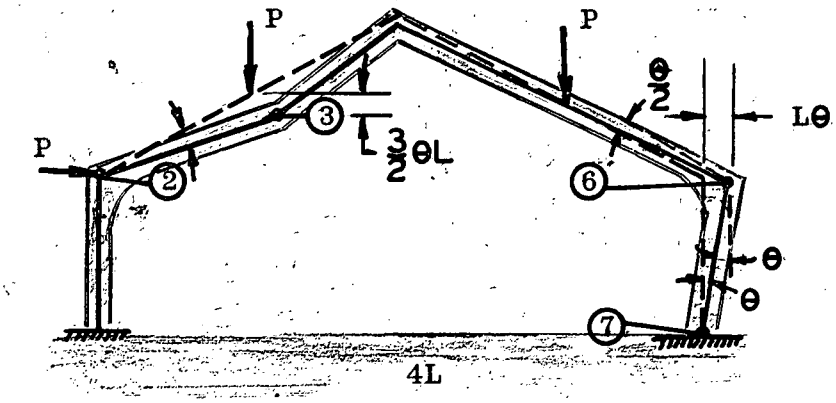

(e) Combination Mechanism
(a) + (d)

If the beam mechanism (a) is combined with the gable mechanism (d), mechanism (e) results having no "hinge" at the gable peak.

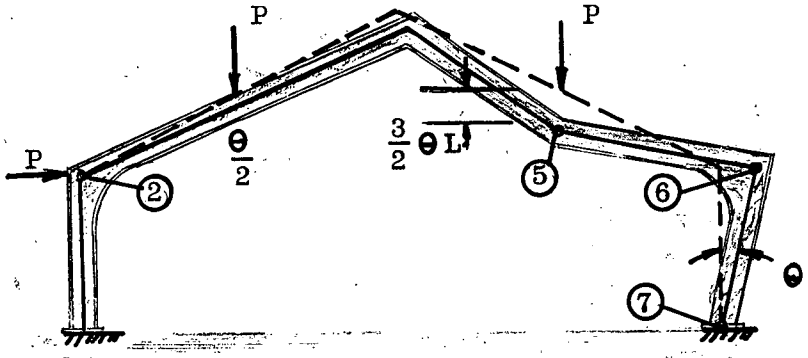

Beam mechanism (b) + gable mechanism (d).

(f) Combined Mechanism (b)+(d)

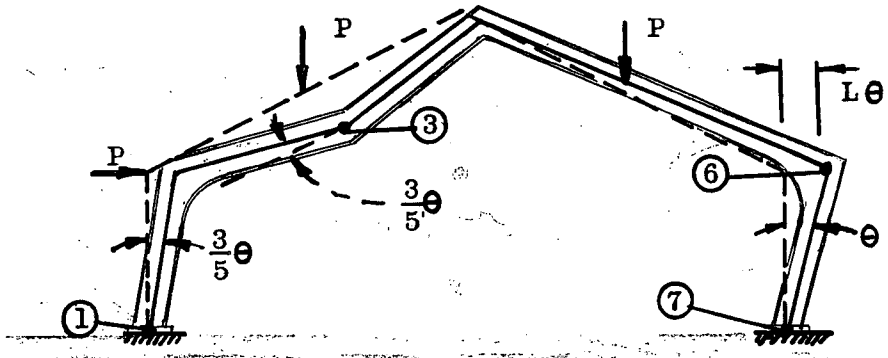

Beam mechanism (a) + sidesway panel mechanism (c).

(g) Combined Mechanism (a)+(c)

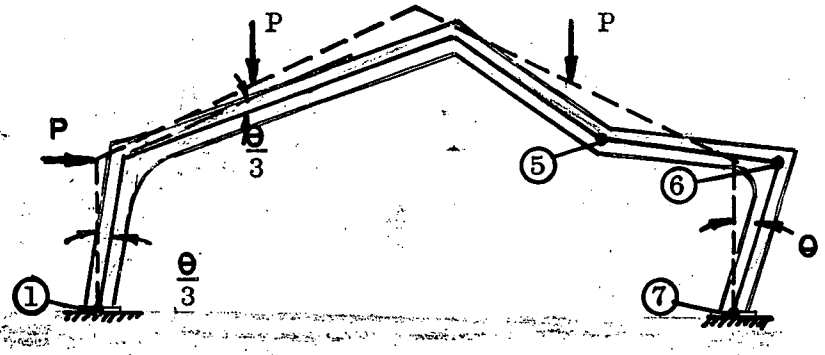

Beam mechanism (b) + sideway panel mechanism (c).

(h) Combined Mechanism (b)+(c)

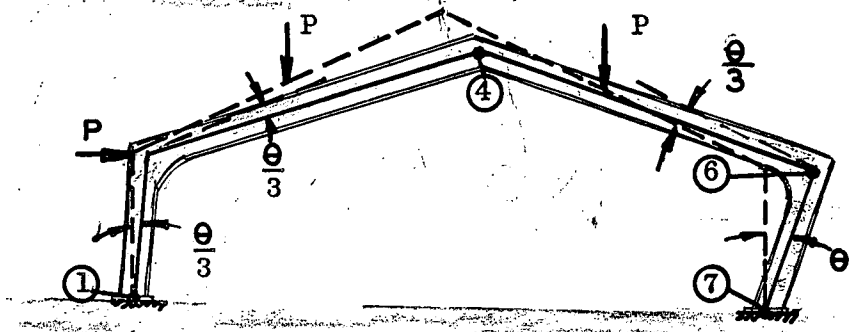

Gable mechanism (d) + panel mechanism (c).

(i) Combined Mechanism (d)+(c)

The next step in the procedure is to determine that critical load P_{cr} corresponding to each assumed mechanism. The largest value of M_{cr} for its corresponding value of P is the solution to the problem.

The critical load is determined by applying the principle of virtual displacements. Before the analyst can apply the principle of virtual displacements, he must fully understand its meaning. Therefore, the principle is stated below.

Principle of Virtual Displacements

If a system of forces in equilibrium is subjected to a virtual displacement, the total work done vanishes, that is, the work done by the external forces equal the work done by the internal forces.

A virtual displacement is one which is geometrically possible, and of small magnitude approaching zero. It must be piecewise continuous within the structure which infers that a "kink" may exist at a hinge.

Beam Mechanism

As an example, working with beam mechanism (a) of figure 1.09, assume that the plastic hinge at point ② rotates through a

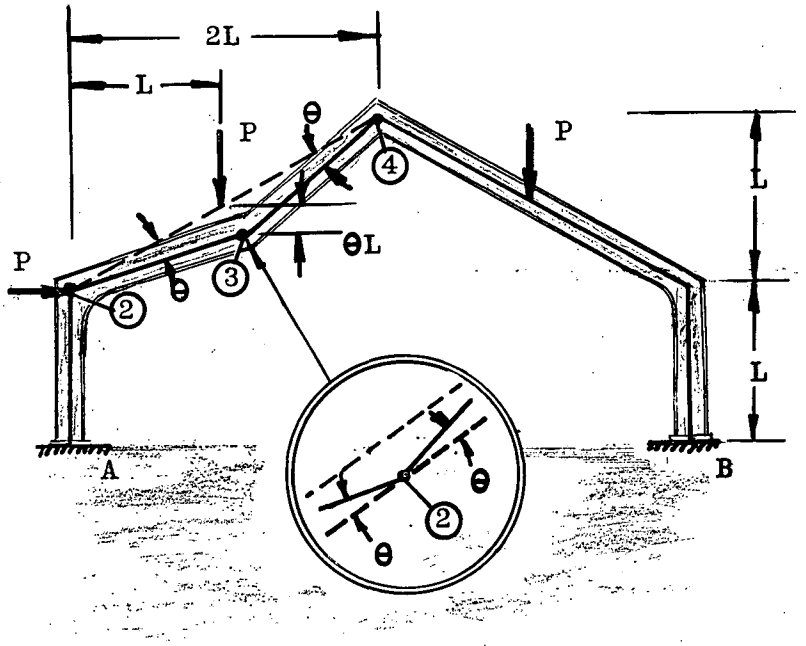

FIGURE 1.11 Beam Mechanism (a)

virtual angle θ. Then the vertical load P will move vertically down through a distance θL. The hinge at ④ rotates through a corresponding angle θ. Since the link ③-④ is the same length as link ② - ③, the point ③ moves to the right $\frac{1}{2}\theta L$ and down θL. The total change in angle at hinge ③ is observed to be twice theta (2θ).

Equating the external to the internal work associated with this assumed deformation configuration as shown in Figure 1.11.

External Work = Internal Work

$$P\theta L = \underbrace{M_p\theta}_{\text{at } 1} + \underbrace{M_p(2\theta)}_{\text{at } 3} + \underbrace{M_p(\theta)}_{\text{at } 4}$$

$$P\theta L = 4M_p\theta$$

$$P_{(a)} = \frac{4M_p}{L} \qquad \text{.....(1.07)}$$

What this expression states is that if the magnitude of P ever approaches the load $P = 4M_p/L$, the structure will fail in the assumed manner. Obviously beam mechanism (b) will give the same result.

Turning to the panel mechanism of Figure (1.12), displace the columns by a virtual rotation of θ. The corresponding geometric relationships are as shown.

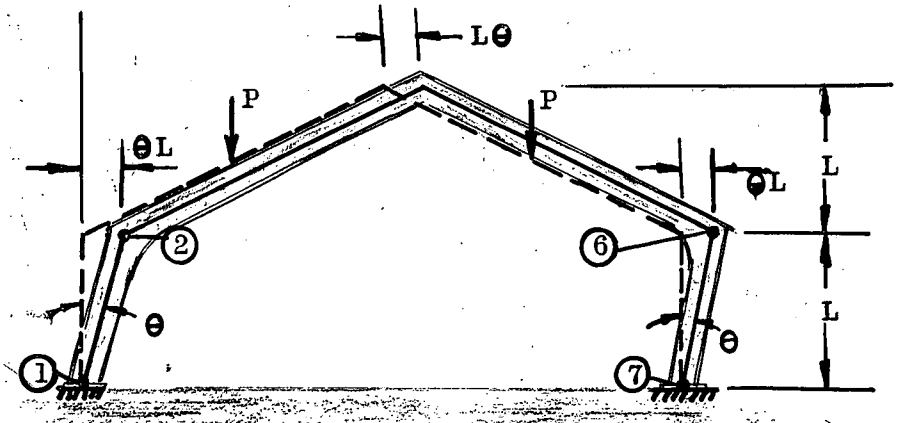

FIGURE 1.12 Panel Mechanism (c)

External Work = Internal Work

$$PL\theta = M_p\,\theta\,(1 + 1 + 1 + 1)$$

$$M_p = \frac{PL}{4} \qquad \text{.....(1.18)}$$

Since both the beam and panel mechanisms have produced the same end result, the interpretation of this coincidence is obviously that, if the load ever reaches this value of $P = 4M_p/L$ both the beam and gable mechanisms will form simultaneously. As will be found later, this is not the correct answer.

From this point on, the geometrical relationships between the rotations at each of the plastic hinges will become much more complex. However, for the immediate solution of the gable mechanism, the same method used in the prior examples will remain as the manner in which this mechanism will first be solved. Returning to the former procedure, consider the gable mechanism shown in Figure 1.13. If the right hand column is given a virtual angle rotation θ, the arc that point ⑥ will describe is equal to θL. Noting compatibility of deflection of the top rafters, at hinge ④ rafter ② - ④ rotates through the same angle as rafter ④ - ⑥, because they are of the same length. Then the hori-

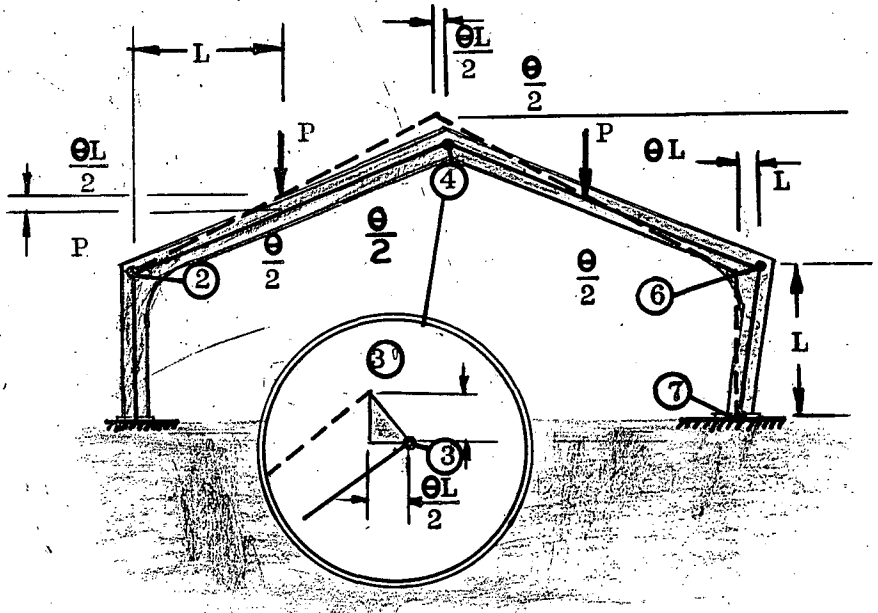

FIGURE 1.13 Gable Mechanism (d)

zontal movement of the rafter peak is exactly half that of point ⑥ or ½ θL. The vertical component of this point is θL. Consequently to satisfy these simultaneous displacements, both rafters must rotate through the same angle $\theta/2$.

Summarizing the total rotations at the various hinges

Hinge ② ..... $\theta/2$

Hinge ④ ..... $\theta/2 + \theta/2 = \theta$

Hinge ⑥ ..... $\theta/2 + \theta = 3\,\theta/2$

Hinge ⑦ ..... θ

Applying the principle of virtual displacements

External Work = Internal Work

$$P\,(L\,\theta/2) + P\,(L\,\theta/2) = M_p\,(\,\theta/2 + \theta + 3\,\theta/2 + \theta\,)$$

$$M_p = \frac{PL}{4} \qquad \text{.....(1.09)}$$

In order to simplify the definition of the geometry associated with any chosen virtual deformation, a "change" in the mechanism method will be interjected at this point. Actually, the use of the instantaneous center does not imply another extraneous method. It truly is only a modification and expedient to the mechanism method, but it is of great consequence in this dissertation because it will be the means employed in solving ring problems. The principle of the instantaneous center is based on a premise of kinematics which states:

> "The instantaneous center of a rigid body having any plane motion is the center about which rotation is taking place at the instant considered."

Reconsider the same mechanism (gable mechanism) as a whole rather than each individual part. Just as before, the left column will remain vertical. Rafter ② - ④ is constrained to rotate

about point ② as its center.

By the same token, the right hand column is compelled to rotate about its base, point ⑦. If the centerlines of these members are extended, they intersect at a point previously defined as the instantaneous center. This is the point about which rafter ④- ⑥ will rotate, since point ⑥ must move practically horizontal and since the end ④ of the rafter must rotate in a direction perpendicular to member ② - ④.

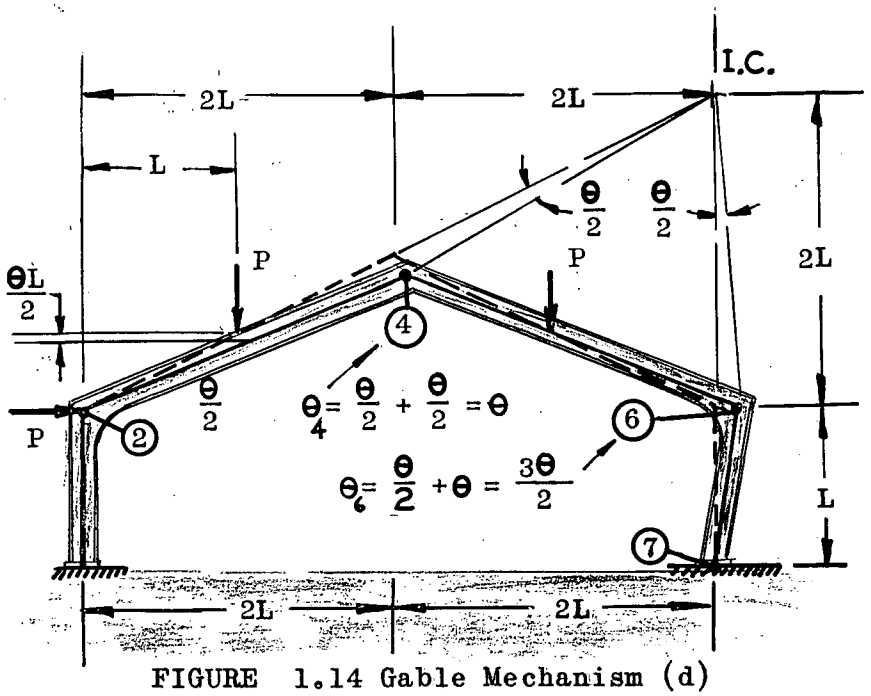

FIGURE 1.14 Gable Mechanism (d) solved by the Instantaneous Center Method

As a reference, the member ⑥- ⑦ is again subjected to a virtual rotation θ, then the amount point ⑥ moves to the right is θL. To be consistent member ④ - ⑥ must translate to the right by the same amount, which necessitates a virtual rotation of rafter ④- ⑥ equal to $\theta L/2L = \theta/2$ about its instantaneous center. In order for point ④ to move in conjunction with the displacement of rafter ④- ⑥, it must shift to the right $\theta L/2$ and vertically down θL. These components are equivalent to the product of the virtual angle $\theta/2$ times the distance from ④ to "I. C.". The rafter ②- ④ must move through an identical

amount $\theta/2$ by virtue of the fact it is the same length as the dimension ④ - I. C.. Hence, summing angles at points ④ and ⑥ and comparing rotations at points ② and ⑦, it is observed that all of the angles are the same as previously ascertained. Furthermore, the resulting solution of this mechanism is also identical.

In as much as the adoption of the instantaneous center procedure (in preference to complexities of geometry) was established. It is hereby employed to solve the remaining mechanisms.

Seeing that mechanism (e) of Figure 1.15 is made up of the beam mechanism (a) and the gable mode (d), the geometry of the mechanism will be very similar to the gable mechanism just solved. The location of the I. C. can be established by the same deductions used before. Column ① - ② is fixed, making it necessary for link ② - ③ to rotate about point ②; column ⑥ - ⑦ must rotate about point ⑦ which in trun locates the instantaneous center of the link ③ - ⑥ a distance 2L vertically above hinges ⑥ and ⑦.

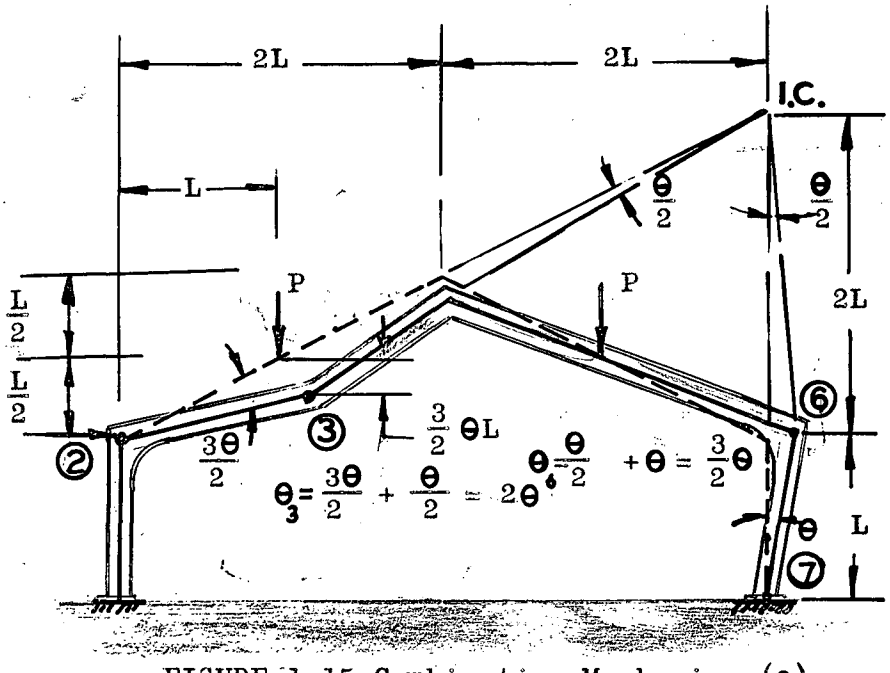

FIGURE 1.15 Combination Mechanism (e)

Now that the geometry is established, let bar ⑥ - ⑦ rotate through a virtual angle θ making it necessary for link ③ - ⑥ to rotate through $\theta L/2L = \theta/2$ correspondingly. Link ⑦ - ③ conforms by rotating through a proportional angle $\frac{3\theta L}{2} / \frac{\theta}{2}\frac{L}{2} = \frac{3\theta}{2}$, since the dimension from the I. C. to point ③ is three times the length of link ② - ③. Hence, the total hinge rotations are summed up in Figure 1.15.

Again applying the principle of virtual work

$$W_{int} = W_{ext}$$

$$M_p \left(3\,\theta/2 + 2\theta + 3\,\theta/2 + \theta\right) = P\,(3\,\theta/2)L + P\,(\theta/2)L$$
$$\qquad\qquad\qquad\qquad\qquad\qquad\qquad\qquad\qquad\qquad\quad @3 \qquad\qquad @5$$

$$M_p = \frac{PL}{3} \qquad \ldots\ldots\ldots\ldots\ldots\ldots\ldots\ldots\ldots\ldots (1.10)$$

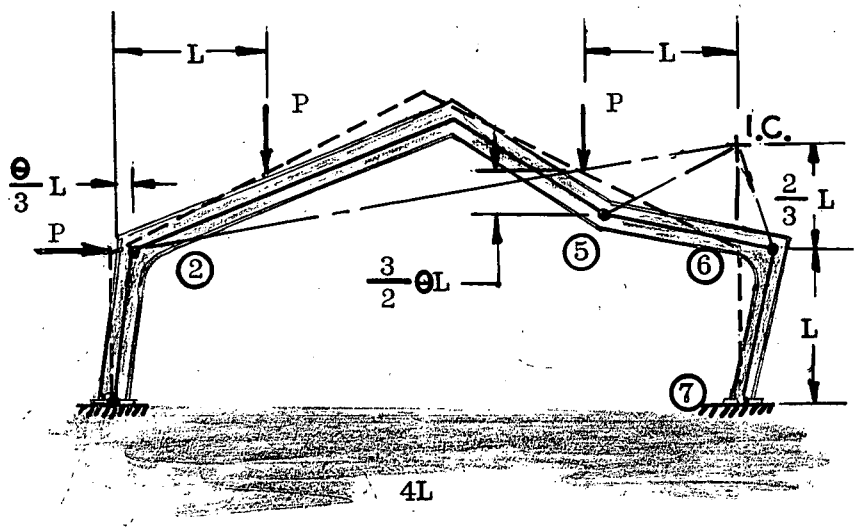

FIGURE 1.16 Combined Mechanism (h)

Continuing the same procedure as before, the location of of the instantaneous center of mechanism (h) is found to exist at a position 2L/3 vertically above point ⑥. Assuming a virtual rotation of θ at ⑦ the corresponding rotations that the other hinges undergo are presented in Figure 1.16. Having the relevant geometry solved, it is only necessary to apply virtual work.

$$W_{int} = W_{ext}$$

$$M_p \underbrace{(\theta/2}_{\text{at 2}} + \underbrace{\theta/2 + 3\,\theta/2}_{\text{at 5}} + \underbrace{3\,\theta/2 + \theta}_{\text{at 6}} \underbrace{+\theta}_{\text{at 7}} = PL\,\theta/2 + PL\,(3\,\theta/2)$$

$$M_p = \frac{PL}{3} \qquad \text{.....(1.11)}$$

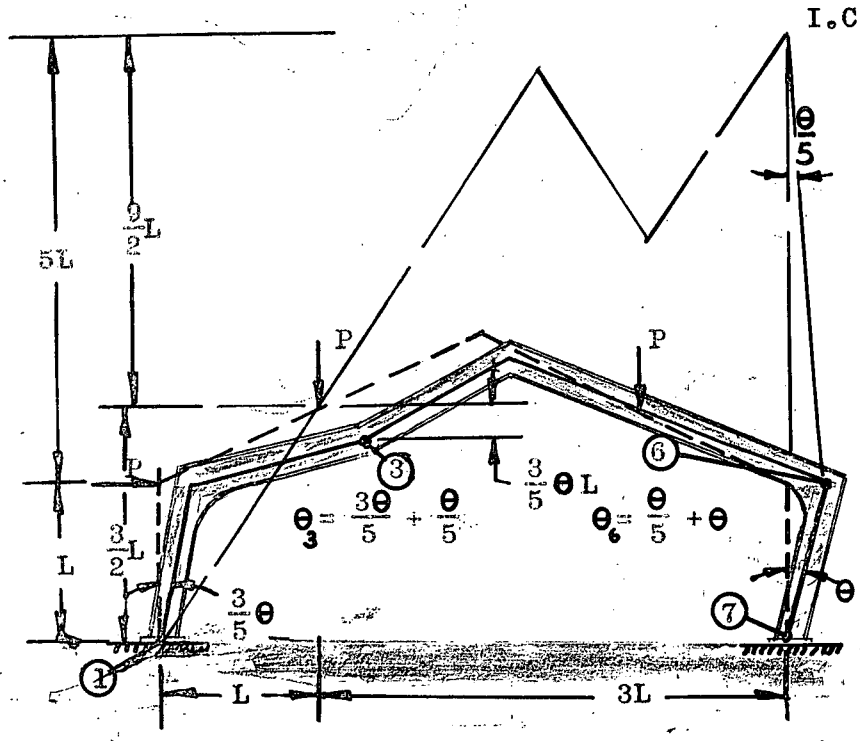

From the geometry of Figure 1.17 the mechanism (g) is solved in the following manner. The instantaneous center of link ③ ⑥ is located 5L above ⑥. From the principle of virtual work.

FIGURE 1.17 Combined Mechanism (g)

$$W_{int} = W_{ext}$$

$$M_p \left(\frac{3\theta}{5} + \frac{3\theta}{5} + \frac{\theta}{5} + \frac{\theta}{5} + \theta + \theta\right) = PL\left(\frac{3\theta}{5}\right) + PL\left(\frac{\theta}{5}\right) + PL\left(\frac{3\theta}{5}\right)$$

$$M_p = \frac{7}{18} PL \qquad \text{.....(1.12)}$$

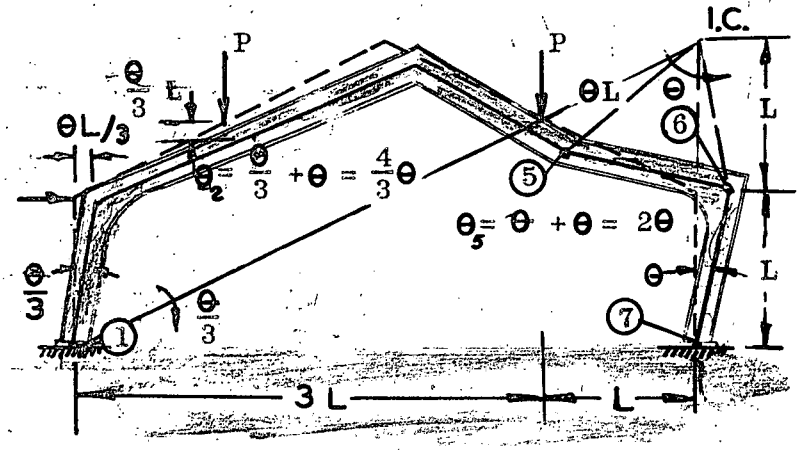

For mechanism (f) the I.C. is L above hinge ⑥.

FIGURE 1.18

$$\frac{14}{3} M_p\theta = P\left(\frac{5}{3} L\right)\theta$$

$$M_p = \frac{5}{14} PL \qquad \text{.....(1.13)}$$

For Figure 1.19

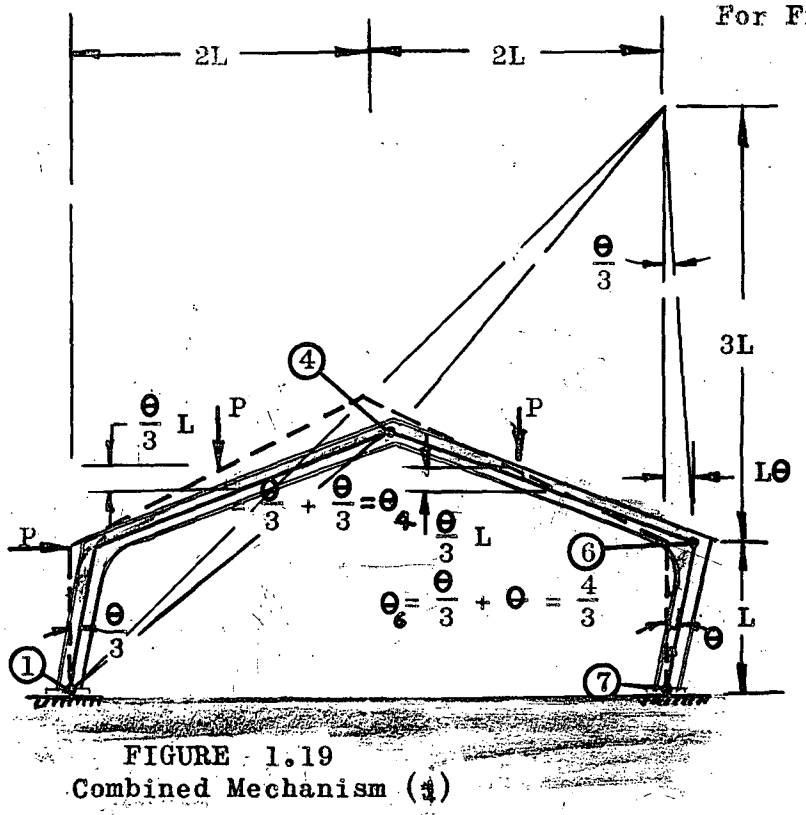

$$M_p\left(\frac{\theta}{3} + \frac{\theta}{3} + \frac{\theta}{3} + \theta + \frac{\theta}{3} + \theta\right)$$

$$= PL\frac{\theta}{3} + PL\frac{\theta}{3} + PL\frac{\theta}{3}$$

$$\frac{10}{3} M_p\theta = \frac{3PL\theta}{3}$$

$$M_p = \frac{3}{10} PL \text{ .....}$$

$$\text{.....(1.14)}$$

FIGURE 1.19
Combined Mechanism (4)

Now that all anticipated possible mechanisms have been analyzed, in order to ascertain whether or not the correct solution has been derived, a plasticity check must be performed. According to the previous line of reasoning, equation 1.12 on page 33 must be the correct solution. If this is the case, the next step is to construct a moment diagram. For the deformed structure shown in Figure 1.20.

Isolating column BD as a free body (Figure 1.20b) and taking moments about D.

$$B = \frac{M_p + M_p}{L} = \frac{2M_p}{L}$$

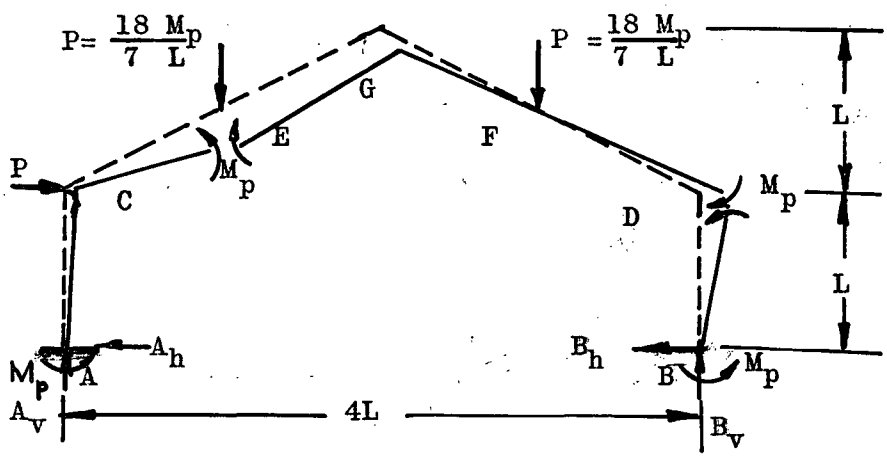

FIGURE 1.20
Failure Mechanism Disjoined

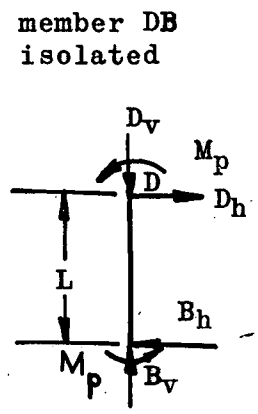

FIGURE 1.20(b)

Then summing horizontal forces

$$P = A_h + B_h$$

$$A_h = \frac{18M_p}{7L} - 2\frac{M_p}{L} = \frac{4M_p}{7L}$$

Considering the complete structure as a free body and taking moments about (A).

$$\Sigma M_A = 0$$

$$2M_p - P(L + L + 3L) + 4LB_v = 0$$

$$B = \frac{-2M_p + \frac{90}{7}M_p}{4L} = 2.71\frac{M_p}{L}$$

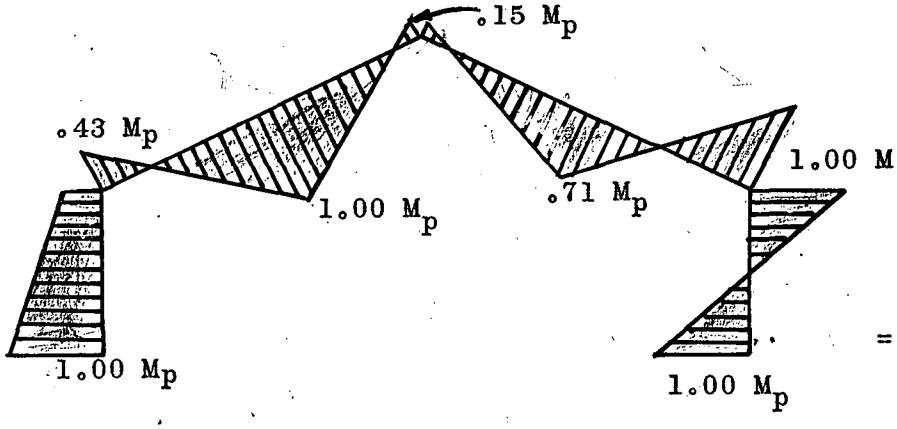

Note: moments plotted on tension side

FIGURE 1.21 Final Moment Diagram

The vertical reaction at (A) is obtained by summing vertical forces.

$$A_v = 2P - B_v$$

$$= \frac{36M_p}{7L} - \frac{19M_p}{7L}$$

$$A_v = 2.43\frac{M_p}{L}$$

As a final conclusion, reviewing the necessary conditions for a plastic solution, a mechanism is formed and the structure is automatically in equilibrium. The plasticity condition was satisfied by the check just performed. Hence, this is the correct solution.

1.07 Conclusions to Introduction

One of the most important premises in this thesis has been established previously on page 24. Although it wasn't emphasized at that point, it is felt that it is necessary to resubstantiate this fact now. As was implied then, statically indeterminate systems require an additional plastic hinge for each redundancy in order to create a general kinematic mechansim. In the case of the single span gable frame where the structure was three times redundant, it always took four plastic hinges to generate a general failure condition. Not only is a continuous ring similar in shape to a rigid frame, but its modes of collapse are of comparable nature, since they both are three times redundant and require exactly four hinges for a general failure mechanism. As will be seen later on, the continuous ring problem can be solved by a sidesway or gable type of mechanism. Hence, the previous illustration with the gable frame should be of extreme value in establishing the methods of analysis for circular rings.

Just as the similarities of the two types of structures have been discussed so their diversities should also be considered. The real distinction between a single span frame and a continuous ring is the nature of their redundancies. Even though they are both inherently redundant three times, the rigid frame is

redundant externally whereas the ring is redundant internally. That is to say, the external redundancies which are part of the solution of the frame are the reactions to the applied loads. On the other hand, for example, the external reactions in the case of the ring may be shears in the skins which are more like an applied load than a reaction, and are by no means internally imparted to the ring. Because of this discrimination, the approach to the ring solution is somewhat different. Since, the locations of the hinges were known in the frame solution, a mechanism was assumed and then checked.

The exact locations of the plastic hinges are seldom known for a ring problem. The hinges are located by assuming a hinge pattern dependent upon unknown angles, and by ascertaining the expression for plastic moment in terms of the unknown angles. The moment expression is maximized with respect to these angles, and then the result is substituted into the expression for the final solution to the problem. Consequently, in ring analysis it is not mandatory to go through a tedious process of seeking a solution from a multitude of mechanisms.

1.08 Modifying Factors

Some of the more significant modifying factors in analyzing rigid frames and rings are apparent from considering the assumptions made prior to developing the simple plastic theories for rigid frames.

Recapitulating, it was assumed

1. Normal forces do not influence the ultimate bending capacity of a member.

2. The influence of shear on the full plastic moment is negligible.

3. No instability occurs prior to the development of a mechanism.

4. The loads are increased proportionally.

5. Failure will not occur due to brittle fracture

When the first two assumptions were considered for rigid frame analysis it was best to make these suppositions, obtain a solution and then take axial load and shear into account by modifying the moment carrying capacity at any section.* However, this is a typical procedure used in accounting for axial load and shear in rigid frame analysis. The effect of axial load and shear is a more significant problem in ring analysis. Later on in the text, a method will be derived to account for this effect.

Local and lateral stability has already been mentioned and the only addition to be advanced at this time is to mention the restrictions to be imposed on the structure in order to eliminate these possibilities. Local instability can be avoided by proportioning the width to thickness of outstanding flanges. In practically all applications that come to mind, rings, fortunately are stabilized laterally because the surrounding skin would have to collapse before the ring could buckle outward.

One of the more uncompromising problems of plastic analysis is the possibility of progressive deformations under varying loads. This phenomenon is commonly known as shakedown (as defined below). If a structure is subjected to several loads, each of

*See reference 5, page 9.1

which may vary between prescribed maximum and minimum limits regardless of the magnitude of the other loads at the same instant, it should be proportioned in such a way that no possible combination of the loads will cause collapse. Consequently, this structure must stabilize itself by a state of residual stress such that further variations of load are supported in a purely elastic manner. In other words, it is important that each of the modes of failure due to varying loads be considered. B.G. Neal* suggests that the problem of shakedown is not as serious as would be anticipated. Many times the shakedown load determined for structures and loadings encountered in practice is only slightly smaller than the load predicted by a simple plastic analysis. However, shakedown is a noteworthy problem for any type of structure, and will be discussed in more detail later.

Concerning the possibility of brittle facture much can be said. Actually, the real problem here lies in the properties of the materials used. All the premises of the simple plastic theory are based on the presumption of ductility. Probably, this section of the text best belongs at the beginning of the thesis, because even before a plastic hinge type of deformation can be assumed it must be established that the materials employed are capable of producing such a distortion. Once before on page 14, the definition of rotation capacity was defined, and it is upon this characteristic of a material that all the theories of plasticity rely. Thus, if a material possesses this property of plasticity, which is a term commonly used in the same sense as

**See references 6 and 8.

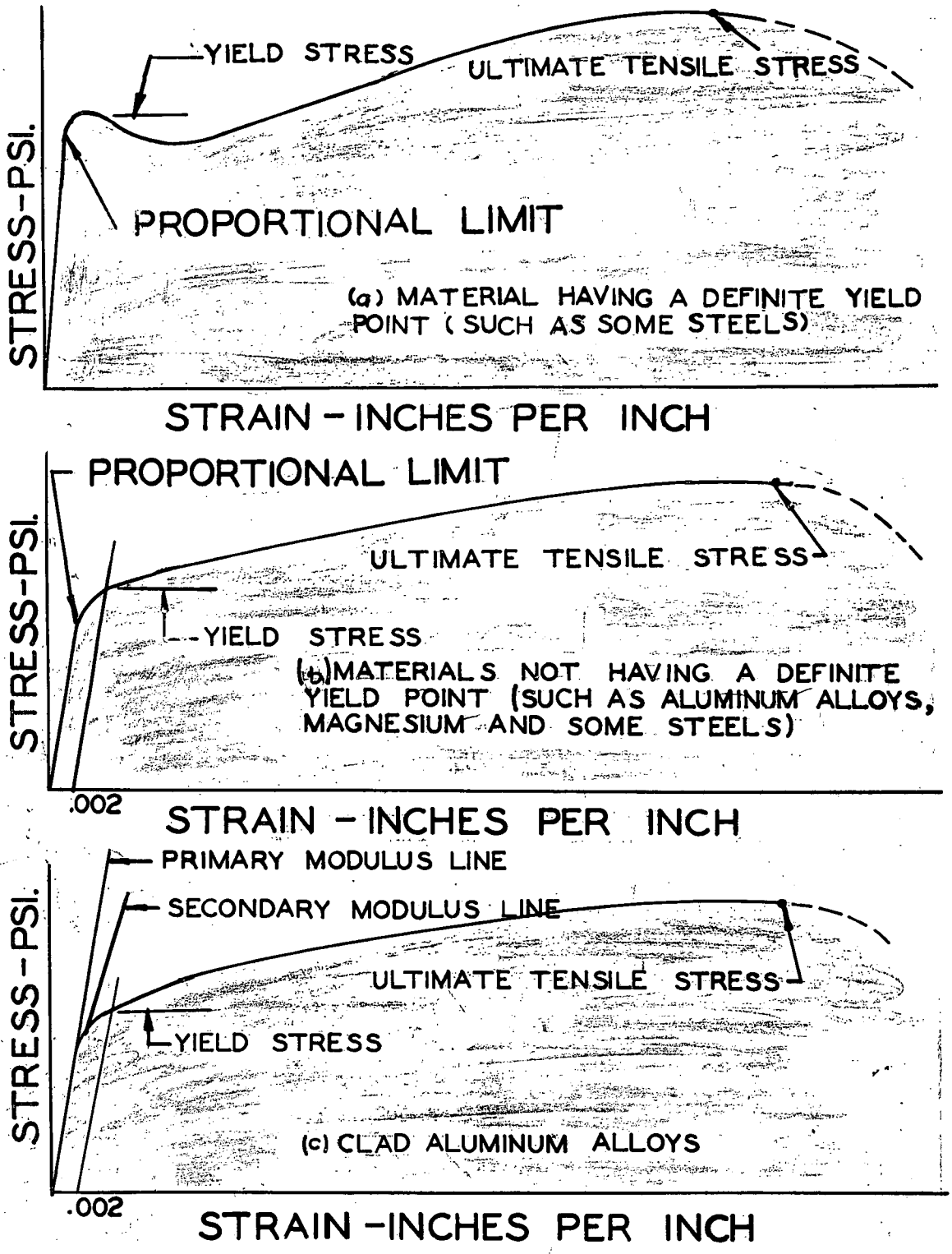

FIGURE 1.22
TYPICAL STRESS STRAIN DIAGRAMS*

*See ANC-5, Strength of Metal Aircraft Elements, March 1955 figure 1.44

we use ductility, it is acceptable for consideration of plastic analysis. In reality, many structural materials fall into this category. A few typical tensile stress-strain diagrams of a select group of structural materials are shown in Figure 1.22 on page 40.

As remote as the possibility may seem, even some pre-stressed concrete structures might possibly be designed by a plasticity method. The thought that comes to mind is the consideration of a pre-stressed concrete slab. If this type of structure were considered in a bending configuration beyond its cracking load, small cracks form running diagonally across the slab. Thus, if a plastic hinge is imagined to form along this crack a mechanism will have been created.

SECTION 2.0.0

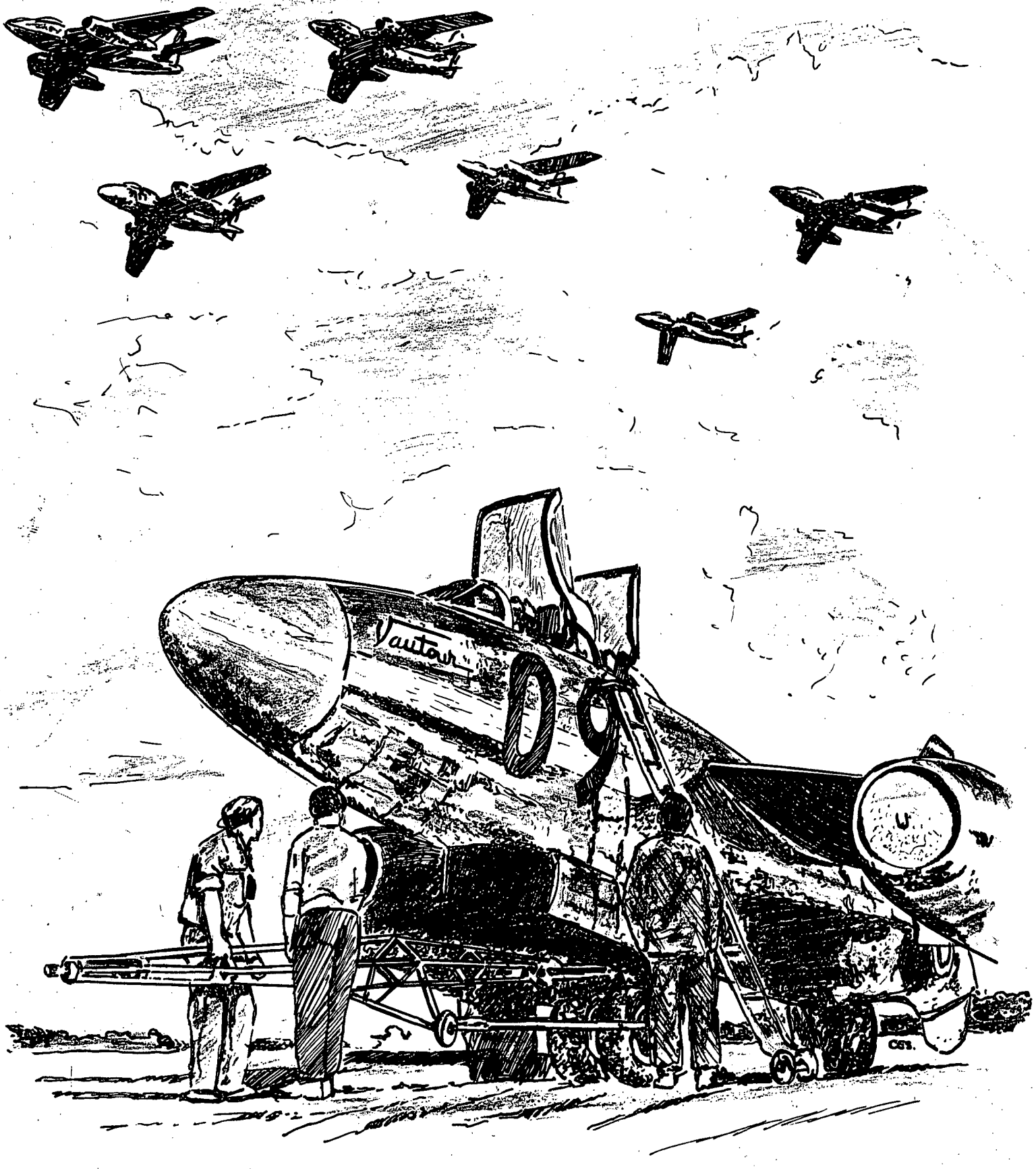

CIRCULAR RINGS

2.0.0 Approach to Solution of Continuous Circular Rings

Justification of the Evolution of Plastic Analysis for Circular Rings

The sole intention of this thesis is to present a systematic procedure for the plastic analysis of continuous circular rings, by means of illustrating the mechanism method for several different examples. The clear-cut distinction between continuous rings and discontinuous ring segments is emphasized to differentiate between ring analysis and arch analysis. There again, arch analysis is much like rigid frame analysis where the external reactions of thrusts and moments must be found, and will therefore constitute no portion of this treatise. Each example was selected with the objective in mind to emphasize some particular peculiarity encountered in simple plastic ring analyses. The elastic solution is presented in the form of graphs and tables with each final general solution presented for purposes of comparison.

The very fact that structures incorporating the use of circular rings are substantially effective is sufficient proof that elastic design methods are adequate enough to produce useful structures. Nevertheless, this same fact does not insinuate that the designer understands the actual working behavior of such structures nor that he has made the best use of the materials included. In other words, because a structure is sufficient, does not imply that it is efficient or an optimum design.

The following pages unfold a method sincerely believed to

be more reasonable and straight forward than elastic methods previously developed for ring analysis. Therefore, without further explanation, the mechanism method of simple plastic analysis in conjunction with the expedient - instantaneous center of rotation - is disclosed.

2.0.1 Loading Condition-Ring I-Radial Force P on a Tangentially Supported Circular Ring

One of the simplest loadings that comes to mind is of the nature shown below in Figure 2.0.1

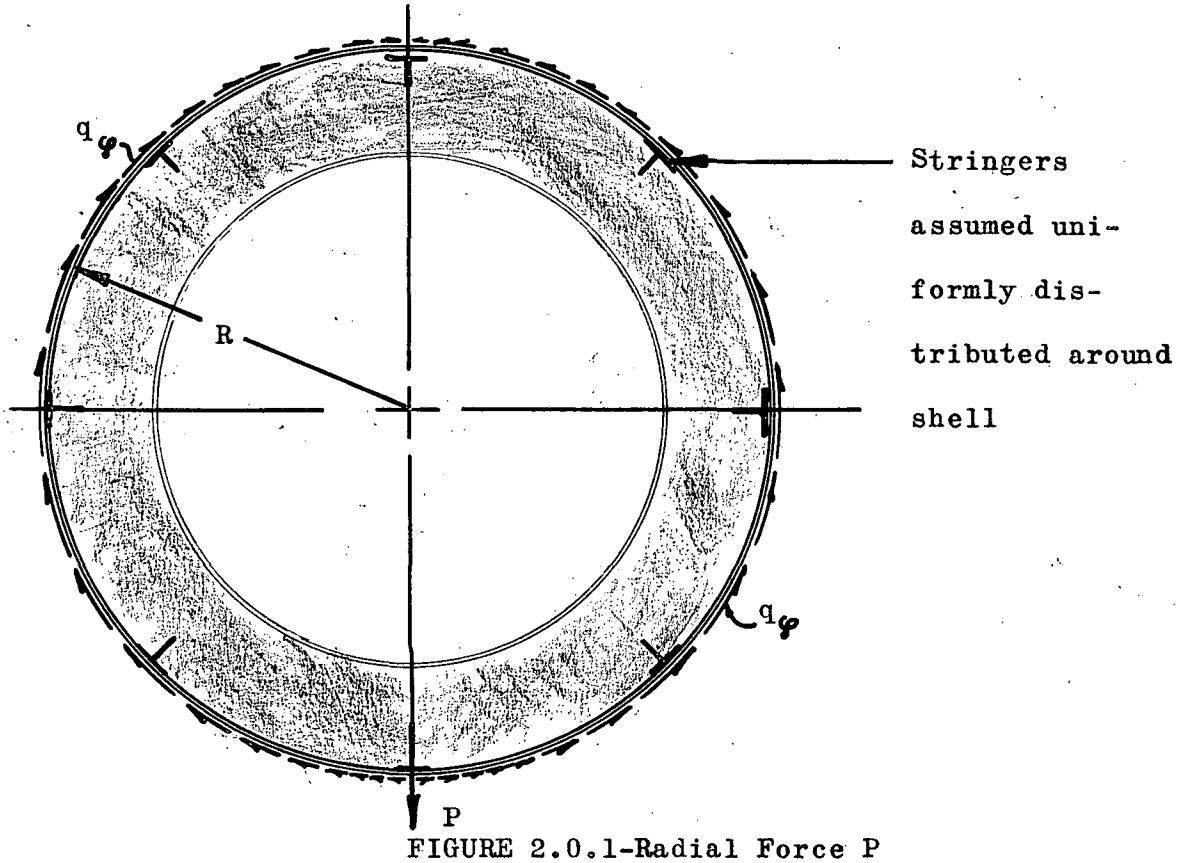

FIGURE 2.0.1-Radial Force P

Since it is not a part of this thesis to determine the manner in which external loads are to be applied, an assumption as to the manner in which the loads are to be carried is of prime necessity. Furthermore, in order to compare the final plastic analysis of a ring to its elastic analysis it is mandatory to be consistent with the same assumptions for transferring loads presumed in the elastic solution. Consequently, if the reader shall imagine this ring contained in a portion of a structure segregated as shown below in Figure 2.0.2.

FIGURE 2.0.2

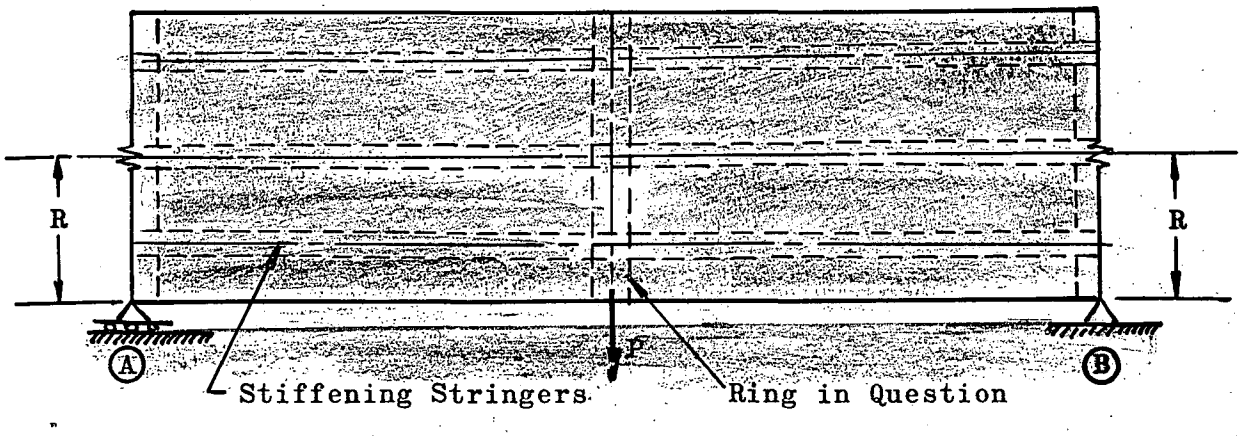

Determination of Shear Load Distribution by

Simple Beam Theory

It is apparent from Figure 2.0.2 that the load P is transferred to the structure's shell by bending. Before the analyst can proceed to solve the problem, he must make some simplifying assumptions. First, it will be assumed that the stiffening members running longitudianlly along the shell are distributed uniformly around the circumference of the semi-monocoque type structure, so that they might be replaced by an effective skin thickness t_e. Upon this simplifying assumption the moment of inertia of the shell may be presumed to be

$$I = \pi R^3 t_e \quad \text{.....(2.0.1)}$$

where t_e is small compared with the radius R.

Also, it must be realized that a ring of this nature is not required to carry any loads or moments out of the plane of the ring. Thus, any loads normal to the plane of the ring must be carried by the stringer longerons and external skins as axial forces in these members.

Segregating that portion of the shell a differential amount

just to the left and right of the ring, results in Figure 2.0.3 (a) and 2.0.3 (b)

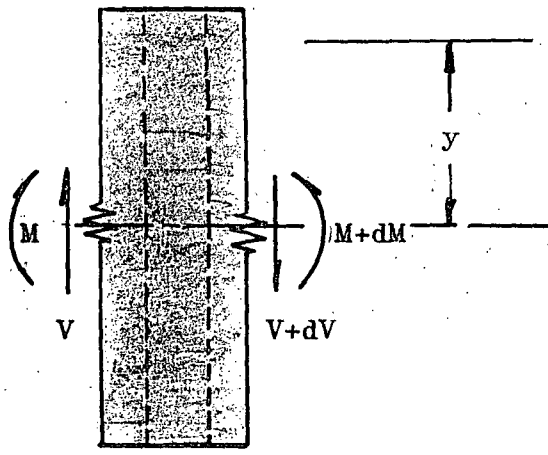

FIGURE 2.0.3 (a)

Section of Shell Including Ring in Question

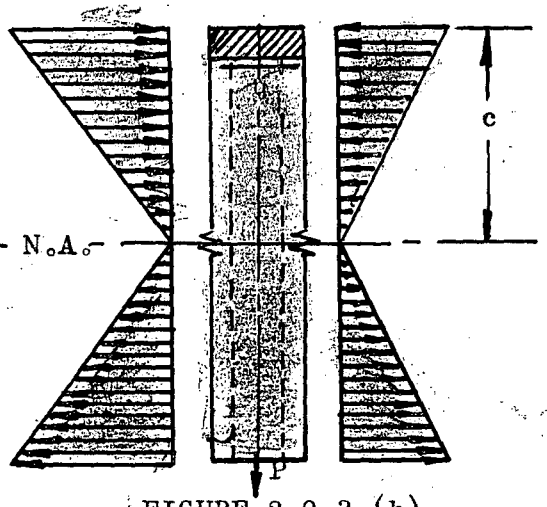

FIGURE 2.0.3 (b)

Bending Stress in Shell Due to Applied P Load

Cutting an element out of the shell a distance "y" above the bending neutral axis of the structure and placing it in equilibrium, (Figure 2.0.4)

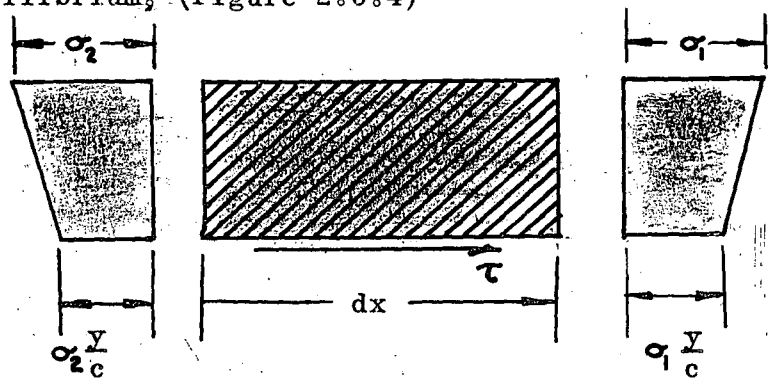

FIGURE 2.0.4
Isolation of a Small Element Above "y" Distance From N.A.

Where τ = Shearing Stress.

It is evident that the shearing force $\tau t = q$ is equal to

$$q = \frac{dM}{dx} \left(\frac{1}{I}\right) \int_y^c y \, dA \quad \text{.....(2.0.2)}$$

or

$$q = \frac{V}{I} \int_{y}^{c} y \, dA = \frac{VQ}{I} \qquad \text{.....(2.0.3)}$$

Where Q = moment with respect to the neutral axis of the shaded portion above "y". Therefore, returning to the ring cross section of Figure 2.0.4

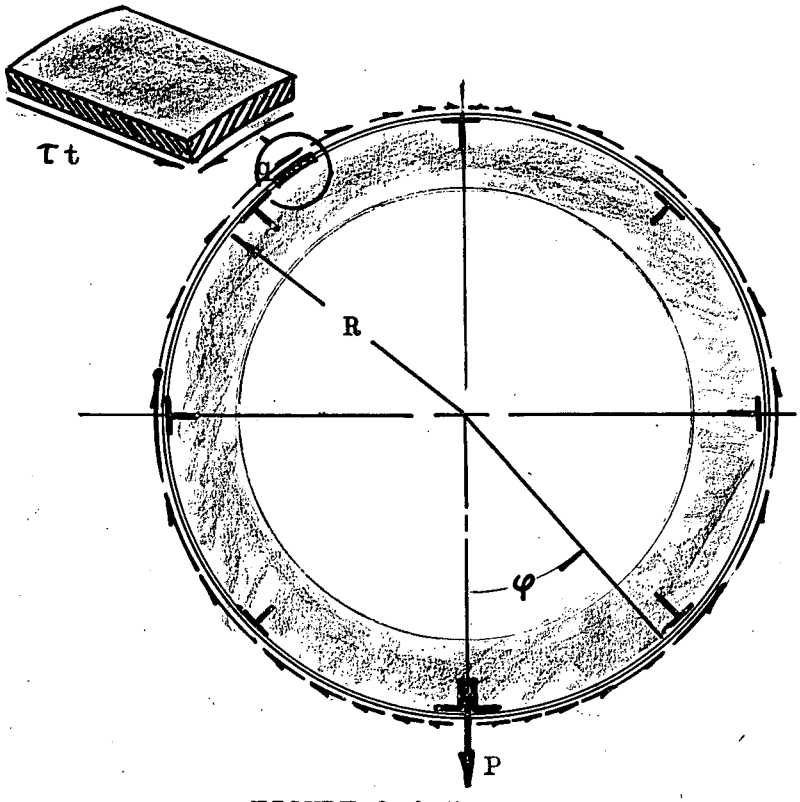

FIGURE 2.0.5

Solving the integral $\int_{y}^{c} y \, dA$ For a circular ring

$$\int_{0}^{\varphi} R \cos\varphi \; Rt_e \, dp$$

$$= R^2 t_e \sin\varphi \text{...(2.0.4)}$$

Substitutuing the values for I (equation 2.0.1) and Q (equation 2.0.4) into equation 2.0.3

$$q = \frac{P}{\pi R^3 t_e} \quad (R^2 t_e \sin\varphi)$$

$$q = \frac{P}{\pi R} \sin^{*}\varphi \text{.....(2.0.5)}$$

This result (2.0.5) is obtained from an elastic interpretation and violates every statement made previously about

*See reference 14 page 483 Niles and Newell

mixing plastic with elastic analysis. However, if the same external loading as used in the elastic analysis is not employed at this point, it will be impossible to compare both final analyses, which is one of the purposes of this thesis. Hence, content with this argument and the fact that a determination of applied and reacted external ring loads is not a part of this text, it follows that all external loads are now defined.

Reiterating the concepts asserted on page 36, four plastic hinges reduce the ring in question to a kinematic mechanism. Observing that the ring geometry is symmetrical and the ring is symmetrically loaded, the hinge pattern in figure 2.0.6 is assumed to be valid.

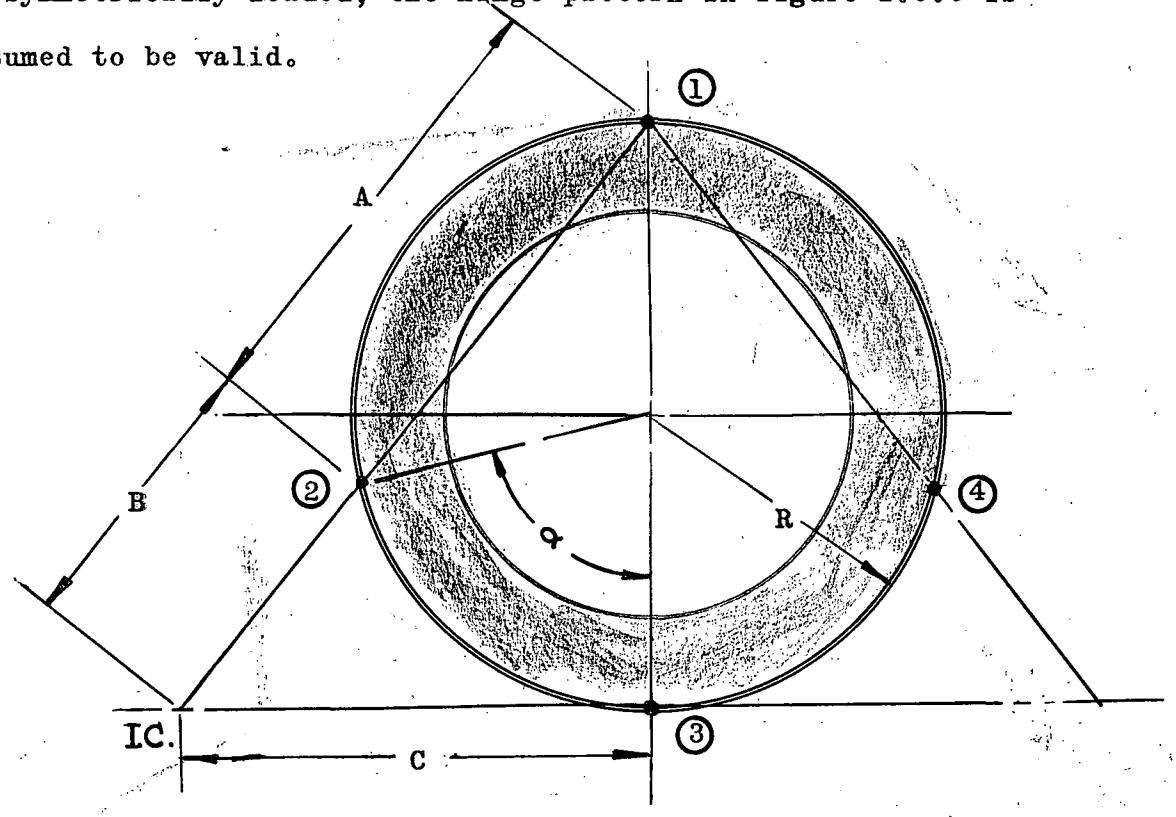

FIGURE 2.0.6
Assumed Hinge Pattern for a Radially Loaded Ring

2.0.2 Determination of Hinge Patterns

Without alluding to any pretenses of simplicity, the whole

crux of the application of plastic theory to ring analyses lies in the ability of the analyst to ascertain the locations of the plastic hinges. Recapitulating, the analyst should recall that there are several conventions which he may resort to in order to define these points. The most important rule to consider is the relationship of shear to moment. That is, by definition maximum moment always occurs at the points of zero shear and vice versa. However, many times the points of zero shear are not quite so apparent, and thus, it may be wise to review the pertinent rules asserted on page 22.

A hinge may form

a.) At the point of a concentrated load.(This is not necessarily a point of zero shear, but is the place where the shear passes from a positive to a negative value.)

b.) At equal angles to a loading axis of symmetry by virtue of geometrical symmetry and symmetry of loading.

c.) At an abrupt change of direction of a member. (This condition could conceiveably be imposed by geometrical restrictions wherein the inner mold line is fixed and a hinge would be compelled to form at an abrupt change of stiffness; similar to a geometrical fixity.)

Once these ideas are instilled in the analyst's mind, he is prepared to apply the rules to individual particular ring problems. In consideration of the ring in question, the hinge pattern (Figure 2.0.6) was ascertained from the following conclusions. The established position of hinge ③ is attributed to rule (a.). According to rule (b.) hinge ① must form 180^{o}

directly opposite hinge ③. This can better be visualized by cutting the ring in half and equilibrating this semi-ring. If each half of the ring is assumed to carry one half the applied load P/2, then the vertical external shear flow $V_y = \int_0^{\pi} \frac{P}{\pi R} \sin\varphi \sin\varphi \, dp = \frac{P}{2}$ exactly equals the applied load. Conversely, the horizontal component of the shear flow must equal zero, that is $V_x = \int_0^{\pi} \frac{P}{\pi R} \sin\varphi \cos\varphi \, d\varphi = 0$. Hence $H_1 = H_2$. The second and fourth hinges ② and ④ must form at equal angles α from the vertical axis of symmetry, because of rule (b.) also. Considering the overall picture (Figure 2.0.7) the only unknown parameter is the value of α, which can eventually be solved for by maximizing the maximum moment with respect to its value.

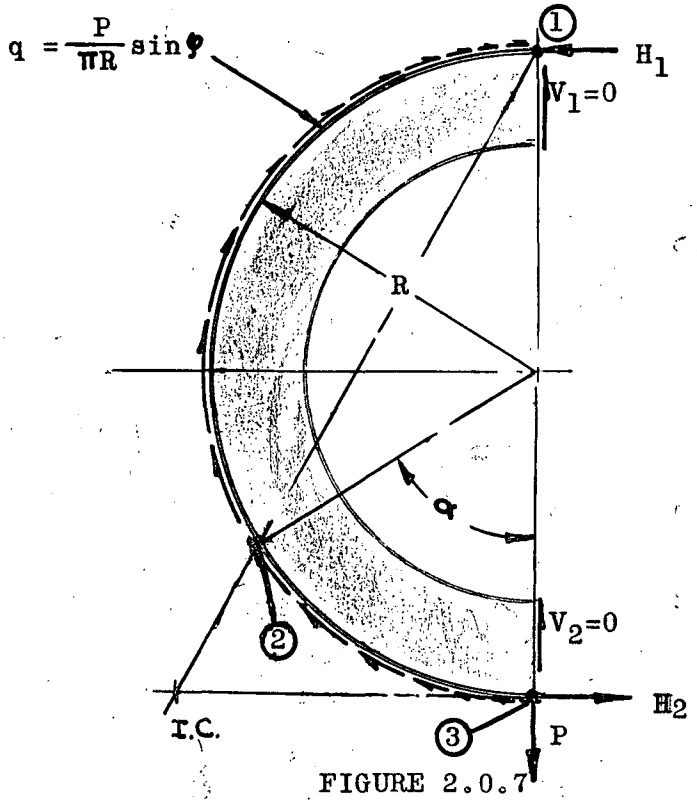

FIGURE 2.0.7

Reconstructing the geometry of Figure 2.0.6 in Figure 2.0.8 and considering only one half the frame because of symmetry, all of the geometry can be resolved from trigonometric relations. Hence, the proportions of the deminsions A, B, and C may all be determined as functions of the radius of the ring and half and

whole trigonometric relations of the unknown angle α.

Although no light has been shed on the subject before, at this point the analyst must use a little inherent ingenuity or discretion. It is entirely without illusion to point out that a lot of time can be avoided by a wise desicision conerning the selection of the point to fix the ring in space. Henceforth, if the analyst is not able to make a wise choice at first, the geometry becomes so complex that he is compelled to abandon this approach and start all over by fixing another hinge point or a section of the ring. Perhaps it is not quite so evident, but it is reasonable to suspect that either point ① or ③ would be a much better choice than point ②.

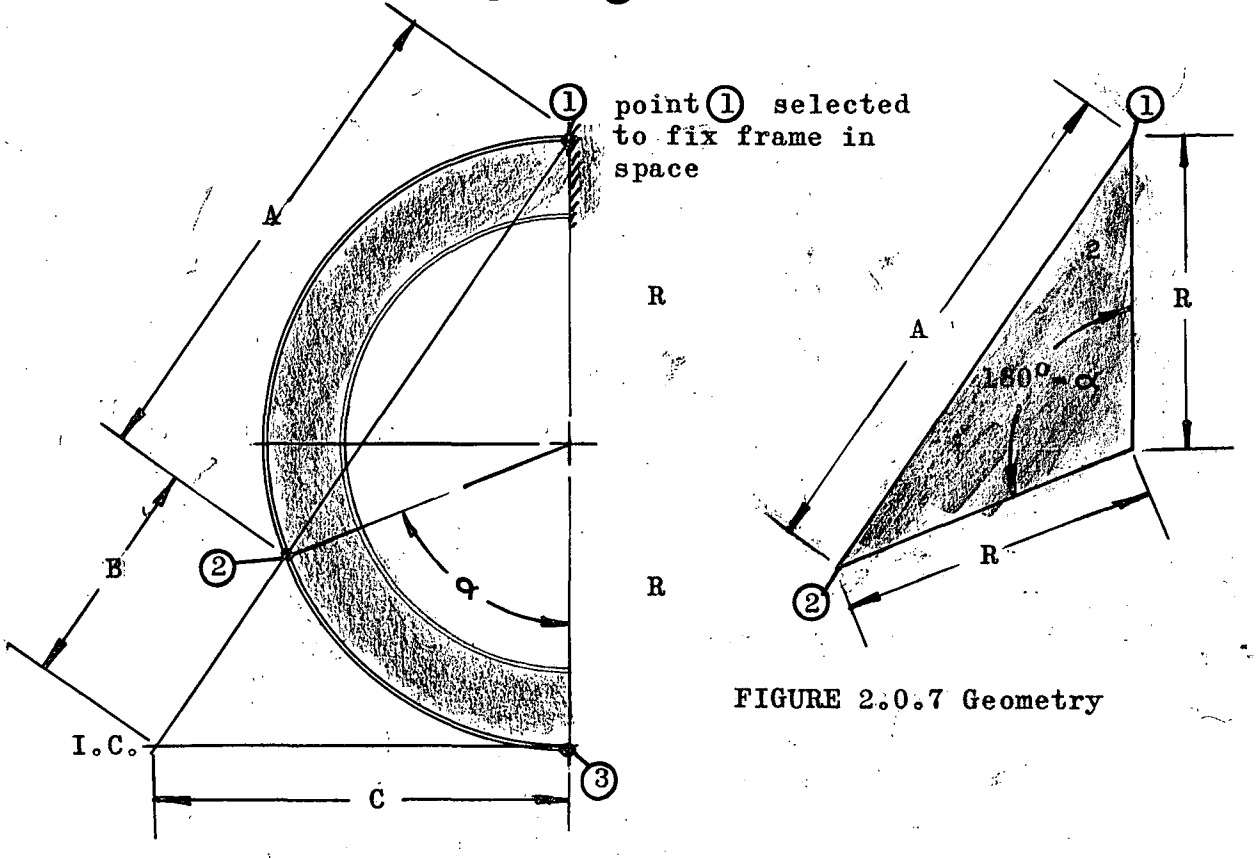

FIGURE 2.0.7 Geometry

From FIGURE 2.0.6

$$\frac{\sin\,(180^\circ - \alpha)}{A} = \frac{\sin\,\left(\frac{\alpha}{2}\right)}{R}$$

$$A = R \frac{\sin (180^{o} - \alpha)}{\sin (\frac{\alpha}{2})}$$

Since point ① is assumed to be fixed in space and link ① - ② must rotate about point ①, its instantaneous center is point ①. Also, if point ③ is restricted to move vertically down due to geometrical symmetry then, the link ② - ③ must rotate about a point along a horizontal line passing through point ③. Link ① - ② must rotate about a line passing through points ① and ②. Where these two lines intersect is the instantaneous center of rotation of segment ② - ③ or ③ - ④ of the structure. Thus, the instantaneous center of rotation is located as shown in Figure 2.0.6.

Also

$$A = R\left[\frac{\sin 180^{o} \cos \alpha - \cos 180^{o} \sin \alpha}{\sin (\frac{\alpha}{2})}\right]$$

$$A = R\left[\frac{-(-1) \sin \alpha}{\sin (\frac{\alpha}{2})}\right] = R\left[\frac{2 \sin (\frac{\alpha}{2}) \cos (\frac{\alpha}{2})}{\sin (\frac{\alpha}{2})}\right] \quad \ldots\ldots(2.0.6)$$

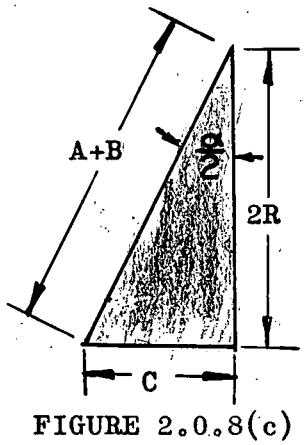

FIGURE 2.0.8(c)

$$A = 2R \cos (\frac{\alpha}{2})$$

$$\tan (\frac{\alpha}{2}) = (\frac{C}{2R})$$

or

$$C = 2R \tan (\frac{\alpha}{2}) = \frac{C}{2R}$$

or

$$C = 2R \tan (\frac{\alpha}{2}) \quad \ldots\ldots\ldots\ldots\ldots\ldots\ldots\ldots\ldots(2.0.7)$$

From Figure 2.0.8 it is evident that

$$\cos (\frac{\alpha}{2}) = \frac{2R}{A + B}$$

Rearranging

$$A + B = \frac{2R}{\cos (\frac{\alpha}{2})} \qquad \text{or} \quad B = \frac{2R}{\cos (\frac{\alpha}{2})} - A$$

Substituting the term A of equation (2.0.6) into the expression

$$B = \frac{2R}{\cos\left(\frac{\alpha}{2}\right)} - 2R\cos\left(\frac{\alpha}{2}\right)$$

$$= 2R\left[\frac{1 - \cos^2\left(\frac{\alpha}{2}\right)}{\cos\left(\frac{\alpha}{2}\right)}\right] = 2R\left[\frac{\sin^2\left(\frac{\alpha}{2}\right)}{\cos\left(\frac{\alpha}{2}\right)}\right]$$

$$B = 2R\sin\left(\frac{\alpha}{2}\right)\tan\left(\frac{\alpha}{2}\right) \quad \text{.....(2.0.8)}$$

Subsequently, in order to apply the principle of virtual displacements, the relationships between the virtual rotations of each component must be investigated, assuming point ① to be fixed and revolving link ① - ② through a virtual counter-clockwise rotation . The results are then as follows

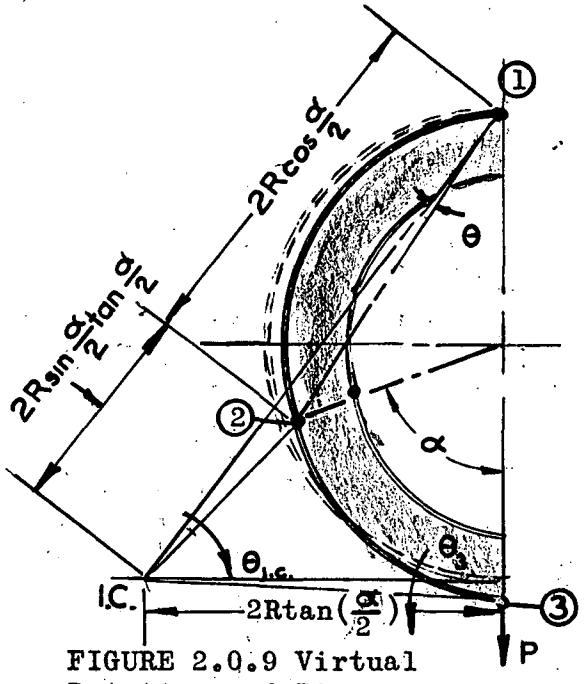

FIGURE 2.0.9 Virtual Rotations of Ring

$$\theta_1 = \theta \quad \text{.....(2.0.9)}$$

$$\theta_{I.C.} = \frac{2R\cos\left(\frac{\alpha}{2}\right)}{2R\sin\left(\frac{\alpha}{2}\right)\tan\left(\frac{\alpha}{2}\right)}$$

$$\theta_{I.C.} = \theta\left[\frac{1}{\tan^2\left(\frac{\alpha}{2}\right)}\right] \quad \text{....(2.0.10)}$$

$$\theta_3 = \theta_{I.C.} = \theta\left[\frac{1}{\tan^2\left(\frac{\alpha}{2}\right)}\right] \quad \text{..(2.0.11)}$$

$$\theta_2 = \theta_1 + \theta_{I.C.}$$

$$= \theta\left[1 + \frac{1}{\tan^2\left(\frac{\alpha}{2}\right)}\right] =$$

$$\theta_2 = \theta\left[\frac{\tan^2\left(\frac{\alpha}{2}\right) + 1}{\tan^2\left(\frac{\alpha}{2}\right)}\right] = \theta\left[\frac{1}{\sin^2\left(\frac{\alpha}{2}\right)}\right] \quad \text{.....(2.0.12)}$$

Summarizing,

$$\theta_1 = \theta \;\Big)$$

$$\left.\begin{aligned} \theta_2 &= \theta \frac{1}{\sin^2(\frac{\alpha}{2})} \\ \theta_3 &= \frac{1}{\tan^2(\frac{\alpha}{2})} \\ \theta_{1.c} &= \theta \frac{1}{\tan^2(\frac{\alpha}{2})} \end{aligned}\right\} \quad \ldots\ldots\ldots\ldots\ldots\ldots\ldots\ldots (2.0.13)$$

2.0.3 Expedient Method for Resolving Ring Shears

At this time, in order to simplify computing the external work done by the "q" shear flow forces, replace the q forces by their equivalent horizontal and vertical forces and moment acting about the center of the ring (Figure 2.0.10).

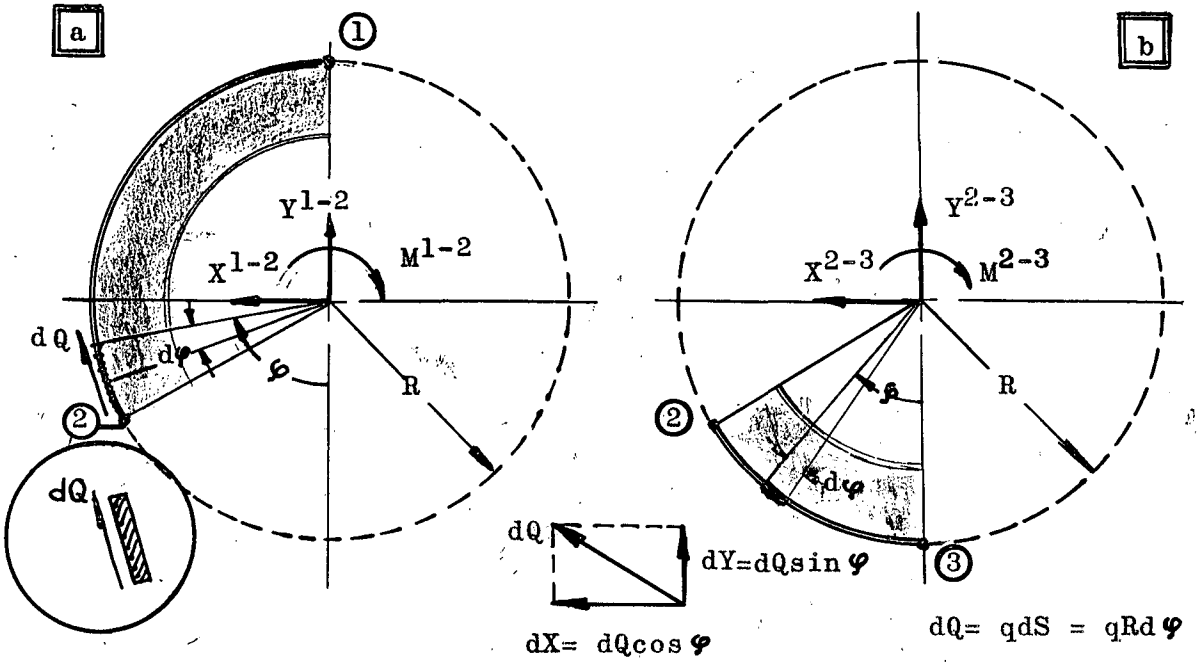

FIGURE 2.0.10 Resolution of Forces

The Equivalent System is Therefore:

$$X = \int q\, R \cos\varphi d\varphi = \frac{PR}{\pi R} \sin\varphi \cos\varphi\, d\varphi =$$

$$Y = \int q\, R \sin\varphi d\varphi = \frac{P}{\pi R} R \sin\varphi \sin\varphi\, d\varphi =$$

$$M = \int q\, R^2 d\varphi = \frac{P}{\pi R} R^2 \sin\varphi\, d\varphi =$$

Which results in

$$X = \frac{P}{\pi} \int \sin\varphi \cos\varphi \, d\varphi = \frac{P}{\pi} \left[\frac{\sin^2\varphi}{2} \right] \begin{matrix} \text{upper limit} \\ \text{lower limit} \end{matrix} \quad \ldots(2.0.14)$$

$$Y = \frac{P}{\pi} \int \sin^2\varphi \, d\varphi = \frac{P}{\pi} \left[\frac{\varphi}{2} - \frac{\sin 2\varphi}{4} \right] \begin{matrix} \text{upper limit} \\ \text{lower limit} \end{matrix} \quad \ldots(2.0.15)$$

$$M = \frac{PR}{\pi} \int \sin\varphi \, d\varphi = \frac{PR}{\pi} \left[-\cos\varphi \right] \begin{matrix} \text{upper limit} \\ \text{lower limit} \end{matrix} \quad \ldots(2.0.16)$$

Evaluating the integrals between hinges ① and ② (α to π)

$$X^{1-2} = \frac{P}{\pi} \left[\frac{\sin^2\pi - \sin^2\alpha}{2} \right] = \frac{P}{\pi} \left[-\frac{\sin^2\alpha}{2} \right] \quad \ldots\ldots\ldots\ldots(2.0.17)$$

$$Y^{1-2} = \frac{P}{\pi} \left[\frac{\pi}{2} - \frac{\sin 2\alpha}{4} - \frac{\alpha}{2} + \frac{\sin 2\alpha}{4} \right] = \frac{P}{\pi} \left[\frac{\pi}{2} - \frac{\alpha}{2} + \frac{\sin 2\alpha}{4} \right] \ldots(2.0.18)$$

$$M^{1-2} = \frac{PR}{\pi} \left[-\cos\pi + \cos\alpha \right] = \frac{PR}{\pi} \left[1 + \cos\alpha \right] \quad \ldots\ldots(2.0.19)$$

Evaluating the integrals between hinges ② and ③ (0 to α)

$$X^{2-3} = \frac{P}{\pi} \left[\frac{\sin^2\alpha}{2} - \frac{\sin^2 0}{2} \right] = \frac{P}{\pi} \left[\frac{\sin^2\alpha}{2} \right] \ldots\ldots\ldots\ldots(2.0.20)$$

$$Y^{2-3} = \frac{P}{\pi} \left[\frac{\alpha}{2} - \frac{\sin^2}{4} - 0 - \frac{\sin 0}{4} \right] = \frac{P}{\pi} \left[\frac{\alpha}{2} - \frac{\sin 2\alpha}{4} \right] \ldots(2.0.21)$$

$$M^{2-3} = \frac{PR}{\pi} \left[-\cos\alpha + \cos 0 \right] = \frac{PR}{\pi} \left[1 - \cos\alpha \right] \ldots\ldots\ldots(2.0.22)$$

The sign convention holds as follows with all forces and moments shown positive

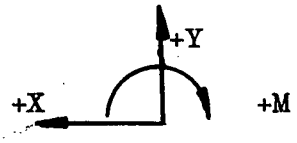

For summarizing the results of equations 2.0.17 through 2.0.22 and computing the external work done by the applied radial load P, consider the ring geometry presented in Figure 2.0.11. The work done by the radial load $\frac{P}{2}$ is equal to its magnitude times the vertical distance through which it is displaced, or

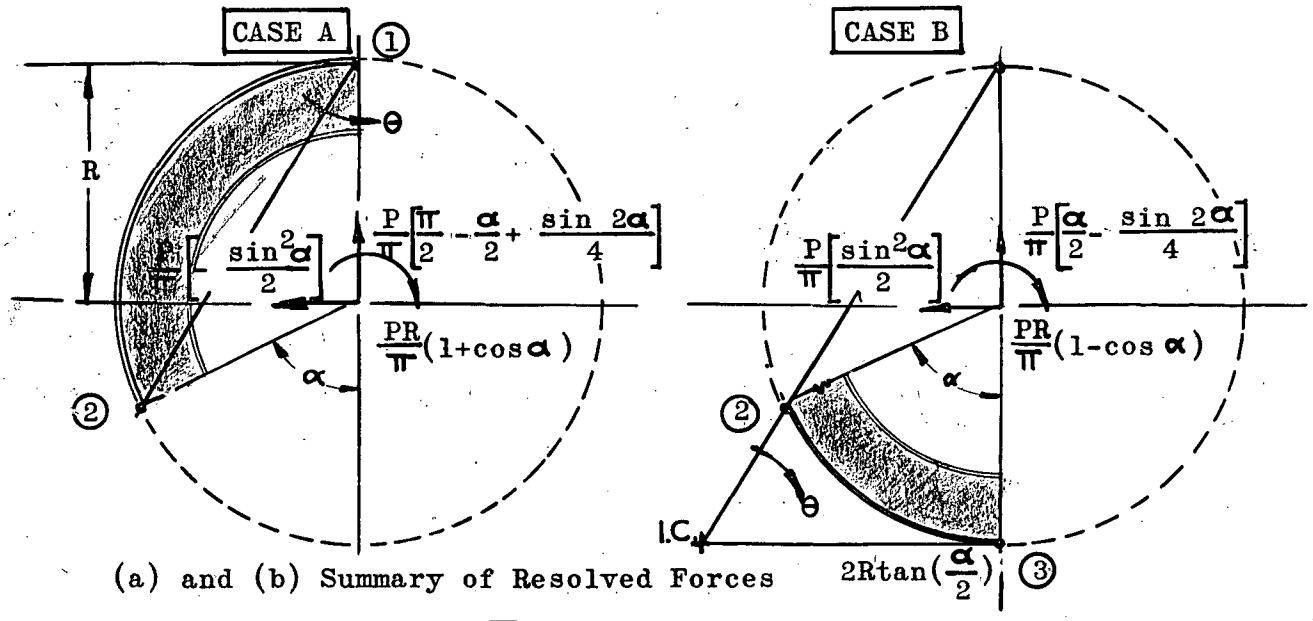

(a) and (b) Summary of Resolved Forces

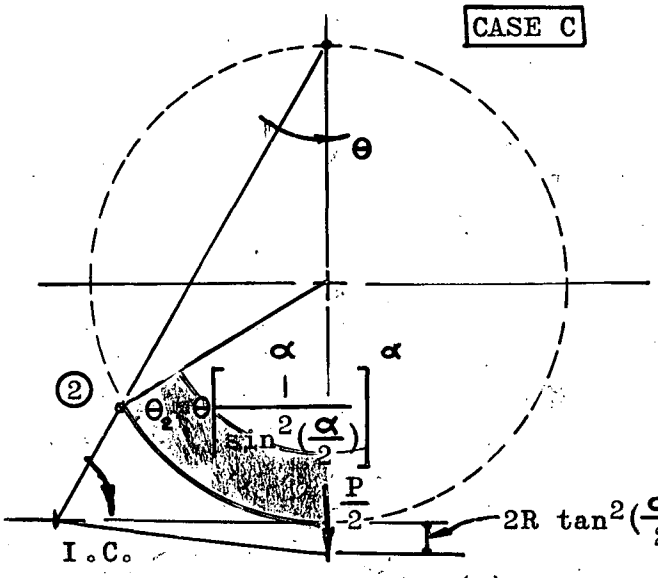

$$W_e = \frac{P}{2}\ 2R\tan^2\left(\frac{\alpha}{2}\right)\left[\frac{1}{\tan^2\left(\frac{\alpha}{2}\right)}\right] \qquad \text{.....(2.0.23)}$$

FIGURE 2.0.11 (c) Computation of External Work Done by the Radial Load P

The last step of the procedure is equating internal to external work.

The internal work is then evaluated by an elementary summation of the internal virtual rotations at each hinge.

Note: The internal work done by the individual virtual rotations always adds, regardless of the direction of the rotations. Therefore, the sign of the work performed by the hinge rotations is automatically defined.

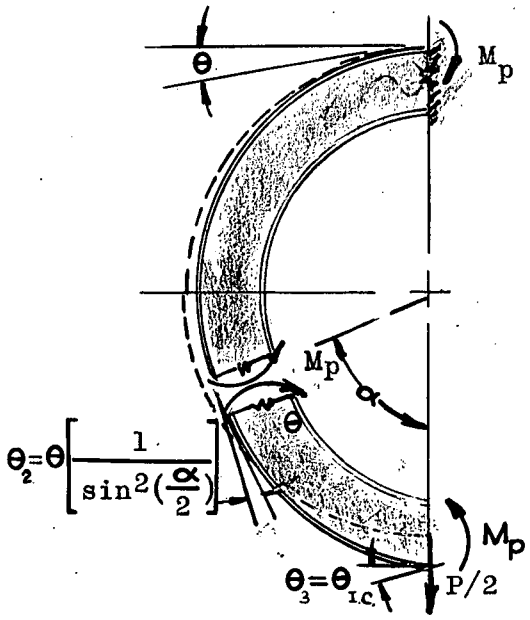

FIGURE 2.0.12 Internal Work

The internal work is simply (see Figure 2.0.12)

$$M_p\left\{1+\frac{1}{\sin^2(\frac{\alpha}{2})}+\frac{1}{\tan^2(\frac{\alpha}{2})}\right\}=\sum M_p\theta$$

$$M_p\left\{\frac{\sin^2(\frac{\alpha}{2})+1+\cos^2(\frac{\alpha}{2})}{\sin^2(\frac{\alpha}{2})}\right\}$$

$$M_p\left\{\frac{2}{\sin^2(\frac{\alpha}{2})}\right\} \quad \ldots\ldots\ldots(2.0.24)$$

The external work is derived by computing the work done by each individual component (i.e. X,Y,M) about its individual instantaneous center. The instantaneous center of vinculum ① - ② is point ① and the instantaneous center of bar ② - ③ is the point I.C. as defined.

Hence:

Case A

$$-\frac{P}{\pi}\left[-\frac{\sin^2\alpha}{2}\right]R\theta-\frac{PR}{\pi}\left[1+\cos\alpha\right]\theta \quad \ldots\ldots(2.0.25)$$

Case B

$$-\frac{P}{\pi}\left(\frac{\sin^2\alpha}{2}\right)R\,\theta\left(\frac{1}{\tan^2(\frac{\alpha}{2})}\right)-\frac{P}{\pi}\left[\left(\frac{\alpha}{2}-\frac{\sin 2\alpha}{4}\right)\right]\theta\left(\frac{1}{\tan^2(\frac{\alpha}{2})}\right)2R\tan\left(\frac{\alpha}{2}\right)$$

$$+\frac{PR}{\pi}\left[(1-\cos\alpha)\,\theta\left(\frac{1}{\tan^2(\frac{\alpha}{2})}\right)\right] \quad \ldots\ldots\ldots\ldots\ldots\ldots(2.0.26)$$

Case C

$$\frac{P}{2}\left[\left(2R\tan\left(\frac{\alpha}{2}\right)\right)\theta\left(\frac{1}{\tan^2(\frac{\alpha}{2})}\right)\right] \quad \ldots\ldots\ldots\ldots\ldots(2.0.27)$$

Summing the external work and equating it to the internal work of equation 2.0.24, $M_p\theta\left[\frac{2}{\sin^2(\frac{\alpha}{2})}\right]=$

$$\frac{PR}{\pi}\left\{\frac{\sin^2\alpha}{2}-1-\cos\alpha-\frac{\sin^2\alpha}{2\tan^2(\frac{\alpha}{2})}-(\alpha-\frac{\sin 2\alpha}{2})\frac{1}{\tan(\frac{\alpha}{2})}+\left[\frac{1-\cos\alpha}{\tan^2(\frac{\alpha}{2})}\right]+\pi(\frac{1}{\tan(\frac{\alpha}{2})})\right\}\theta$$

.....(2.0.28)

Hence,

$$M_p\left[\frac{2}{\sin^2(\frac{\alpha}{2})}\right]=$$

$$\frac{PR}{\pi}\left\{\frac{\sin^2\alpha}{2}-1-\cos\alpha-2\cos^4(\frac{\alpha}{2})-\frac{\alpha}{\tan(\frac{\alpha}{2})}+\frac{\sin 2\alpha}{2\tan(\frac{\alpha}{2})}+2\pi\left[\frac{1}{\tan(\frac{\alpha}{2})}\right]+\frac{1-\cos\alpha}{\tan^2(\frac{\alpha}{2})}\right\}$$

Simplifying,

$$M_p\left[\frac{2}{\sin^2(\frac{\alpha}{2})}\right]=$$

$$\frac{PR}{\pi}\left\{\frac{\sin^2\alpha}{2}-(1+\cos\alpha)+\frac{1}{\tan(\frac{\alpha}{2})}(1-\cos\alpha)-\frac{\sin^2\alpha}{2}-\alpha-(\frac{\sin^2\alpha}{2})\tan(\frac{\alpha}{2})\right\}$$

$$\frac{M_p}{PR}=\frac{1}{2\pi}\left\{\sin^2(\frac{\alpha}{2})(\frac{\sin^2\alpha}{2}-1-\cos\alpha)+\pi\sin(\frac{\alpha}{2})\cos(\frac{\alpha}{2})\right.$$

$$\left.+\cos^2(\frac{\alpha}{2})(1-\cos\alpha-\frac{\sin^2\alpha}{2}-(\alpha-\frac{\sin^2\alpha}{2})\tan(\frac{\alpha}{2}))\right\}$$

$$\frac{M_p}{PR}=\frac{1}{2\pi}\left\{-\frac{\sin^2(\frac{\alpha}{2})}{2}(\cos^2\alpha+2\cos\alpha+1)+\frac{\pi\sin\alpha}{2}+\cos^2(\frac{\alpha}{2})(1-\cos\alpha)\right.$$

$$\left.-\cos^2(\frac{\alpha}{2})\frac{\sin^2\alpha}{2}-\cos^2(\frac{\alpha}{2})\tan(\frac{\alpha}{2})(\alpha-\frac{\sin 2\alpha}{2})\right\}$$

Expanding $\cos^2(\frac{\alpha}{2})\tan(\frac{\alpha}{2})\,\alpha-\frac{\sin 2\alpha}{2}=\frac{1}{2}(\sin\alpha)(\alpha-\frac{\sin 2\alpha}{2})$

$$\frac{M_p}{PR}=\frac{1}{2\pi}\left\{\frac{\sin\alpha}{2}\left[\pi-\alpha+\frac{\sin 2\alpha}{2}\right]-\frac{\sin^2(\frac{\alpha}{2})}{2}(1+\cos\alpha)^2+\cos^2(\frac{\alpha}{2})(1-\cos\alpha-\frac{\sin^2\alpha}{2})\right\}$$

$$\frac{M_p}{PR}=\frac{1}{2\pi}\left\{\frac{\sin\alpha}{2}(\pi-\alpha+\frac{\sin 2\alpha}{2})-\frac{\sin^2(\frac{\alpha}{2})}{2}(1+\cos\alpha)^2+\frac{\cos^2(\frac{\alpha}{2})}{2}(1-\cos\alpha)^2\right\}$$

$$\frac{M_p}{PR} = \frac{1}{4\pi}\left\{\sin\alpha(\pi-\alpha+\sin\alpha\cos\alpha) - \sin^2\left(\frac{\alpha}{2}\right)\left(1+\cos\alpha\right)^2 + \cos^2\left(\frac{\alpha}{2}\right)\left(1-\cos\alpha\right)^2\right\}$$

$$= \frac{1}{4\pi}\left\{\sin\alpha\,(\pi-\alpha+\sin\alpha\cos\alpha) + \cos\alpha - 2\cos\alpha + \cos^3\alpha\right\}$$

$$= \frac{1}{4\pi}\left\{\sin\alpha\,(\pi-\alpha) + \cos\alpha\sin^2\alpha - \cos\alpha + \cos\alpha\cos^2\alpha\right\}$$

$$= \frac{1}{4\pi}\left\{\sin\alpha\,(\pi-\alpha) + \cos\alpha(\sin^2\alpha + \cos^2\alpha) - \cos\alpha\right\}$$

$$\frac{M_p}{PR} = \underline{\underline{\frac{1}{4\pi}\left\{\sin\alpha\,(\pi-\alpha)\right\}}} \qquad \ldots\ldots\ldots\ldots\ldots\ldots\ldots\ldots\ldots\ldots (2.0.29)$$

Thus, the dimension less moment coefficient $\frac{M_p}{PR}$ reduces to the simple expression of equation 2.0.29. The only unknown in the expression is the angle α. In order to obtain the appropriate angle α which yields the maximum value of M_p, the function $\frac{1}{4\pi}\left\{\sin\alpha\,(\pi-\alpha)\right\}$ must be maximized with respect to α. This result is acheived by differentiating the function M_p with respect to α and setting the end product equal to 0. Since the shear is essentially the first derivative of the moment, this performance is equivalent to the determination of the location of zero shear.

$$\frac{d\,M_p}{d\,\alpha} = \frac{1}{4\pi}\left[\frac{d}{d\alpha}\left(\sin\alpha\right)\left(\pi-\alpha\right)\right]$$

$$= \frac{1}{4\pi}\left[\pi\cos\alpha - \alpha\cos\alpha - \sin\alpha\right] = 0$$

Thus transposing,

$$(\pi-\alpha)\,(\cos\alpha) = \sin\alpha.$$

$$\mathrm{Tan}\,\alpha = (\pi-\alpha) \qquad \ldots\ldots\ldots\ldots (2.0.30)$$

The exact angle α which fulfills this expression is found by a process known as Newton's iteration method. This method is very simply outlined as follows.

If a function is expressed by

$$F = f(x) = 0 \qquad \ldots\ldots\ldots\ldots\ldots\ldots\ldots\ldots (2.0.31)$$

To obtain successive approximations to roots of algebraic and transcendental equations, a first approximation to the roots of equation 2.0.31 must be obtained. Then denoting the first approximation of the roots by x_o, and h by the difference between the first approximation and its next approximation, expand $f(x_o+h)$ in a taylor's series....

$$f(x_o+h) = f(x_o) + h f'(x_o) + \frac{h^2}{2} f''(x_o) + \ldots\ldots$$

Neglecting higher powers of h

$$h_o = -\frac{f(x_o)}{f'(x_o)} \qquad \ldots\ldots\ldots\ldots\ldots\ldots\ldots\ldots (2.0.32)$$

Applying this method to equation 2.0.30 and noting the graphical representation of the two functions tan α and $(\pi - \alpha)$ from Figure 2.0.13, it appears that the value $\alpha = 1.00$ rad. is a close first approximation.

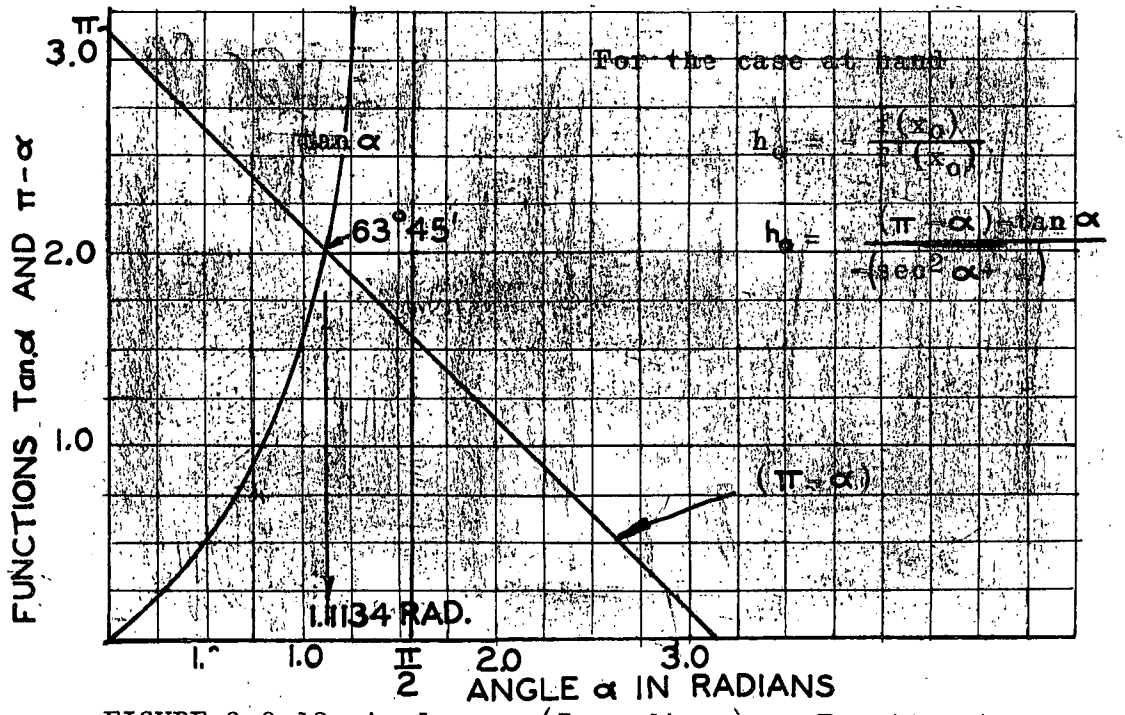

FIGURE 2.0.13 Angle α = (In radians) vs. Function tan α and $\pi - \alpha$

$$h_o = -\frac{(3.141596-1) - \tan 1.00}{\text{Tan}^2\ 1.00 + 2}$$

$$= \frac{2.1416 - 1.5577}{(1.5577)^2 + 2} = \frac{.5839}{4.4261}$$

$$h_o = .132$$

As a next approximation try $\alpha = 1 + .132 = 1.132$ rad.

Proceeding,

$$h_o = -\frac{(3.141596 - 1.132) - \tan 1.132}{\text{Tan}^2\ 1.132 + 2} = \frac{2.0096 - 2.1315}{(2.1315)^2 + 2}$$

$$h_o = -.0186$$

$\alpha = 1.132 - .0186 = 1.1134$ radions or $63^o\ 45'$

Use $\alpha = 63^o\ 45'$ .....(2.0.33)

Substituting this value of α into the expression for moment

$$M_p = \frac{PR}{4\pi}\left[(\sin 63^o\ 45')\ (\pi - 1.1134)\right]$$

$$\underline{M_p = .14480\ PR} \quad .....(2.0.34)$$

2.0.4 Plasticity Check for Ring I

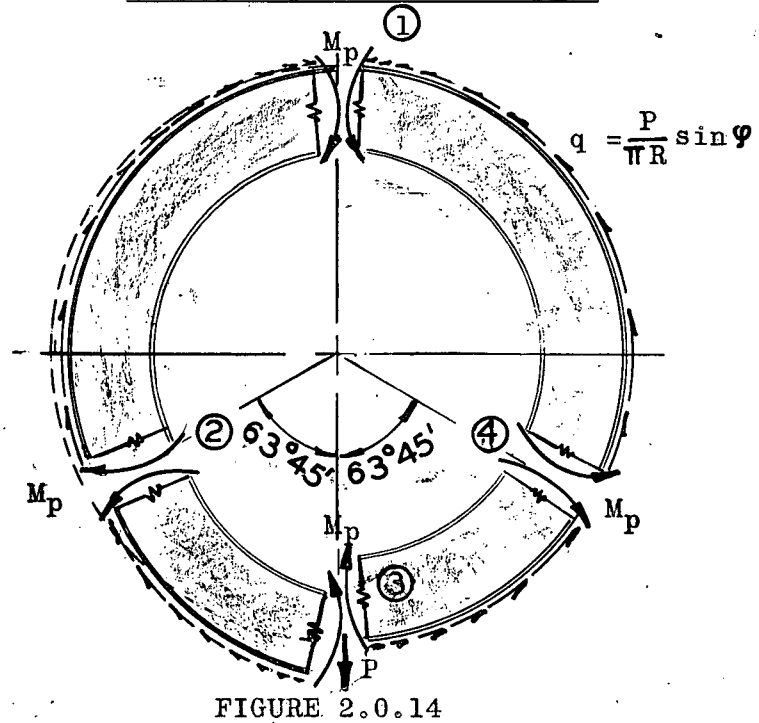

FIGURE 2.0.14
Collapse Mehcanism-Plasticity Check.

The resulting failure configuration is as shown in Figure 2.0.14. The next step is to determine the various values of the internal forces all of the way around the ring.

Note: The direction of the maximum moments M_p is always such as to restore the deformed structure to its original shape or position.

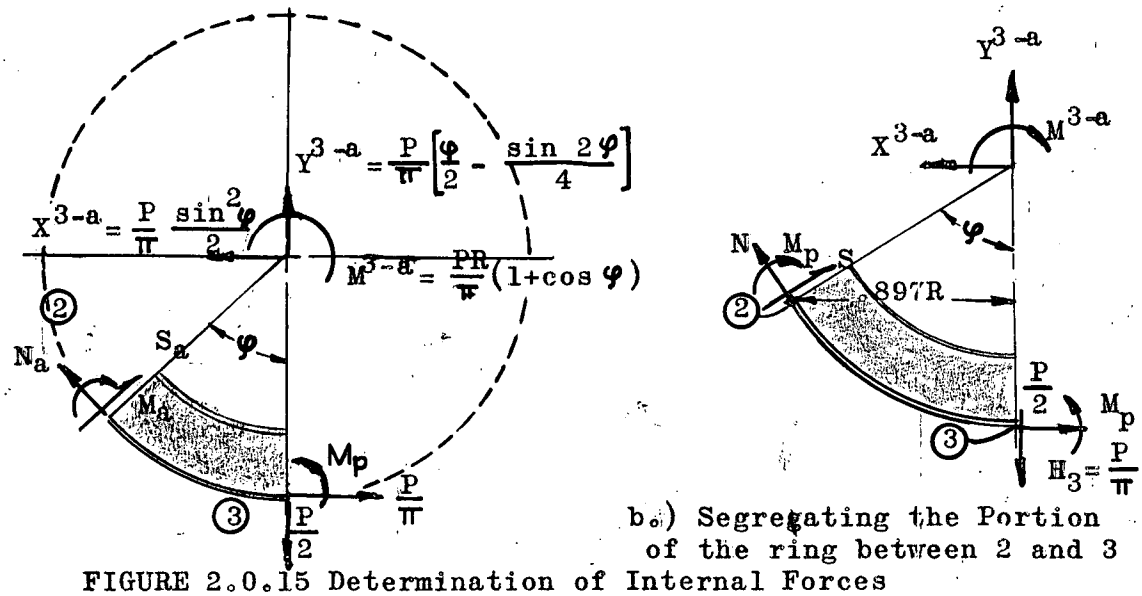

b.) Segregating the Portion of the ring between 2 and 3

FIGURE 2.0.15 Determination of Internal Forces

Considering the geometry of the ring above, the expressions for moment, shear, and axial load are

$$M_a = M_p - \frac{PR}{\pi}\left[\frac{\pi}{2}\sin\varphi - (1-\cos\varphi) + (1-\cos\varphi) - \left(\frac{\varphi}{2} - \frac{\sin 2\varphi}{4}\right)\sin\varphi - \frac{\sin^2\varphi}{2}\cos\varphi\right]$$

$$M_a = .1448\ PR - \frac{PR}{\pi}\left[\sin\varphi\left(\frac{\pi}{2} - \frac{\varphi}{2}\right)\right] \quad \text{.....(2.0.35)}$$

$$N_a = \left[\frac{P}{\pi} - \frac{P}{\pi}\frac{\sin^2\varphi}{2}\right]\cos\varphi + \frac{P}{2} - \frac{P}{\pi}\left[\left(\frac{\varphi}{2} - \frac{\sin 2\varphi}{4}\right)\right]\sin\varphi$$

$$N_a = \frac{P}{\pi}\left[\cos\varphi + \sin\varphi\left(\frac{\pi}{2} - \frac{\varphi}{2}\right)\right] \quad \text{.....(2.0.36)}$$

$$S_a = \left[\frac{P}{2} - \frac{P}{\pi}\left(\frac{\varphi}{2} - \frac{\sin 2\varphi}{4}\right)\right]\cos\varphi - \left[\frac{P}{\pi} - \frac{P}{\pi}\frac{\sin^2\varphi}{2}\right]\sin\varphi$$

$$S_a = \frac{P}{\pi}\left[-\frac{\sin\varphi}{2} + \cos\varphi\left(\frac{\pi}{2} - \frac{\varphi}{2}\right)\right] \quad \text{.....(2.0.37)}$$

Segregating the portion of the structure between hinges ① and ②, results in the same equations as between hinges ② and ③. Therefore, in setting up the expressions for moment, shear and axial load in tabular form, only one expression for each is necessary all the way around the ring.

RADIAL FORCE P ON A TANGNTIALLY SUPPORTED CIRCULAR RING

TABLE 2.0.1

Comparison of Plastic to Elastic Moment, Shear and Axial Load Coefficients						
Angle φ From Vertical	Plastic Moment Coeff.	Elastic* Moment Coeff.	Plastic Shear Coeff.	* Elastic Shear Coeff.	Plastic Axial Load Coeff.	Elastic* Axial Load Coeff.
0	-.144800	-.2387	.500000	.5000	.318310	.239
5	-.102431		.470386		.359466	
10	-.062799		.437407		.395476	
15	-.026174	-.1174	.401489	.422	.426091	.350
20	+.007209		.363205		.451122	
25	+.037161		.322955		.470449	
30	+.063532	+.0197	.281267	.321	.483999	.415
35	+.086244		.238655		.491788	
40	+.105172		.195597		.493810	
45	+.120366	+.0497	.152626	.209	.490246	.434
50	+.131825		.110199		.481231	
55	+.139627		.068947		.467003	
60	+.143875	+.0897	.028831	.097	.447830	.408
63 45'	+.144814		.0		.430399	
65	+.144716		-.009240		.424040	
70	+.142324		-.045053		.395993	
75	+.136930	+.1020	-.078243	0	.364115	.343
80	+.128750		-.108500		.328832	
85	+.118084		-.135548		.290628	
90	+.105198	+.0908	-.159155	.0796	.249998	.250

*For elastic coefficients see reference 4, Graph 2

RADIAL FORCE P ON A TANGENTIALLY SUPPORTED CIRCULAR RING

TABLE 2.0.2

Comparison of Plastic to Elastic Moment, Shear and Axial Load Coefficients						
Angle φ From Vertical	Plastic Moment Coeff.	Elastic Moment Coeff.	Plastic Shear Coeff.	Elastic Shear Coeff.	Plastic Axial Load Coeff.	Elastic Axial Load Coeff.
95	.090412		-.179128		.207468	
100	.074046		-.195325		.163572	
105	.056589	.0627	-.207695	-.1310	.119004	.1395
110	.037916		-.216061		.073848	
115	.018840		-.220550		.029306	
120	-.000465	-.0250	-.221167	.1523	-.014821	.0250
125	-.019652		-.218002		-.057428	
130	-.038406		-.211195		-.098213	
135	-.056411	-.0145	-.200929	-.1445	-.136691	-.0803
140	-.073270		-.187419		-.172308	
145	-.089035		-.170928		-.204979	
150	-.103135	-.0486	-.151744	-.1087	-.234001	-.160
155	-.115633		-.130200		-.259321	
160	-.125799		-.106638		-.280112	
165	-.134016	-.0715	-.081436	-.0608	-.296681	-.220
170	-.139977		-.054993		-.308652	
175	-.143589		-.027708		-.315887	
180	-.144800	-.0796	0	0	-.318310	-.239

*For elastic coefficients see reference 4, Graph 2

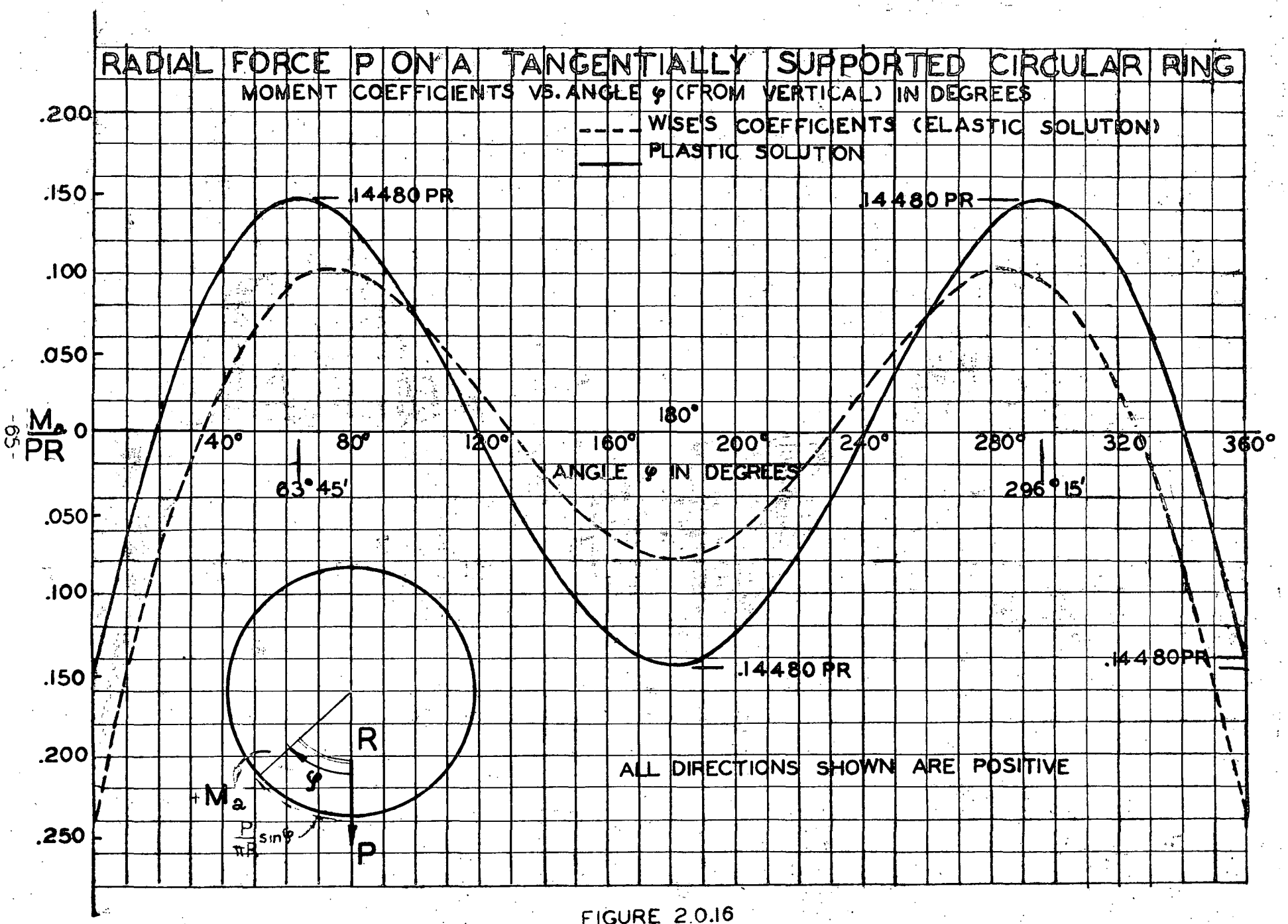

FIGURE 2.0.16
MOMENT CURVES

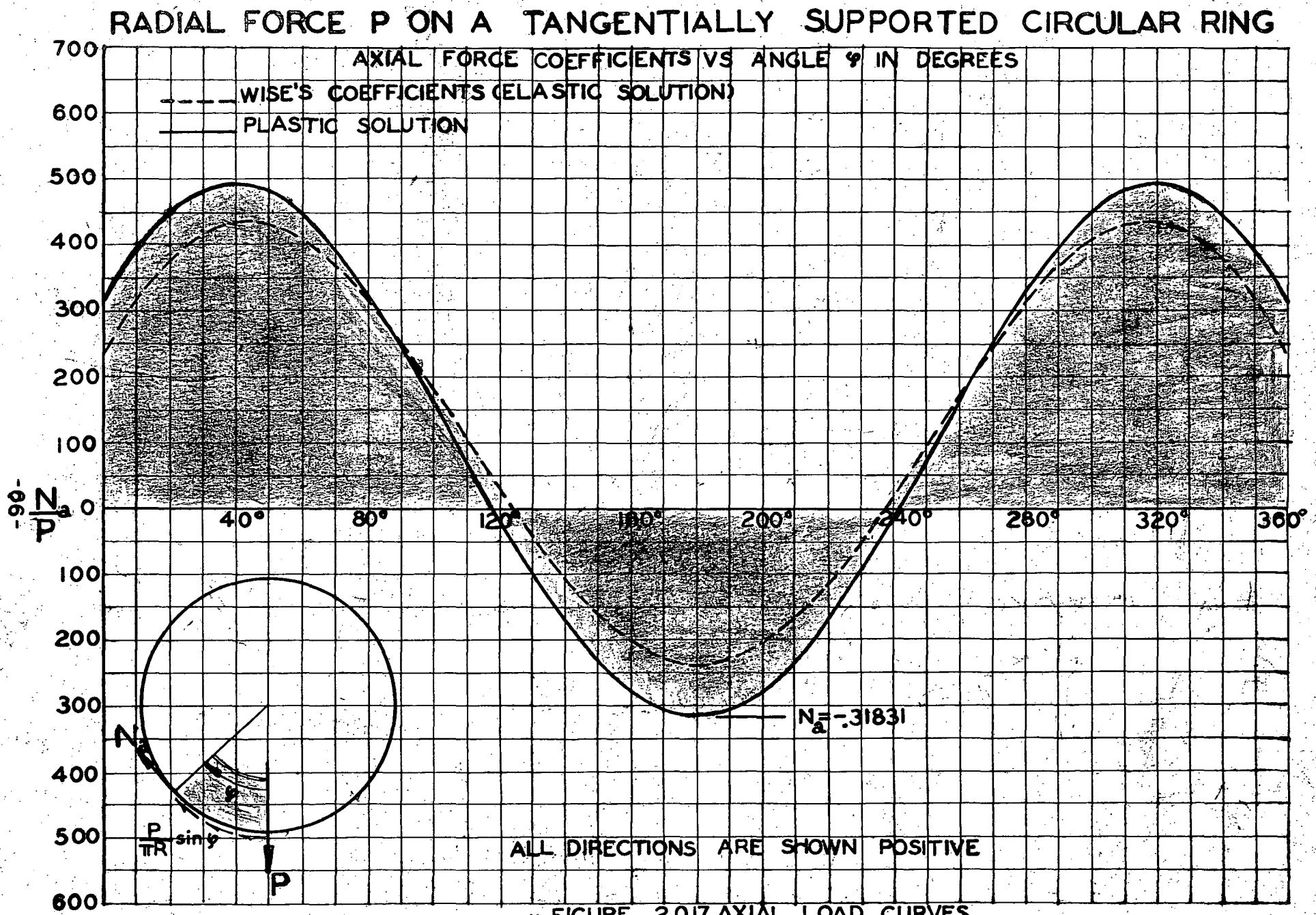

FIGURE 2.0.17 AXIAL LOAD CURVES

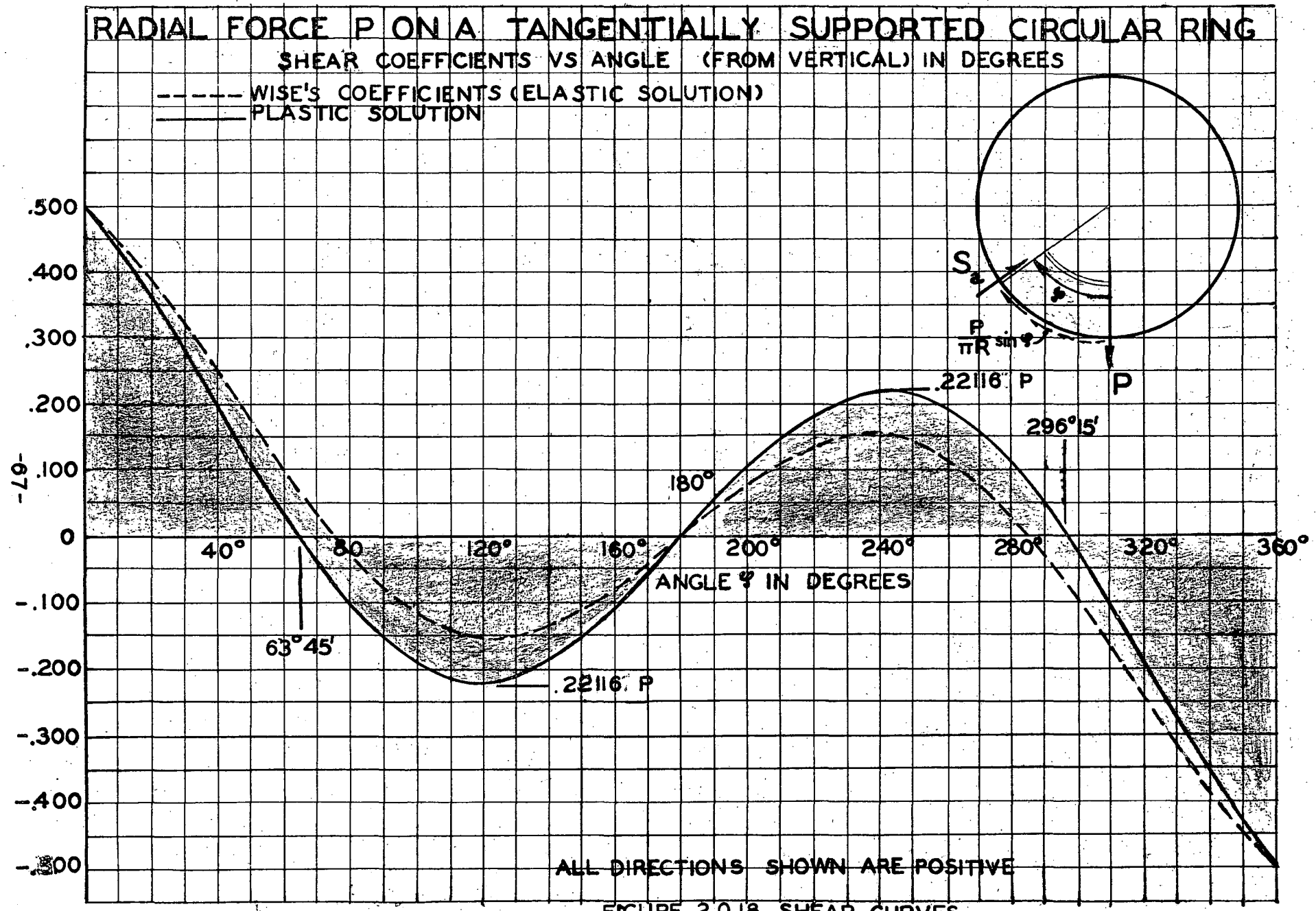

FIGURE 2.0.18 SHEAR CURVES

Values of φ for every 5^{o} were substituted into the expressions, and tables 2.0.1 and 2.0.2 were developed to compare the elastic solution with the plastic solution. The plot of the functions of φ for moment, axial load, and shear are presented on pages 65, 66, 67 respectively. The maximum and minimums are noted on all graphs in order to be able to visualize the difference between the two solutions. It may be argued that even though the moment curves emphasize the fact that the moment is distributed much more evenly for the plastic solution, the combination of axial load and moment may suggest that nothing is gained by analyzing plastically. This is a very important consideration, since it is the combination of moment and axial load which promotes either the endorsement or the undoing of plastic analysis. A means of including the effect of axial load on the ultimate bending capacity of the beam will be discussed in a later portion of this thesis.

2.0.5 Conclusions and Discussion of Ring I

It may be of interest to conclude the discussion of this particular ring loading by observing certain features of this category of loading. One of the more significant observations, which is immediately suggested from Figure 2.16, is the influence of concentrated load upon the location of maximum moment. It will be noted that the point of maximum moment, at about 70^{o} from the vertical for the elastic solution, appears to shift toward the location of the concentrated load above the elastic limit, (yielding of hinge ③). The cause of this consequence is not quite so evident. However, it will be further noted that the axial load also peaks about 50^{o} to the vertical, and also

shifts toward the concentrated load beyond the yielding of hinge ③. What may be concluded from these two observations is that the hinge ③ rotates permitting redistribution of moment. This action is manifested by a distinct increase of axial load with the maximum value shifting toward the point of application of the load.

Another suggested point of interest is the apparent proportional increase of all three internal forces. Not only do the moment and axial load diagrams indicate a pronounced increase, but the shear plot also suggests a proportional rise in magnitude. However, even though all three functions show a marked increase in amplitude the basic shape of each curve shows no radical digression from the original, but remains very nearly the same.

Another quandary that may mislead the reader at first is the seemingly reduced magnitude of moment (at the concentrated load) between the elastic and the plastic solution. Further comprehension of the above quandary may be attained by reviewing the cycle of loading from the elastic range up to the collapse load. As the circular frame is loaded, the ring first sustains the load in a manner whereby the maximum moment occurs at the point of the applied load (see Figure 2.0.19). Throughout the elastic range the shape of the moment diagram remains the same, proportional to the magnitude of the load. At a certain load, however, the structure yields at hinge ③ under the applied load. At this point the structure may be designed by the elastic method. Beyond this point the elasticity condition is violated and

consequently the moment curve changes shape. When the first hinge (at ③) forms, the structure has not reached its ultimate carrying capacity, but actually is capable of sustaining much greater loads. Further increase in applied radial load causes the portion of the ring between points ② and ④ to assume sort of a "catenary effect" whereby the loads are sustained partially by hoop tension (see Figure 2.0.20(b)). This could be one reason why the internal axial forces increases proportionally between those two points. As the load is progressively increased, the moment at points ② and

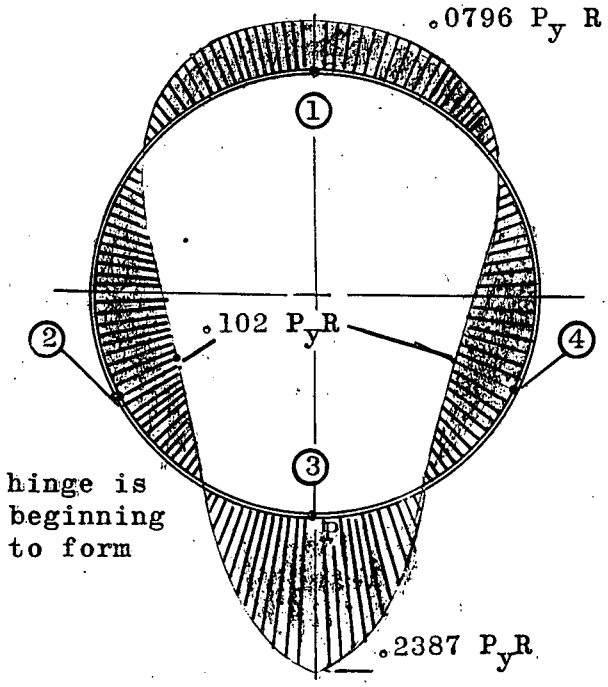

FIGURE 2.0.19 Elastic Configuration

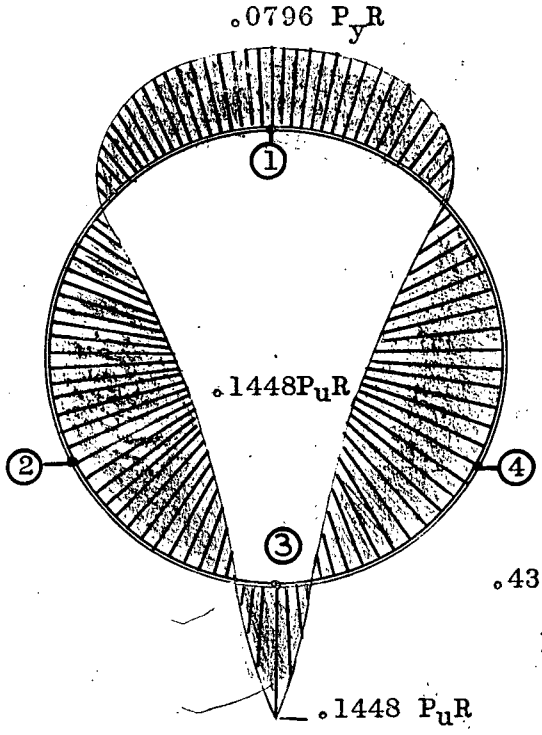

FIGURE 2.0.20
Elastic-Plastic Configuration

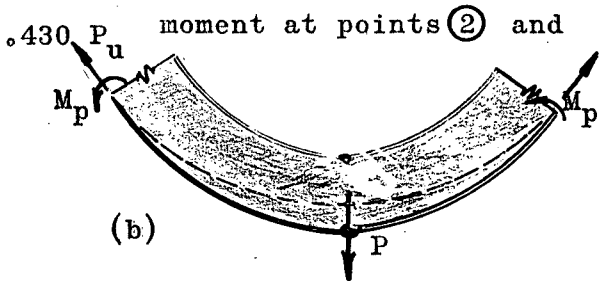

④ come closer and closer to the computed M_p moment. At a certain value of the applied load the structure strains to yield at points ② and ④ simultaneously. The ring, however, can still carry addition load because the structure above hinges ② and ④ is still strained within its elasticity capacity (see Figure 2.0.21). Thus, this elastic portion remains comparatively rigid and is still capable of sustaining further load. The lower portion of the frame merely acts as a transmitter of load. If the load is again increased until the structure yields at point ①, a kinematic mechanism is formed (Figure 2.0.22) and the structure collapses because further application of load results in markedly increased rotations and deflections. This, then, is truly the ultimate load of the structure. The magnitude of the ultimate load P_{cr} is much larger than the load which first caused yielding at point ③. Thus,

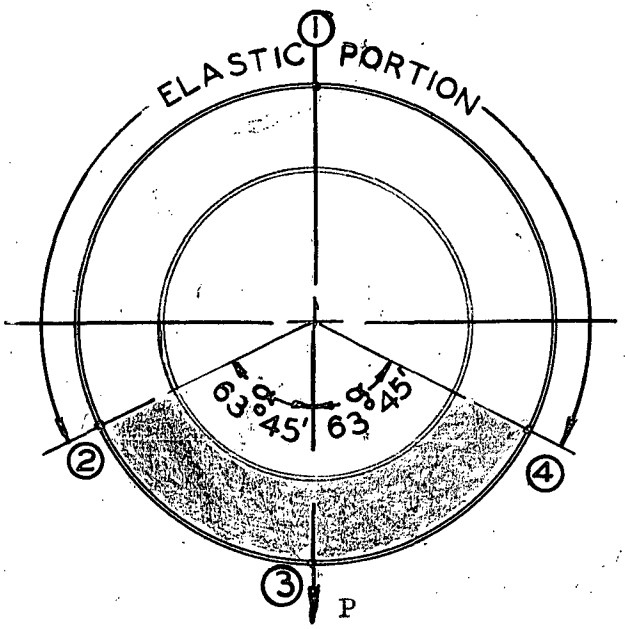

FIGURE 2.0.21 Elastic-Plastic Configuration

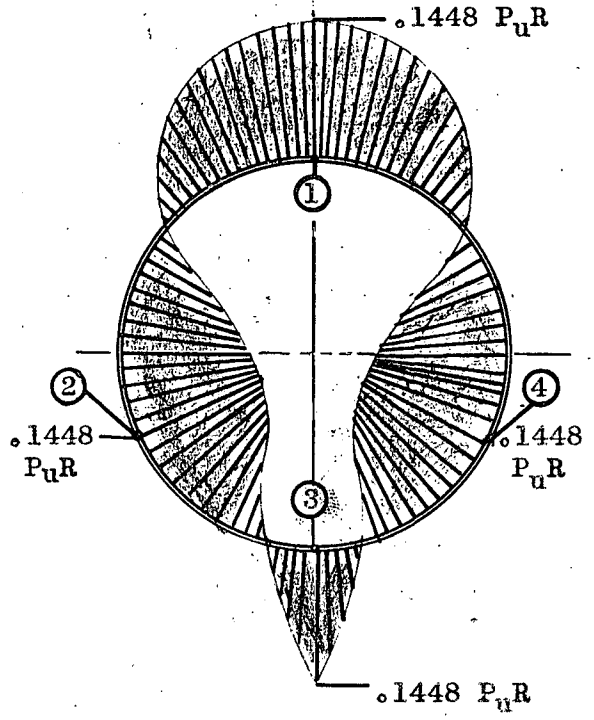

FIGURE 2.0.22 Collapse Configuration

the moment at point ③ is no smaller for the plastic solution than it is for the elastic solution. If one were required to design the structure, however, the plastic solution would require the smaller moment value.

The reader may be confused because the two moment diagrams are plotted on the same axis, but if it is kept in mind that the value of P is actually a variable instead of a constant (as assumed for either an elastic or a plastic solution), the picture is much clearer.

As was asserted previously, each particular loading was chosen to emphasize a special phase of ring analysis. The radial loading was chosen because of its simplicity and its generality. The elastic solution was readily available for purposes of comparison, and the effect of concentrated load on the moment, shear, and axial load variables was of interest.

2.1.0 Loading Condition-Ring II-Tangential Force P on a Tangentially Supported Circular Ring

Another simple loading, which is brought to mind, is the loading configuration of a circular ring laden by a single tangential load.

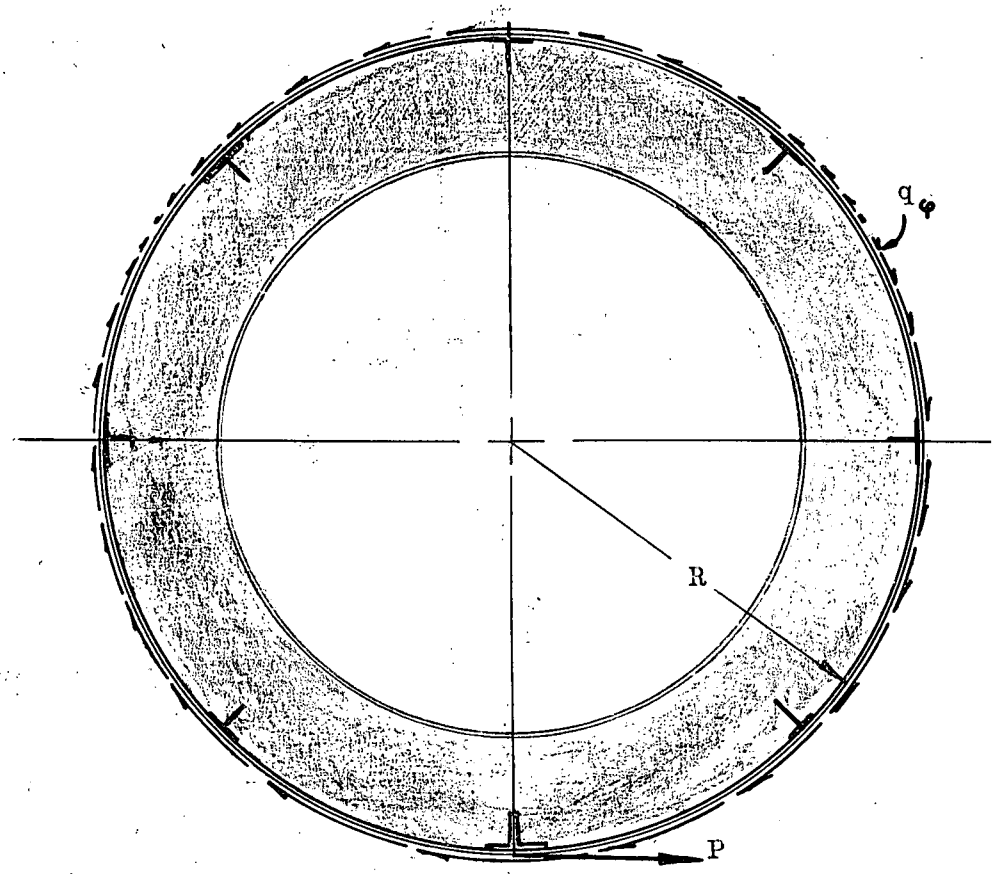

FIGURE 2.1.0 External Loading Condition

Recalling from the previous example, the first step in the procedure of solution is to determine the relative positions of the hinges which characterize the formation of a kinematic mechanism for this loading. Suppose, for simplicity that the ring loading is divided into two separate loadings. An equivalent loading would be composed of a shear load (Figure 2.1.2) and a twist (Figure 2.1.3)

with their respective equilibrating shears. Referring to Figure 2.0.6, it was seen that the hinge pattern was symmetrical about the vertical center line. As it turns out for this case the hinge pattern will again be symmetrical about this axis. It can be concluded that there is no internal moment at the point of tangential load, since the internal axial load and shear are a maximum at this point. It will also be deduced that another point of zero moment is directly opposite (180^{o} away) the external tangential loading because of symmetrical ring geometry. Therefore, it is reasonable to conclude that the other two points of zero moment are located symmetrically about the vertical axis. Conversely, just as the points of zero moment were established, so also may the points of maximum moments be determined. As a result, the hinge pattern is deduced to be arranged in the symmetrical manner delineated in Figure 2.1.1.

In order to simplify the task of deriving the virtual work expressions, the frame loading may be imagined to be composed of three cases which shall later be added together.

2.1.1 Breakup of Tangential Loading

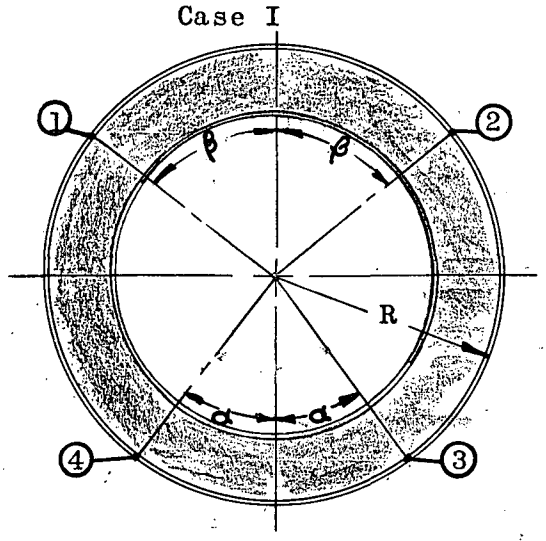

Case I (Figure 2.1.1) is the geometry of the ring for the applied load. Case II (Figure 2.1.2) represents the shear flow due to just the horizontal shear, and Case III

FIGURE 2.1.1-Hinge Pattern for Tangential Loading

(Figure 2.1.3) represents the shear flow due to the twist.

Case II

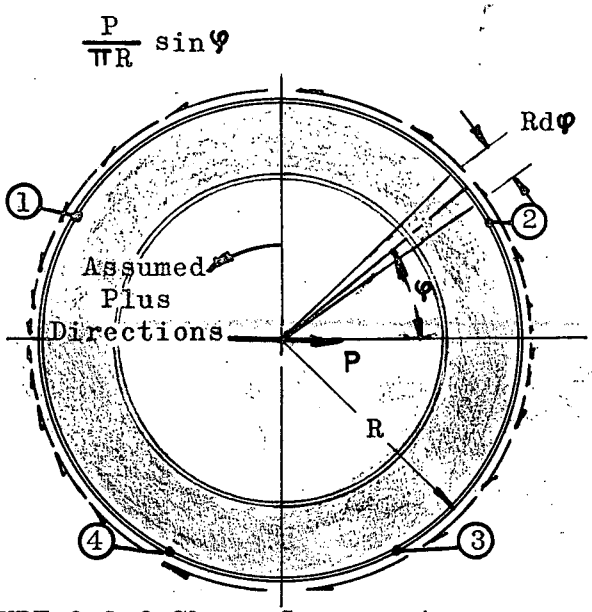

FIGURE 2.1.2 Shear Component

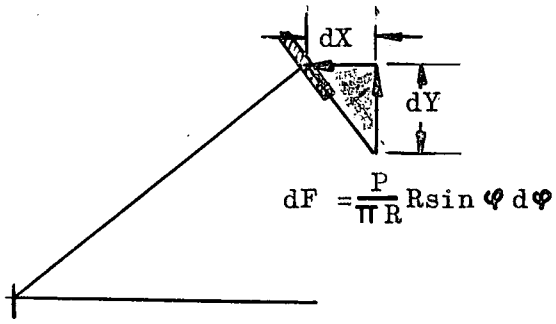

$$dM = \frac{PR}{\pi} \sin\varphi\, d\varphi \quad \ldots.(2.1.1)$$

$$dX = \frac{P}{\pi} \sin^2\varphi\, d\varphi \quad \ldots.(2.1.2)$$

$$dY = \frac{P}{\pi} \sin\varphi\cos\varphi\, d\varphi \ldots(2.1.3)$$

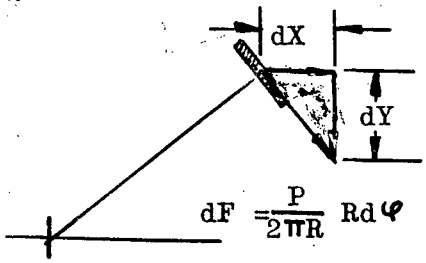

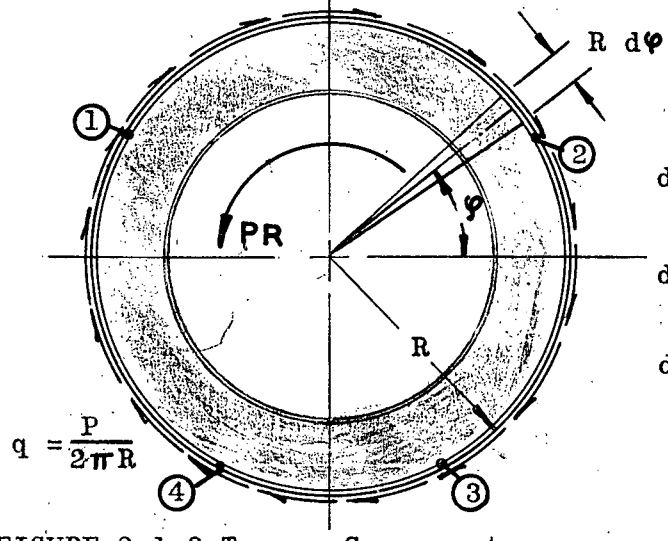

FIGURE 2.1.3 Torque Component

$$dM = -\frac{PR}{2\pi} d\varphi$$

$$dX = -\frac{P}{2\pi} \sin\varphi\, d\varphi$$

$$dY = -\frac{P}{2\pi} \cos\varphi\, d\varphi$$

For Assumed Plus Directions

Just as before, the next logical step is to determine the point or section of the ring which is to be fixed in space. Since it was emphasized on page 51 that even though the analyst may not make a prudent choice of ring fixity at first, complicated geometry almost compels him to make another choice. Perhaps this

example can shed some light on what constitutes a wise selection. Suppose that the analyst elects to fix the ring section between ① and ②. Then the geometrical relations of this collapse mechanism is shown in Figure 2.1.4. It is evident that, if the frame is given a virtual angle θ about the instantaneous center, the virtual displacements and relations between the angular rotations are trigonometric functions of angles α and β and their half angles. By the time the external work is equated to the internal work, the expressions become so complicated and confused that the analyst is completely discouraged from attempting the final general solution.

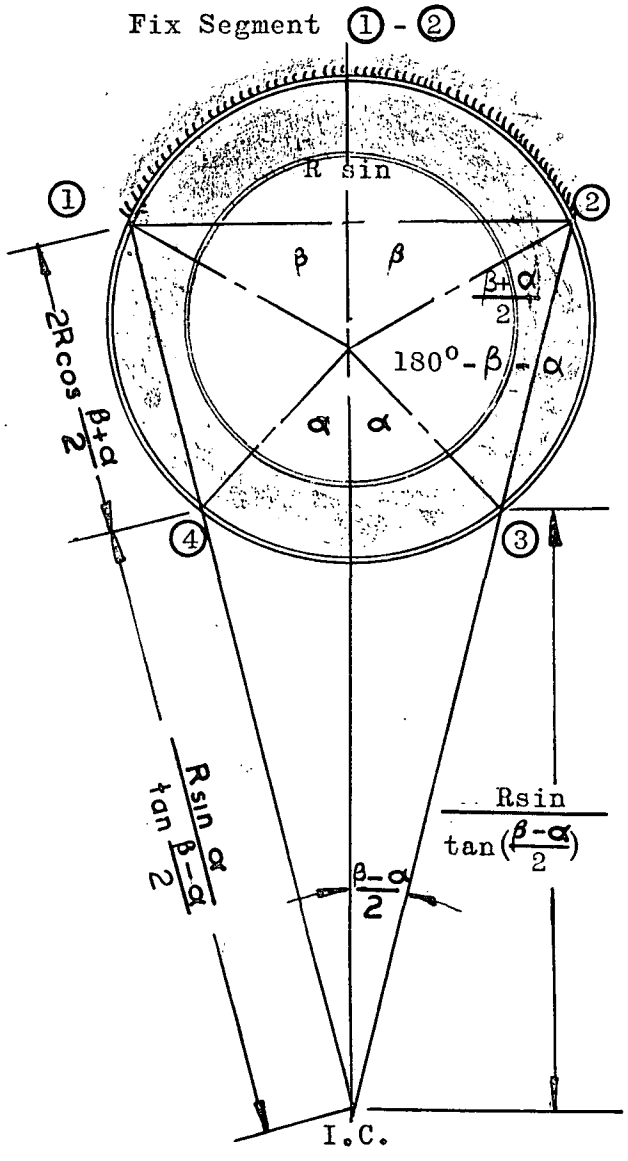

FIGURE 2.1.4
Failure Configuration for

Accordingly, the next logical step to take is to fix some other portion of the ring, and determine the geometry based on this choice. Careful study of the hinge pattern confirms the fact that, if either the portion between hinges ① and ④ or ② and ③ is fixed in space, both mechanisms yield the same result. The ad-

vantageous conclusion of this option is that the top portion (between hinges ① and ②) must rotate about point ① (or ②) and its instantaneous radius of rotation is through points ①-②. Verily, the same line of reasoning implies that the lower portion of the ring (between hinges ③ and ④) must rotate about ④ (or ③). It is obvious that the axis of rotation do not intersect. Therefore, the instantaneous center of rotation must be located at infinity. If this is the case this configuration is exactly identical to the action of a sidesway mechanism for an unequal legged rectangular rigid frame (see Figure 2.1.5). The relationships of the angles relative to each other are found by giving link ③ - ④ a virtual rotation θ.

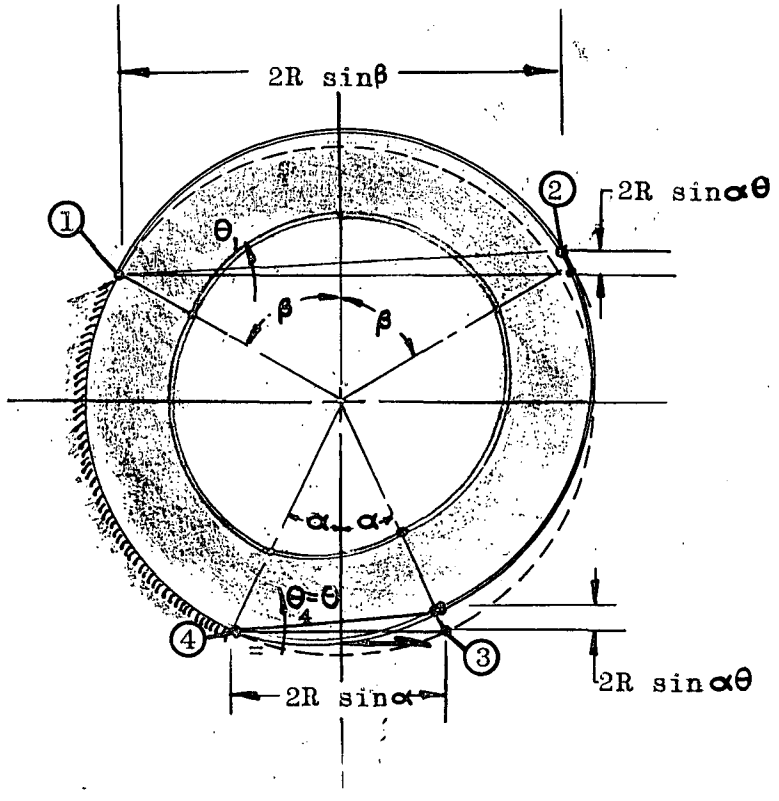

FIGURE 2.1.5 Failure configuration

Then,

$$\theta_1 = \frac{2R\,\theta \sin\alpha}{2R\sin\beta} = \frac{\sin\alpha}{\sin\beta}\theta \qquad \ldots\ldots(2.1.4)$$

$$\theta_2 = \theta_1 = \frac{\sin\alpha}{\sin\beta}\theta \qquad \ldots(2.1.5)$$

$$\theta_3 = \theta \qquad \ldots\ldots(2.1.6)$$

$$\theta_4 = \theta \qquad \ldots\ldots(2.1.7)$$

θ_1 is concluded from from the observation that when the frame sways, the vertical deformation must be equal for both the top and bottom portion of the ring. Hence, they both scribe an arc length of $(2R \sin\alpha)\theta$. The part of the structure between

② and ③ just translates vertically (it does not rotate) and, thus, only the vertical component of the shear flow (Y^{2-3}) does any work.

2.1.2 Internal and External Work

From Figure 2.1.5, the internal work may be derived by summing the product of the resisting plastic moments and rotations at each of these hinges.

$$M_p \left[\theta_1 + \theta_2 + \theta_3 + \theta_4\right] = M_p \theta \left[1+1+\frac{\sin\alpha}{\sin\beta} + \frac{\sin\alpha}{\sin\beta}\right]$$

$$W_{int} = 2M_p \theta \left[1+ \frac{\sin\alpha}{\sin\beta}\right] \quad \text{.....(2.1.8)}$$

From Case II, Figure 2.1.2

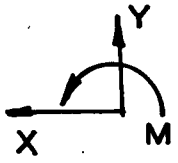

$$X = \int R\sin\varphi \; d\varphi = \frac{P}{\pi R}\int R\sin^2\varphi \; d\varphi$$

$$X = \frac{P}{\pi}\int \sin^2\varphi \; d\varphi$$

$$Y = \int qR\cos\varphi \; d = \frac{P}{\pi R}\int R\sin\varphi\cos\varphi \; d\varphi = \frac{P}{\pi}\int \sin\varphi\cos\varphi \; d\varphi$$

$$M = \int q\, R^2 d\varphi = \frac{P}{\pi R}\int R^2\sin\varphi \; d\varphi = \frac{PR}{\pi}\int \sin\varphi \; d\varphi$$

Integrating to determine the equivalent force system

$$X = \frac{P}{\pi}\int \sin^2\varphi d\varphi = \frac{P}{\pi}\left[\frac{\varphi}{2} - \frac{\sin 2\varphi}{4}\right]_{\text{lower limit}}^{\text{upper limit}} \quad \text{.....(2.1.9)}$$

$$Y = \frac{P}{\pi}\int \sin\varphi\cos\varphi \; d\varphi = \frac{P}{\pi}\left[\frac{\sin^2\varphi}{2}\right]_{\text{lower limit}}^{\text{upper limit}} \quad \text{.....(2.1.10)}$$

$$M = \frac{PR}{\pi}\int \sin\varphi \; d\varphi = \frac{PR}{\pi}\left[-\cos\varphi\right]_{\text{lower limit}}^{\text{upper limit}} \quad \text{.....(2.1.11)}$$

As before, rather than deal directly with the shear flow, it is broken up into three components shown above.

Commencing with Case II, between hinges ① and ②,

$$X_{II}^{1-2} = \frac{P}{\pi}\left[\frac{\varphi}{2} - \frac{\cos\varphi \sin\varphi}{2}\right]_{\frac{\pi}{2}-\beta}^{\frac{\pi}{2}+\beta}$$

$$= \frac{P}{\pi}\left[\frac{\pi}{4}+\frac{\beta}{2}-\frac{1}{2}\cos(\frac{\pi}{2}+\beta)\sin(\frac{\pi}{2}+\beta)-\frac{\pi}{4}+\frac{\beta}{2}+\frac{1}{2}\cos(\frac{\pi}{2}-\beta)\sin(\frac{\pi}{2}-\beta)\right]$$

$$X_{II}^{1-2} = \frac{P}{\pi}\left[\beta + \sin\beta\cos\beta\right]$$

$Y_{II}^{1-2} = 0$ (From observation)

$$M_{II}^{1-2} = \frac{PR}{\pi}\left[-\cos\varphi\right]_{\frac{\pi}{2}-\beta}^{\frac{\pi}{2}+\beta} = -\frac{PR}{\pi}\left[\cos(\frac{\pi}{2}+\beta)-\cos(\frac{\pi}{2}-\beta)\right] = \frac{2PR}{\pi}\sin\beta$$

Between hinges ② and ③,

$$X_{II}^{2-3} = \frac{P}{\pi}\left[\frac{\varphi}{2}-\frac{1}{2}\cos\varphi\sin\varphi\right]_{-(\frac{\pi}{2}-\alpha)}^{\frac{\pi}{2}-\beta}$$ This component does no work during the virtual displacement.

$$Y_{II}^{2-3} = \frac{P}{2\pi}\left[\frac{\sin^2\varphi}{2}\right]_{\alpha-\frac{\pi}{2}}^{\frac{\pi}{2}-\beta} = \frac{P}{2\pi}\left[\sin^2(\frac{\pi}{2}-\beta)-\sin^2(\alpha-\frac{\pi}{2})\right] = \frac{P}{2\pi}\left[\cos^2\beta-\cos^2\alpha\right]$$

$M_{II}^{2-3} = -\frac{PR}{\pi}\left[\cos\varphi\right]_{\alpha-\frac{\pi}{2}}^{\frac{\pi}{2}-\beta}$ There is no rotation of link ② - ③, hence this component does no work.

Between hinges ③ and ④,

$$X_{II}^{3-4} = \frac{P}{\pi}\left[\frac{\varphi}{2}-\frac{1}{2}\cos\varphi\sin\varphi\right]_{-(\frac{\pi}{2}+\alpha)}^{\alpha-\frac{\pi}{2}} = \frac{P}{\pi}\left[\alpha+\sin\alpha\cos\alpha\right]$$

$Y_{II}^{3-4} = 0$

$$M_{II}^{3-4} = \frac{PR}{\pi}\left[-\cos\varphi\right]_{-(\frac{\pi}{2}+\alpha)}^{\alpha-\frac{\pi}{2}} = -\frac{PR}{\pi}\left[\cos(\alpha-\frac{\pi}{2})-\cos(-\frac{\pi}{2}-\alpha)\right] = -\frac{2PR}{\pi}\sin\alpha$$

Considering Case III next, and resolving the shear flow into its components,

$$X_{III} = \int qR\sin\varphi\,d\varphi = \frac{P}{2\pi R}\int R\sin\varphi\,d\varphi = -\frac{P}{2\pi}\left[-\cos\varphi\right]_{\text{lower limit}}^{\text{upper limit}}$$

$$Y_{III} = \int qR\cos\varphi\,d\varphi = \frac{P}{2\pi R}\int R\cos\varphi\,d\varphi = -\frac{P}{2\pi}\left[\sin\varphi\right]_{\text{lower limit}}^{\text{upper limit}}$$

$$M_{III} = \int qR^2 d\varphi = \frac{P}{2\pi R}\int R^2\, d\varphi = -\frac{PR}{2\pi}\Big[\varphi\Big]\ \begin{matrix}\text{upper limit}\\ \text{lower limit}\end{matrix}$$

Commencing with the shear flow between hinges ① and ②,

$$X_{III}^{1-2} = -\frac{P}{2\pi}\Big[-\cos\varphi\Big]_{\frac{\pi}{2}-\beta}^{\frac{\pi}{2}+\beta} = -\frac{PR}{2\pi}\Big[\cos(\tfrac{\pi}{2}+\beta)-\cos(\tfrac{\pi}{2}-\beta)\Big] = -\frac{P}{\pi}\sin\beta$$

$$Y_{III}^{1-2} = 0 \qquad \text{(From previous considerations)}$$

$$M_{III}^{1-2} = -\frac{PR}{2\pi}\Big[\varphi\Big]_{\frac{\pi}{2}-\beta}^{\frac{\pi}{2}+\beta} = -\frac{PR}{2\pi}\Big[\tfrac{\pi}{2}+\beta-(\tfrac{\pi}{2}-\beta)\Big] = -\frac{PR}{\pi}\beta$$

Between hinges ② and ③

$$X_{III}^{2-3} = -\frac{P}{2\pi}\Big[-\cos\varphi\Big]_{-(\frac{\pi}{2}-\alpha)}^{\frac{\pi}{2}-\beta}$$ As stated previously this component does no work.

$$Y_{III}^{2-3} = -\frac{P}{2\pi}\Big[\sin\varphi\Big]_{-(\frac{\pi}{2}-\alpha)}^{\frac{\pi}{2}-\beta} = -\frac{P}{2\pi}\Big[\sin(\tfrac{\pi}{2}-\beta)-\sin(\alpha-\tfrac{\pi}{2})\Big] = -\frac{P}{2\pi}\Big[\cos\beta+\cos\alpha\Big]$$

$$M_{III}^{2-3} = -\frac{PR}{2\pi}\Big[\varphi\Big]_{-(\frac{\pi}{2}-\alpha)}^{\frac{\pi}{2}-\beta}$$ This component does no work.

Between hinges ③ and ④,

$$X_{III}^{3-4} = -\frac{P}{2\pi}\Big[-\cos\varphi\Big]_{-(\frac{\pi}{2}+\alpha)}^{\alpha-\frac{\pi}{2}} = \frac{P}{2\pi}\Big[\cos(\alpha-\tfrac{\pi}{2})-\cos(-\tfrac{\pi}{2}-\alpha)\Big] = \frac{P}{\pi}\sin\alpha$$

$$Y_{III}^{3-4} = 0$$

$$M_{III}^{3-4} = -\frac{PR}{2\pi}\Big[\varphi\Big]_{-(\frac{\pi}{2}+\alpha)}^{\alpha-\frac{\pi}{2}} = -\frac{PR}{2\pi}\Big[\alpha-\tfrac{\pi}{2}+(\tfrac{\pi}{2}+\alpha)\Big] = -\frac{PR}{\pi}\alpha$$

Summarizing the previous expressions, figures 2.1.7, 2.1.8, 2.1.9 are constructed, and the external work is computed immediately adjacent to the sketch to the sketch.

In consecutive order, adding the components for Cases I and II, the net result between hinges ① and ② are shown in

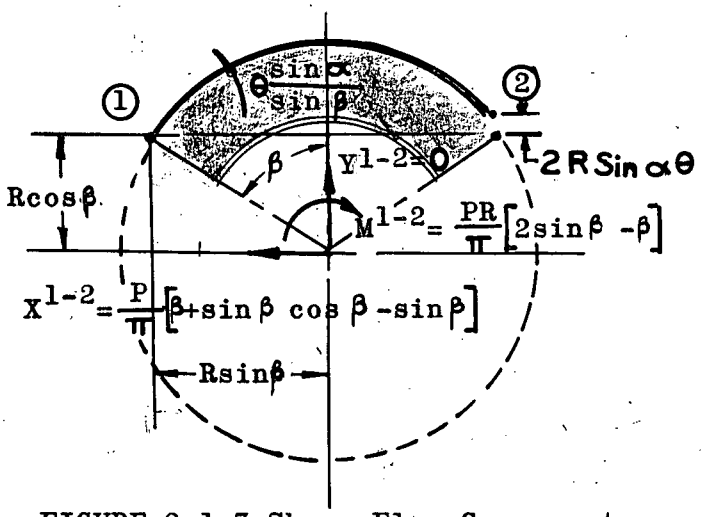

Figure 2.1.7.

Note: Positive moment is that moment which assists the rotation of the failure configuration.

FIGURE 2.1.7 Shear Flow Components

$$W_e^{1-2} = -\frac{P}{\pi}\left[\beta+\sin\beta\cos\beta-\sin\beta\right]\left[R\cos\beta\right]\left[\frac{\sin\alpha}{\sin\beta}\right]\theta + \frac{PR}{\pi}\left[2\sin\beta-\beta\right]\left[\frac{\sin\alpha}{\sin\beta}\right]\theta$$

$$= -\frac{PR\theta}{\pi}\left[(\beta+\sin\beta\cos\beta-\sin\beta)\left[\frac{\sin\alpha\cos\beta}{\sin\beta}\right]+(2\sin\beta-\beta)\left[\frac{\sin\alpha}{\sin\beta}\right]\right]$$

$$= -\frac{PR}{\pi}\theta\left[\frac{\sin\alpha\cos\beta+\sin\alpha\sin\beta\cos2\beta-\sin\alpha\sin\beta\cos\beta-2\sin\alpha\sin\beta+\sin\alpha\beta}{\sin\beta}\right]$$

Note: Components X and M do no work .....(2.1.12)

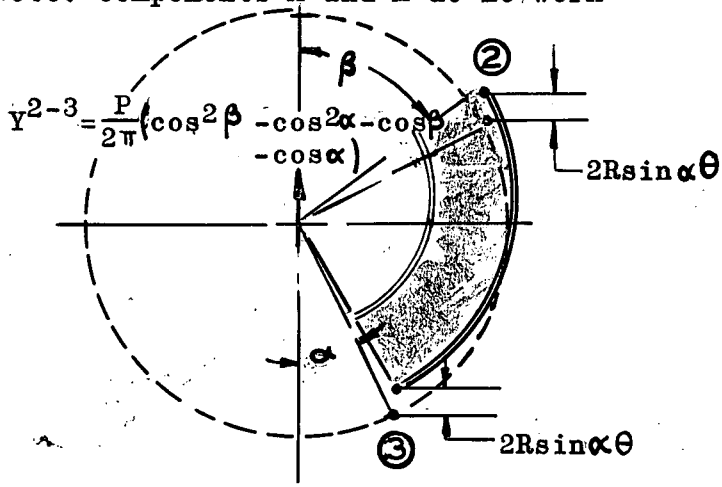

Adding components of Cases II and III, the net result between hinges ②-③ is shown in Figure 2.1.8 with its corresponding virtual displacement.

FIGURE 2.1.8 Shear Flow Components

The external work is evaluated very simply.

$$W_e^{2-3} = Y^{2-3}2R\sin\alpha\theta$$

$$= \frac{P}{2\pi}(\cos^2\beta\cos^2\alpha-\cos\beta-\cos\alpha)\theta\sin\alpha\,2R$$

$$= \frac{PR}{\pi}\theta\left[\cos^2\beta\sin\alpha - \cos^2\alpha\sin\alpha - \cos\beta\sin\alpha - \sin\alpha\cos\alpha\right] \ldots (2.1.13)$$

Between hinges ③ and ④,

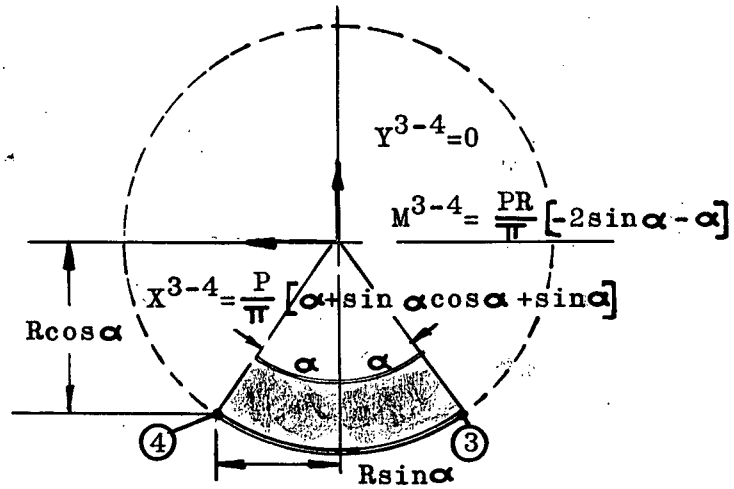

FIGURE 2.1.9 Shear Flow Components

If the same procedure is carried out for the link ③ - ④, the results are summarized in Figure 2.1.9. The external work is as shown below.

$$W^{3-4} = \frac{P}{\pi}\left[\alpha+\sin\alpha\cos\alpha+\sin\alpha\right]R\cos\alpha\theta + \frac{PR}{\pi}\left[-2\sin\alpha-\alpha\right]\theta$$

$$= \frac{PR}{\pi}\left[\alpha\cos\alpha+\sin\alpha\cos^2\alpha+\sin\alpha\cos\alpha-2\sin\alpha-\alpha\right]\theta \quad \ldots.(2.1.14)$$

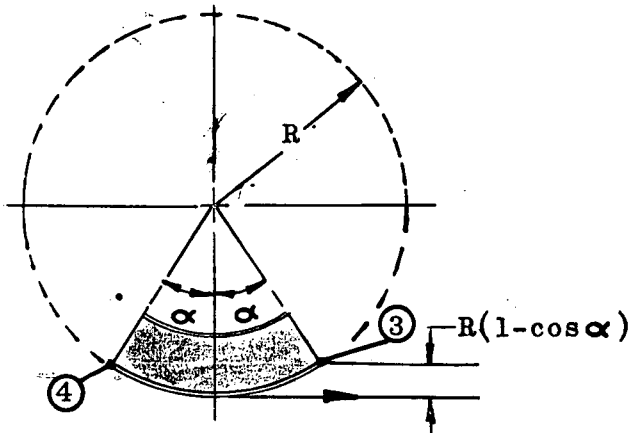

FIGURE 2.1.10 External Work of the Applied Tangential Loading

Returning to Case I temporarily in order to derive the external work of the applied load,

W_e = $PR(1-\cos\alpha)$ ...(2.1.15)

If the expressions for all the separate links are added together (i.e., equations 2.1.12+2.1.13+2.1.14+2.1.15) and equated to expression 2.1.8, then the resultant is the execution of the principle of virtual displacement. Thus, evolves

$$2\,M_p\left[1+\frac{\sin\alpha}{\sin\beta}\right] = \underbrace{PR(1-\cos\alpha)}_{2.1.15}$$

$$-\frac{PR}{\pi}\theta\Big[\underbrace{\sin\alpha\cos\beta+\sin\alpha\sin\beta\cos^2\beta-\sin\alpha\sin\beta\cos\beta-2\sin\alpha\sin\beta+\beta\sin\alpha}_{2.1.12}\Big]$$

$$+\frac{PR}{\pi}\theta\Big[\cos^2\underbrace{\sin\alpha-\cos^2\alpha\sin\alpha-\cos o\sin\alpha-\sin\alpha\cos\alpha}_{2.1.13}\Big]$$

$$+\frac{PR}{\pi}\theta\Big[\underbrace{\alpha\cos\alpha+\sin\alpha\cos^2\alpha+\sin\alpha\cos\alpha-2\sin\alpha-\alpha}_{2.1.14}\Big] \quad \ldots\ldots(2.1.16)$$

Rearranging,

$$2M_p\Big[\sin\beta+\sin\alpha\Big] = PR(1-\cos\alpha)\sin\alpha$$

$$-\frac{PR}{\pi}\Big[\beta\sin\alpha\cos\beta+\cancel{\sin\alpha\sin\beta\cos^2\beta}-\cancel{\sin\alpha\sin\beta\cos\beta}-\cancel{2\sin\alpha\sin\beta}+\beta\sin\alpha\Big]$$

$$+\frac{PR}{\pi}\Big[\cancel{\cos^2\beta\sin\alpha\sin\beta}-\cancel{\cos^2\alpha\sin\alpha\sin\beta}-\cancel{\cos\beta\sin\alpha\sin\beta}-\cancel{\sin\alpha\sin\beta\cos\alpha}+\alpha\sin\beta\cos\alpha\Big]$$

$$+\frac{PR}{\pi}\Big[\cancel{\sin\alpha\sin\beta\cos^2\alpha}+\cancel{\sin\alpha\sin\beta\cos\alpha}-\cancel{2\sin\alpha\sin\beta}-\alpha\sin\beta\Big]$$

Collecting the remaining terms,

$$2M_p = \frac{\frac{PR}{\pi}(\pi\sin(1-\cos\alpha)+\alpha\sin\beta\cos\alpha-\alpha\sin\beta-\beta\sin\alpha\cos\beta-\beta\sin\alpha)}{\sin\beta+\sin\alpha}$$

which reduces to the fairly simple expression,

$$\frac{M_p}{PR} = \frac{1}{2\pi(\sin\beta+\sin\alpha)}\Big[(\pi-\alpha)\sin\beta(1-\cos\alpha)-\beta\sin\alpha(1+\cos\beta)\Big] \quad \ldots(2.1.17)$$

In reality, this is a fairly simple expression since the maximum moment is a function of two unknown angles α and β.

2.1.3 Maximizing for a Complete Solution

In order to solve for the angles which satisfy this expression, the equation must be maximized with respect to each angle individually. This process yields two equations, which must be solved simultaneously for the complete solution to the problem.

Thus,

$$\frac{\partial M_p}{\partial \alpha} = 0$$

$$\frac{2\pi(\sin\beta+\sin\alpha)(\pi\sin\beta\sin\alpha-\alpha\sin\beta\sin\alpha+\sin\beta\cos\alpha-\sin\beta-\beta\cos\alpha\cos\beta-\beta\cos\alpha}{(\sin\beta+\sin\alpha)^2}$$

$$-\frac{2\pi(\cos\alpha)(\pi-\alpha)\sin\beta-(1-\cos\alpha)-\beta\sin\alpha(1+\cos\beta)}{(\sin\beta+\sin\alpha)^2} = 0$$

$$=(1-\cos\alpha)(\pi-\alpha-\sin\beta-\sin\alpha)+(\pi-\alpha)(\sin\alpha\sin\beta)-\beta\cos\alpha(1+\cos\beta)= \quad ..(2.1.18)$$

$$\frac{\partial M_p}{\partial \beta} = 0$$

$$\frac{2\pi(\sin\beta+\sin\alpha)(\pi-\alpha)\sin\beta(1-\cos\alpha)-\sin\alpha+\beta\sin\alpha\sin\beta-\sin\alpha\cos\beta}{(\sin\alpha+\sin\beta)^2}$$

$$+\frac{2\pi\cos\beta(\pi-\alpha)\sin\beta(1-\cos\alpha)-\beta\sin\alpha(1+\cos\beta)}{(\sin\beta+\sin\alpha)^2} = 0$$

$$=(\beta-\sin\beta-\sin\alpha)(1+\cos\beta)+(\pi-\alpha)\cos\beta(1-\cos\alpha)+\beta\sin\alpha\sin\beta=0$$

$$\ldots\ldots\ldots\ldots(2.1.19)$$

Rather than attempt a simultaneous solution of the two equations 2.1.18 and 2.1.19, the author decided to refer to the elastic solution as found in any of the references 1 , 2 , 3 , and 4 listed in section VI. A check revealed that the points of maximum moment for an elastic solution fell around 35° from the vertical axis for an approximation to α and 50° from the vertical for the angle β . Recapitulating, it will be recalled that the points of maximum moment for the solution to the radially loaded ring shifted toward the applied load. Thus, an attempt was made to satisfy the expressions 2.1.18 and 2.1.19 one at a time. First of all several different values of α were assumed while holding β fixed. If β were assumed to be 52° and α were given the different values of 25°, 30°, 35°, a graph of

expression 2.1.18 could be plotted versus the angle α. This plot would peak at some value of α (it turned out to be approximately $31^\circ\ 30'$). With this value of α as a first approximation, several different values of β, 45°, 50°, 55°, were substituted into expression 2.1.19. Again a plot of this function was sketched and the curve culminated around an angle of $53^\circ\ 50'$. Further manipulation led to the final interpolation.

$$\alpha = 31^\circ\ 23' \quad \text{.....(2.1.20)}$$

$$\beta = 53^\circ\ 47' \quad \text{.....(2.1.21)}$$

These angles satisfy the two expressions simultaneously, and thus were in turn substituted into the expression for maximum moment 2.1.17.

Reflecting:

$$\frac{M_p}{PR} = \frac{(\pi-\alpha)\sin\beta(1-\cos\alpha)-\beta\sin\alpha(1+\cos\beta)}{2\pi(\sin\beta+\sin\alpha)} \quad \text{.....(2.1.17)}$$

$$\frac{M_p}{PR} = \frac{(3.1416-.54774)(.80679)(1-.8537)-.9387(.52076)(1+.59084)}{2(3.1416)(.80679+.52076)}.$$

Thus,

$$M_p = .05653\ PR \quad \text{.....2.122}$$

2.1.4 Plasticity Check

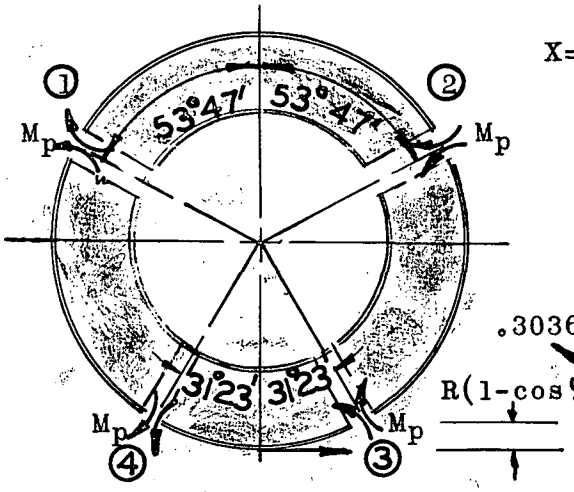

FIGURE 2.1.11 Plasticity Check

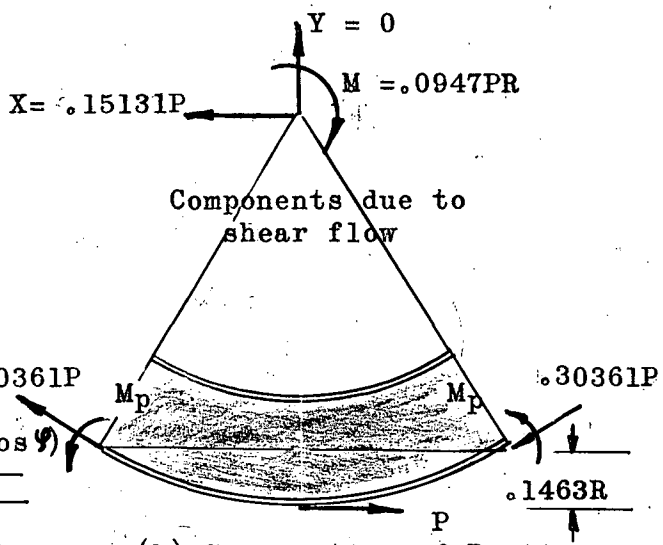

(b) Segregation of Portion of Ring Between Hinges ③ & ④

From Figure 2.1.11(a)and(b), it may be perceived that the ring is in equilibrium with the prescribed loads. Thence, the completeness of the plasticity check is substantiated by a plot of the internal moment diagram. Observing that the moment is zero at the point of loading, this is a good starting place for plotting the moment curve. Resolving the components of moment, axial load, and shear of the shear flow between 0^o and some arbitrary angle φ (as shown in Figure 2.1.12), the moment, axial load and shear at some section φ^o from the vertical are determined from the following expressions.

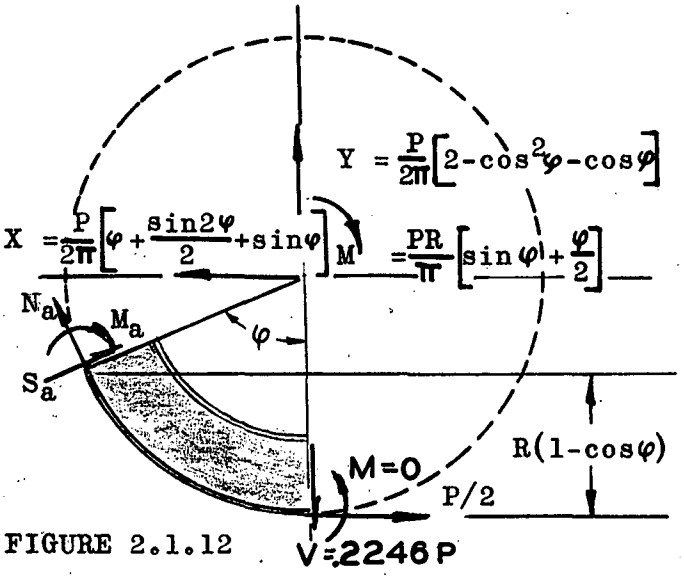

FIGURE 2.1.12

Moment,

$$M_a = \frac{P}{2}(1-\cos\varphi)R+\frac{P}{2}\left[\varphi+\sin\varphi\cos\varphi+\sin\varphi\right]R\cos\varphi+\frac{P}{2\pi}\left[2-\cos^2\varphi-\cos\varphi R\sin\varphi\right]$$

$$-\frac{PR}{\pi}\left[\sin\varphi+\frac{\varphi}{2}\right]$$

$$M_a = \frac{PR}{2\pi}\left[(\pi-\varphi)(1-\cos\varphi)-.4491\pi\sin\varphi\right] \quad \ldots\ldots\ldots\ldots\ldots\ldots (2.1.23)$$

Axial Load,

$$N_a = \frac{P}{2\pi}\left[\varphi+\sin\varphi\cos\varphi+\sin\varphi\right]\cos\varphi+\frac{P}{2\pi}\left[2-\cos^2\varphi-\cos\varphi\sin\varphi-.2245P\right]\sin\varphi-\frac{P}{2}\cos\varphi$$

$$N_a = \frac{P}{2\pi}\left[(2-.4491\pi)\sin\varphi-(\pi-\varphi)\cos\varphi\right] \quad \ldots\ldots\ldots\ldots\ldots\ldots (2.1.24)$$

Shear,

$$S_a = \frac{P}{2\pi}\left[\varphi+\sin\varphi\cos\varphi+\sin\varphi\right]\sin\varphi-\frac{P}{2}\sin\varphi-\frac{P}{2\pi}\left[2-\cos^2\varphi-\cos\varphi\right]\cos\varphi+.2910P\cos\varphi$$

$$S_a = \frac{P}{2\pi}\left[(\pi - \varphi)\sin\varphi + (.4491\pi - 1)\cos\varphi + 1\right] \quad \ldots\ldots\ldots\ldots\ldots\ldots\ldots (2.1.25)$$

Values of φ for every 5^o were substituted into expressions 2.1.23, 2.1.24, and 2.1.25, and the coefficients were tabulated in Tables 2.1.1 and 2.1.2. These coefficients are plotted on pages 90,91,92 (Figures 2.1.13,2.1.14,2.1.15).

Curiously enough for this loading, the concurrence of the applied load has the same effect on internal axial load and moment as it did in the preceding example, even though it is not quite so pronounced. It is discernible from the moment curve (Figure 2.1.13) that the peaks of moment shift from about 35^o and 130^o for the elastic solution to $31^o\ 23'$ and $126^o\ 13'$ for the plastic solution, respectively. All of the distinctions of the structural behavior of this loading seem to be conforming with the former case, except that they are not quite so conspicuous this time. The crown of the axial load and shear curves seem to heighten very little, whereas, there is a marked redistribution and increase of moment.

Although a direct comparison is impossible because the yield load is much different from the ultimate collapse load, this particular case affords an opportunity to advance a brief discrimination between an elastic and a plastic interpretation of a loading. If the axial load and shear coefficients for a loading are very nearly the same and if a design were based on moment adequacy alone, it is plausible to presume that the plasticity solution would yield a more adequate distribution of bending stiffness.

In order to elucidate the previous statement, suppose that the acheivement of the mechanism just developed is outlined in more

TANGENTIAL FORCE P ON A TANGENTIALLY SUPPORTED CIRCULAR RING

TABLE 2.1.1

Comparison of Plastic to Elastic Moment, Shear and Axial Load Coefficients						
Angle φ From Vertical	Plastic Moment Coeff.	Elastic * Moment Coeff.	Plastic Shear Coeff.	Elastic* Shear Coeff.	Plastic Axial Load Coeff.	Elastic * Axial Load Coeff.
0	0	0	.224545	.239	-.50000	-.50000
5	.017720		.181895		-.476086	
10	.031820		.141551		-.448768	
15	.042465	.04538	.103686	.1175	-.418414	-.423
20	.049995		.068593		-.385572	
25	.054559		.036458		-.350592	
30	.056452	.06354	.007452	.002	-.314818	-.321
31 23'	.056538		0		-.303603	
35	.056014		-.018311		-.276165	
40	.053352		-.040725		-.237634	
45	.048944	.05898	-.059773	-.0498	-.198868	-.2085
50	.043018		-.075438		-.160295	
55	.035874		-.087766		-.122356	
60	.027796	.04008	-.096827	-.0903	-.085468	-.0979
65	.019067		-.102726		-.050028	
70	.009954		-.105608		-.016401	
75	.000718	.01442	-.105650	-.1015	.015016	0
80	-.008407		-.103049		.044100	
85	-.017199		-.098029		.070402	
90	-.025455	-.01127	-.090845	-.0908	.093760	.0796

*For Elastic coefficients see reference 4, Graph 3

TANGENTIAL FORCE P ON A TANGENTIALLY SUPPORTED CIRCULAR RING

TABLE 2.1.2

Comparison of Plastic to Elastic Moment, Shear and Axial Load Coefficients						
Angle φ From Vertical	Plastic Moment Coeff.	Elastic* Moment Coeff.	Plastic Shear Coeff.	Elastic* Shear Coeff.	Plastic Axial Load Coeff.	Elastic* Axial Load Coeff.
95	-.033001		-.081756		.113982	
100	-.039677		-.071047		.130925	
105	-.045596	-.03166	-.059159	-.0628	.144528	.131
110	-.049946		-.045928		.154609	
115	-.053548		-.032120		161282	
120	-.055537	-.04325	-.017879	-.0248	.164532	.152
125	-.056472		-.003500		.164434	
126 13'	-.056508		0		.163915	
130	-.056155		.010728		.161101	
135	-.054610	-.04458	.024528	.002	.154687	.1445
140	-.051891		.037642		.145384	
145	-.048067		.049826		.133418	
150	-.043230	-.03614	.060858	.0486	.119049	.112
155	-.037486		.070542		.102563	
160	-.030963		.078707		.084273	
165	-.023794	-.02092	.085213	.0716	.064511	.0608
170	-.016141		.089934		.043637	
175	-.008154		.092803		.022009	
180	0	0	.093765	.0796	0	0

*For Elastic coefficients see reference 4, Graph 3

TANGENTIAL FORCE P ON A TANGENTIALLY SUPPORTED RING

MOMENT COEFFICIENTS VS ANGLE φ (FROM VERTICAL) IN DEGREES

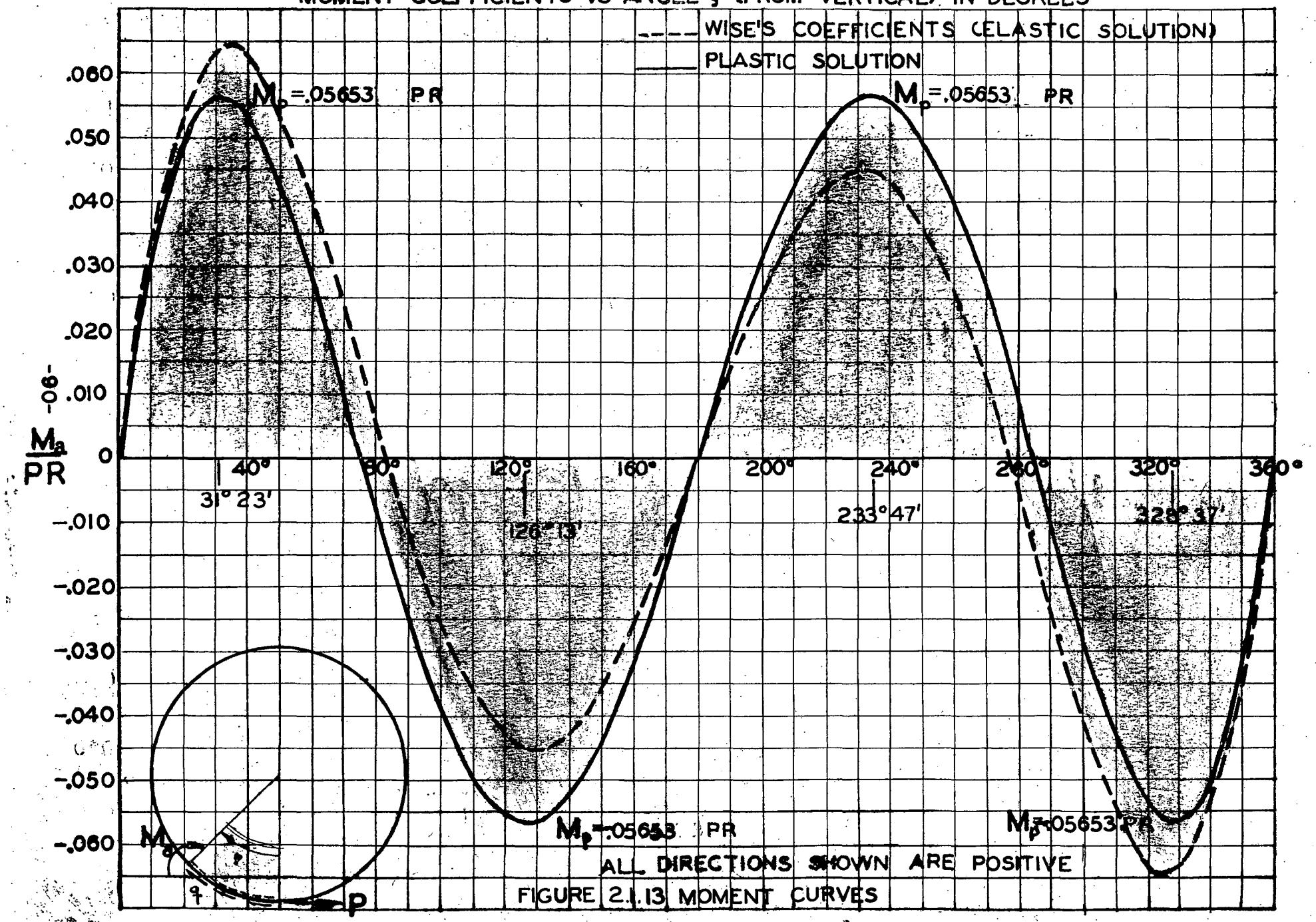

ALL DIRECTIONS SHOWN ARE POSITIVE

FIGURE 2.1.13 MOMENT CURVES

TANGENTIAL FORCE P ON A TANGENTIALLY SUPPORTED RING

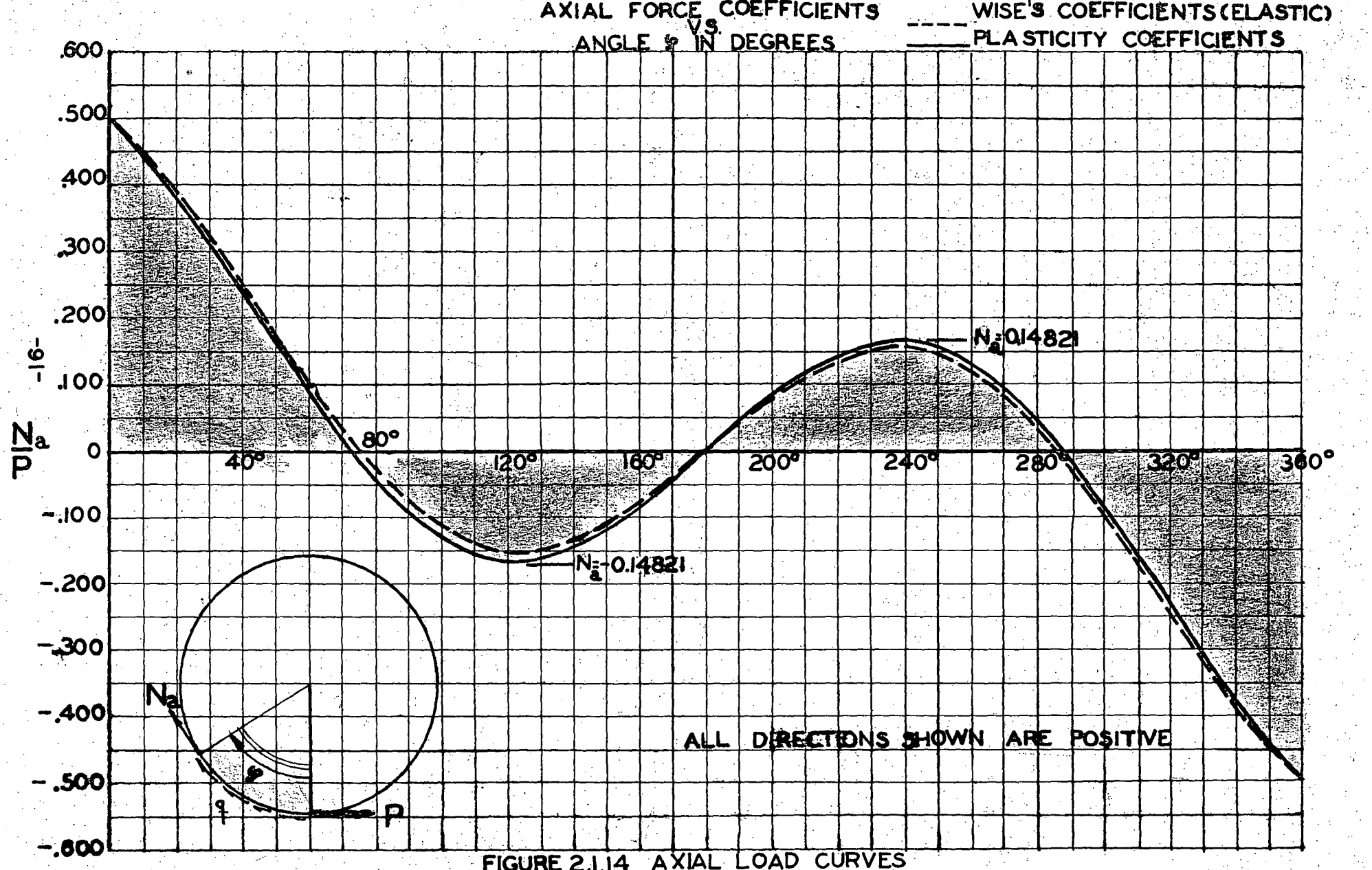

FIGURE 2.1.14 AXIAL LOAD CURVES

TANGENTIAL FORCE P ON A TANGENTIALLY SUPPORTED RING

SHEAR COEFFICIENTS VS ANGLE φ (FROM VERTICAL) IN DEGREES

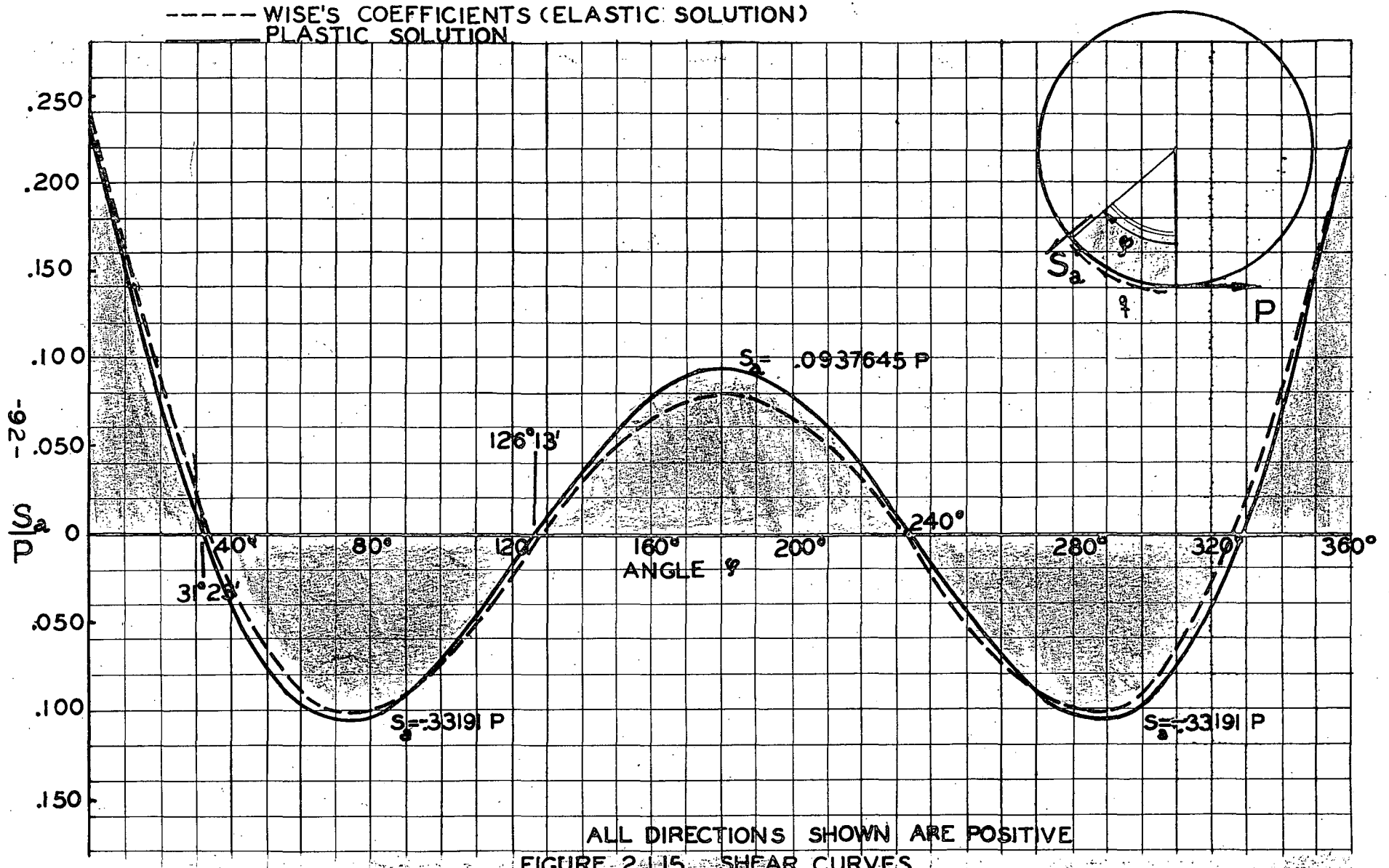

ALL DIRECTIONS SHOWN ARE POSITIVE

FIGURE 2.1.15 SHEAR CURVES

detail. Reviewing the procedure of Ring Loading I, the first hinges form simultaneously at points ③ and ④. This is concluded from the observation of the maximum moments of the elastic solution. Once a certain value of P is acheived which causes yielding at ③ and ④, the structure yields at these locations while the portion of the ring above ③ and ④ remains intact and strained well within the limits of yielding. As the load is progressively increased, the shape of the moment diagram changes concurrently until it attains its final plastic configuration (2.1.13, the solid line). At this point the applied load has reached its ultimate intensity and collapse will prevail.

The bending stiffness of the ring for the plastic solution conforms to the shape of the plastic moment curve. On the other hand, since the bending stiffness was assumed to be constant for the elastic solution, it is dependent on the maximum moment at hinges ③ and ④ (dotted curve of Figure 2.1.13). Thus, when the two solutions (elastic and plastic) are compared with each other, it is reasonable to conclude that a design based on the plastic solution will surpass the comparable elastic design.

2.2.0 Loading Condition Ring III-Twisting Moment PRsin γ on a Tangentially Supported Circular Ring

The third loading which is to be considered in this thesis is a general case consisting of a torque applied to a circular ring, applied by two P forces acting at some constant angle γ, measured from the vertical axis. (See Figure 2.2.1).

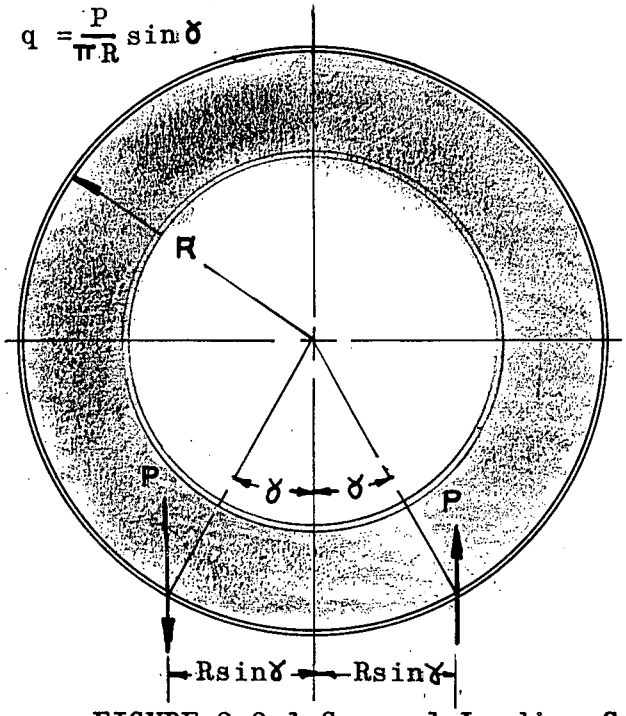

FIGURE 2.2.1 General Loading Case
Ring III-Twisting Moment 2PRsin γ

If the P forces are located at some arbitrary angle from the vertical, then the twisting moment, T, imposed on the ring is 2PRsin γ, and the resulting shear flow is

$$q = \frac{T}{2A}$$

$$= \frac{P(2R\sin\gamma)}{2\pi R^2}$$

$$= \frac{P\sin\gamma}{\pi R} \qquad \ldots\ldots(2.2.1)$$

Considering the previous examples, it is recalled that the most significant part of the procedure is the designation of the relative hinge locations. There is a certain range of γ wherein two of the hinges will always form at the point of concentrated loads, and there is an upper range of γ where there is a transition from this general case. There is a lower range of γ when the frame no longer fails in bending, but instead it fails in shear. The upper range or bound could be found by assuming

the hinges do fall between the concentrated loads P, and maximizing the solution of M_p with respect to two unknown variable angles as done in the preceding example, loading 2.1.0. The lower range or bound could be determined by letting the angle δ approach a very small angle. At some value of δ, the magnitude of the shear at the location of the concentrated loads becomes so intense that the section will fail in shear rather than in bending. The range where the lower hinges form exactly at the applied loads constitute the larger percentage of the practical cases, and only this scope of loading will be considered first. The other two cases will be discussed later on.

Two of the hinges are located immediately at the applied loads, and hence, it is only necessary to figure out the locations of the two remaining hinges necessary to generate a mechanism. The position of the remaining hinge locations may be ascertained from rule b, page 49. By virtue of geometrical symmetry and symmetry of loading the other two hinges will form at some unknown angle β with respect to the vertical axis of symmetry (as shown in Figure 2.2.2). Summarizing the preceding conclusions, two hinges from at the predetermined angles δ defined by the location of the applied loads, and the other two hinges form at an arbitrary angle β, which is to be obtained for a complete solution.

After the arrangement of the hinges has been ascertained, it is only necessary to pick the segment or point on the ring which is to be fixed in space, before applying the principle of virtual displacement. The condition of hinge pattern symmetry

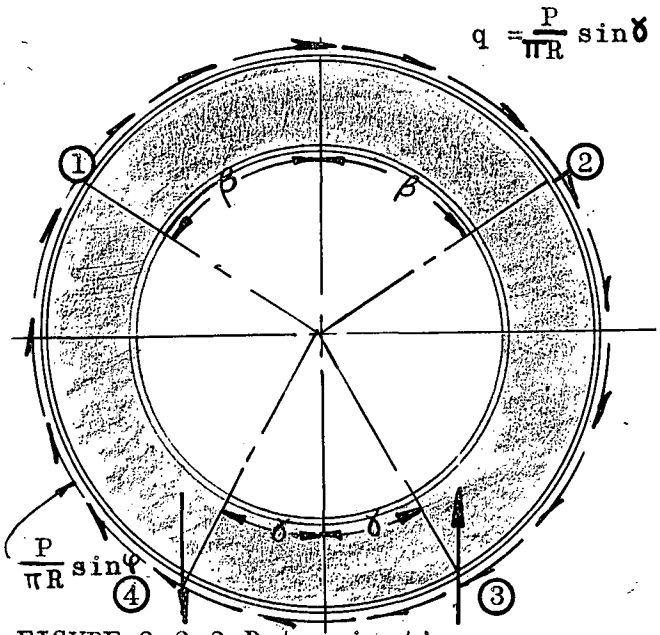

FIGURE 2.2.2 Determination of Hinge Pattern

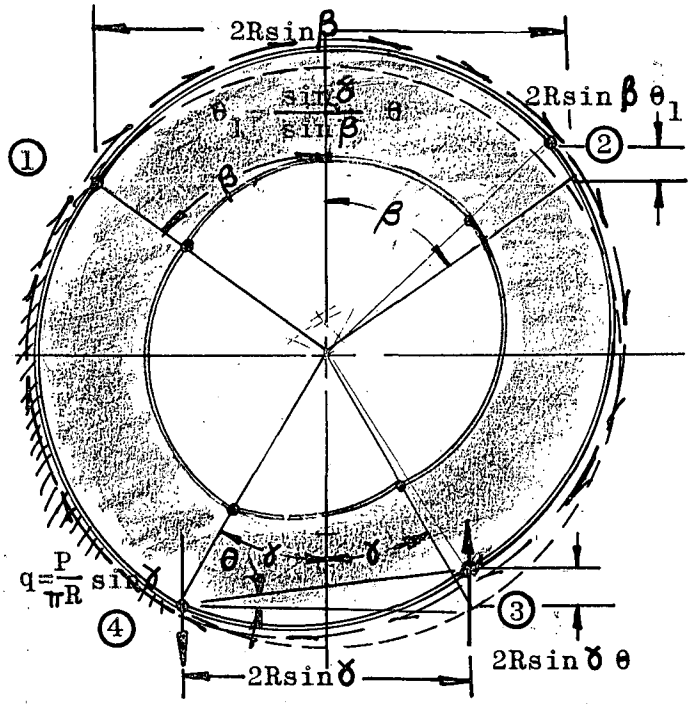

FIGURE 2.2.3 Relationships of the Various Virtual Rotations and Deflection

lends itself to the use of a sidesway or panel type mechanism. Therefore, it is logical to fix the segment of the structure which permits a sidesway mode of failure, because this procedure always simplifies the geometry and, consequently, the external work expressions.

It was decided to hold the segment between hinges ① and ④ fast, and give the structure a virtual rotation θ about the point ④. From compatibility of structural deformation, it is evident from Figure 2.2.3 that the vertical deflection of segment ①-② must be identical to the vertical deflection of section ③-④. It is perceivable that the hinge pattern for this loading is equivalent to the hinge pattern of the preceding case, loading 2.1.0. The only exception is the substitution of

the angle γ for the angle α. As a result the trigonometric relationships between the virtual rotations of the various parts of the structure remain the same as the expressions on page 77, or

$$\theta_1 = \frac{2R\theta \sin\gamma}{2R\sin\beta} = \frac{\sin\gamma}{\sin\beta}\,\theta \qquad \ldots\ldots\ldots(2.2.2)$$

$$\theta_2 = \theta_1 = \frac{\sin\gamma}{\sin\beta}\,\theta \qquad \ldots\ldots\ldots(2.2.3)$$

$$\theta_3 = \theta \qquad \ldots\ldots\ldots\ldots\ldots\ldots\ldots\ldots(2.2.4)$$

$$\theta_4 = \theta \qquad \ldots\ldots\ldots\ldots\ldots\ldots\ldots\ldots(2.2.5)$$

2.2.1 Resolution of Shear Flow into Equivalent Components

The expedient for replacing the shear flow with its equivalent by resolving it into vertical, horizontal and moment components at the center of the ring is inserted into the procedure now.

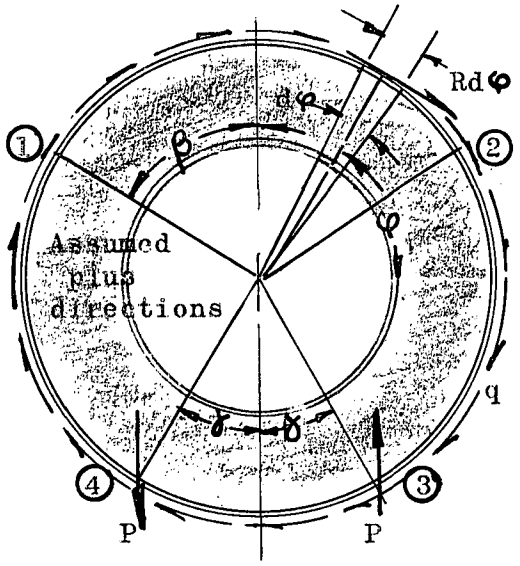

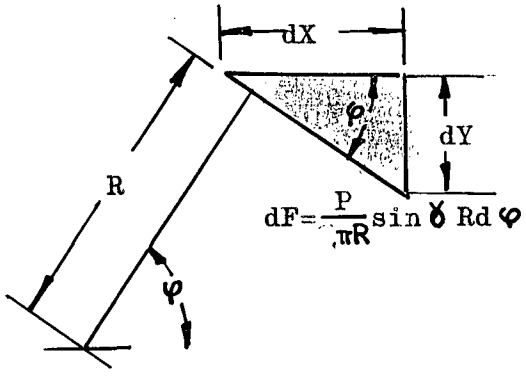

FIGURE 2.2.4 Resolution of Shear Flow into Components

$$dX = \frac{P\sin\gamma}{\pi}\sin\varphi \ldots(2.2.6)$$

$$dY = \frac{P\cos}{\pi}\sin\varphi \ldots(2.2.7)$$

$$dM = \frac{PR^2}{R\pi}\sin\varphi \ldots(2.2.8)$$

Referring to Figure 2.2.4, the equivalent components may be obtained by integrating equations 2.2.6, 2.2.7 and 2.2.8.

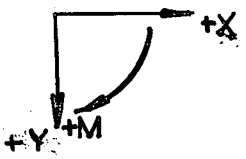

$$X = \int qR\sin\varphi\, d\varphi = \frac{P\sin\gamma}{\pi R}\int R\sin\varphi\, d\varphi$$

$$X = \frac{P\sin\gamma}{\pi R}\left[-\cos\varphi\right]_{\text{lower limit}}^{\text{upper limit}} \quad \ldots\ldots\ldots\ldots (2.2.6)$$

$$Y = \int qR\cos\varphi\, d\varphi = \frac{P\sin\gamma}{\pi R}\int R\cos\varphi\, d\varphi = \frac{P}{\pi}\sin\gamma\left[\sin\varphi\right]_{\text{lower limit}}^{\text{upper limit}} \quad \ldots (2.2.7)$$

$$M = \int qR^2 d\varphi = \frac{P\sin\gamma}{R}\int R^2 d\varphi = \frac{PR\sin\gamma}{\pi}\left[\varphi\right]_{\text{lower limit}}^{\text{upper limit}} \quad \ldots\ldots (2.2.8)$$

Commencing with the shear flow between hinges ① and ②

$$X^{1-2} = \frac{P\sin\gamma}{\pi}\left[-\cos\varphi\right]_{\frac{\pi}{2}-\beta}^{\frac{\pi}{2}+\beta} = \frac{P\sin\gamma}{\pi}\left[-\cos\left(\frac{\pi}{2}+\beta\right)+\cos\left(\frac{\pi}{2}-\beta\right)\right] = \frac{2P\sin\gamma\sin\beta}{\pi}$$

$$Y^{1-2} = 0$$

$$M^{1-2} = \frac{PR\sin\gamma}{\pi}\left[\varphi\right]_{\frac{\pi}{2}-\beta}^{\frac{\pi}{2}+\beta} = \frac{PR\sin\gamma}{\pi}\left[\frac{\pi}{2}+\beta-\left(\frac{\pi}{2}-\beta\right)\right] = \frac{2PR\sin\gamma}{\pi}\beta$$

Between hinges ② and ③

$$X^{2-3} = \frac{P\sin\gamma}{\pi}\left[-\cos\varphi\right]_{\frac{3\pi}{2}+\beta}^{\frac{\pi}{2}+\beta}$$ This component does no work because segment ② - ③ just translates vertically

$$Y^{2-3} = \frac{P\sin\gamma}{\pi}\left[\sin\varphi\right]_{\frac{3\pi}{2}+\gamma}^{\frac{\pi}{2}-\beta} = \frac{P\sin\gamma}{\pi}\left[\sin\left(\frac{\pi}{2}-\beta\right)-\sin\left(\frac{3\pi}{2}+\gamma\right)\right] = \frac{P\sin\gamma}{\pi}\left[\cos\beta+\cos\gamma\right]$$

$$M^{2-3} = \frac{PR\sin\gamma}{\pi}\left[\varphi\right]_{\frac{3\pi}{2}+\gamma}^{\frac{\pi}{2}-\beta}$$ The moment does no work because segment ② - ③ does not rotate

Between hinges ③ and ④

$$X^{3-4} = \frac{P\sin\gamma}{\pi}\left[-\cos\varphi\right]_{\frac{3\pi}{2}-\gamma}^{\frac{\pi}{2}+\gamma} = \frac{P\sin\gamma}{\pi}\left[-\cos\left(\frac{3\pi}{2}+\gamma\right)+\cos\left(\frac{3\pi}{2}-\gamma\right)\right] = \frac{2P\sin^2\gamma}{\pi}$$

$$Y^{3-4} = 0$$

$$M^{3-4} = \frac{PR\sin\gamma}{\pi}\left[\varphi\right]_{\frac{3\pi}{2}-\gamma}^{\frac{3\pi}{2}+\gamma} = \frac{PR\sin\gamma}{\pi}\left[\frac{3\pi}{2}+\gamma-\left(\frac{3\pi}{2}-\gamma\right)\right] = \frac{2PR}{\pi}\gamma\sin\gamma$$

2.2.3 Evaluation of Internal and External Work

All of the shear components which do work have been determined, and now the analyst is ready to ascertain the internal and external work.

The internal work is obtained by adding together the magnitude of the moment at the individual hinges multiplied by their virtual internal rotations, or

$$M_p \left[\theta_1+\theta_2+\theta_3+\theta_4\right] = M_p\,\theta\left[1+1+\frac{\sin\gamma}{\sin\beta}+\frac{\sin\gamma}{\sin\beta}\right]$$

$$W_{int} = 2M_p\theta\left[\frac{\sin\beta+\sin\gamma}{\sin\beta}\right] \qquad \text{.....(2.2.9)}$$

The external work is obtained by summing the products of the shear components on each segment and their respective virtual rotations. Note: Positive moment is that moment which assists the rotation of the failure configuration.

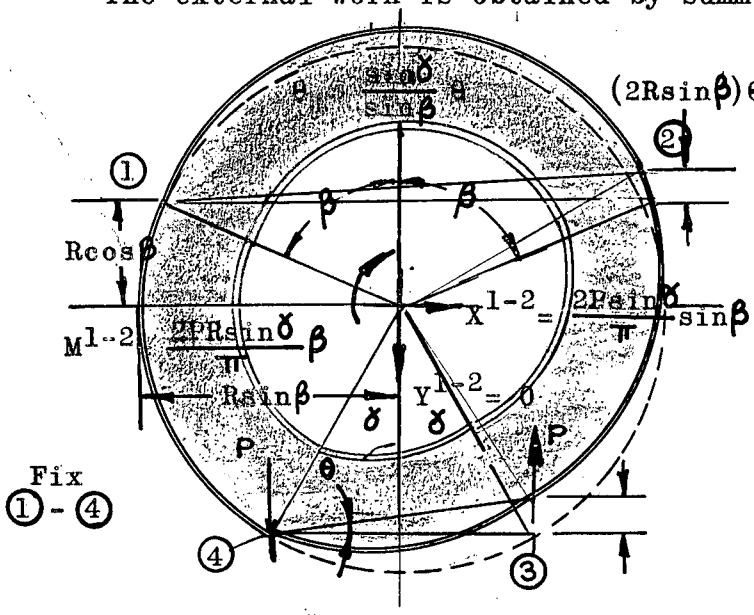

FIGURE 2.2.5
External Work Done on Segment
1 - 2

For segment

$$W_e^{1-2} = \frac{2P\sin\gamma\,\sin\beta}{\pi}R\cos\beta\left[\frac{\sin\gamma}{\sin\beta}\right]\theta - 2\,\frac{PR\sin\gamma}{\pi}\beta\left(\frac{\sin\gamma}{\sin\beta}\right)\theta \quad \text{...(2.2.10)}$$

Note: X and M components do no work.

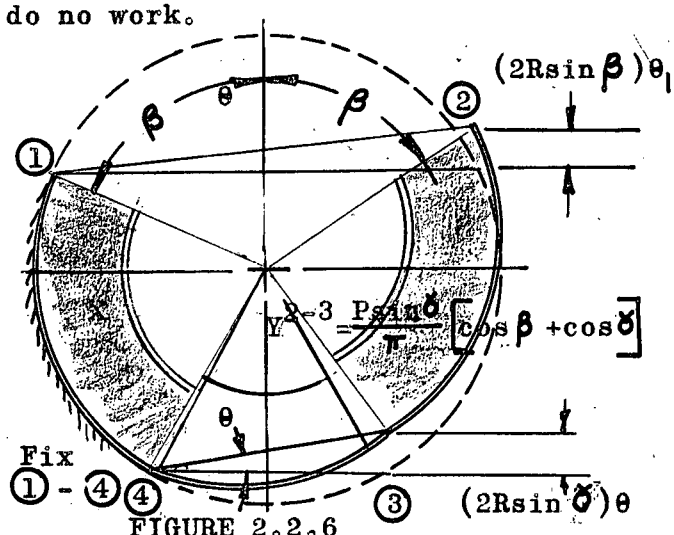

FIGURE 2.2.6
External Work on Segment ② - ③

Since segment ② - ③ just translates vertically, the external work done on segment ② - ③ is

$$W_e^{2-3} = -\frac{P\sin\gamma}{\pi}(\cos\beta+\cos\gamma)2R\sin\gamma\,\theta \quad \ldots\ldots\ldots\ldots(2.2.11)$$

The external work done on segment ③ - ④ is illustrated in Figure 2.2.7.

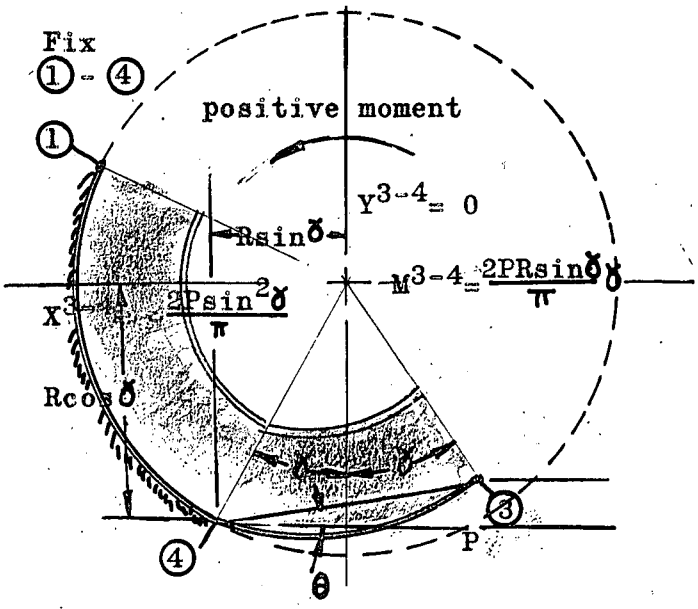

$$W_e^{3-4} = -\frac{2P\sin^2\gamma}{\pi}(-R\cos\gamma)\theta - \frac{2PR}{\pi}(\sin\gamma)\theta \ldots(2.2.12)$$

The work done by the applied load can be ascertained from Figure 2.2.7

$$W_e^{P} = 2PR(\sin\gamma)\theta \ldots(2.2.13)$$

The principle of virtual work is executed by summing equations 2.2.10, 2.2.11, 2.2.12, 2.2.13 and equating the result to equation 2.2.9. Performing this addition leads to

$$\underbrace{2\,M_p\theta\left[\frac{\sin\beta+\sin\gamma}{\sin\beta}\right]}_{2.2.9} =$$

$$\underbrace{\left[\frac{2P\sin\gamma\sin\beta}{\pi}\right]R\cos\beta\left(\frac{\sin\gamma}{\sin\beta}\right)\theta - 2\frac{PR\sin\gamma}{\pi}\beta\left(\frac{\sin\gamma}{\sin\beta}\right)\theta}_{2.2.10} - \underbrace{\frac{P\sin\gamma}{\pi}(\cos\beta+\cos\gamma)2R\sin\gamma\theta}_{2.2.11}$$

$$\underbrace{\frac{2P\sin^2\delta}{\pi}(-R\cos\delta)\theta - \frac{2PR}{\pi}\delta\theta}_{2.2.12} + \underbrace{2PR\sin\delta\,\theta}_{2.2.13}$$

$$2M_p\theta\left[\frac{\sin\delta+\sin\beta}{\sin\beta}\right] =$$

$$\frac{2PR\sin}{\pi}\left\{\sin\beta\cos\beta\frac{\sin\delta}{\sin\beta} - \sin\beta\cos\beta - \sin\delta\cos\delta + \sin\delta\cos\delta - \delta + \pi + \beta\frac{\sin\delta}{\sin\beta}\right\}$$

$$M_p = \frac{PR\sin}{(\sin\beta+\sin\delta)}\left\{\sin\beta\cos\beta\sin\delta - \beta\sin\delta - \sin\delta\cos\beta - \sin\delta\cos\delta\sin\beta + \sin\delta\cos\delta\sin\beta - \delta\sin\beta + \pi\sin\beta\right\}$$

Collecting terms

$$M_p = \frac{PR\sin\delta}{\pi(\sin\beta+\sin\delta)}\left\{(\pi-\delta)\sin\beta - \beta\sin\delta\right\} \quad \text{.....(2.2.14)}$$

The maximization of this expression should not be very difficult since there is only one unknown variable β, δ being a constant. In order to obtain the maximum value of M_p, equation 2.2.14 must be maximized with respect to

$$\frac{dM}{d\beta}p =$$

$$PR\sin\delta\left\{\frac{(\sin\beta+\sin\delta)\left[(\pi-\delta)\cos\beta - \sin\delta\right] - \cos\beta\left[(\pi-\delta)\sin\beta - \beta\sin\delta\right]}{(\sin\beta+\sin\delta)^2}\right\}$$

$$\text{.....(2.2.15)}$$

Setting equation 2.2.15 equal to zero results in

$$(\pi-\delta)\sin\beta\cos\beta - \sin\delta\sin\beta + (\pi-\delta)\sin\delta\cos\beta - \sin^2\delta - (\pi-\delta)\sin\beta\cos\beta + \beta\sin\delta\cos\beta - (\cos\beta)(\pi-\delta+\beta) - \sin\beta - \sin\delta = 0$$

$$\frac{\sin\delta+\sin\beta}{\cos\beta} = \pi - \delta + \beta \quad \text{.....(2.2.16)}$$

Therefore, once a certain value of δ is selected the cor-

responding value of β may be deduced by using Newton's Iteration Method outlined on page 60. From expression 2.0.32

$$h_o = - \frac{f(x_o)}{f'(x_o)} \qquad \text{.....(2.0.32)}$$

since δ appears to be an unknown variable, the analyst must assign some value to it for a complete particular solution. If δ is arbitrarily alloted the value of 30^o , then the solution to the general equation becomes

$$\frac{f(x_o)}{f'(x_o)} = - \frac{-\cos\beta\,(\pi - \delta - \beta) - \sin\beta - \sin\delta}{-\sin\beta\,(\pi - \delta + \beta) - \cos\beta} \qquad \text{.....(2.2.17)}$$

then, if $\delta = 30^o$

$$\frac{f(x_o)}{f'(x_o)} = - \frac{-\cos\beta(3.1416 - .5236 + \beta) - \sin\beta - .5000}{-\sin\ (3.1416 - .5236 + \beta) - \cos\beta} \qquad \text{.....(2.2.18)}$$

The expression does not appear to be simplifying enough to obtain an exact solution. Accordingly, the next best thing to do is to guess some value of β and substitute it into equation 2.2.18 to find out if it satisfies this limitation. After several unsuccessfull attempts were made, it was eventually discovered that the angle 68^o very nearly satisfied expression 2.2.18.

Thus,

$$\beta = - \frac{.37461(3.1416 - .5236 + 1.1868) - .9272 - .5000}{.92718\ (3.1416 - .5236 + 1.1868) - .51461}$$

$$\beta = \frac{1.4272 - 1.4253}{.9272(1.4312) - .37461}$$

$$\beta = -.000524$$

Try $\beta = 1.18692 - .0005237 = 1.186768$ or $\beta = 67^o\ 58'$

$$= -\frac{.3752(2.6180+1.18624)-.9270-.5000}{.9270\ (3.8042)\ -.37515} = \text{negligible amount}$$

Use $\beta = 67^{o}\ 58'$

Substituting this evaluated angle of β and the assigned value of γ into expression 2.2.14.

$$M_p = \frac{PR\sin\gamma}{\pi(\sin\beta + \sin\gamma)}\left\{(\pi-\gamma)\sin\beta - \beta\sin\beta\right\} \ldots\ldots(2.2.14)$$

$$= \frac{PR(.5000)}{3.1416(.927+.500)}\left[(3.1416-.5236)(.92697)-.5931\right]$$

$$M_p = .20452PR \qquad \ldots\ldots\ldots\ldots\ldots\ldots\ldots\ldots\ldots\ldots\ldots\ldots\ldots(2.2.19)$$

Consequently the collapse mechanism for $\gamma = 30^{o}$ assumes the configuration shown in Figure 2.2.8.

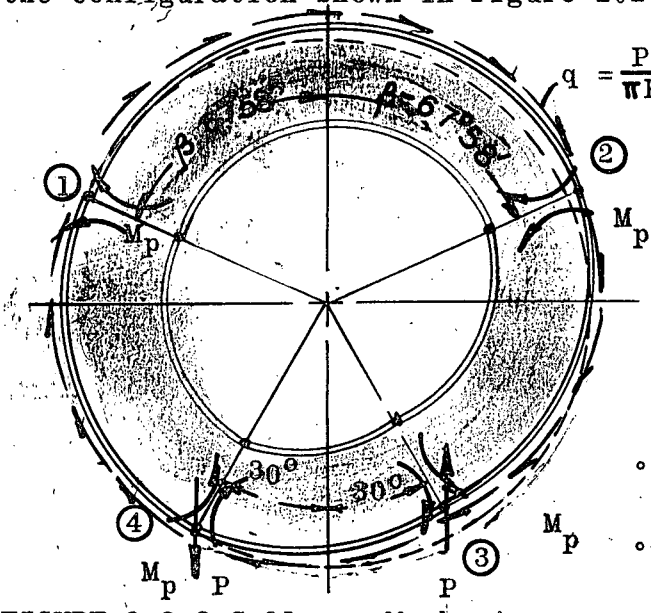

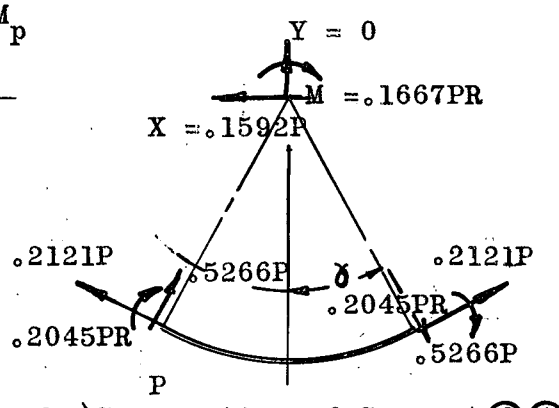

FIGURE 2.2.8 Collapse Mechanism b.)Segregation of Segment ③④

Note: The direction of M_p is always imposed on the structure opposite to the rotation of the deformed structure. That is, it attempts to restore it to its original shape.

The completeness of the plasticity check is verified only after all of the internal forces and moments have been evaluated, and

after the condition $M_a \quad M_p$ has been satisfied. Figures 2.2.9 (a) and (b) were constructed to verify the plasticity condition, $M_a \leq M_p$

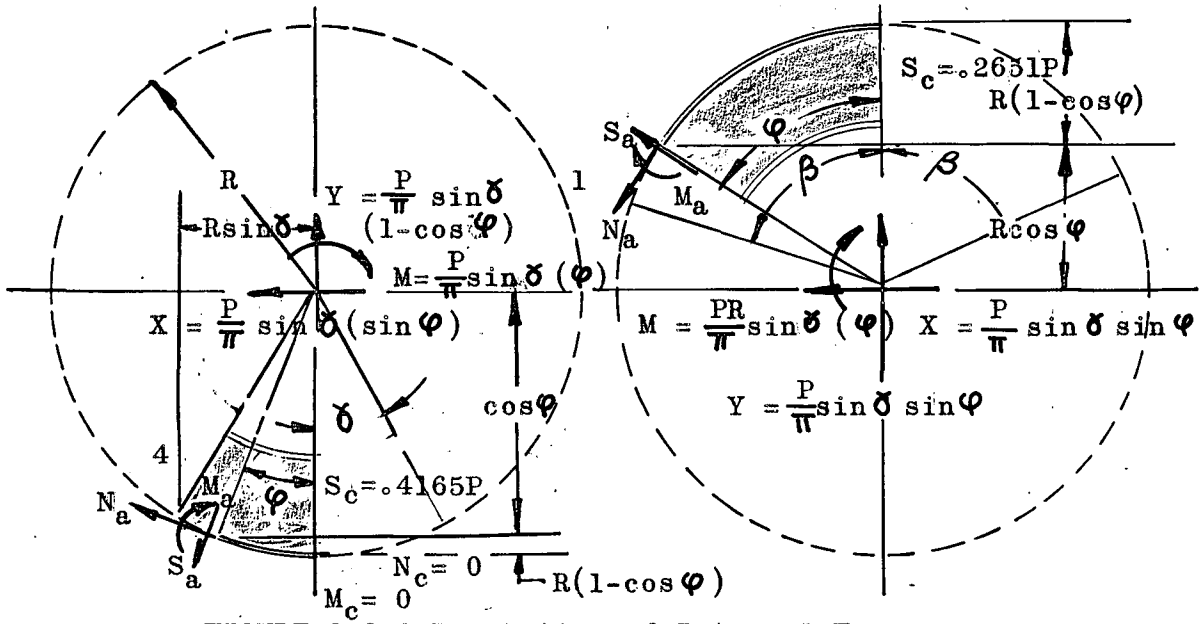

FIGURE 2.2.9 Resolution of Internal Forces

Since the concentrated applied loads have a pronounced effect on internal shear, axial load and moment, the equations for these internal forces and moments must be derived within two separate sectors.

Referring to Figure 2.2.9(a) and commencing with the internal forces and moments in the sector $(0^o$ to $30^o)$

$$M_a = .4165P(R\sin\varphi) + \frac{P}{\pi}\sin\delta\,(1-\cos\varphi)R\sin\varphi + \frac{P}{\pi}\sin\delta\sin\varphi\,R\cos\varphi - \frac{PR}{\pi}\sin\delta(\varphi)$$

$$M_a = \frac{PR\sin\delta}{\pi}\left[3.6172\sin\varphi - \varphi\right] \qquad \ldots\ldots\ldots\ldots\ldots\ldots\ldots\ldots\ldots\ldots (2.2.20)$$

$$N_a = \frac{P\sin}{\pi}\left[\frac{.4165\pi}{\sin\delta} + (1-\cos\varphi)\right] \sin\varphi + \frac{P}{\pi}\sin\delta\,(\sin\varphi)\cos\varphi$$

$$N_a = \frac{P\sin\delta}{\pi}(3.6172\sin\varphi) \qquad \ldots\ldots\ldots\ldots\ldots\ldots\ldots\ldots\ldots\ldots (2.2.21)$$

$$S_a = \frac{P\sin\delta}{\pi}\left[\frac{.4165\pi}{\sin\delta} + (1-\cos\varphi)\right]\cos\varphi - \frac{P}{\pi}\sin\delta\,(\sin\varphi)\sin\varphi$$

$$S_a = \frac{P\sin\delta}{\pi}(3.6172\cos\varphi - 1) \qquad \ldots\ldots\ldots\ldots\ldots\ldots\ldots\ldots\ldots\ldots (2.2.22)$$

From Figure 2.2.9(b), the expressions for internal forces between δ and 180° become

$$M_a = .2651(R\sin\varphi) + \frac{P}{\pi}\sin\delta\,(\sin\varphi)R\cos + \frac{P}{\pi}\sin\delta\,(1-\cos\varphi)\sin\varphi - \frac{PR}{\pi}\sin\delta\,(\varphi)$$

$$M_a = \frac{PR}{\pi}\sin\delta\left[2.666\sin\varphi - \varphi\right] \qquad \ldots\ldots\ldots\ldots\ldots\ldots\ldots\ldots\ldots\ldots (2.2.23)$$

$$N_a = \left[.2651P + \frac{P\sin}{\pi}(1-\cos\varphi)\right]\sin\varphi + \left[\frac{P\sin\delta}{\pi}\sin\varphi\right]\cos\varphi$$

$$N_a = \frac{P}{\pi}\sin\delta\,(2.666\sin\varphi) \qquad \ldots\ldots\ldots\ldots\ldots\ldots\ldots\ldots\ldots\ldots (2.2.24)$$

$$S_a = \left[.2651P + \frac{P\sin}{\pi}(1-\cos\varphi)\right]\cos\varphi - \left[\frac{P\sin\delta}{\pi}\sin\varphi\right]\sin\varphi$$

$$S_a = \frac{P}{\pi}\sin\delta\,(2.666\cos\varphi - 1) \qquad \ldots\ldots\ldots\ldots\ldots\ldots\ldots\ldots\ldots\ldots (2.2.25)$$

Values of φ from 0° to 30° must be substituted into 2.2.20, 2.2.21, 2.2.22 and values of φ from 0° to 150° must be substituted into equations 2.2.23, 2.2.24, 2.2.25. This is evident since the equations for the internal forces and moments within the range $180^\circ > \varphi > \delta = 30^\circ$ initiate at the very top of the ring and proceed around the ring counterclockwise, whereas the equations for the lower portion of the ring begin at 0° and advance clockwise.

The equations for the internal forces and moments have been ascertained, and all that remains is to give φ definite incremental angles of 5°, and substitute them into equations 2.2.20 through 2.2.25. As a consequence of this operation, Tables 2.2.1, and 2.2.2 were composed and Figures 2.2.10,

TWISTING MOMENT 2PR sin δ ON A TANGENTIALLY SUPPORTED CIRCULAR RING

Where $\delta = 30^{\circ}$

TABLE 2.2.1

Comparison of Plastic to Elastic Moment, Shear and Axial Load Co						
Angle φ From Vertical	Plastic Moment Coeff.	Elastic* Moment Coeff.	Plastic Shear Coeff.	Elastic* Shear Coeff.	Plastic Axial Load Coeff.	Elastic* Axial Load Coeff.
0	0	0	.41655	.52884	0	0
5	.03629	.04637	.41435	.52618	-.05178	-.06062
10	.07219	.09300	.40780	.51827	-.09997	-.12077
15	.10734	.13834	.39693	.50514	-.14900	-.18001
20	.14022	.18232	.38183	.48689	-.19690	-.23787
25	.17386	.22449	.36261	.46367	-.24330	-.29393
30	.20452	.26442	.33942	.43566	-.28785	-.34775
30	.20452	.26442	-.52661	-.42286	.21215	.15225
35	.15941	.22813	-.50672	-.40859	.24337	.17466
40	.11615	.19316	-.48418	-.39241	.27274	.19573
45	.07497	.15969	-.45918	-.37447	.30003	.21531
50	.03608	.12785	-.43189	-.35488	.32503	.23326
55	-.00343	.09779	-.40252	-.33381	.34756	.24943
60	-.03412	.06963	-.37130	-.31141	.36746	.26371
65	-.06510	.04347	-.3385	-.28784	.38455	.27597
70	-.09315	.01942	-.30427	-.26330	.39871	.28613
75	-.11818	-.00246	-.26897	-.23797	.40984	.20413
80	-.14008	-.02210	-.23283	-.21203	.41785	.29987
85	-.15879	-.03945	-.19614	-.18570	.42268	.30334
90	-.17430	-.05450	-.15915	-.15916	.42430	.30450

*See reference 2, Table IV, Case No. X for Elastic Equations

TWISTING MOMENT $2PR\sin\delta$ ON A TANGENTIALLY SUPPORTED RING

Where $\delta = 30^{\circ}$

TABLE 2.2.2

Comparison of Plastic to Elastic Moment, Shear and Axial Load Coefficient						
Angle From Vertical	Plastic Moment Coeff.	Elastic* Moment Coeff.	Plastic Shear Coeff.	Elastic* Shear Coeff.	Plastic Axial Load Coeff.	Elastic* Axial Load Coeff.
95	-.18657	-.06551	-.12217	-.13262	.42268	.30334
100	-.19563	-.07765	-.08548	-.10633	.41785	.29987
105	-.20151	-.08563	-.04934	-.08034	.40984	.29413
110	-.20427	-.09169	-.01404	-.05501	.39871	.28613
$112^{\circ}2'$	-.20452		0		.39331	
115°	-.20399	-.0954	.02016	-.03047	.38455	.27597
120	-.20079	-.09704	.05299	-.00691	.36746	.26371
125°	-19479	-.09665	.08421	.01550	.34756	.24943
130°	-.18614	-.09437	.11358	.03657	.32503	.23326
135	-.17503	-.09031	.14087	.05616	.30003	.21532
140	-.16162	-.08462	.16588	.07410	.27274	.19573
145	-.14615	-.07743	.18841	.09028	.24337	.17466
150	-.12882	-.06892	.20830	.10455	.21215	.15225
155	-.10987	-.05924	.22539	.11682	.17932	.12869
160	-.08956	-.04860	.23955	.12698	.14512	.10414
165	-.06815	-.03714	.25069	.13497	.10982	.07881
170	-.04590	-.02510	.25870	.14072	.07368	.05288
175	-.02309	-.01265	.26353	.14418	.03698	.02654
180	0	0	.26514	.14535	0	0

*See reference 2, Table IV, Case No. X for Elastic Equations

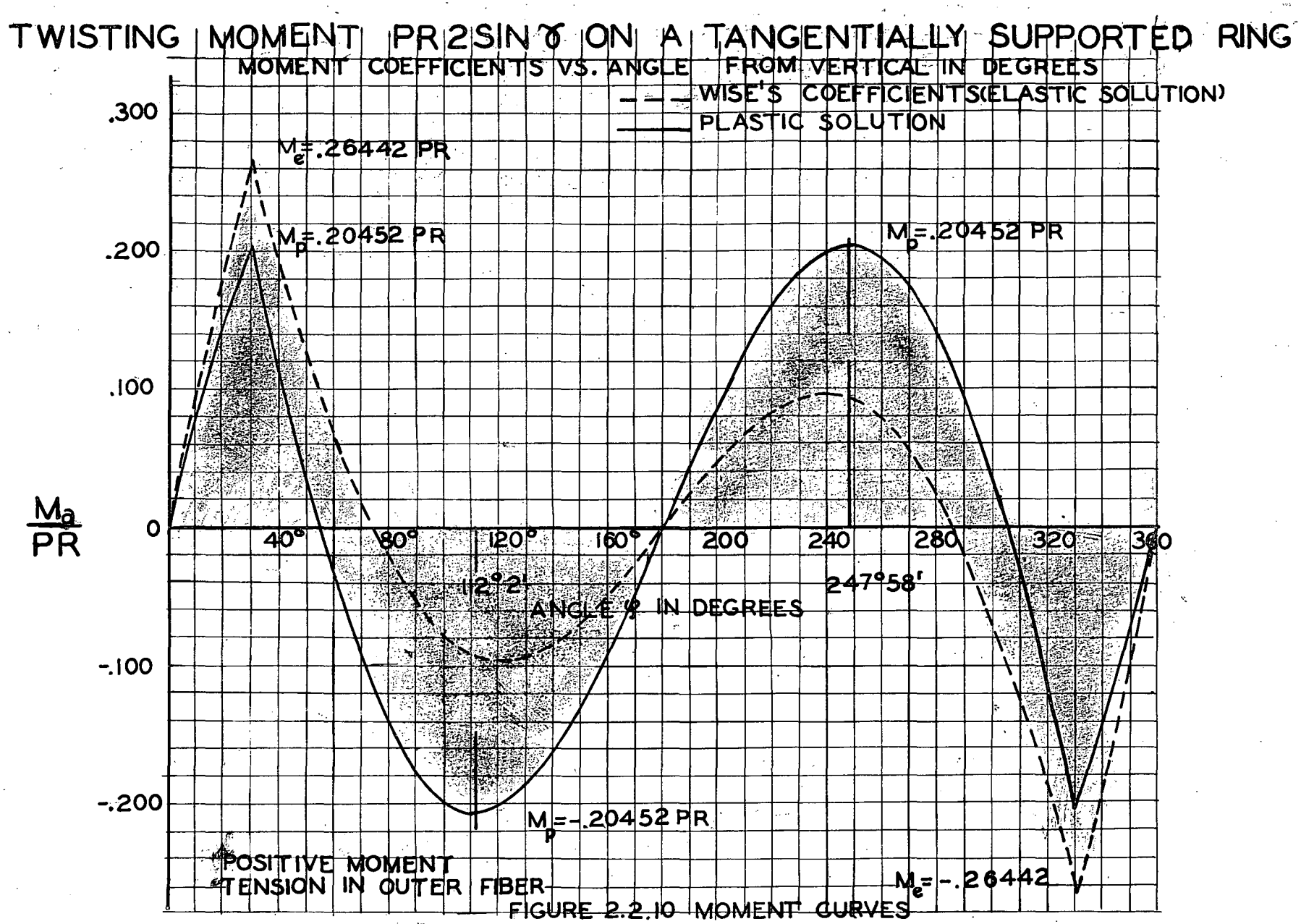

FIGURE 2.2.10 MOMENT CURVES

TWISTING MOMENT $2PRS\sin\gamma$ ON A TANGENTIALLY SUPPORTED RING

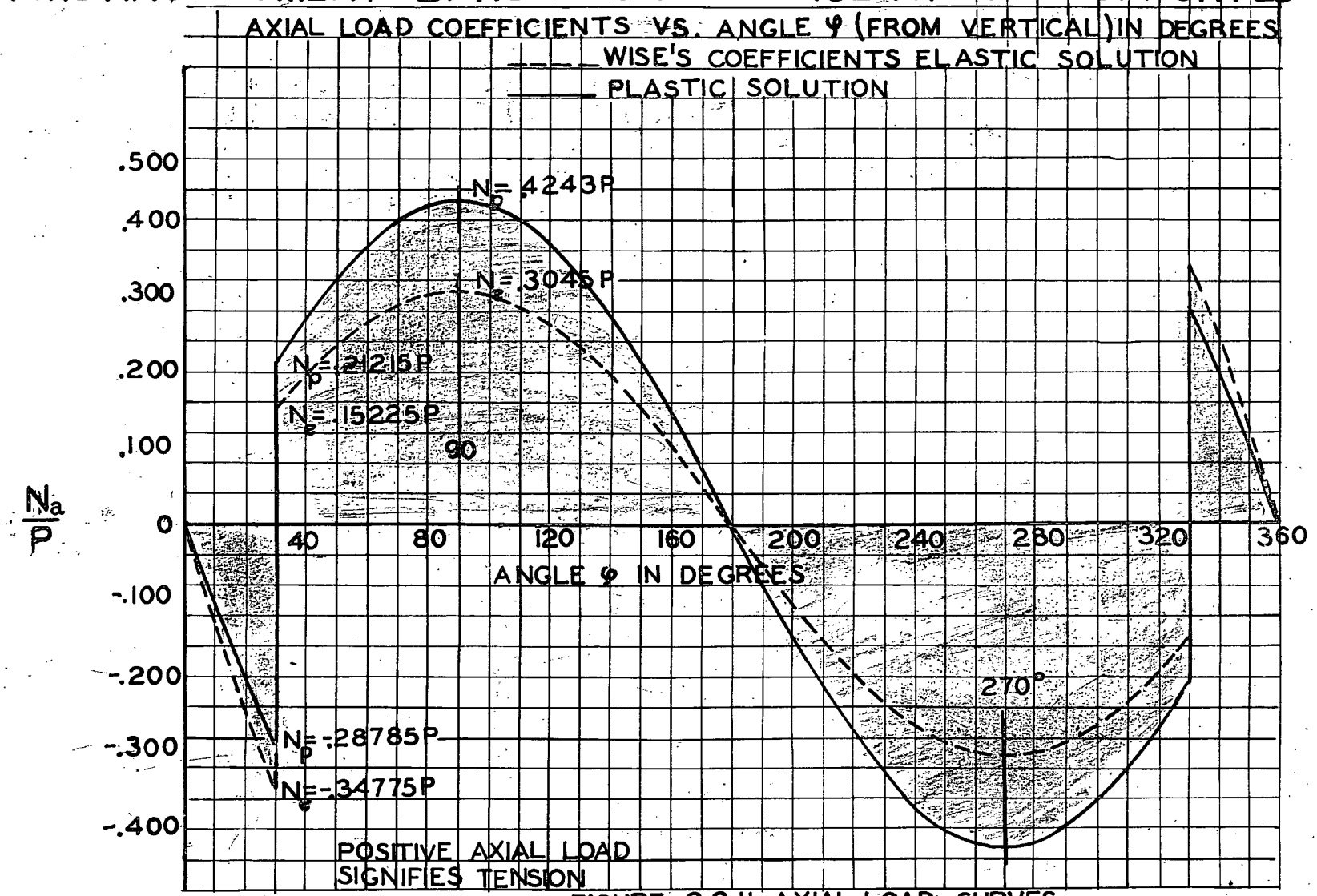

FIGURE 2.2.11 AXIAL LOAD CURVES

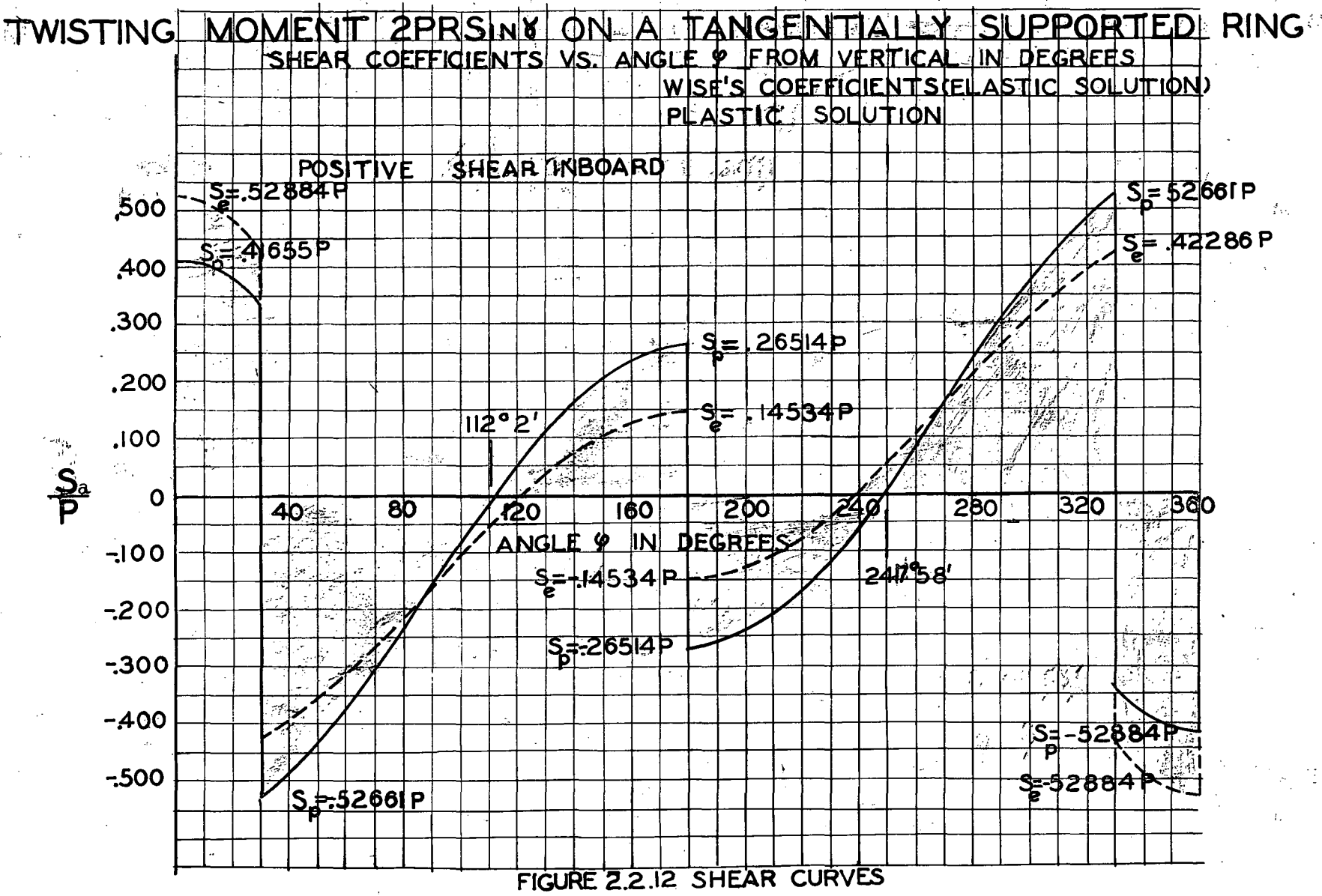

FIGURE 2.2.12 SHEAR CURVES

2.2.11, and 2.2.12 were constructed. Since the plot of the moment never exceeded the maximum plastic moment, M_p = .20452PR, this is the exact solution to the problem.

A noteworthy observation comes from Figures 2.2.10, 2.2.11, and 2.2.12. In the other cases when the moment was redistributed after the yield point was reached, the axial load always seem to redistribute in a similar manner, with its crests shifting in the same direction as the peak moments. However, this is not true for this loading. There is a definite redistribution of moment with the crests shifting from 120° and 240° (for the elastic solution) to 112° and 248° (for the plastic solution) respectively, but the crests of the axial load curve remain stationary at 90° and 270°. Also, of noteworthy mention is the fact that the elastic and plastic shear curves intersect at these same angles of 90° and 270°. The explanation for these pecularities may be clarified by segregating a quarter sector of the ring.

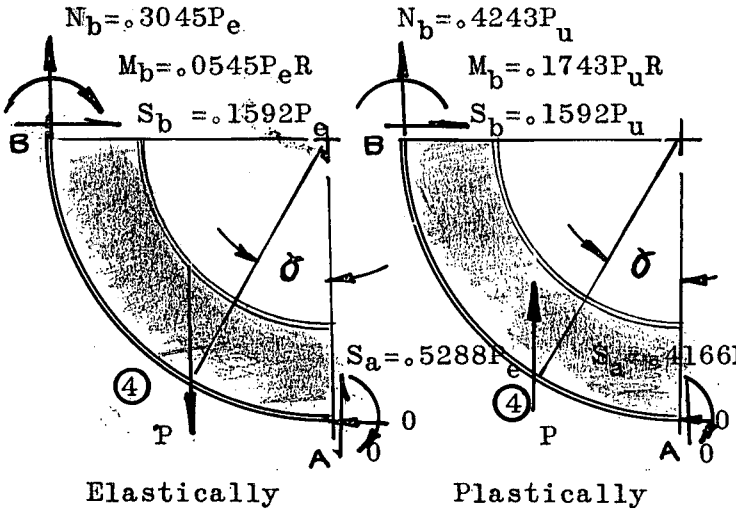

FIGURE 2.2.13
Elastic and Plastic Explanation

Referring to Figure 2.2.13, it can be seen that the shear flow and the shear at B is a linear function dependent only on P. That is, the external shear flow and internal shear at

90^{o} increase in the same linear proportions as the applied load. Also, the elastic and plastic axial loads and moments do not change at A, but remain zero. Thus, as P is increased above the yield load, the shear at A decreases necessitating an increase in the axial load at B for equilibrium of vertical forces. If moments are equilibrated about point B, it may be discerned that the moment must increase at B for the plastic case since the shear decreases and since the only other equilibrating force is the shear flow which increases in same proportion as the load. This explains the shifting of moment crest.

The justification of the assertion that the axial load does not redistribute stems from the observation that the only horizontal forces which might influence the magnitude of the axial load at any point are the shear at the point and the external shear flow. Since these loads both increase linearly, they just balance out each other, and hence the axial load at B is always a maximum at this point being dependent on the vertical forces only.

2.2.4 Lower Bound of Loading 2.2.0 (Shear Influence)

As mentioned on page 95, there is some lower bound of this loading where the hinges form at the location of the concentrated loads, but the shears produced by the large loads are so intense that the ring fails in combined shear distortion and bending. In solving this problem, it will be assumed that the bending stresses and deflections are of such small proportions relative to the shear stresses and deflections that the bending moment can be neglected. Referring to 2.2.15, the problem can be

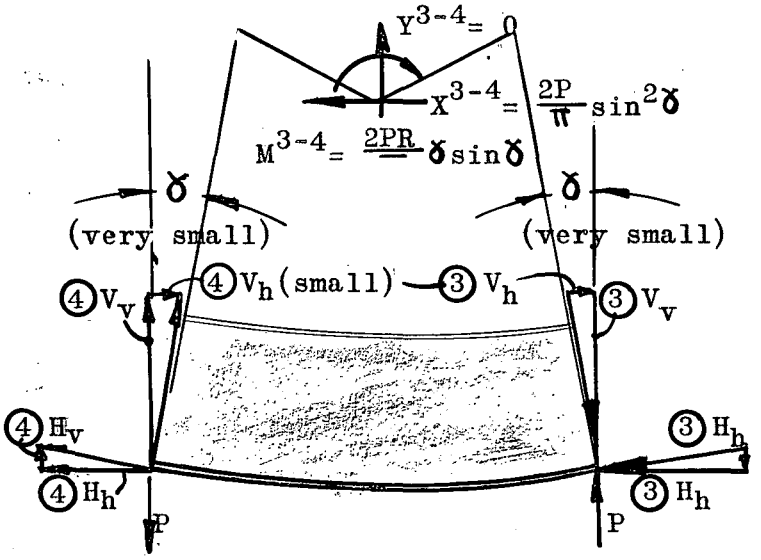

FIGURE 2.2.15 Lower Bound

reduced from a complex situation to one of relative simplicity by making a few assumptions. It is noticeable from Figure 2.2.15 that, since the angle is comparatively small, the vertical component of the axial loads are insignificant as contrasted with the vertical component of the shears. Hence, if moments are taken about hinge ③ the only unknown is $4V_v$ (if $4H_v$ is neglected).

Summing moments about hinge ③,

$$\sum M_3 = 0$$

$$\frac{2P\sin^2\delta}{\pi}\delta R\cos\delta - \frac{2PR}{\pi}\delta\sin\delta - 2M_p + 2PR\sin\delta - 2\,④V_v\sin\delta\, R$$

Collecting terms,

$$④V_v\sin = P\sin\delta - M_p - \frac{P}{\pi}\delta\sin\delta + \frac{P\sin^2\delta}{\pi}\delta\cos\delta$$

$$④V_v = P - M_p\sin\delta - \frac{P}{\pi}\delta + \frac{P}{\pi}\delta\sin\delta\cos\delta$$

$$④V_v = \frac{P}{\pi}\left[\pi - \frac{\pi M_p}{\sin\delta} - \delta + \delta\sin\delta\cos\delta\right] \quad \text{.....(2.2.26)}$$

According to equation 2.2.14, for small values of δ, M_p approaches zero, and consequently it may be eliminated from 2.2.25. Expression 2.2.25 reduces to

$$④V_v = \frac{P}{\pi}\left[\pi - \delta + \delta\sin\delta\cos\delta\right] \quad \text{.....(2.2.27)}$$

Assuming that the section fails in combined shear and axial stress due to ④H_H or ③H_H. According to Stimoshenko, "Strength of Materials, Part II", D. Van Nostrand Company, Page 454, combined axial tension and shear stresses result in the principal stresses.

$$\sigma_1^* = \frac{\sigma}{2} + \sqrt{\frac{\sigma^2}{4} + \tau^2} \quad , \sigma_2^* = \frac{\sigma}{2} - \sqrt{\frac{\sigma^2}{4} + \tau^2} \quad \text{.....(2.2.28)},$$

and the condition of yielding becomes

$$\sigma^2 + 3\tau^2 = \sigma_{Y.P.}^2 \quad \text{.....(2.2.29)}$$

where σ and τ denote axial stress and shear stress, and $\sigma_{Y.P.}$ the yield stress in tension, respectively.

Assuming that each horizontal component is half of X in Figure 2.2.15, then ④$H \approx \frac{P\sin^2}{\pi}$ the expression for ④V_V, and axial load ④H are substituted into 2.2.28.

$$\left[\frac{P\sin^2\delta}{A}\right]^2 + 3\left[\frac{P(\pi - \delta + \delta\sin\delta\cos\delta)}{A}\right]^2 = \sigma_{Y.P.}^2 \text{....(2.2.30)}$$

where A = cross sectional area at critical section.

It can be seen that the axial stress $\left[\frac{P\sin^2\delta}{A}\right]^2$ is insignificant compared with the shearing stress. Since δ is a very small angle, $\frac{P\sin^2\delta}{\pi}$ will even be smaller by the square, the influence of the axial stress is even smaller yet when the bracket is squared. However, the shear stress is exactly equal to $\frac{P}{A}$ if the rest of the parenthesis, $-\delta + \delta\sin\delta\cos\delta$, is neglected. Hence, expression 2.2.29 could very readily be reduced to

$$\left[\frac{P}{\pi}(\pi - \delta + \delta\sin\delta\cos\delta)\right] = \frac{\sigma_{Y.P.}A}{\sqrt{3}} \quad \text{.....(2.2.31)}$$

*See Section V for exact definition of terms

The exact value of δ which corresponds to a shear distortion failure depends on the yield stress of the material employed and the size of the cross section. Since it is felt that selecting a material and solving for δ extends very little additional clarity to the problem, it shall be left up to the analyst to employ the preceding method to his own particular analysis.

Upper Bound of Ring Loading 2.2.0

Just as there is a lower bound, there is an upper bound of the problem, wherein there is a transition of the lower hinges ③ and ④ away from the concentrated loads. In order to find this angle, a hinge pattern as suggested in Figure 2.2.16 is employed. The procedure applied is outlined as followed.

First assume that the hinges form at an angle α (less than δ), solve the problem using the resulting hinge pattern (see Figure 2.2.16), and then maximize the maximum moment, M_p, obtained, with respect to α and β. The exact point at which the lower hinge locations (③ and ④) diverge from the position of the concentrated loads may be ascertained by permiting δ to approach α (or $\delta - \alpha \to 0$).

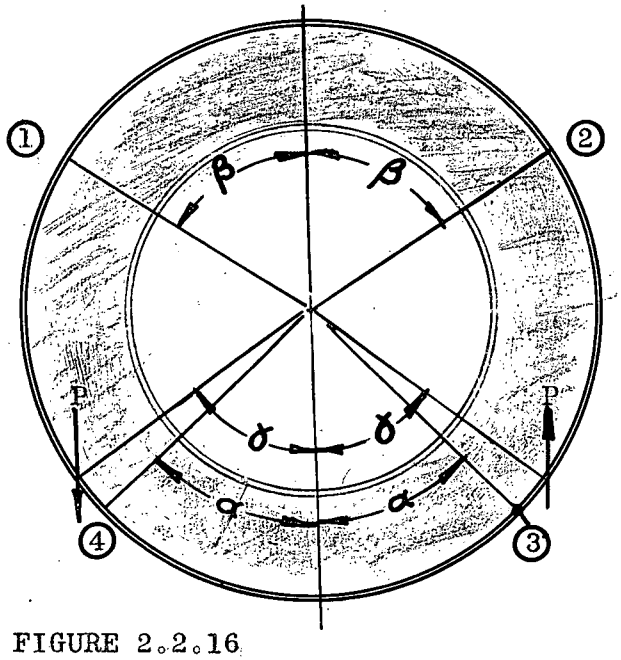

FIGURE 2.2.16
Hinge Pattern for Upper Bound

To begin this procedure, the structure may be held again between

hinges ① and ④ to permit a sidesway or "panel" type mechanism. If segment ③-④ is given a virtual rotation of θ, then the basic geometry assumes the disposition shown in Figure 2.2.17. The only real diversity between the geometry of Figure 2.2.3 and that of Figure 2.2.17 is the replacement of angle δ of the former case with α in the latter case. Hence, all of the trigonometric relations pertaining to the virtual rotations and deflections hold true with the substitution of α for δ

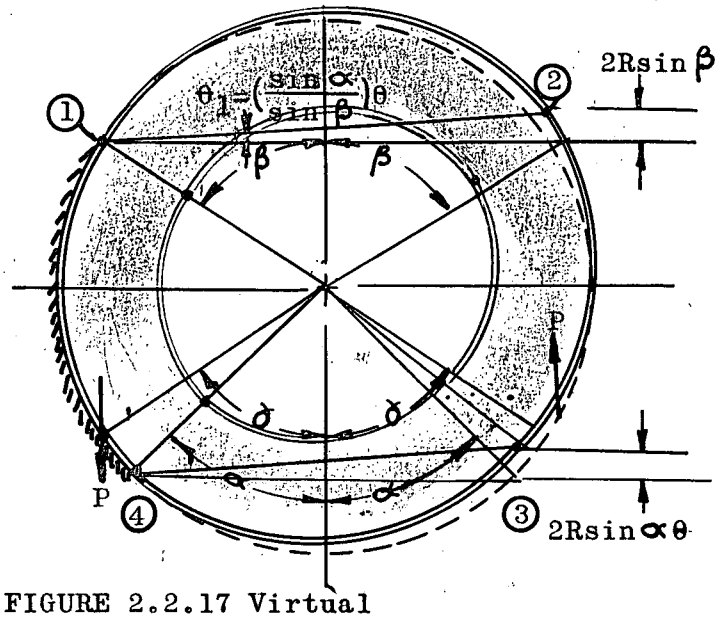

FIGURE 2.2.17 Virtual Rotations and Deflections

$$\theta_1 = \frac{(\sin\alpha)}{(\sin\beta)}\ \theta \quad ..(\text{See eq. } 2.2.2) \quad ....(2.2.32)$$

$$\theta_2 = \left(\frac{\sin\alpha}{\sin\beta}\right)\theta \quad ..(\text{See eq. } 2.2.3) \quad ....(2.2.33)$$

$$\theta_3 = \theta \quad ....(\text{See eq. } 2.2.4) \quad ....(2.2.34)$$

$$\theta_4 = \theta \quad ....(\text{See eq. } 2.2.5) \quad ....(2.2.35)$$

Referring to Figure 2.2.4 and equations 2.2.6, 2.2.7, and 2.2.8, the resolution of the shear flows must again be evaluated in order to obtain a solution to this new problem.

Between hinges ① and ② the equivalent shear components

remain the same. (See page 98)

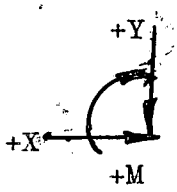

$$X^{1-2} = \frac{2P}{\pi} \sin\delta \sin\beta$$

$$Y^{1-2} = 0$$

$$M^{1-2} = \frac{PR}{\pi}(\sin\delta)\beta$$

Between hinge (2) and the applied load the equivalent shear components are identical to the evaluation between hinges (2) - (3) of Figure 2.2.3.

X^{2-P} = This moment does no work

$$Y^{2-P} = \frac{P\sin}{\pi}\left[\cos\beta + \cos\alpha\right]$$

M^{2-P} = This moment does no work

Between the applied load and hinge (3)

X^{P-3} = This component does no work

$$Y^{P-3} = \frac{P\sin}{\pi}\left[\sin\varphi\right]_{\frac{3\pi}{2}+\alpha}^{\frac{3\pi}{2}+\delta} = \frac{P\sin\delta}{\pi}\left[\sin(\tfrac{3\pi}{2}+\delta) - \sin(\tfrac{3\pi}{2}+\alpha)\right] = \frac{P\sin\delta}{\pi}(\cos\alpha - \cos\delta)$$

M^{P-3} = This moment does no work

Between hinges (3) and (4),

$$X^{3-4} = \frac{P\sin\delta}{\pi}\left[-\cos\varphi\right]_{\frac{3\pi}{2}-\alpha}^{\frac{3\pi}{2}+\alpha} = \frac{P\sin}{\pi}\left[-\cos(\tfrac{3\pi}{2}+\alpha) + \cos(\tfrac{3\pi}{2}-\alpha)\right] = -\frac{2P}{\pi}\sin^2\alpha$$

$Y^{3-4} = 0$ (From observation)

$$M^{3-4} = \frac{PR\sin\delta}{\pi}\left[\varphi\right]_{\frac{3\pi}{2}-\alpha}^{\frac{3\pi}{2}+\alpha} = \frac{PR\sin\delta}{\pi}\left[\tfrac{3\pi}{2}+\alpha-(\tfrac{3\pi}{2}-\alpha)\right] = \frac{2PR}{\pi}\alpha\sin\delta$$

The evaluation of the internal work is exactly the same as before (see equation 2.2.9).

$$W_{int} = 2M_p\theta\left[\frac{\sin\beta+\sin\alpha}{\sin\beta}\right] \quad \text{.....(2.2.36)}$$

The external work isascertained in a similar manner as used before by performing the addition of the products of external forces and moments and their corresponding virtual movements. Referring to Figures 2.2.5 through 2.2.7,

$$W_e^{1-2} = \left[\frac{2P\sin\delta\sin\beta}{\pi}\right] R\cos\beta\left(\frac{\sin\alpha}{\sin\beta}\right)\theta - \frac{2PR\sin\delta}{\pi}\left(\frac{\sin\alpha}{\sin\beta}\right)\theta \text{...(2.2.37)}$$

$$W_e^{2-P} = \frac{-P\sin\delta}{\pi}\left[\cos\beta+\cos\delta\right] 2R\sin\alpha\theta + 2P\sin\alpha R\theta \quad \text{.....(2.2.38)}$$

$$W_e^{P-3} = \frac{P\sin\delta}{\pi}\left[\cos\alpha-\cos\delta\right] 2R\sin\alpha\theta \quad \text{.....(2.2.39)}$$

$$W_e^{3-4} = \frac{-2P\sin\delta}{\pi}\sin\alpha(-R\cos\alpha\theta) - \frac{2PR}{\pi}\sin\delta(\theta)\alpha \quad \text{.....(2.2.40)}$$

The principle of virtual displacements is employed by equating equation 2.2.36 to the sum of 2.2.37 through 2.2.40.

$$2\,M_p\theta\underbrace{\left[\frac{\sin\beta+\sin\alpha}{\sin\beta}\right]}_{2.2.36} =$$

$$\underbrace{\left[\frac{2P\sin\delta\sin\beta}{\pi}\right] R\cos\beta\left(\frac{\sin\alpha}{\sin\beta}\right)\theta - \frac{2PR}{\pi}\sin\delta\left(\frac{\sin\alpha}{\sin\beta}\right)\theta\beta}_{2.2.37}$$

$$\underbrace{-\frac{P\sin\delta}{\pi}\left[\cos\beta+\cos\delta\right] 2R\sin\alpha\theta - 2PR\theta\sin\alpha}_{2.2.38} \underbrace{-\frac{P\sin\delta}{\pi}\left[\cos\alpha-\cos\delta\right] 2R\theta\sin\alpha}_{2.2.39}$$

$$\underbrace{-\frac{2P\sin\delta}{\pi}\left[\sin\alpha\right](-R\cos\ \ 0) - \frac{2PR}{\pi}\sin\delta\,\theta\,\alpha}_{2.2.40}$$

$$2M_p\ \theta\left[\frac{\sin\beta+\sin\alpha}{\sin\beta}\right]$$

$$\frac{2PR\sin\delta}{\pi}\left\{\sin\beta\cos\beta\frac{\sin\alpha}{\sin\beta} - \beta\frac{\sin\alpha}{\sin\beta} - \sin\alpha\cos\beta - \sin\alpha\cos\alpha + \pi\frac{\sin\alpha}{\sin\delta}\right.$$

$$-\sin\alpha\cos\alpha+\sin\alpha\cos\alpha-\alpha+\sin\alpha\cos\delta\Big]$$

$$M_p = \frac{PR\sin\delta}{\pi(\sin\beta+\sin\alpha)}\left\{(\pi\frac{\sin\alpha}{\sin\delta}-\alpha)\sin\beta-\beta\sin\alpha\right\}. \quad \ldots\ldots\ldots (2.2.41)$$

Note the similarity of expression 2.2.41 to 2.2.14.

In order to obtain a solution to the problem at hand expression 2.2.39 must be maximized with respect to both angles α and β. If the exact angle at which the lower hinges translate away from the concentrated loads is desired, δ must approach the angle α for this to transpire.

Equation 2.2.41 becomes

$$M_p = \frac{PR\sin\alpha}{(\sin\beta+\sin\alpha)}\left\{(\pi-\alpha)\sin\beta-\beta\sin\alpha\right\} \quad \ldots\ldots\ldots\ldots (2.2.42)$$

if $\alpha=\delta$.

To maximize the solution $\frac{\partial M_p}{\partial\alpha} = 0$

$$=PR\sin\delta\left[\frac{(\sin\beta+\sin\alpha)(-\sin\beta-\beta\cos\alpha)-\cos\alpha(\pi-\alpha)\sin\beta-\beta\sin\alpha}{(\sin\beta+\sin\alpha)^2}\right]$$

$$= -\sin\beta-\beta\cos\alpha-\sin\alpha-\pi\cos\alpha+\alpha\cos\alpha$$

$$=-\cos(\pi+\beta-\alpha)-\sin\beta-\sin\alpha \quad \ldots\ldots\ldots\ldots\ldots\ldots (2.2.43)$$

and $\frac{\partial M_p}{\partial\beta} = 0$

$$PR\sin\delta\left\{\frac{(\sin\beta+\sin\alpha)\left[(\pi-\alpha)\cos\beta-\sin\alpha\right]-\cos\beta\left[(\pi-\alpha)\sin\beta-\beta\sin\alpha\right]}{(\sin\beta+\sin\alpha)^2}\right\}$$

$$= -\sin\beta+(\pi-\alpha)\cos\beta-\sin\alpha+\beta\cos\beta$$

$$= \cos\beta(\pi+\beta-\alpha)-\sin\beta-\sin\alpha \quad \ldots\ldots\ldots\ldots\ldots\ldots (2.2.44)$$

Subtracting expression 2.2.43 from 2.2.44

$$\cos\alpha(\pi+\beta-\alpha)+\cos\beta(\pi+\beta-\alpha)=0$$

Therefore,

$$\cos\alpha = -\cos\beta \qquad \text{.....(2.2.45)}$$

Observation of equations 2.2.41, 2.2.42 and 2.2.45 reveals that α and β must be equal in order to satisfy the equations. From the solution of the limiting case, loading 7.1.0, this fact is borne out as specified. The solution to this problem was

$$\alpha = \beta = 50^{\circ}\ 27'$$

Using Newtons' iteration process on page 102

$$h_o = \frac{-\cos\beta(\pi-\alpha+\beta)-\sin\beta-\sin\alpha}{-\sin\beta(\pi-\alpha+\beta)-\cos\beta} \qquad \text{.....(2.2.46)}$$

For h_o to vanish the top part of equation 2.2.46 must equal zero, or if $\alpha=\beta$

$$\pi\cos\beta = 2\sin\beta$$

$$\frac{\pi}{2} = \tan\beta$$

$$\beta = \alpha = 57^{\circ}\ 30' \qquad \text{.....(2.2.47)}$$

Thus as the angle δ approaches the value $57^{\circ}\ 31'$, the lower hinges form immediately at the position of the concentrated load, and β is always larger than δ but is getting smaller. When δ reaches the value $57^{\circ}\ 30'$, the lower hinges form at the locations of the concentrated loads and $\beta=\delta=\alpha$. Once δ has progressed beyond the magnitude $57^{\circ}31'$, α equals β but both are less than δ.

The conclusion that α must equal β may also be determined in another manner to substantiate this deduction. Returning to equation 2.2.41, suppose that the analyst does not eliminate δ by letting it equal α and β as before.

$$\frac{\partial M_p}{\partial \alpha} = \frac{(\sin\beta+\sin\alpha)\left[(\pi\frac{\cos\alpha}{\sin\delta}-1)\sin\beta-\beta\cos\alpha\right]-\cos\alpha\left[(\pi\frac{\sin\alpha}{\sin\delta}-\alpha)\sin\beta-\beta\sin\alpha\right]}{(\sin\alpha+\sin\beta)^2}$$

This reduces to

$$\cos\alpha(\pi\frac{\sin\beta^*}{\sin\alpha}+\alpha-\beta)-\sin\alpha-\sin\beta = 0 \quad \text{.....(2.2.48)}$$

Also $\frac{\partial M_p}{\partial \beta} = 0$

$$= \frac{(\sin\beta+\sin\alpha)\left[(\pi\frac{\sin\alpha^*}{\sin\delta}-\alpha)\cos\beta-\sin\alpha\right]-\cos\beta\left[(\pi\frac{\sin\alpha}{\sin\delta}-\alpha)\sin\beta-\beta\sin\alpha\right]}{(\sin\beta+\sin\alpha)^2}$$

This reduces to

$$\cos\beta(\pi\frac{\sin\alpha^*}{\sin\delta}-\alpha+\beta)-\sin\alpha-\sin\beta = 0 \quad \text{.....(2.2.49)}$$

The only difference between 2.2.49 and 2.2.45 is the term $\frac{\sin\alpha^*}{\sin\delta}$, and likewise between 2.2.48 and 2.2.44 is the term $\frac{\sin\beta^*}{\sin\alpha}$. If α approaches δ both of these * terms must drop out of the expression.

$$\text{or } \sin\delta = \sin\alpha = \sin\beta$$

$$\delta = \alpha = \beta \quad \text{.....(2.2.50)}$$

for a solution. Hence the solution to the upper bound or upper range problem was very simple.

This particular loading was chosen not only for its generality of loading, but also to study the influence of the position of the concentrated load within different sectors of the lower half of the ring. It was interesting to investigate the upper bound, or the position of the applied load at which the lower hinges translate away from this load. Of equal interest, is the revelation that the lower bound was dependent on the

strength of the material and the area of the cross section.

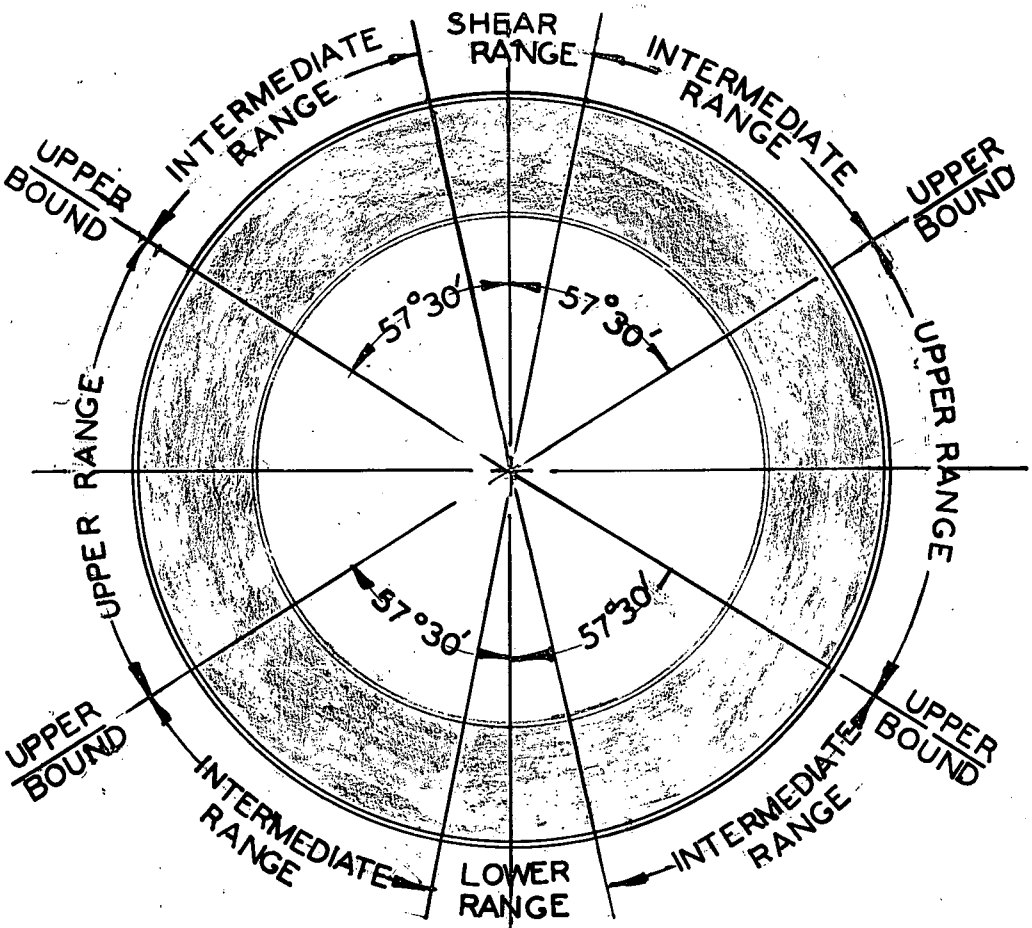

FIGURE 2.2.18
Representation of Upper and Lower Ranges of δ Which Determine the Upper and the Lower Bound for Loading 2.0.0

In order to visualize the picture better, Figure 2.2.18 was constructed. Note: no applied loads are shown; just the boundaries.

2.3.0 Loading condition-Ring IV-Equal Vertical Loads at Equal Angles to the Vertical Axis

The last loading condition of section IV is another general loading case. The problem at hand is a circular ring laden with two equal vertical down loads imposed at equal angles to the vertical axis of symmetry as shown in Figure 2.3.1.

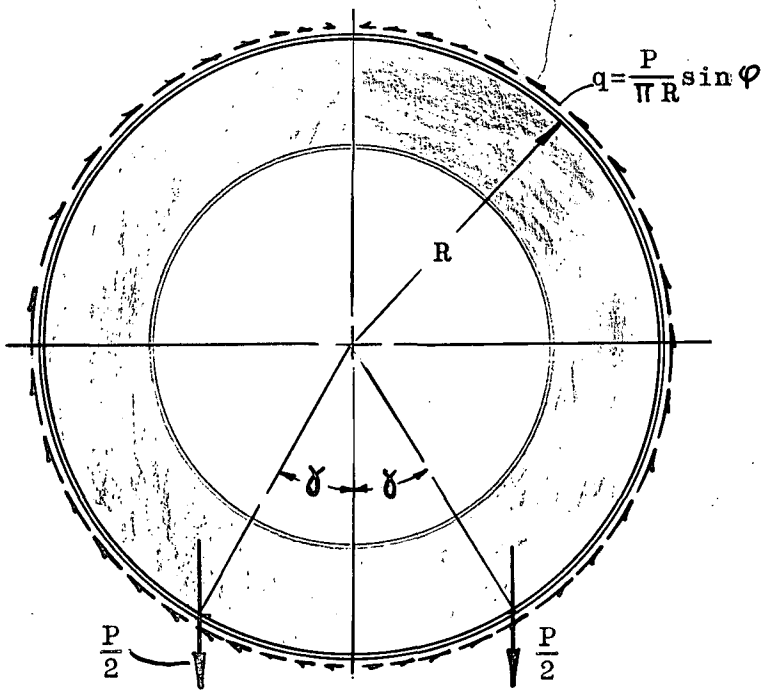

FIGURE 2.3.1 General Loading Condition-Ring IV

This loading is similar in nature to the preceding loading also has an upper and lower bound or range. The lower bound is very readily obtained since it depends upon γ approaching zero. When γ exactly equals zero, Loading 2.3.0 reduces to loading condition 2.0.0 (see Figure 2.0.1). The upper range is not so easily perceivable.

It is proposed to first determine the range of loading which constitutes the greater percentage of practical loading cases. The proposed procedure is to leave the angle, γ , in a general form and then later assign a value to it to obtain a specific answer to the problem.

The first step in the procedure is to ascertain the arrangement of the maximum moments around the ring, or the hinge pattern.

Actually the hinge pattern for this particular loading is not as easily conceivable as it may appear. From previous considerations, the concept that four plastic hinges reduce the ring to a kinematic mechanism was confirmed by the three example loadings preceding this case. Up to this case, four plastic hinges always created a mechanism failure. However, this problem is an exception to this general rule. Proceeding on the pretense that it is not known that four hinges do not induce failure, an attempt will be made to determine the hinge pattern. According to the rules employed in locating the hinges around the ring. The analyst is almost certain that two of the hinges will fall at the position of the concentrated loads. The other two hinge locations may be deduced from rule b on page 49. If δ is not a large angle (less than 50° say), then from the rule of symmetry it might be suspected that the hinges form at some unknown angle β. (See Figure 2.3.2) If for the first trial it is assumed that segment ① - ② is fixed in space, it is soon discovered the frame can't move vertically. With this

Case I-Fix Segment ① - ②

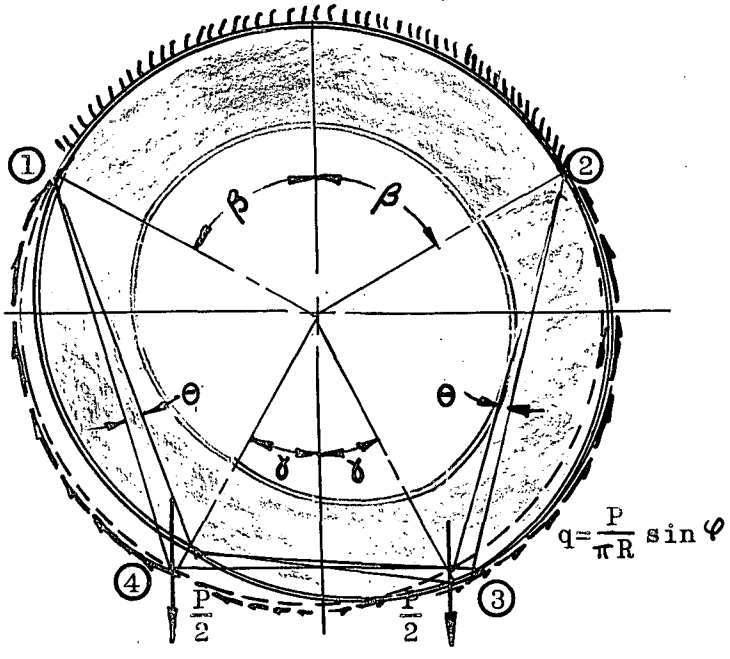

FIGURE 2.3.2 Assumed Hinge Pattern Trial 1

fixity no vertical movement is possible. Since only vertical loads are applied and no vertical deflection is possible, this failure configuration is not possible. The next resort to a solution is to fix some other point in space. It is obvious that

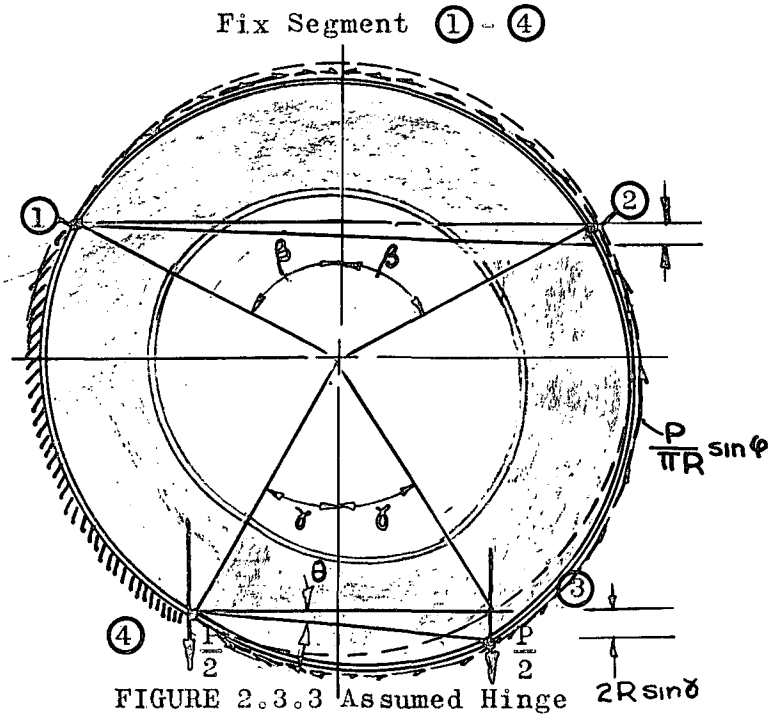

FIGURE 2.3.3 Assumed Hinge Pattern Trial 2

the same dilemma as before exists if segment ③ - ④ is fixed. Since the only other two possibilities yield the same result, assume segment ① - ④ is fixed and let the frame sway as shown in Figure 2.3.3. This possibility implies that segment ① - ④ translates vertically with respect to ② - ③ , but this is not physically possible because segment ③ - ④ just translates vertically and does not rotate. All failure possibilities have been eliminated and now the analyst is completely perplexed.

At this point the analyst will possibly realize that because of the symmetry of the applied load, it is conceivable that two of the hinges comprising the failure configuration will develop simultaneously. It may therefore be required that five hinges develop in order that the structure be reduced to

a mechanism. As will be demonstrated in the following, this is actually what happens.

Suppose that Figure 2.3.2 is ammended by inducing one more hinge at the upper most point of the ring (on the vertical axis). The next hinge pattern is as shown in Figure 2.3.4. By assuming hinge ① fixed in space, the failure assimilates that of Loading 2.0.0 (Figure 2.0.6).

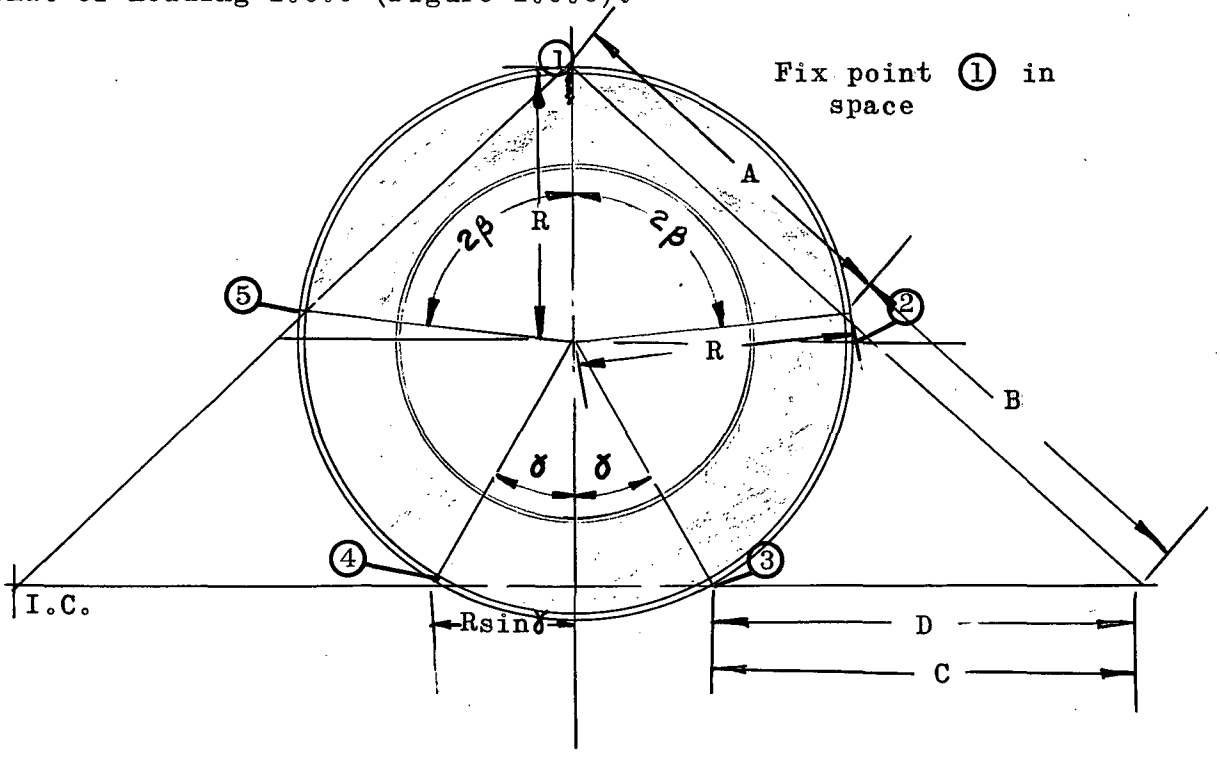

FIGURE 2.3.4 Assumed Hinge Pattern

The geometry of the failure configuration is resolved from noting Figure 2.3.4

$$\frac{R(1+\cos\gamma)}{A+B} = \sin\beta$$

$$A+B = \frac{R(1+\cos\gamma)}{\sin} \quad \text{.....(2.3.1)}$$

$$\frac{C}{A+B} = \cos\beta \quad \text{or} \quad C = (A+B)\cos\beta$$

$$C = \frac{R(1+\cos\gamma)}{\tan\beta} \qquad \text{.....(2.3.2)}$$

From the law of sines,

$$\frac{\sin 2\beta}{A} = \frac{\sin(90^\circ-\beta)}{R}$$

$$A = 2R\sin\beta \qquad \text{.....(2.3.3)}$$

Dimension B may now be determined from equations 2.3.1 and 2.3.3.

$$B = \frac{R(1+\cos\gamma)}{\sin\beta} - 2R\sin\beta$$

or

$$B = R\left[\frac{(1+\cos\gamma)-2\sin^2\beta}{\sin\beta}\right] \qquad \text{.....(2.3.4)}$$

and $D = C - R\sin\gamma$

$$D = \frac{(1+\cos\gamma)}{\tan\beta} - \sin\gamma \qquad \text{.....(2.3.5)}$$

Reconstructing the geometry just derived in Figure 2.3.5

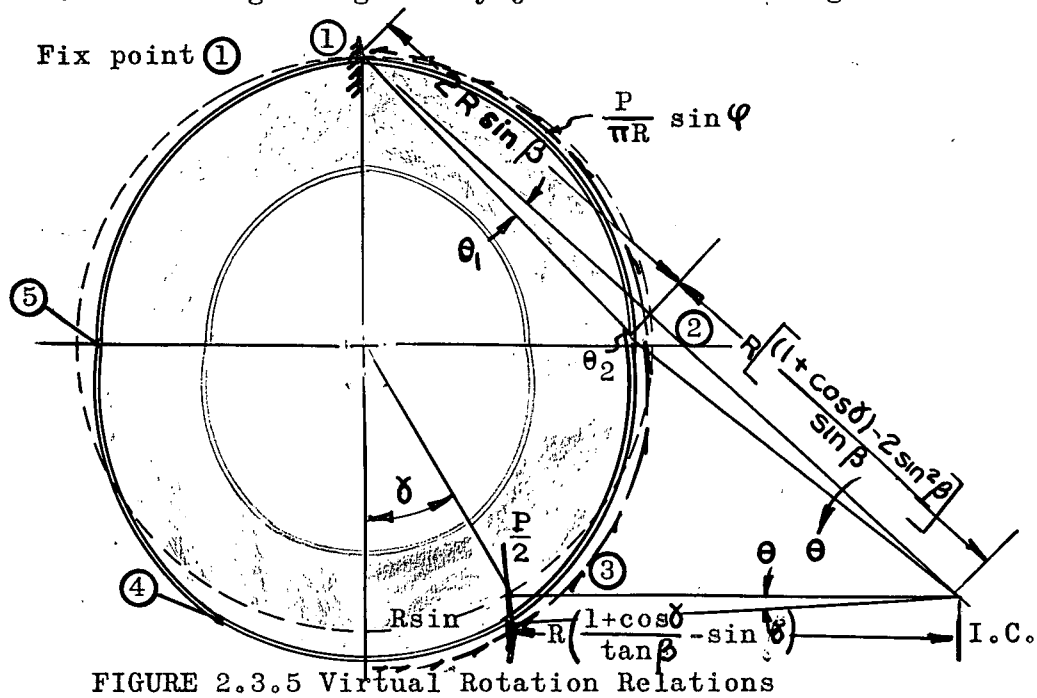

FIGURE 2.3.5 Virtual Rotation Relations

If a segment ② - ③ is given a virtual rotation of θ about the I.C. of segment ② - ③ of the mechanism, the resulting virtual rotations of the other segments are ascertained as follows:

$$\theta_1 = \frac{R\left[\frac{(1+\cos\delta)-2\sin^2\beta}{\sin\beta}\right]}{2R\sin\beta} = \theta\left[\frac{(1+\cos\delta)-2\sin^2\beta}{2\sin^2\beta}\right]$$

or summarizing,

$$\theta_1 = \theta\left[\frac{(1+\cos\delta)}{2\sin^2\beta} - 1\right]$$

$$\theta_2 = \theta + \theta_1 = \theta\left[\frac{1+\cos\delta}{2\sin^2\beta}\right]$$

$$\theta_3 = \theta$$

Before resolving the shear flows into their respective components as formerly proposed in the other examples, it was decided to amend the procedure for this problem. It is suggested to compute the internal work at this time, instead of resolving shear flows.

Hence,

$$W_{int} = M_p\left[\theta_1+\theta_2+\theta_3+\theta_4\right] = M_p\left[\frac{(1+\cos\delta)}{2\sin^2\beta} - 1 + \frac{(1+\cos\delta)}{2\sin^2\beta} + 1\right]$$

$$W_{int} = M_p\theta\left[\frac{1+\cos\delta}{\sin^2\beta}\right] \qquad \text{.....(2.3.7)}$$

In order to illustrate the external work a little better and eliminate the process of integrating for shear components with a summary afterwards, it was decided to illustrate the external work as the components are progressively integrated.

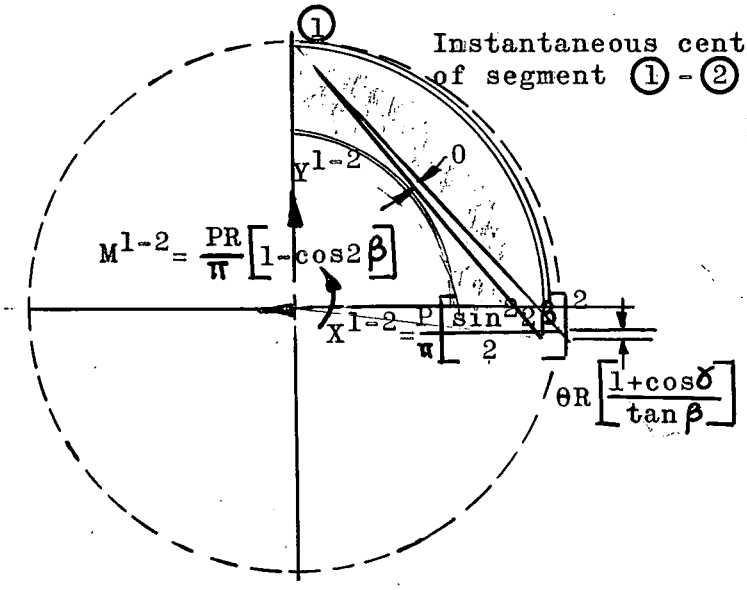

Note: The Y^{1-2} component does no work since its centerline passes through the instantaneous center of segment

FIGURE 2.3.6 External Work Done on Segment 1-2

Since Case I, Loading 2.0.0 is the limiting case of this loading, the expressions for the equivalent force system of the shear flows is the same as shown on pages 44 and 45. Referring to Figure 2.0.0 and equations 2.0.14, 2.0.15, and 2.0.16

$$X = \int \frac{P}{\pi} \sin\varphi \cos\varphi \, d\varphi = \frac{P}{\pi}\left[\frac{\sin^2\varphi}{2}\right]_{\text{lower limit}}^{\text{upper limit}} \quad \text{.....(2.0.14)}$$

$$Y = \int \frac{P}{\pi} \sin\varphi \sin\varphi \, d\varphi = \frac{P}{\pi}\left[\frac{\varphi}{2} - \frac{\sin 2\varphi}{4}\right]_{\text{lower limit}}^{\text{upper limit}} \quad \text{.....(2.0.15)}$$

$$M = \int \frac{PR}{\pi} \sin\varphi \, d\varphi = \frac{PR}{\pi}\left[-\cos\varphi\right]_{\text{lower limit}}^{\text{upper limit}} \quad \text{.....(2.0.16)}$$

Note: The integration of Case 2.0.0 was performed by commencing at the bottom of the ring and progressing clockwise. The integration of this case will be acheived by beginning at the top of the ring and progressing clockwise.

Integrating between hinges 1 and 2

$$X^{1-2} = \frac{P}{\pi}\left[\frac{\sin^2\varphi}{2}\right]_0^{2\beta} = \frac{P}{\pi}\left[\frac{\sin^2 2\beta}{2}\right]$$

$$Y^{1-2} = \frac{P}{\pi}\left[\frac{\varphi}{2} - \frac{\sin 2\varphi}{4}\right]_0^{2\beta}$$ This component does not need to be determined since it passes through the instantaneous center of segment ① - ②.

$$M^{1-2} = \frac{P}{\pi}\left[-\cos\varphi\right] = \frac{P}{\pi}\left[-\cos 2\beta + \cos(0)\right] = \frac{PR}{\pi}\left[1-\cos 2\beta\right]$$

See Figure 2.3.6 for a summary of these integrals.

Integrating between hinges ② - ③

$$X^{2-3} = \frac{P}{\pi}\left[\frac{\sin^2\varphi}{2}\right]_{2\beta}^{\pi-\delta} = \frac{P}{\pi}\left[\frac{\sin^2(\pi-\delta)}{2} - \frac{\sin^2 2\beta}{2}\right] = \frac{P}{\pi}\left[\frac{\sin^2\delta}{2} - \frac{\sin^2 2\beta}{2}\right]$$

$$Y^{2-3} = \frac{P}{\pi}\left[\frac{\varphi}{2} - \frac{\sin 2\varphi}{4}\right]_{2\beta}^{\pi-\delta} = \frac{P}{\pi}\left[\left(\frac{\pi-\delta}{2}\right) - \left(\frac{2\beta}{2}\right) - \frac{\sin 2(\pi-\delta)}{4} + \frac{\sin 2(2\beta)}{4}\right]$$

$$Y^{2-3} = \frac{P}{2\pi}\left[\pi - \delta - 2\beta + \sin\delta\cos\delta + (\sin 2\beta)(\cos 2\beta)\right]$$

$$M^{2-3} = \frac{PR}{\pi}\left[-\cos\varphi\right]_{2\beta}^{\pi-\delta} = \frac{PR}{\pi}\left[-\cos(\pi-\delta) + \cos 2\beta\right] = \frac{PR}{\pi}\left[\cos 2\beta + \cos\delta\right]$$

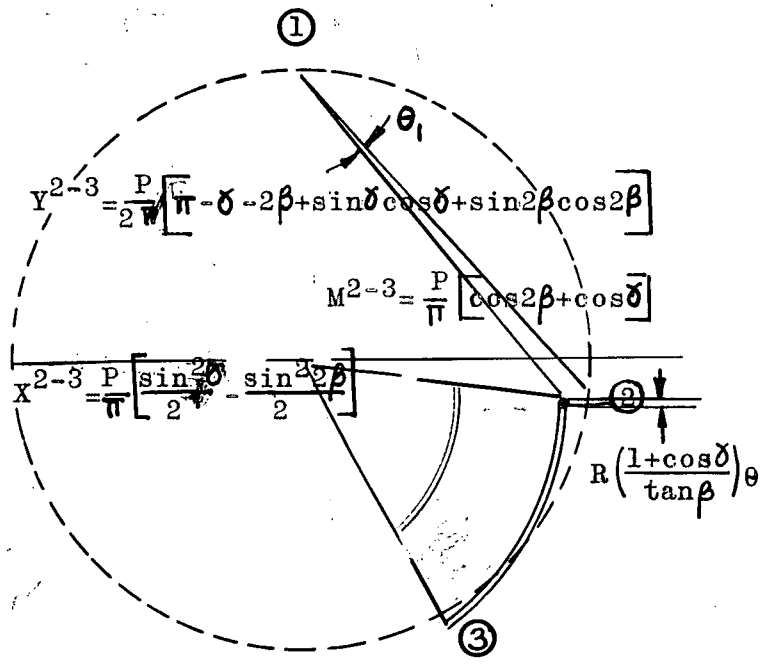

FIGURE 2.3.7 External Work Done on Segment ② - ③

The summary of the shear flow components and the virtual displacement of segment ① - ② are illustrated in Figure 2.3.7. Perhaps it may be more obvious to the reader, now, to point out that segment ② - ② was given a virtual rotation of θ instead of segment ① -

②, because only two components enter into the external work of segment ①-② whereas all three enter into the work expression for segment ②-③. Also, the expressions of ②-③ are more involved than the equations of ①-②. Thus, it was feasible to make the virtual rotaion of ②-③ as simple as possible.

Integrating between ③ and ④

$X^{3-\text{¢}}$ = This component does no work since segment ③-④ just translates vertically and does not rotate.

$$Y^{3-\text{¢}} = \frac{P}{\pi}\left[\frac{\varphi}{2} - \frac{\sin 2\varphi}{4}\right]_{\pi-\delta}^{\pi} = \frac{P}{\pi}\left[\frac{\pi}{2} - \frac{\sin 2\delta}{4} - \frac{(\pi-\delta)}{2} + \frac{\sin 2(\pi-\delta)}{4}\right] = \frac{P}{\pi}\left[\delta - \frac{\sin 2\delta}{4}\right]$$

$M^{3-\text{¢}}$ = The moment does no work because segment ③-④ does not rotate.

FIGURE 2.3.8 Work Done on Segment ③-④

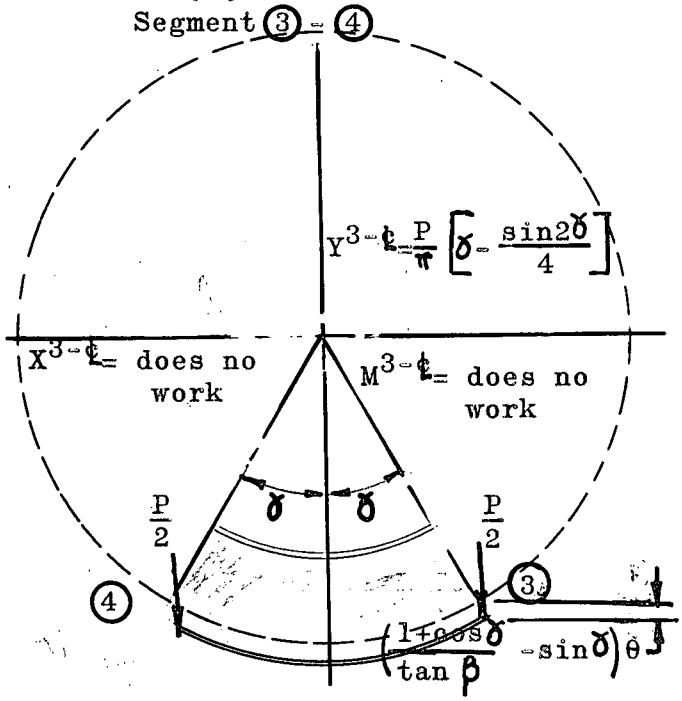

The summary of the equivalent components and their virtual rotations may be perceived in Figure 2.3.8. It is noteworthy to point out that the X component and moment, M, do no work since segment ③-④ just translates vertically and does not rotate.

The external work is now easily ascertained since three of the nine components vanish from the work expression. Therefore, the external work becomes

$$W_e = X^{1-2}R\theta_1 - M^{1-2}\theta_1 + X^{2-3}\theta R\cos\delta - Y^{2-3}\theta C + M^{2-3}\theta - Y^{3-c}\theta D + \frac{P}{2}\theta D$$

$$\frac{W}{\theta}e=\left[\frac{PR}{2\pi}(\sin 2\delta-\sin^2 2\beta)\cos\delta\right]-\left[\frac{PR}{2\pi}(\pi-\delta-2\beta+\sin\delta\cos\delta+\sin 2\beta\cos 2\beta)\left(\frac{1+\cos\delta}{\tan\beta}\right)\right]$$

$$+\left[\frac{PR}{\pi}(\cos\delta+\cos 2\beta)\right]-\left[\frac{PR}{2\pi}(\delta-\frac{\sin 2\delta}{2})\left(\frac{1+\cos\delta}{\tan\beta}-\sin\delta\right)\right]+\left[\frac{PR}{2}\left(\frac{1+\cos\delta}{\tan\beta}-\sin\delta\right)\right]$$

$$\frac{W}{\theta}e=\frac{PR}{\pi}\left\{\frac{(1+\cos\delta)\sin^2(2\beta)}{4\sin^2\beta}-\frac{\sin^2(2\beta)}{2}-\frac{(1-\cos 2\beta)(1+\cos\delta)}{2\sin^2\beta}+1-\cos 2\beta+\frac{\cos\delta\sin^2\delta}{2}\right.$$

$$-\frac{\cos\delta\sin^2(2\beta)}{2}-\pi\frac{(1+\cos\delta)}{2\tan\beta}+\delta\frac{(1+\cos\delta)}{2\tan\beta}+\beta\frac{(1+\cos\delta)}{\tan\beta}-\frac{(\sin\delta\cos\delta)(1+\cos\delta)}{2\tan\beta}$$

$$-\frac{\sin 2\beta(\cos 2\beta)(1+\cos\delta)}{2\tan\beta}+\cos\delta+\cos 2\beta-\delta\frac{(1+\cos\delta)}{2\tan\beta}+\frac{\delta\sin\delta}{2}+\frac{\sin 2\delta(1+\cos\delta)}{4\tan\beta}$$

$$\left.-\frac{\sin 2\delta(\sin\delta)}{4}+\frac{\pi}{2}\frac{(1+\cos\delta)}{\tan\beta}-\frac{\pi}{2}\sin\delta\right\}$$

By manipulating the remaining terms, the expression reduces to

$$W_e=\frac{PR}{\pi}\left[\frac{\beta}{\tan\beta}(1+\cos\delta)-\frac{\sin\delta}{2}(\pi-\delta)\right]\theta \qquad \text{.....(2.3.9)}$$

Equating expression 2.3.9 to 2.3.7 results in the execution of the principle of virtual displacements.

$$M_p\theta\left[\frac{1+\cos\delta}{\sin^2\beta}\right]=\frac{PR}{\pi}\theta\left[\frac{\beta}{\tan}(1+\cos\delta)-\frac{\sin\delta}{2}(\pi-\delta)\right]$$

$$M_p=\frac{PR}{\pi}\left[\beta\sin\beta\cos\beta-\frac{\sin^2\beta}{1+\cos\delta}\left(\frac{\sin\delta}{2}(\pi-\delta)\right)\right] \qquad \text{.....(2.3.10)}$$

For a specific problem, the angle δ is a constant, and hence equation 2.3.10 is maximized by differentiating with respect to β only.

$$\frac{dM}{d\beta}p=0$$

$$\beta\sin^2\beta+\beta\cos^2\beta+\sin\beta\cos\beta-\frac{\sin\beta\cos\beta\sin\delta}{1+\cos\delta}(\pi-\delta)$$

$$0=\beta(\cos^2\beta-\sin^2\beta)+\sin\beta\cos\beta\left[1-\frac{\sin\delta}{1+\cos\delta}(\pi-\delta)\right]$$

$$\beta(\cos^2\beta)+\frac{1}{2}\sin 2\beta\left[1-\frac{\sin\delta}{1+\cos\delta}(\pi-\delta)\right]$$

$$\text{or}\quad \frac{\tan 2\beta}{\beta}=\frac{2}{\left[1-\frac{\sin\delta}{1+\cos\delta}(\pi-\delta)\right]} \qquad \text{.....(2.3.11)}$$

In order to obtain a value of β which satisfies equation 2.3.10, the angle δ must be chosen. Just to be consistent with the selection of the previous example, choose $\delta = 30^{\circ}$ for this illustration.

Equation 2.3.11 reduces to

$$\frac{\tan 2\beta}{\beta}=\frac{2}{.29851}=-6.7 \qquad \text{.....(2.3.12)}$$

If the function $\tan 2\beta$ is plotted against the angle β as shown in Figure 2.3.9, it is seen that an angle of approximately $\beta = .88$ rad. or 50° is the solution to the problem.

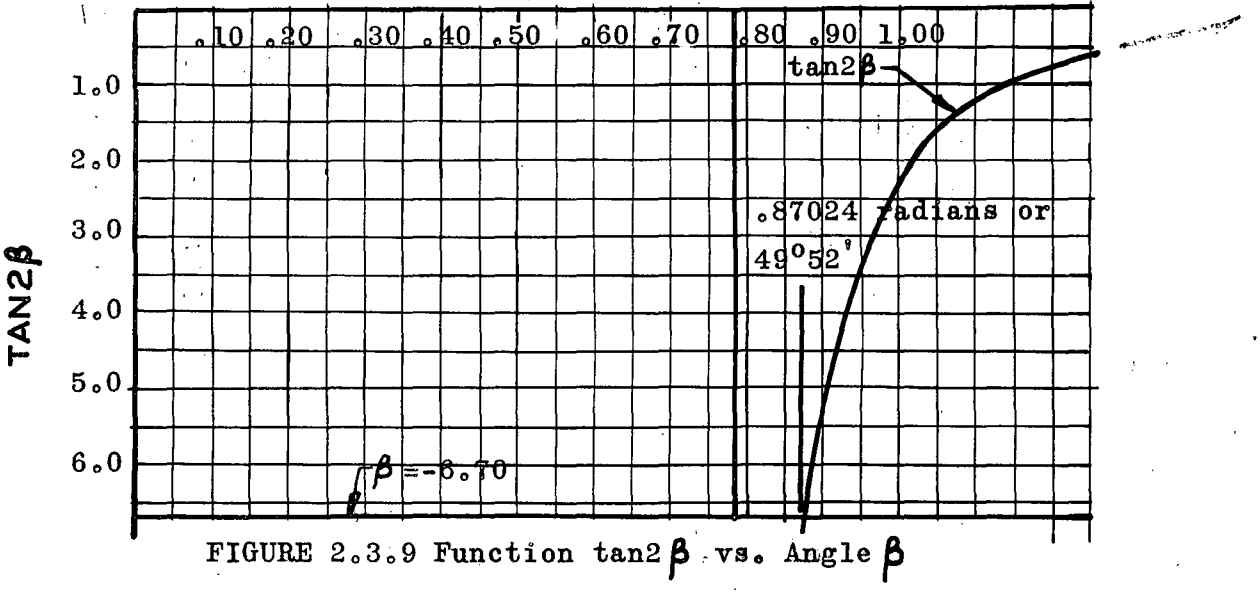

FIGURE 2.3.9 Function $\tan 2\beta$ vs. Angle β

Using Newton's Iteration Method as outlined on page 60 with $\beta = 50^{\circ}$

$$\frac{f(x_o)}{f'(x_o)}=-h_o \qquad \text{.....(2.0.32)}$$

$$\text{or} \qquad h_o = -\frac{\tan^2\beta + 6.70}{2\sec^2\beta + 6.70}$$

$$h_o = -\frac{(-5.671) + 6.70(.8727)}{2(1.56)^2 + 6.70} = .0024 \text{ rad.}$$

As a next approximation try

$= .873 - .0024 = .8703$ rad. or $\beta = 49^\circ\ 52'$

$$h_o = -\frac{(-5.83) + 6.70(.8703)}{2(1.55)^2 + 6.70} = \text{(negligible amount)}$$

It appears that $\beta = 49^\circ\ 52'$ satisfies the expression within the nearest minute of angle. Substituting these values of δ and β into the function for M_p,

$$M_p = \frac{PR}{\pi}\left\{(.8703)(.7646)(.6446) - \frac{(.7646)^2}{1.866}\left[.250(2.618)\right]\right\}$$

$$M_p = .07127PR \qquad \ldots\ldots\ldots\ldots\ldots\ldots\ldots\ldots\ldots\ldots (2.3.13)$$

2.3.1 Plasticity Check

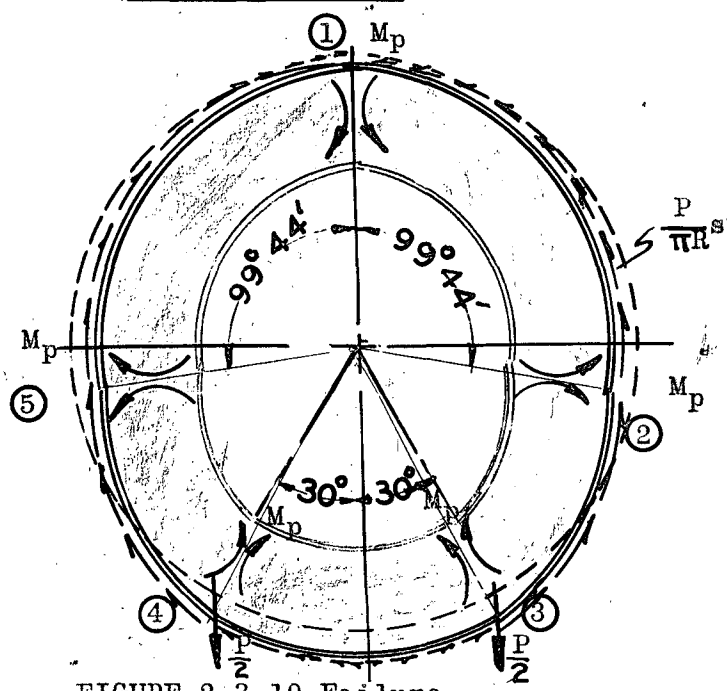

FIGURE 2.3.10 Failure Configuration

Note: The hinge moments are induced to oppose the rotation of the frame, so as to restore the deformed structure to its initial undeformed shape.

From the assumed hinge pattern, the plastic hinges are clustered

around the ring as shown in Figure 2.3.10. To substantiate the solution, the equations for internal moments, shears and thrusts must be derived. Referring to Figure 2.3.10, it may be discerned that one expression is not sufficient to designate each of these internal variables around the ring, because of the influence of the concentrated loads at 30^{o} to the vertical axis.

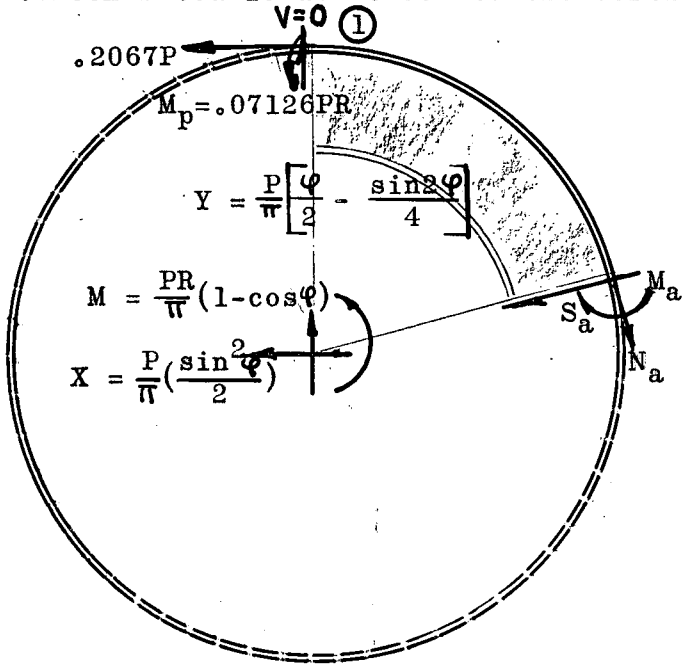

FIGURE 2.3.11 Plasticity Check

Figure 2.3.11 was drawn to assist in deriving the following equations. The expressions had to be deduced within two intervals. The first sector was between hinge ① and hinge ③ .

Commencing with the interval between ① and ③ at any cross section a,

$$M_a = M_p - (.2067)(1-\cos\varphi) + \frac{PR}{\pi}\left[1-\cos\varphi\right] - \frac{P}{\pi}\left[\frac{\sin^2\varphi}{2}\right]R\cos\varphi - \frac{PR}{\pi}\left[\frac{\varphi}{2} - \frac{\sin 2\varphi}{4}\right]\sin\varphi$$

$$M_a = \frac{PR}{\pi}\left[.5746 - .3508\cos\varphi - \varphi\frac{\sin\varphi}{2}\right] \quad \ldots\ldots\ldots\ldots\ldots\ldots (2.3.14)$$

$$N_a = \left[.2067 - \frac{P}{\pi}\left(\frac{\sin^2\varphi}{2}\right)\right]\cos\varphi - \left[\frac{P}{\pi}\frac{\varphi}{2} - \frac{\sin 2\varphi}{4}\right]\sin\varphi$$

$$N_a = \frac{P}{\pi}\left[.6492\cos\varphi - \frac{\varphi}{2}\sin\varphi\right] \quad \ldots\ldots\ldots\ldots\ldots\ldots\ldots\ldots (2.3.15)$$

$$S_a = \left[.2067 - \frac{P}{\pi}\frac{\sin^2\varphi}{2}\right]\sin\varphi + \frac{P}{\pi}\left[\left(\frac{\varphi}{2} - \frac{\sin 2\varphi}{4}\right)\right]\cos\varphi$$

$$S_a = \frac{P}{\pi}\left[.1492\sin\varphi + \frac{\varphi}{2}\cos\varphi - \frac{\sin\varphi}{2}\right] \quad \ldots\ldots\ldots\ldots\ldots\ldots (2.3.16)$$

VERTICAL FORCES $\frac{P}{2}$ AT A RANDOM ANGLE

TABLE 2.3.1

Comparison of Plastic to Elastic Moment, Shear and Axial Load Co.						
Angle From Vertical	Plastic Moment Coeff.	Elastic Moment Coeff.	Plastic Shear Coeff.	Elastic Shear Coeff.	Plastic Axial Load Coeff.	Elastic Axial Load Coeff.
0	.04457		0		.20666	
5	.04536		.01798		.11992	
10	.04771		.03560		.03467	
15	.05156		.05254		-.04842	
20	.05677		.06824		-.12882	
25	.06347		.08302		-.20597	
30	.07128		.0959		-.27936	
30	.07129		-.33709		.38731	
35	.04336		-.30269		.40031	
40	.01848		-.26737		.40828	
45	-.00329		-.23158		.41130	
50	-.02193		-.19573		.40946	
55	-.03746		-.16025		.40296	
60	-.04993		-.12553		.39201	
65	-.05441		-.09151		.37685	
70	-.06602		-.05987		.35781	
75	-.06991		-.02960		.33522	
80	-.07125		-.00145		.30945	
$80^{\circ}16'$	-.07126		0		.30799	
85	-.07024		.02432		.28090	
90	-.06708		.04751		.25000	

VERTICAL FORCES $\frac{P}{2}$ AT A RANDOM ANGLE

TABLE 2.3.2

Comparison of Plastic to Elastic Moment, Shear and Axial Load Co.						
Angle From Vertical	Plastic Moment Coeff.	Elastic Moment Coeff.	Plastic Shear Coeff.	Elastic Shear Coeff.	Plastic Axial Load Coeff.	Elastic Axial Load Coeff.
95	-.06203		.06790		.21720	
100	-.05532		.08537		.18296	
105	-.04722		.09981		.14775	
110	-.03799		.11114		.11204	
115	-.02792		.11936		.07630	
120	-.01728		.12447		.04101	
125	-.00681		.12654		.00661	
130	.00475		.12567		-.02644	
135	.01557		.12198		-.05774	
140	.02596		.11566		-.08689	
145	.03568		.10688		-.11352	
150	.04455		.09592		-.13731	
155	.05237		.08302		-.15795	
160	.05899		.06845		-.17520	
165	.06427		.05254		-.18883	
170	.06813		.03561		-.19870	
175	.07047		.01797		-.20466	
180	.07127		0		-.20666	

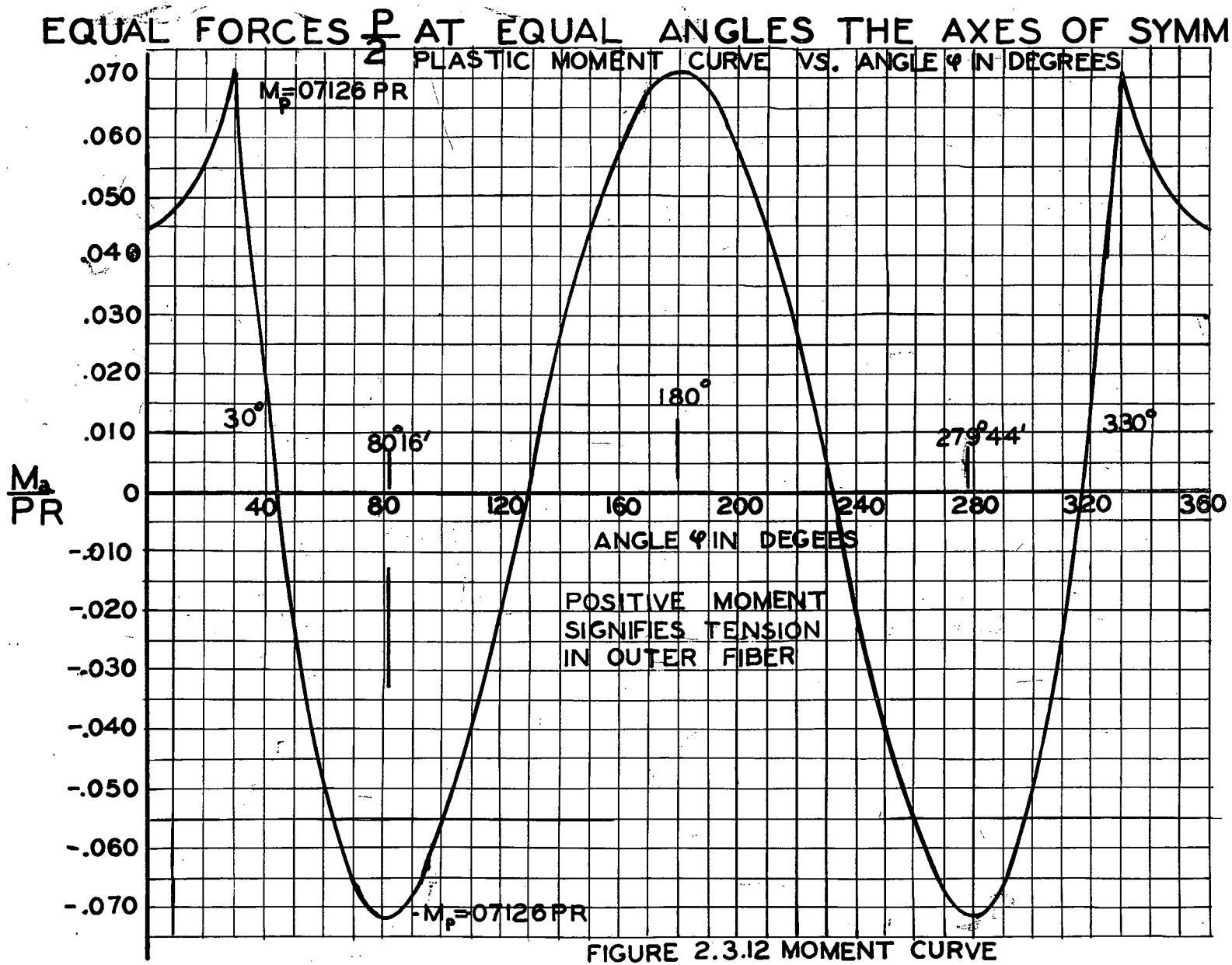

FIGURE 2.3.12 MOMENT CURVE

EQUAL FORCES $\frac{P}{2}$ AT EQUAL ANGLES TO THE AXES OF SYMMETRY

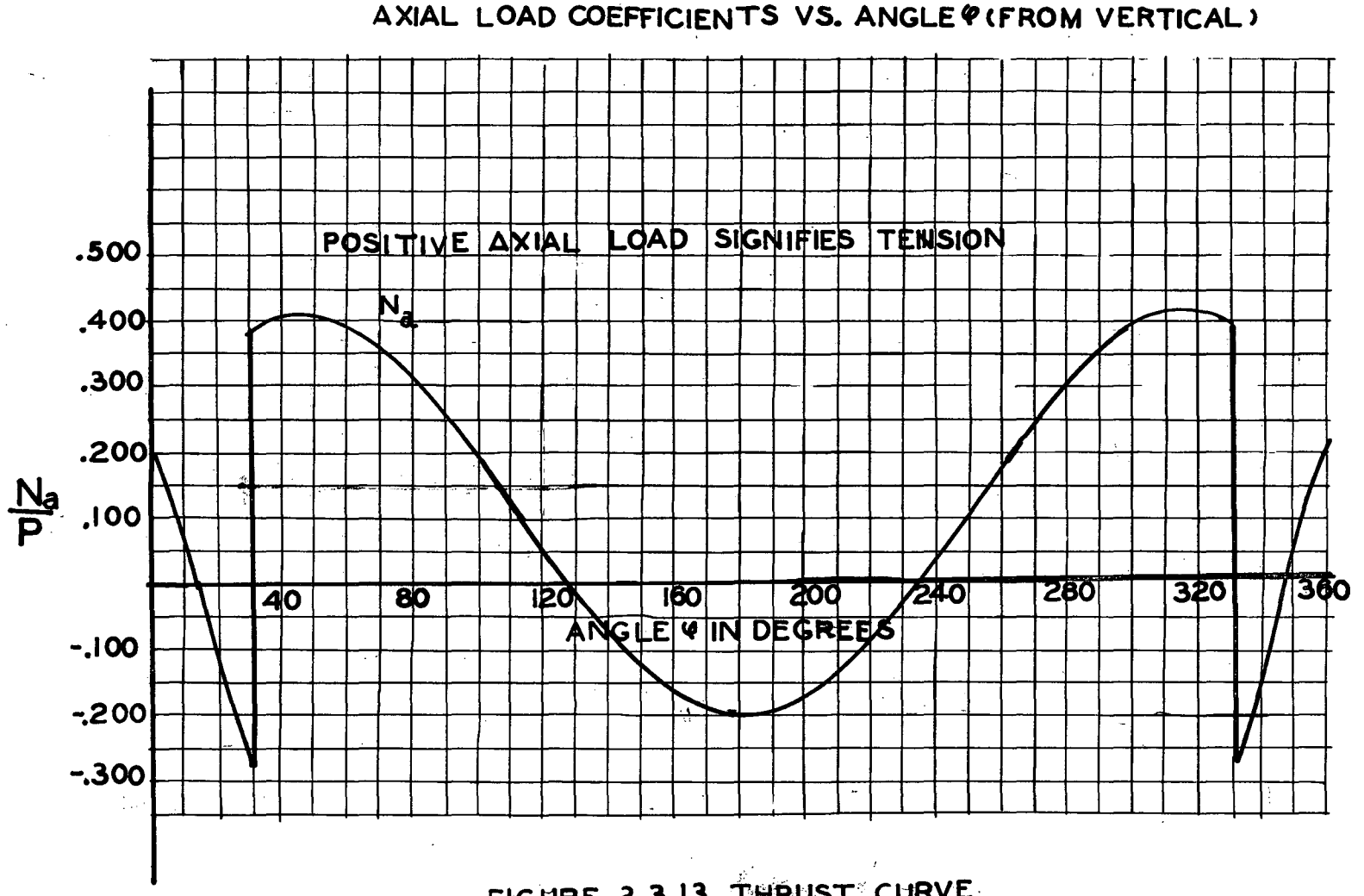

FIGURE 2.3.13 THRUST CURVE

EQUAL FORCES $\frac{P}{2}$ AT EQUAL ANGLES TO THE AXES OF SYMMETRY

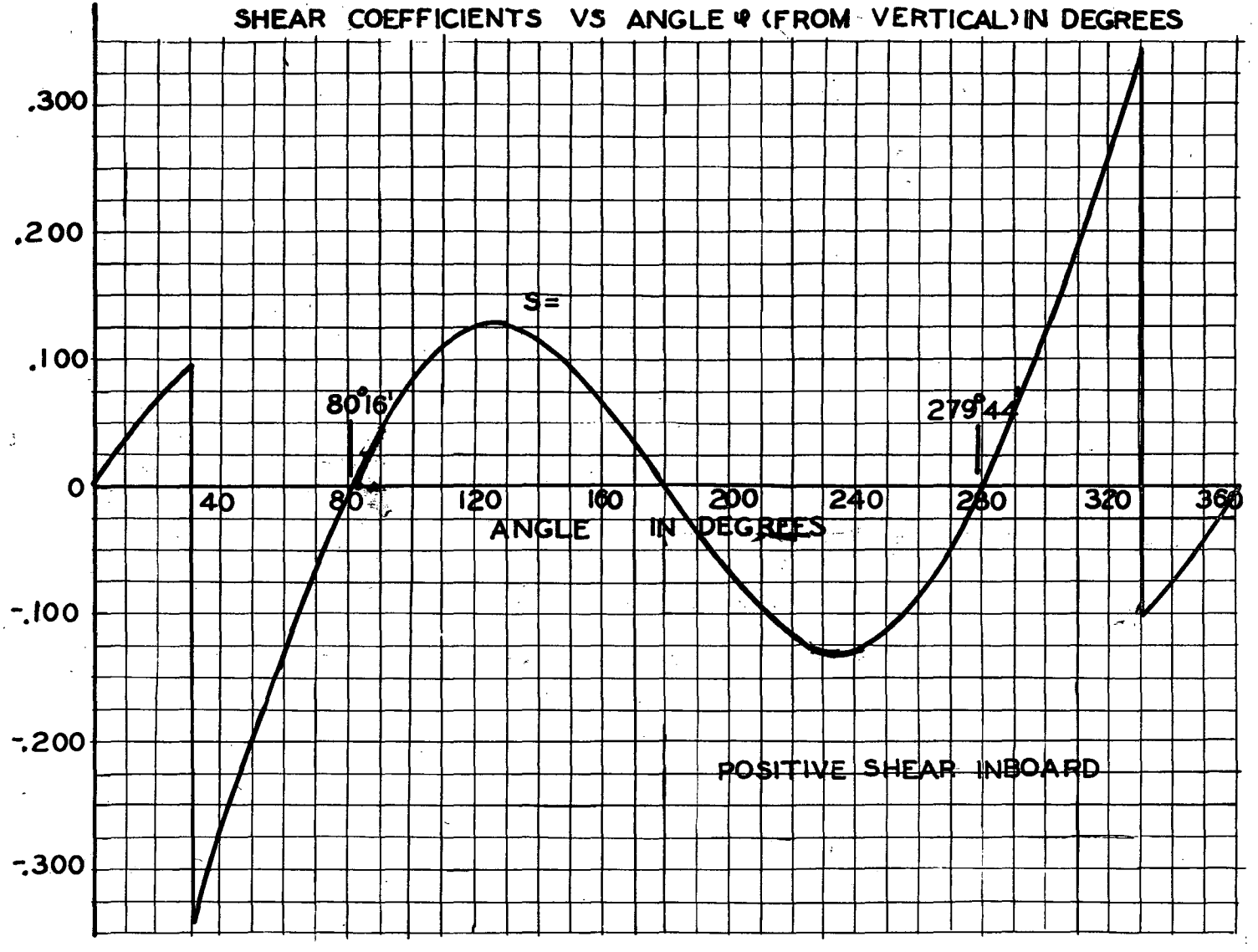

$\frac{S_a}{P}$

FIGURE 2.3.14 SHEAR CURVE

Either starting from the bottom of the ring or including the influence of the vertical P load in the expressions above results in the same or equivalent internal force equations.

$$M_a = \frac{PR}{\pi}\left[.5746 - .3508\cos\varphi - \varphi\frac{\sin\varphi}{2}\right] - \frac{PR}{2}(\sin\delta - \sin\varphi)$$

$$M_a = \frac{PR}{\pi}\left[-.2108 - .3508\cos\varphi + \sin\left(\frac{\pi}{2} - \frac{\varphi}{2}\right)\right] \qquad \text{.....(2.3.17)}$$

$$N_a = \frac{P}{\pi}\left[.6492\cos\varphi - \frac{\varphi}{2}\sin\varphi - \frac{P}{2}\sin\varphi\right]$$

$$N_a = \frac{P}{\pi}\left[.6492\cos\varphi - \sin\varphi\left(\frac{\pi}{2} - \frac{\varphi}{2}\right)\right] \qquad \text{.....(2.3.18)}$$

$$S_a = \frac{P}{\pi}\left[.1492\sin\varphi - \frac{\varphi}{2}\cos\varphi + \frac{\sin\varphi}{2}\right] + \frac{P}{2}\cos\varphi$$

$$S_a = {}^{P}\left[.1492\sin\varphi + \cos\varphi\left(\frac{\pi}{2} - \frac{\varphi}{2}\right)\right] \qquad \text{.....(2.3.19)}$$

Since equations 2.3.14 through 2.3.19 represent the internal forces in the ring, all that remains to do is to substitute values of φ every 5^{o} into these formulas. The results of these calculations may be seen in Figures 2.3.12, 2.3.13, and 2.3.14. The tabulation of the results are shown in tables 2.3.1 and 2.3.2. There is one point of interest which will be pointed out at this time. Observing the moment diagram, Figure 2.3.12, one may notice that the moment did not change its sign at the centerline from that at either hinges ③ or ④ . The reason for this will be explained presently.

Since nowhere did the moment curve exceed the maximum moment value, M_p = .07127PR, this is the true or correct solution to the problem.

2.3.2 Lower Limiting Case

Just as in the previous example, the boundaries for this

problem will be discussed. Beginning with the lower limit it is obvious after careful study of the elastic moment diagram (Figure 2.3.12) that, as δ is decreased, the hinges will keep forming at the point of concentrated load and β will become larger and larger. Further, it is obvious from symmetry of loading that hinge ① must always form at the vertical axis at the top of the ring regardless of where the load, P/2 is applied. Returning to the former, as δ is progressively decreased the lower hinges (③ and ④) form closer and closer to the vertical and the angle 2β approaches the value (180° - 63° 45'). (63° 45' comes from Loading condition 2.0.0 where $\alpha = 63^\circ$ 45'). As the two concentrated loads converge on the centerline, loading condition 2.0.0 is realized. The cusp on the moment diagram (see Figure 2.3.12) begins to flatten out as this condition is approached, and thus the moment at the centerline (refer to discussion on page 136) does not change to a sign opposite from the moment at hinge ③ or ④.

Returning to equation 2.3.10, as the lower bound is approached the angle ($180^\circ - 2\beta$) may be replaced by α (Case I). The angle α now locates the lower hinges ③-④. Hinges ② and ⑤ disappear with a hinge forming at the centerline (or the lowest point on the ring).

If 2β is replaced by $180^\circ - \alpha$, expression 2.3.10 reduces to

$$M_p = \frac{PR}{\pi}\left\{\frac{\sin}{2}(\pi-\alpha)\left[\frac{1}{2} - \frac{\cos^2\delta}{1+\cos\delta}\right]\right\} \quad \text{.....(2.3.22)}$$

As δ approaches zero, 2.3.26 reduces further to

$$M_p = \frac{PR}{4}\left[-\sin\alpha(\pi-\alpha)\right]$$

which is identical to equation 2.0.29(Case 2.0.0).

2.3.4 Upper Limit of Loading Condition 2.3.0

If different values of δ are selected and their corresponding moment curves are drawn, it will be seen that as δ is increased the moment at the bottom of the ring becomes smaller and smaller until it assumes a sign opposite to that of hinges ③ and ④. The angle 2β becomes smaller and smaller until, for a given value of 2β, the preferred hinge system changes, a hinge developing at the base of the ring. This is the upper limit of the solution given for equation 2.3.21. Its hinge pattern and assumed failure configuration are shown in Figure 2.3.15. Figure 2.3.15 is identical in form to Figure 2.0.14 page 61. It will be noticed that the only difference in the solution to the upper bound problem and loading 2.0.0 is the determination of the external work of the applied loads. Reviewing equations 2.0.25, 2.0.26 on page 58 and substituting δ for α.

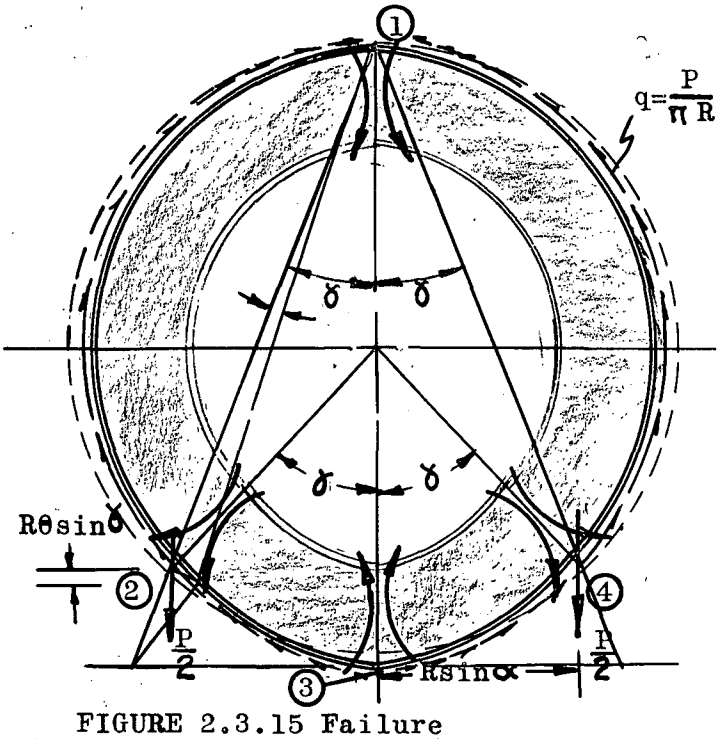

FIGURE 2.3.15 Failure Configuration of Upper Bound

$$-\frac{P}{\pi}\left[-\frac{\sin^2\delta}{2}\right]R\theta-\frac{PR}{\pi}\left[1+\cos\delta\right]\theta \quad \text{....(See 2.0.35).....(2.3.22)}$$

$$-\frac{P}{\pi}\left(\frac{\sin^2\delta}{2}\right)R\theta\left(\frac{1}{\tan^2(\frac{\delta}{2})}\right)-\frac{P}{\pi}\left(\frac{\delta}{2}-\frac{\sin 2\delta}{4}\right)\theta\left(\frac{1}{\tan^2(\frac{\delta}{2})}\right)2R\tan\left(\frac{\delta}{2}\right) \quad \text{..(2.3.23)}$$

and finding the work done by the $\frac{P}{2}$ force

$$\frac{P}{2}(\theta)R\sin\delta \quad \text{.....(2.3.24)}$$

Equating the summation of equations 2.3.22, 2.3.23, and 2.3.24 to the internal work equation (which is the same as 2.0.24)

$$M_p\theta\left[\frac{2}{\sin^2(\frac{\delta}{2})}\right]=$$

$$\theta\frac{PR}{\pi}\left\{\frac{\sin^2\delta}{2}-1-\cos\delta-\left(\frac{\sin^2\delta}{2\tan^2(\frac{\delta}{2})}\right)-\left(\delta-\frac{\sin 2\delta}{2}\right)\left|\frac{1}{\tan(\frac{\delta}{2})}\right|+\frac{1-\cos\delta}{\tan^2(\frac{\delta}{2})}\Bigg|+\pi\left|\frac{\sin^2(\frac{\delta}{2})}{\tan(\frac{\delta}{2})}\right|\right\}$$

this eventually reduces to

$$M_p=\frac{PR}{\pi}\sin\delta\left(\pi\sin^2\frac{\delta}{2}-\delta\right) \quad \text{.....(2.3.25)}$$

In order to ascertain the upper bound, the maximum moment, M_p, which satisfies both equations 2.3.25 and 2.3.10 simultaneously, must be found. This situation will occur for some specific angles of δ and β. These are the two unknowns of the problem. An obvious method for determining this condition is to equilibrate the two equations, 2.3.25 and 2.3.10, and solve for δ in terms of β. The solution would be acheived by finding the angle δ of equation 2.3.10 which gives the identically same solution for M_p (with its corresponding value of β) as the same value of yields for equation 2.3.25. This process becomes tediously involved however.

Therefore another method of attack will be proposed instead. It is observed from equation 2.3.11 that the expression $\frac{\tan 2\beta}{\beta}$ is some function of the angle δ . If the analyst sets up a table involving all of the variables of equation 2.3.11, then he is able to plot the angle β which suffices the function $\frac{\tan 2\beta}{\beta}$ against the angle δ which satisfies the right hand side of 2.3.11 (corresponding to equivalent values of the β function) as shown in Figure 2.3.16. As long as the curve is smooth and there are no abrupt changes in the curve (discontinuities), this method of solution is permissible.

With the relationship between the angle β and δ now available, the function for M_p, as specified by equation 2.3.10 may be plotted versus the angle δ . If the same angles for δ are employed in solving equation 2.3.25, the two functions of $\frac{M_p}{PR}$ may be plotted against their respective angles δ, as shown in Figure 2.3.17. Where the two curves intersect is naturally the solution to the problem. From Figure 2.3.17, it is beheld that the two curves intersect at an approximate angle of $36^{\circ}6'$.

This approach to the problem is accurate enough for the analyst's purposes. The upper bound for this loading condition may be very useful to the analyst since he is interested in knowing where the problem diverges from a five hinge solution to a four hinge solution. He must know this in order to educe the arrangement of the plastic hinges (or hinge pattern around the ring) for a specific angle of δ .

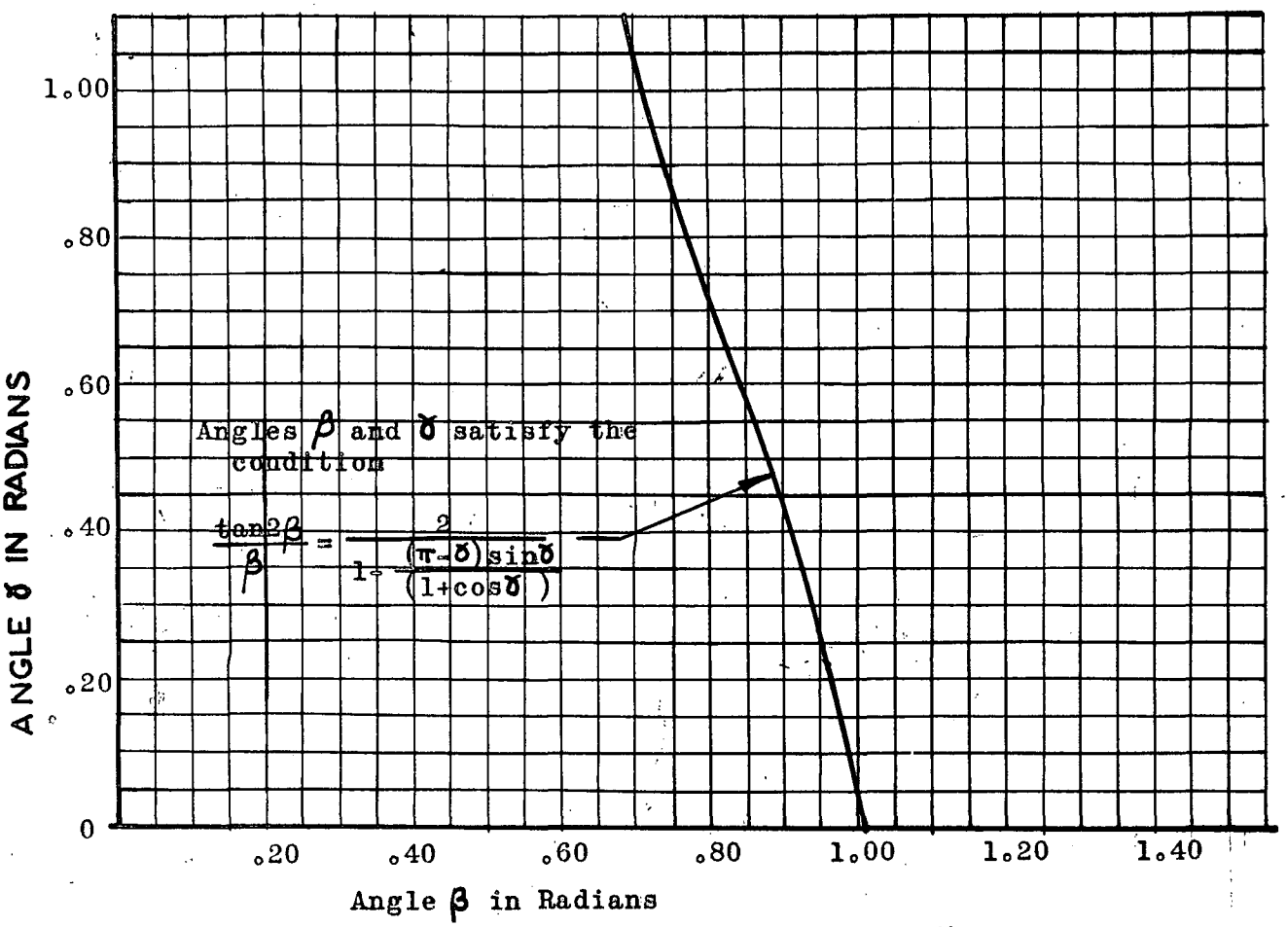

FIGURE 2.3.16 Relation of Angle β to Angle δ

This loading condition was chosen for a very special purpose. Besides its generality of loading, it was an excellent example of an exception to the general rule that it takes only four plastic hinges to create a kinematic mechanism of failure. Prior to this loading condition, it was established that four hinges are necessary to propagate a collapse mode. If the analyst had encountered a problem similar in nature to this case, he would be baffled by the fact that there is no evident solution, when considering only four plastic hinges. Thus, this case was submitted for consideration to establish the fact that it may take more than four hinges to acheive a failure mechanism.

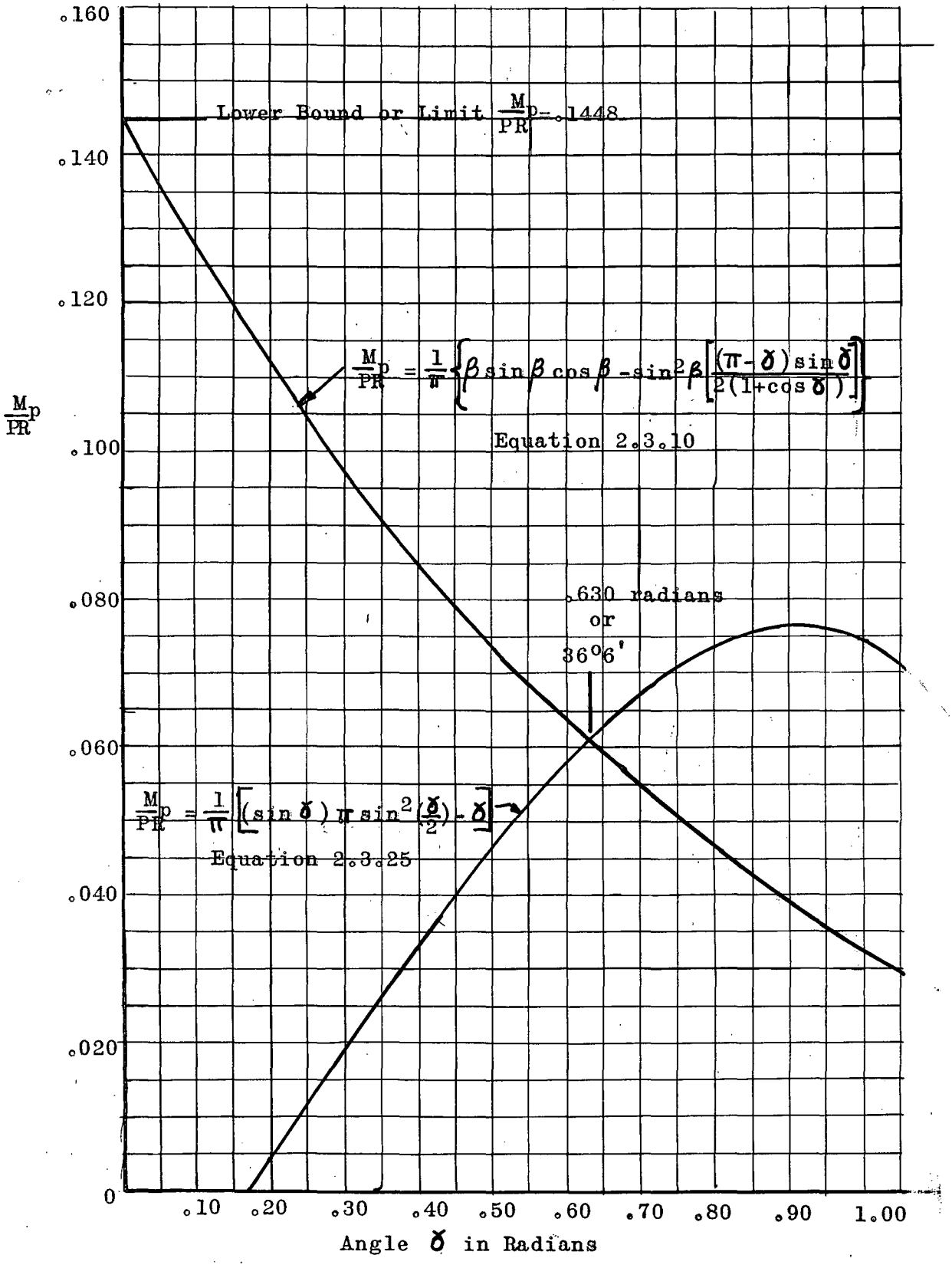

FIGURE 2.3.17 $\frac{M}{PR}p$ Vs. Angle δ in Radians

SECTION 3.0.0

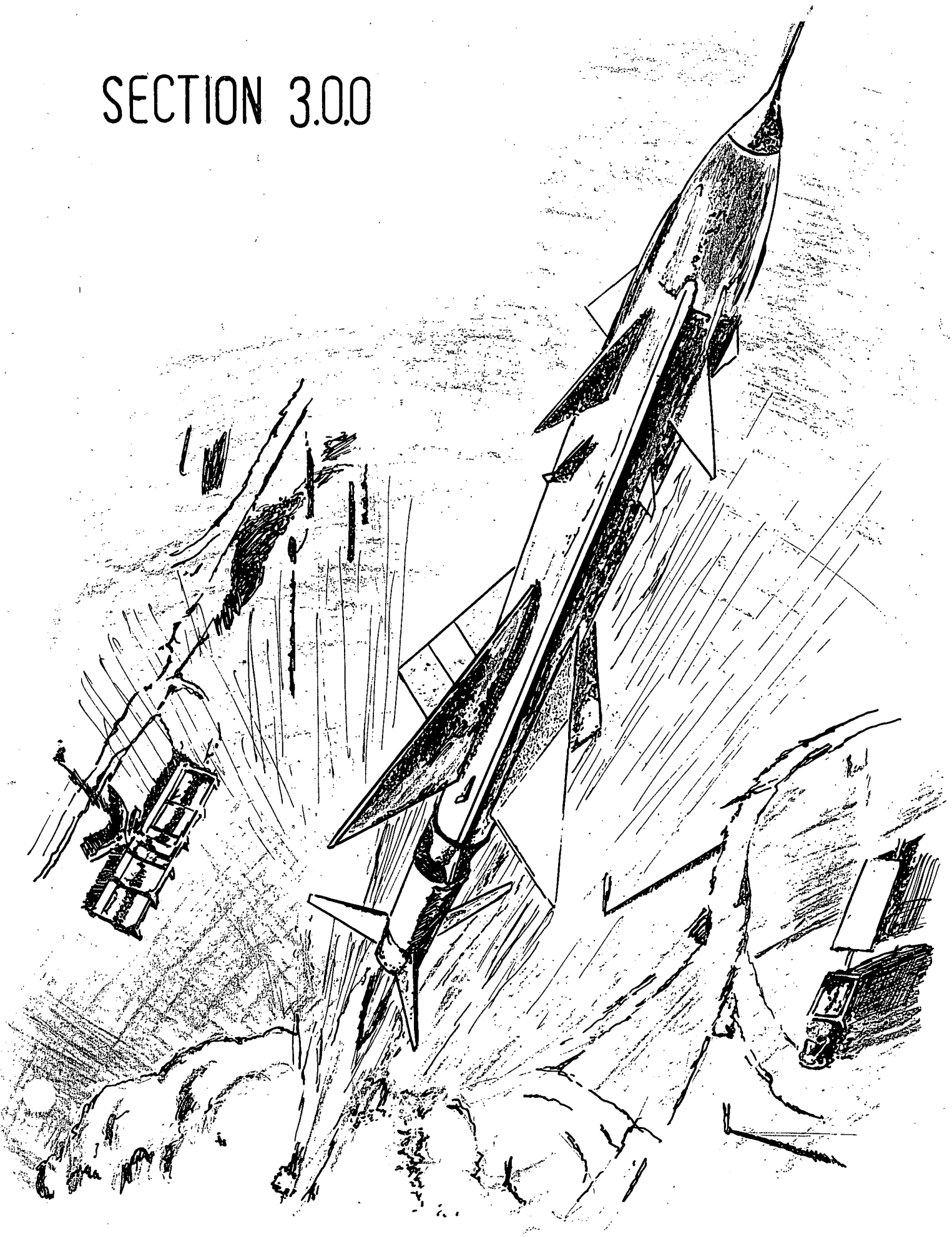

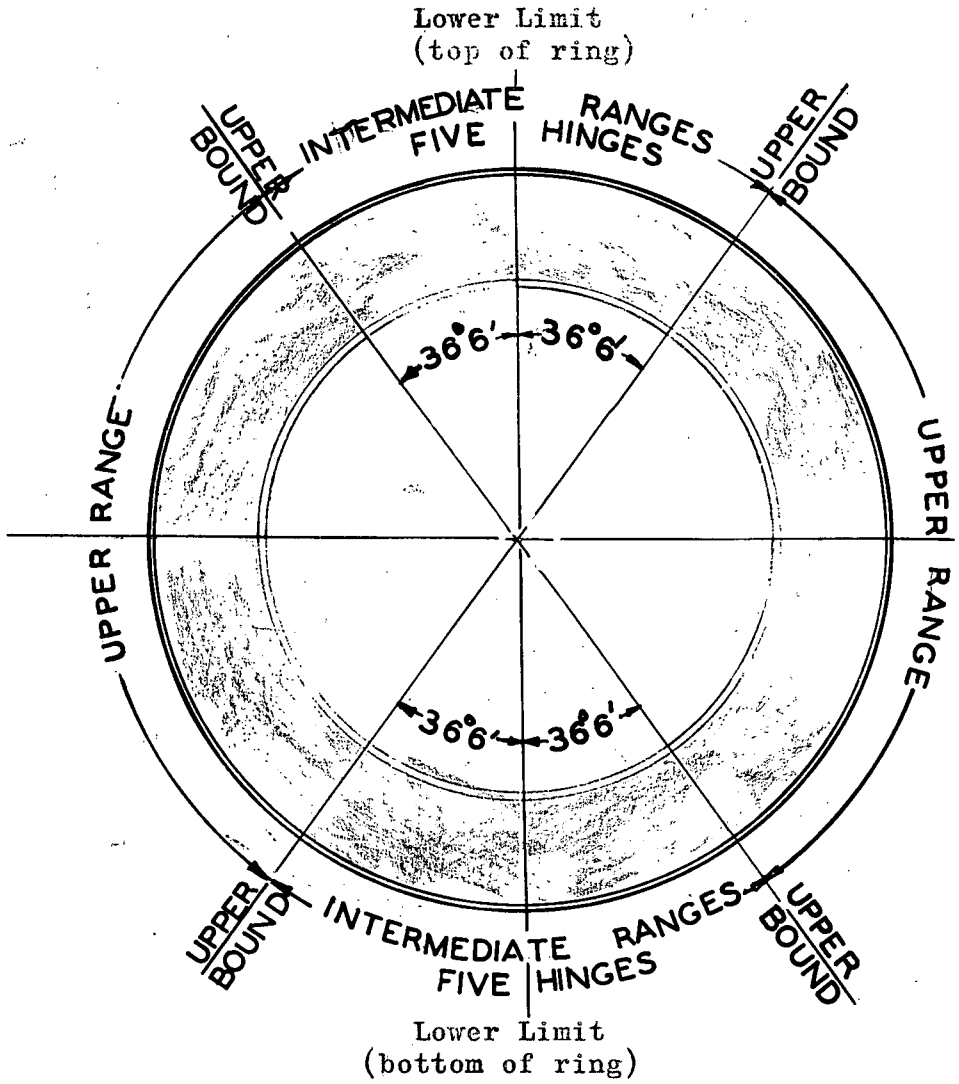

FIGURE 2.3.18

Representation of Upper and Lower Ranges of σ Which Determine the Upper and Lower Bounds for Loading 2.3.0

Figure 2.3.18 was drawn to illustrate the summary of the limiting boundaries just discussed. Note: No applied loads are shown; just the boundaries.

III SOME MODIFYING FACTORS

3.0.0 Derivation of Expressions for the Combination of Axial Load and Moment

It was stated on page 38 that it was assumed axial load did not affect the ultimate bending capacity of any section in the ring for a simple plastic solution. It was decided at that time to make this supposition, achieve a solution and then modify the cross section in order to account for this factor. It is the specific purpose of section 3.0.0 and 3.1.0 of this dissertation to develope a general method for combining axial load and moment, and to derive a foolproof, systematic procedure for determining ring bending stiffness.

3.0.1 Expression for Combining Axial Load with Bending Moment at Any Cross Section around the Ring

Before proceding with the derivation, it will be necessary to make a few assumptions concerning the shape of the cross section of the ring. Since a multitude of cross sectional shapes would impart a multitude of answers to the problem, a constant width rectangular cross section is surmised to be the simplest choice. Because of the easiness of working with such an elementary section, the "interaction" expressions will be rendered in much simpler terms.

Certain nomenclature will be defined at this time in order to facilitate the development of the expressions, rather than to refer the reader to the section containing the nomenclature. It is handier to do this since these definitions are specifically related to this section of the paper.

Let

$M^{original}$ = Moment determined from "simple plastic theory" neglecting thrust and size of cross section,

$N^{original}$ = Thrust or axial load determined from the "simple plastic theory" study,

M^{final} = Moment of section after considering the effect of axial load

M_p^{final} = Final full plastic moment at hinge points

N_y^{final} = Axial yield load of the section

To abridge the terminology only the first letter of the script, will be retained throughout the following derivation.

To begin the discussion, there is interaction relationship between the moment and axial load at a cross section and their corresponding full plastic moment and yield load capacities, for a rectangular cross section.

If a stress distribution for a fully plastic rectangular cross section (including the effect of an axial thrust) is assumed as shown in Figure 3.0.1(a), the equivalent stress distribution may be represented by dividing it into two parts.

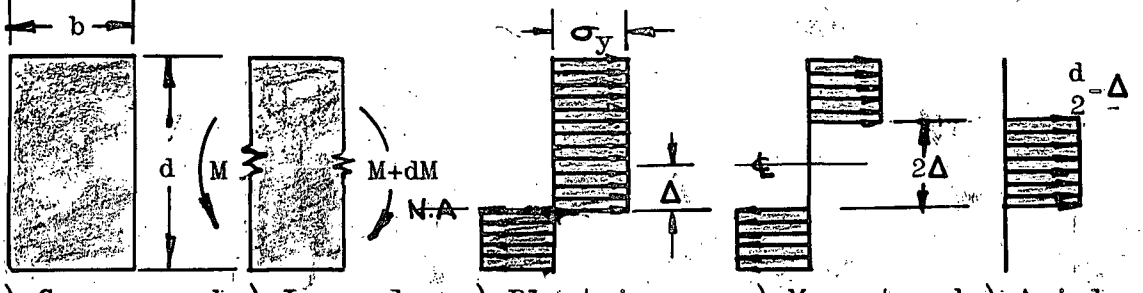

a.) Cross Section b.) Imposed Moment c) Plastric Stress Distrib. c.) Moment Contribution d.) Axial Load

FIGURE 3.0.1 Fully Plastic Bending Section

The moment resistance of the section may be obtained in terms of the distance from 3.0.1(c)

$$M^o = \left(\frac{d}{2} + \Delta\right) \quad \left(\frac{d}{2} - \Delta\right) \sigma_y b \qquad \text{.....(3.0.1)}$$

and the axial load may be represented by

$$N^o = 2\,\Delta b\,\sigma_y \qquad \text{.....(3.0.2)}$$

The full plastic moment is readily available

$$M_p = \frac{bd^2}{4}\sigma_y \qquad \text{.....(3.0.3)}$$

and the stabilized maximum thrust resistance is evaluated from

$$N_y = bd\,\sigma_y \qquad \text{.....(3.0.4)}$$

An interaction of the moment and axial load may be obtained from the ratios of moment to full plastic moment and axial load to yield load.

$$\frac{M^o}{M_p} = \frac{4\left[\left(\frac{d}{2}\right)^2 - \Delta^2\right]}{d^2} \qquad \text{.....(3.0.5)}$$

$$\frac{N^o}{N_y} = \frac{2\Delta}{d} \qquad \text{.....(3.0.6)}$$

Thus, if $\frac{N}{N_y}$ is substituted into 3.0.5 everywhere $\frac{2\Delta}{d}$ arises.

$$\frac{M^o}{M_p} = \frac{d^2 - 4\Delta^2}{d^2} = 1 - \frac{4\Delta^2}{d^2}$$

$$\frac{M^o}{M_p} = 1 - \left(\frac{N^o}{N_y}\right)^2 \qquad \text{.....(3.0.7)}$$

For the special case at hand,

$$\frac{M^o}{M_p^f} = 1 - \left(\frac{N^o}{N_y^f}\right)^2 \qquad \text{.....(3.0.8)}$$

and

$$N_y^f = bd\sigma_y \qquad \text{.....(3.0.9)}$$

$$M_p^f = \frac{bd^2}{4}\sigma_y \qquad \text{.....(3.0.10)}$$

By manipulating equations 3.0.9 and 3.0.10, the subsequent equation arises.

$$M_p^f = \frac{d}{4} N_y^f \qquad \text{.....(3.0.11)}$$

Replacing M_p^f in equation 3.0.8 with the expression 3.0.11,

$$\frac{M^o}{\frac{d}{4} N_y^f} = 1 - \left(\frac{N^o}{N_y^f}\right)^2 \qquad \text{.....(3.0.12)}$$

Cross multiplying,

$$\frac{4}{d} M^o \, N_y^f = (N_y^f) - (N^o)^2$$

Rearranging the terms,

$$(N_y^f)^2 - (N_y^f)\frac{4}{d} M^o - (N^o)^2 = 0 \qquad \text{.....(3.0.13)}$$

Equation 3.0.13 is recognized as a homogeneous quadratic equation, which possesses the roots

$$(N_y^f) = \frac{2M_p^o}{d}\left[1 \pm \sqrt{1 + \frac{d^2(N^o)^2}{4(M^o)^2}}\right] \qquad \text{.....(3.0.14)}$$

Only the positive root will be investigated because the negative root has no physical significance. Furthermore, if the dimensionless moduli of the moment and axial load expressions which have been determined from previous analysis (i.e., the tables and graphs at the end of each loading condition) are designated by variable coefficients, then

$$\frac{M^o}{PR} = q_m \qquad M^o = q_m\, PR$$

or

$$\frac{N^o}{P} = q_n \qquad N^o = q_n\, P \qquad \text{.....(3.0.15)}$$

where q_m denotes the moment coefficient and q_n the thrust coefficient at any cross section in the ring. These coefficients may be obtained from any of the plasticity checks at the end of the loading cases.

When equations 3.0.15 are substituted into 3.0.14,

$$(N_y^f) = \frac{2(q_m PR)}{d}\left[\sqrt{1 + \frac{(\frac{d}{R})^2}{4}\left(\frac{q_n}{q_m}\right)^2} + 1\right]$$

or

$$\frac{N_y^f}{P} = \frac{2\, q_m}{\frac{d}{R}}\left[1 + \sqrt{1 + \frac{1}{4}\left(\frac{d}{R}\right)^2 \left(\frac{q_n}{q_m}\right)^2}\right] \qquad \text{.....(3.0.16)}$$

3.0.16 is not as involved as a quick glance might suggest. Regarding the expression closely, it is noticed that the only unknown parameter in the expression for a given practical problem is $\frac{d}{R}$. The coefficients q_m and q_n may be obtained from the plots of moment and thrust previously obtained for a particular loading. Any of the six tables of coefficients succeeding the solution of the individual cases would be good examples.

The radius of the ring is normally circumscribed by structural limitations. Since everything is known except the depth of the section in question, this can be evaluated by a systematic process around the entire frame.

Prior to educing this method of solving the problem, equation 3.0.12 may be further refined by taking into consideration the depth of the cross section.

3.1.0 Evaluation of Bending Stiffness in a Methodical Manner

Considering the ring to have depth and constant breadth, the moment and axial load may be translated to the center line of the cross section. This course of action presupposes that the structural yield properties of the material being used are the same in compression as in tension. This is not an erratic presumption, since it was assumed from the very beginning that the structure was stabilized against crippling or buckling phenomena and most ductile materials do display almost equal yield properties. It also presumes that the stress distribution is as shown in Figure 3.0.1(a).

Although it was not definitely asserted in the text, the ring was considered to be a line (the thickness shown in the Figures was employed to give the illustrations girth) prior to this discussion.

An elastic analysis demands some assumption concerning the distribution of structural stiffness in order to even obtain a solution. In each of the elastic solutions previously cited it was assumed that the ring was of constant cross section. To avoid any further confusion concerning the assumptions of

bending stiffness for a plastic solution, it is hereby specified that the method employed in this thesis does not presume any structural stiffness for a solution. It does presume, however, that the section will deliver (in the presence of any thrust, etc.) at the final points of hinge formation a magnitude of moment M_p. Therefore, the moment may be adjusted to the centerline of the cross section and the section determined will be that capable of delivering this moment value.

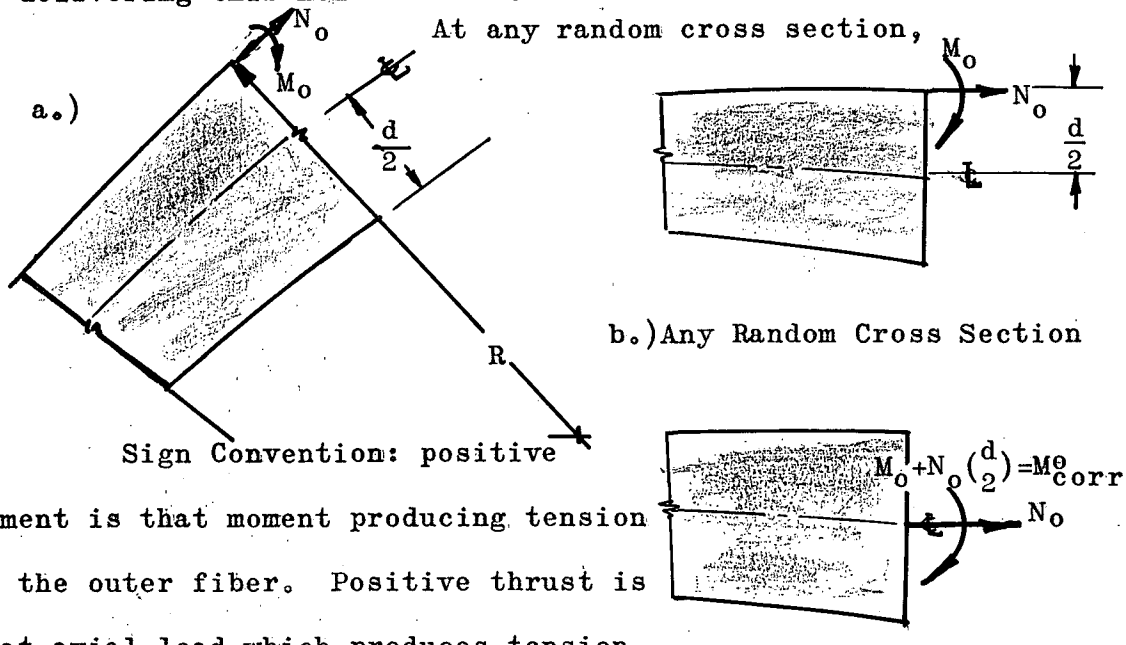

FIGURE 3.1.1 Adjusted Moment

From Figure 3.1.1, the adjusted moment is

$$M^{original}_{correct} = M^{original} + N^{original}\left(\frac{d}{2}\right) \qquad \text{.....(3.1.1)}$$

Reviewing expressions 3.0.11,

$$M^o_c = q_m \; PR + P \; q_n \left(\frac{d}{2}\right)$$

or rearranging,

$$M_c^o = q_m + \frac{1}{2}(q_n)\left(\frac{d}{R}\right) = q_m^{corrected} \quad \ldots\ldots\ldots\ldots\ldots\ldots (3.1.2)$$

The sign between the two terms depends on the sign of the moment and the axial thrust. However, the sign is automatically satisfied by establishing a sign convention. As shown in Figure 3.1.1, positive moment presumes tension in the outer fiber, and positive thrust is that load which produces axial tension.

If equation 3.1.2 is substituted in equation 3.0.16,

$$\frac{N_y^f}{P} = \frac{2}{d/R}\left[q_m + \frac{1}{2}\, q_n\left(\frac{d}{R}\right)\right]\left[1 + \sqrt{1 + \frac{1}{4}\left(\frac{d}{R}\right)^2\left[\frac{q_n}{q_m + \frac{1}{2}\, q_n\left(\frac{d}{R}\right)}\right]^2}\right]$$

$$\frac{N_y^f}{P} = \frac{2}{d/R}\left\{q_m + \frac{1}{2}\, q_n\left(\frac{d}{R}\right)\right\}\left\{1 + \sqrt{1 + \left[\frac{\frac{1}{2}\left(\frac{d}{R}\right) q_n}{q_m + \frac{1}{2}\, q_n\left(\frac{d}{R}\right)}\right]^2}\right\} \quad \ldots (3.1.3)$$

$$\frac{N_y^f}{P} = \frac{2q_m}{d/R}\left\{1 + \frac{1}{2}\left(\frac{d}{R}\right)\frac{q_n}{q_m}\right\}\left\{1 + \sqrt{1 + \left[\frac{\frac{1}{2}\left(\frac{d}{R}\right)\frac{q_n}{q_m}}{1 + \frac{1}{2}\,\frac{q_n}{q_m}\left(\frac{d}{R}\right)}\right]^2}\right\} \quad \ldots (3.1.4)$$

Equation 3.1.3 holds for all points of the interaction relation, but 3.1.4 does not hold for the condition of zero moment and some magnitude of axial load.

Just as stated on page 153 concerning 3.0.12, the only unknown in expressions 3.1.3 or 3.1.4 is the depth d. With a particular problem in mind, all the analyst need do for a solution is to assume various ratios of $\frac{d}{R}$ and then plot the resulting curves. This was done for cases, Ring I, Loading 2.0.0 for values of d/R of .05, .10, .15, .20, .25 using expression 3.1.3. Figures 3.1.2, 3.1.3, 3.1.4 were constructed in conjunction with these computations. These curves appear

INTERACTION CURVES - LOADING CONDITION 2.0.0

TABLE 3.1.1

Tabulation of Ordinates for Interaction Curves						
Angle φ From Vertical	$\frac{d}{R}$ = .100	$\frac{d}{R}$ = .125	$\frac{d}{R}$ = .15	$\frac{d}{R}$ = .200	$\frac{d}{R}$ = .25	$\frac{d}{R}$ = .300
0	-5.175		-3.256	-2.304	-1.739	-1.369
10	-1.808		-1.035	-.691	-.517	-1.550
20	1.641		1.244	1.202	.850	.750
30	3.575		2.747	2.339	2.096	1.936
40	5.241		3.855	3.168	2.759	2.488
50	6.272		4.529	3.662	3.145	2.803
60	6.681		4.774	3.826	3.259	2.884
$63^{o}45'$	6.680		4.785	3.806	3.235	2.856
70	6.509		4.621	3.681	3.119	2.747
80	5.826		4.117	3.266	2.757	2.419
90	4.732		3.324	2.628	2.211	1.935
100	3.297		2.313	1.823	1.529	1.334
110	1.668		1.163	.912	.762	.661
120	-.052		-.047	-.044	-.042	-.049
130	-1.738		-1.228	-.974	-.871	-.721
140	-3.289		-2.316	-1.831	-1.541	-1.349
150	-4.605		-3.235	-2.553	-2.144	-1.872
160	-5.606		-3.935	-3.102	-2.603	-2.272
170	-6.232		-4.372	-3.445	-2.890	-2.521
180	-6.443		-4.521	-3.561	-2.988	-2.606

INTERACTION EQUATION 3.1.3
VS.
ANGLE IN RADIANS
for
Loading Condition 2.0.0

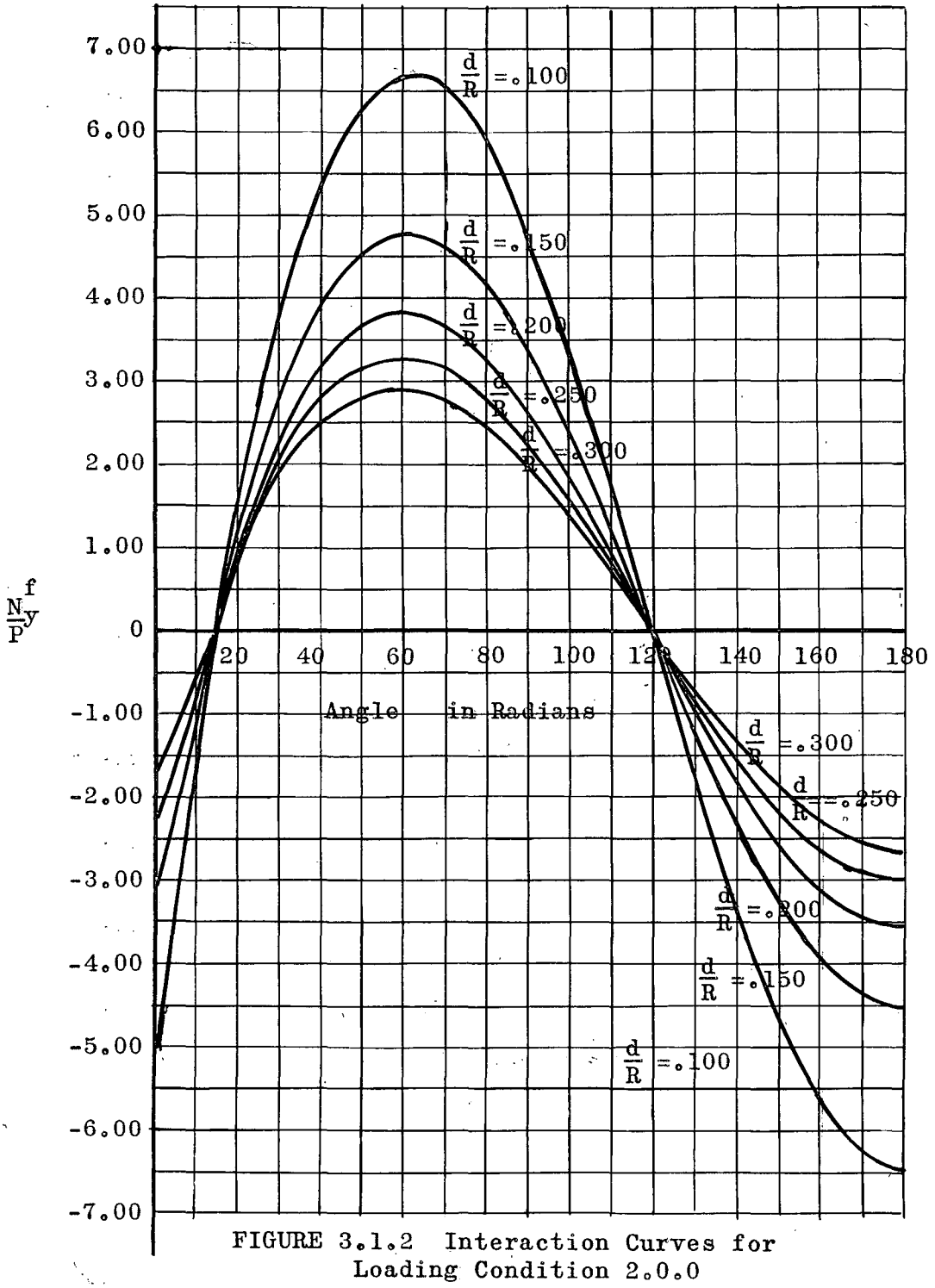

FIGURE 3.1.2 Interaction Curves for
Loading Condition 2.0.0

INTERACTION CURVES - LOADING CONDITION 2.1.0

TABLE 3.1.2

Tabulation of Ordinates for Interaction Curves						
Angle φ From Vertical	$\frac{d}{R}$ = .05	$\frac{d}{R}$ = .06	$\frac{d}{R}$ = .08	$\frac{d}{R}$ = .100	$\frac{d}{R}$ = .150	$\frac{d}{R}$ = .200
0	1.207	1.207	1.207	1.207	1.207	1.207
10	-1.762	-1.371	-.914	-.674	.473	.598
20	-3.274	-2.619	-1.737	-1.340	-.758	-.517
30	-3.912	-3.165	-2.237	-1.687	-.977	-.652
$31^{\circ}23'$	-3.939	-3.191	-2.261	-1.708	-.993	-.663
40	-3.808	-3.100	-2.218	-1.692	-1.004	-.675
50	-3.129	-2.557	-1.844	-1.408	-.857	-.584
60	-2.056	-1.685	-1.225	-.949	-.583	-.403
70	-.764	-.631	-.465	-.366	-.234	-.168
80	.588	.477	.388	.256	.149	.100
90	1.880	1.516	1.094	.841	.509	.347
100	2.918	2.391	1.732	1.338	.817	.562
110	3.693	3.029	2.199	1.703	1.046	.723
120	4.121	3.382	2.459	1.907	1.175	.815
$126^{\circ}13'$	4.199	3.447	2.508	1.946	1.2014	.835
130	4.177	3.429	2.496	1.938	1.197	.832
140	3.870	3.175	2.313	1.800	1.112	.775
150	3.225	2.649	1.931	1.501	.930	.648
160	2.311	1.899	1.385	1.076	.668	.466
170	1.205	.989	.722	.562	.349	.243
180	0	0	0	0	0	0

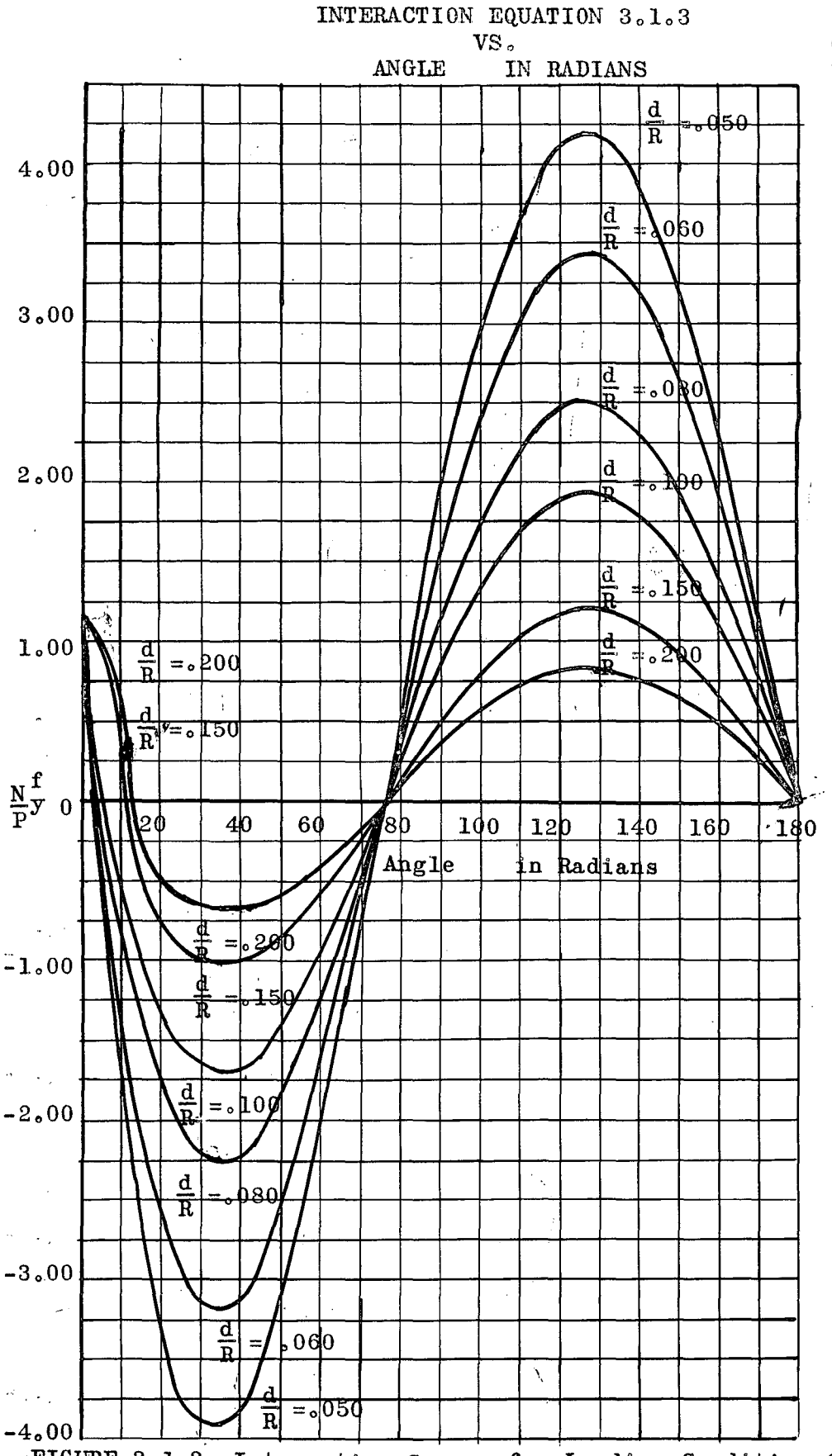

FIGURE 3.1.3 Interaction Curves for Loading Condition 2.1.0

INTERACTION CURVES - LOADING CONDITION 2.2.0

TABLE 3.1.3

Tabulation of Ordinates for Interaction Curves						
Angle From Vertical	$\frac{d}{R}$ = .10	$\frac{d}{R}$ = .125	$\frac{d}{R}$ = .15	$\frac{d}{R}$ = .200	$\frac{d}{R}$ = .25	$\frac{d}{R}$ = .30
0	0	0	0	0	0	0
10	2.691	2.115	1.732	1.251	.965	.776
20	5.222	4.103	3.357	2.427	1.870	1.502
30	7.616	5.983	4.895	3.538	2.727	2.189
30	8.610	6.976	5.886	4.525	3.709	3.166
40	5.206	4.280	3.663	2.894	2.434	2.116
50	2.143	1.853	1.675	1.445	1.308	1.218
60	-.634	-.587	-.0465	-.394	.047	.053
70	-2.982	-2.254	-1.776	-1.198	-.901	-.679
80	-4.800	-3.675	-2.959	-2.051	-1.520	-1.180
90	-6.153	-4.767	-3.846	-2.704	-2.029	-1.589
100	-7.010	-5.457	-4.421	-3.133	-2.368	-1.866
110	-7395	-5.767	-4.684	-3.336	-2.534	-2.005
$112^{o}2'$	-7.415	-5.785	-4.701	-3.351	-2.546	-2.017
120	-7.315	-5.714	-4.649	-3.322	-2.528	-2.009
130	-6.811	-5.326	-4.338	-3.107	-2.356	-1.888
140	-5.932	-4.643	-3.784	-2.714	-2.076	-1.655
150	-4.738	-3.710	-3.004	-2.173	-1.664	-1.327
160	-3.298	-2.584	-2.108	-1.515	-1.161	-.927
170	-1.692	-1.326	-1.082	-.778	-.596	-.476
180	0	0	0	0	0	0

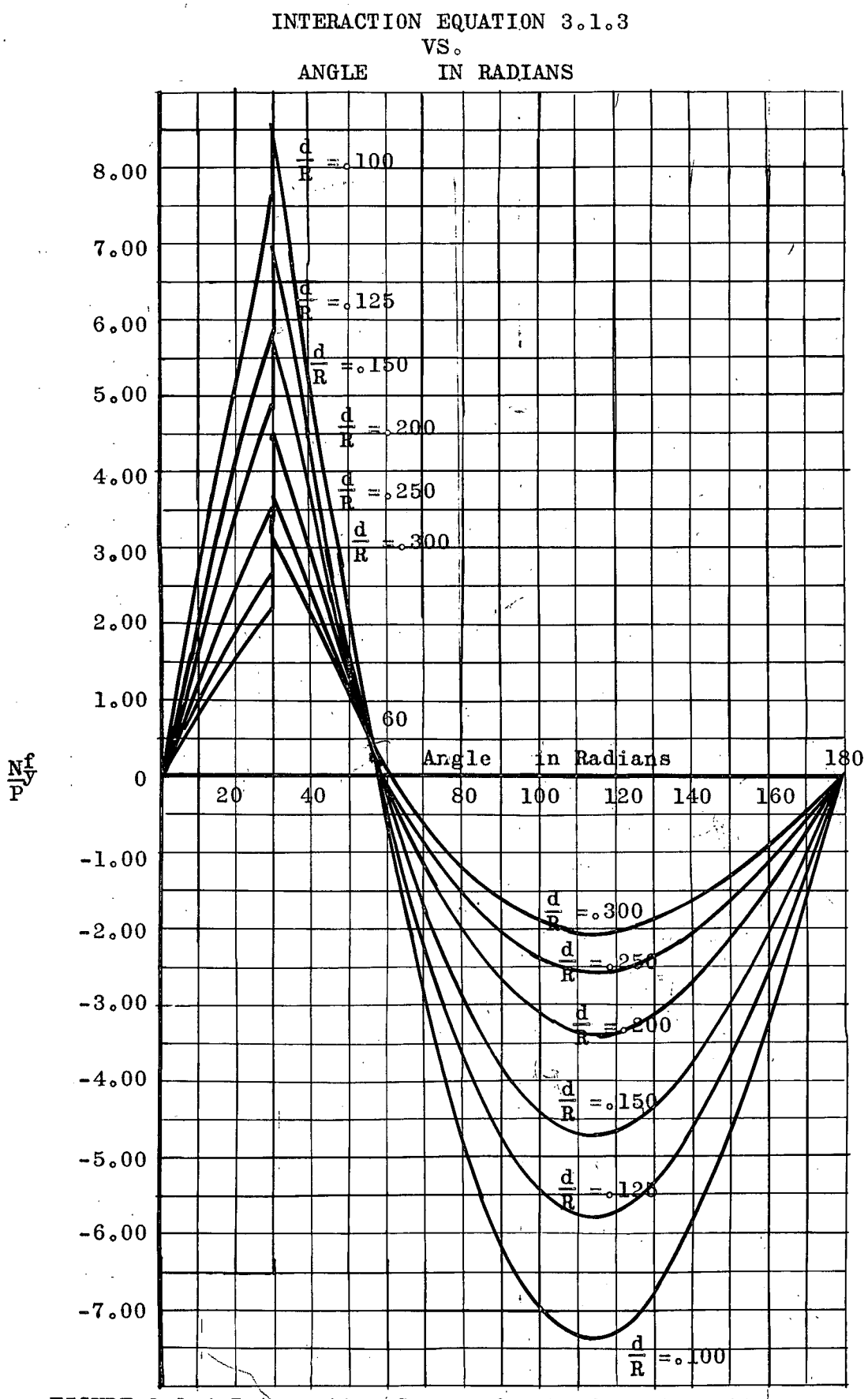

FIGURE 3.1.4 Interaction Curves for Loading Condition 2.2.0

to simulate the moment curves with their crests and troughs shifted by the influence of axial load.

Some interesting observations concerning the interaction curves may be made. First of all in the instance of loading 2.1.0, Figure 3.1.3, as the ratio of d/R increased near the applied load (φ approaching zero) there is a definite cusp in the curve. The explanation for this phenomenon is the high axial loads as compared to moments approaching zero in this area. In fact, at $\varphi = 0$ there is no moment, but there is an ordinate on the curve because of the axial load at this point. Actually the interaction curve almost assumes the shape of the axial load curve, having an ordinate at zero determined completely by axial load alone.

It will be observed that the interaction curves assume the shape of the moment curve in all cases. Even the intersection of the curves with the zero axis are the same as the crossing points of the moment curves for loadings 2.0.0 and 2.1.0, shifting only slightly in loading case 2.2.0 (Figure 3.1.4). The peak of the interaction curve does not necessarily fall immediately at the peak of the corresponding moment curve, but may be affected enough by the axial thrust to shift towards the peak of the axial thrust curve. Also, it may be observed in Figure 3.1.4 that there is a sharp discontinuity in the interaction curves at $\varphi = 30^{\circ}$. This phenomenon is due to the extreme influence of axial load, which has a transition from a negative to a positive value (see Figure 2.2.10) at this angle.

Once the interaction curves have been drawn (Figures 3.1.7, 3.1.3, 3.1.4), the analyst is ready to proceed to design the frame.

3.1.1 Systematic Procedure for Designing a Circular Frame with a Constant Thickness Rectangular Section

For most practical designs a structure is normally designed for more than one loading condition. However, only one loading may be treated at a time. Begining with the interaction curve, Figure 3.1.2, loading condition 2.0.0 will first be dealt with as a precedent.

The succeeding method is arbitrary and flexible, and is proposed in such a manner that the analyst is given much freedom of design.

1.) Given the value of P and the radius of the circular frame, the only tool necessary for a solution is the interaction curve of moment and axial load for a specific loading condition. (Take Figure 3.1.2 as an example).

2.) First of all, determine the greatest dimension of the ring. This is the greatest ordinate (plus or minus) on the interaction curve. (Note: It is not necessary to pick this point, any other would do just as well).

The greatest dimension is obtained in the following manner. (Refer to Figure 3.1.2).

a.) Assume that d/R at this position on the curve is a certain value. As an example let $\frac{d}{R} = .200$ (point A Figure 3.1.2)

b.) This corresponds to a certain value of $\frac{N^F}{P}$, but

$$\frac{N_y^F}{P} = bd \quad \frac{\sigma_y}{P} \qquad \text{.....(3.1.4)}$$

For this example

$$bd \quad \sigma_y = 3.826P$$

c.) Assume a value for b. Just for purposes of illustration let b = 1.0 (unity). Then d can be found by

$$d = \frac{3.826P}{\sigma_y}$$

d.) This d would be divided by "R" to see what the ratio d/R is for the section chosen.

$$\frac{d}{R} = \frac{3.826P}{\sigma_y R}$$

If this ratio is different from the selected d/R (e.g. 0.200), the process would be repeated by selecting a new value of $\frac{d}{R}$ and undergoing the previous steps. The method converges quickly, and eventually the analyst has the correct ratio of $\frac{d}{R}$ corresponding to the applied loads, and the strength of the material being used.

3.) Once the parameter d/R is known for one point, the analyst is ready to progress around the frame estimating the profile of the stiffness at various sections. Since one of the primary suppositions was a constant thickness of ring section, the depth of ring, "d", is the only variable. Furthermore, since "d" is known for one place, an elementary computation determines d at any other section of the ring. This is obvious from Figure 3.1.5

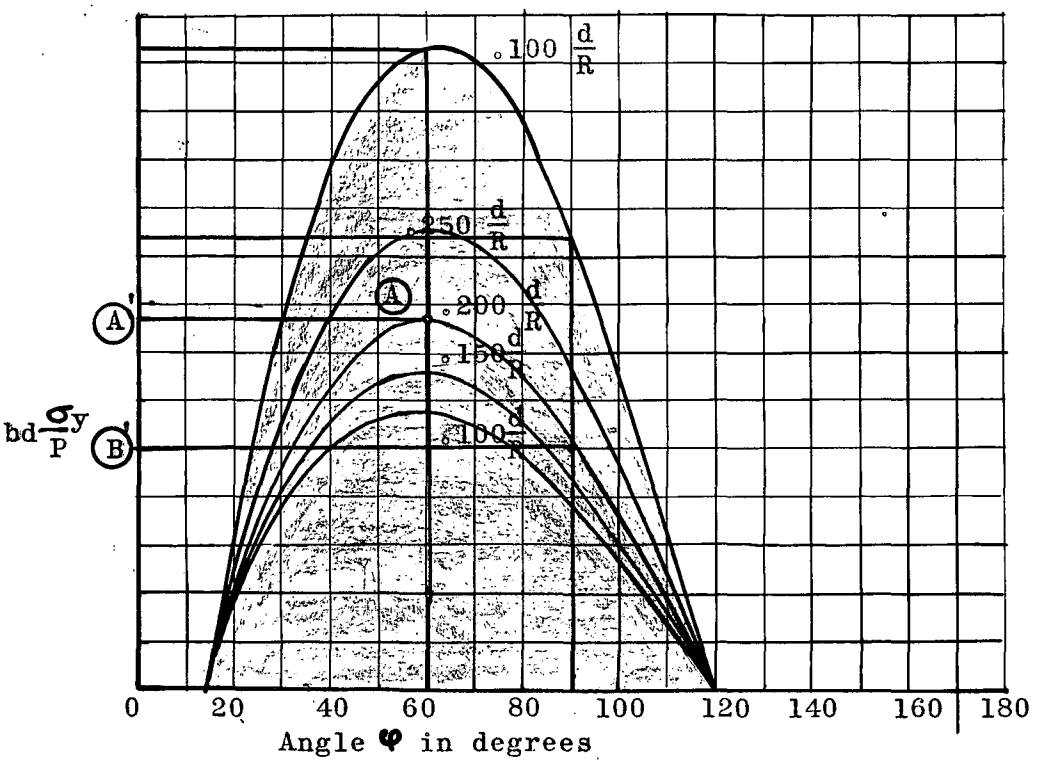

FIGURE 3.1.5 Loading Condition Ring I-2.0.0 Interaction Curves

Returning to the previous illustration, suppose it is desired to find the depth of section at 90^{o}. From Figure 3.1.5, all that has to be done to obtain the depth at the cross section 90^{o} is to get the ratio of the d/R at the new point with respect to the known d/R to equal the ratio of the new $bd\frac{\sigma_y}{P}$ to that for the original $bd\frac{\sigma_y}{P}$. This may be expressed in equation form as follows

$$\frac{\text{(A)}'}{.200} = \frac{\text{(B)}'}{\frac{d}{R}\ \text{New}} \qquad \text{.....(3.1.5)}$$

That is

$$\frac{bd(\frac{\sigma}{P}y)\text{Point (A)}}{(\frac{d}{R})\text{Point (A)}} = \frac{bd(\frac{\sigma}{P}y)\text{Point (B)}}{(\frac{d}{R})\text{Point (B)}} \qquad \text{.....(3.1.6)}$$

A complete design would be acheived by determining the correct $\frac{d}{R}$ (or $bd\frac{\sigma_y}{p}$) at various sections. After the method as outlined is completed, the results may be presented in the manner shown in Figure 3.1.6 or as shown in Figure 3.1.7.

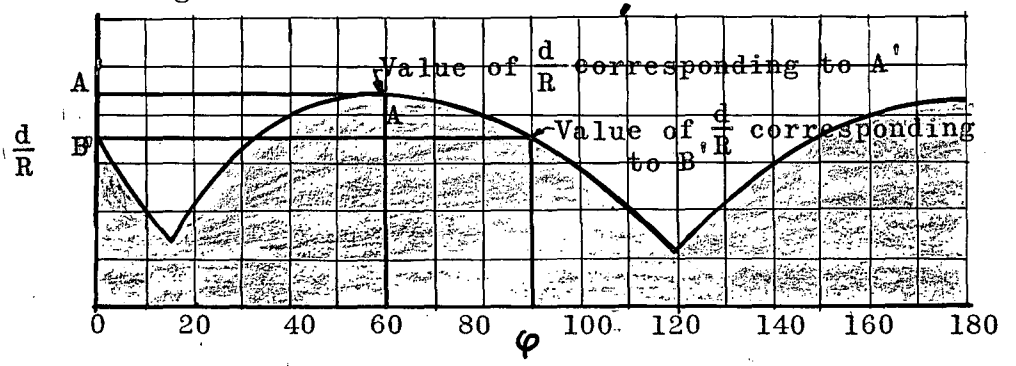

FIGURE 3.1.6 Method of Presenting Ring Stiffness

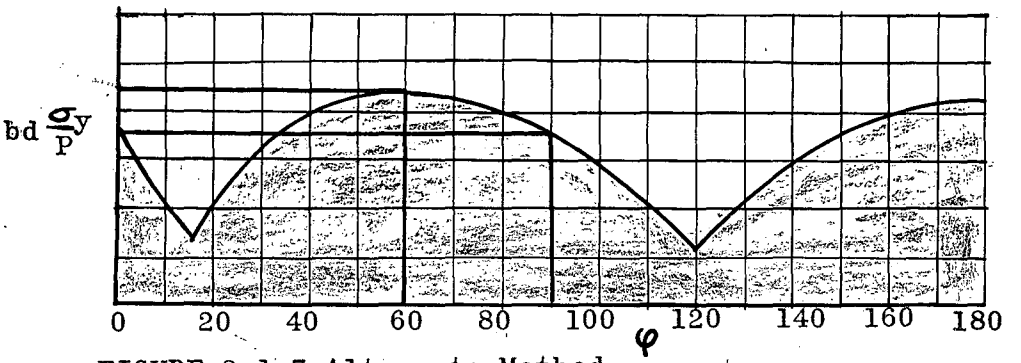

FIGURE 3.1.7 Alternate Method

Note: The maximum point on the curve may arbitrarily be assigned the value of unity so that all values of stiffness would be related to the maximum value of d

To gain an overall picture of the method, it was decided to go through an example. Subsequently, the succeeding problem is proposed (See Figure 3.1.8).

P_v = 30,000 lb.

P_h = 40,000 lb.

$P_{t@\ 30^o}$ = 30,000 lb.

Note: All loads are limit loads and not the ultimate loading

R = 15 inches

σ_y = 40,000 psi. (24ST Bar Aluminum, according to the ANC-5) "Strength of Metal Aircraft Elements"

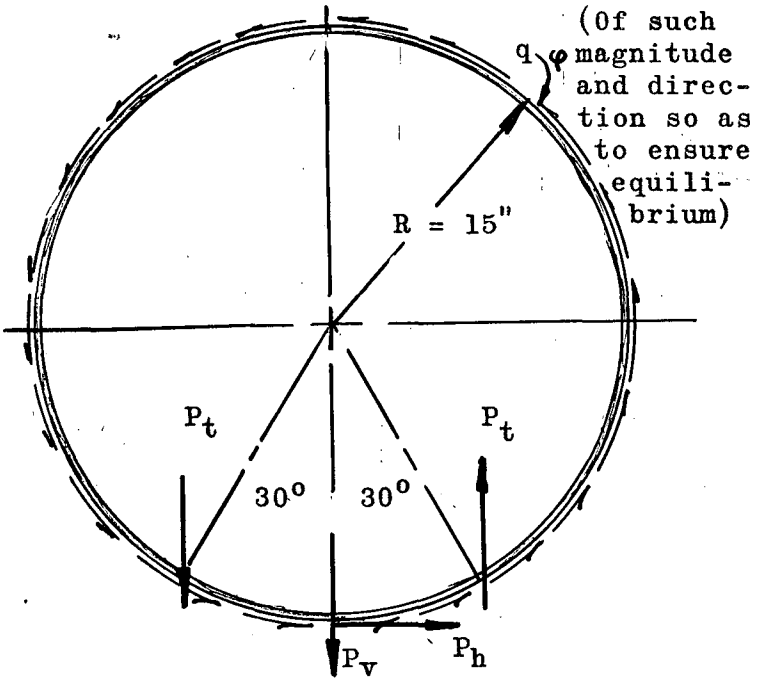

FIGURE 3.1.8 Example Loading

Plastic Analysis is not adaptable to superposition of loading. Consequently, each loading must be analyzed individually. It is assumed that shear flows will be such as to ensure external equilibrium.

Commencing with the vertical load, P_v = 20,000 lb., assume a constant width of section = .80 in. The maximum ordinate on any of the interaction curves of Figure 3.1.2 is located at an angle $\varphi = 60^\circ$ (the maximum ordinate is shifted from the crest of the moment curve because of the influence of the axial thrust). If this is the first position selected, then a d/R = .20 is a good estimate. If (for a first trial) d/R = .250, then

$$bd \frac{\sigma_y}{P} = 3.235 \qquad \text{(From table 3.1.1)}$$

$$d = \frac{30,000}{40,000} \quad \frac{3.235}{.8} = 3.04$$

$$\text{or} \quad \frac{d}{R} = \frac{3.04}{15} = .202$$

Try a value of d/R between .202 and .250

Try $\frac{d}{R} = .225$

$$bd \frac{\sigma_y}{P} \approx 3.50$$

$$d = \frac{30,000}{40,000} = \frac{3.50}{.8} = 3.28 \text{ in.}$$

$$\frac{d}{R} = \frac{3.28}{15.0} = .219$$

The process is converging. After a few trial and error attempts, it was finally established that a $\frac{d}{R} = .220$ satisfies the process most aptly.

Now that a single stiffness value has been obtained, other succeeding values may be obtained with the assistance of expression 3.1.6

$$\text{or } \frac{3.50}{.220} = \frac{bd \frac{\sigma_y}{P} \text{ other point}}{\left(\frac{d}{R}\right)_{\text{other point}}} \qquad \ldots\ldots\ldots\ldots (3.1.6(a))$$

It is reasonable to presume that $\frac{d}{R}$ will be smaller at other points. If the section at 90^o is to be ascertained next, it is found that $\frac{d}{R} = .180$ satisfies 3.1.6(a))

$$\text{or } \frac{3.50}{.220} = \frac{2.85}{.180}$$

If an exaggerated curve of the nature shown in Figure 3.1.6 is plotted with a few random initial values taken from the process above excellent accuracy may be obtained by picking off the remaining stiffnesses.

As the analyst proceeds around the ring, he obtains the curve A, Figure 3.1.8.

The same means of ascertaining $\frac{d}{R}$ for the horizontal load, P_h, and the twisting moment P_t Rsin 30° may be employed as outlined in the immediate preceding method. The execution of this procedure results in Figures 3.1.8 A, B, C.

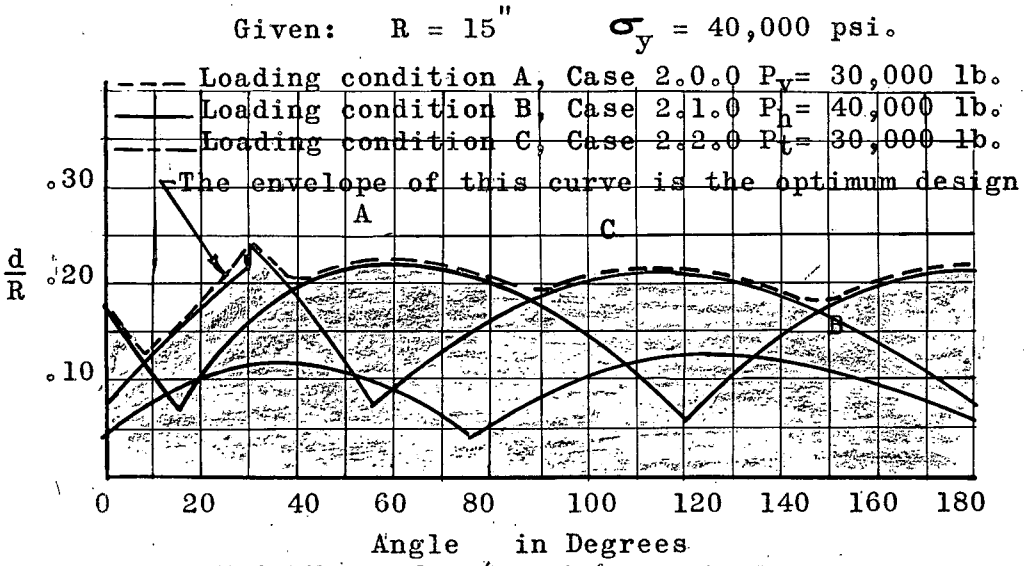

FIGURE 3.1.8 d/R ratio vs. Angle

The various stiffness curves resulting from the trial and error process is shown in Figure 3.1.8. The solution of the example is shown in Figure 3.1.9.

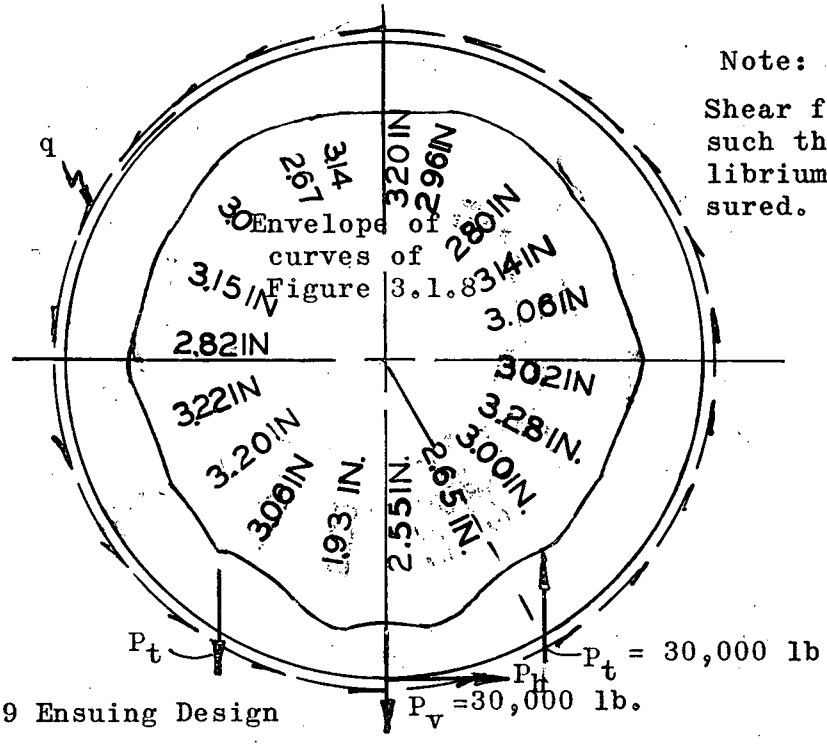

Note:

Shear flows are such that equilibrium is ensured.

FIGURE 3.1.9 Ensuing Design

It may be seen from Figure 3.1.8 that the envelope of the curves is the optimum design. Since anywhere outside this envelope ample stiffness is supplied to sustain any of the design loads, then it is believed that a frame designed by the proposed method yields the most favorable bending stiffness.

The importance of this corollary cannot be over emphasized. It is not possible to employ such a method in conjunction with elastic analysis, becuase each time the stiffness is changed the resulting solution is altered. Elastic analysis is a trial and error procedure entirely dependent on the original assumed bending stiffness. A solution to a plastic analysis is based on the positions of the loads and geometry of the structure. It does not presuppose any conformity of structural stiffness, nor does it restrictively rely on the strength properties of a material. Thus, any method for designing a frame, such as just was proposed, is plausible for a plastic solution.

3.2.0 Influence of Shear

Unfortunately the influence of shear can not be separated in the same manner in which the influence of axial thrust was formulated in the preceding section.

According to Mise's stress theory (see page 113 of this thesis) the principal stresses which result from combined axial stress and shear stresses are

$$\sigma_1 = \frac{\sigma}{2} + \sqrt{\frac{\sigma^2}{4} + \tau^2} \quad , \quad \sigma_2 = \frac{\sigma}{2} - \sqrt{\frac{\sigma^2}{4} + \tau^2} \qquad \text{.....(2.2.28)}$$

and the condition of yielding becomes

$$\sigma^2 + 3\tau^2 = \sigma^2_{Y.P.} \qquad \text{.....(2.2.29)}$$

If the axial stress is assumed zero then 2.2.29 reduces to

$$\tau_{max} = \frac{\sigma_{Y.P.}}{\sqrt{3}} \quad \text{.....(3.2.1)}$$

However, the combination of high shear and high moment can only occur where the moment gradient is high, that is, where two hinges of opposite signs approach each other. However, yielding will be restricted in this vicinity, and the area may go into strain-hardening, thus increasing the ultimate moment capacity. Therefore, it is not anticipated that shear will have a significant effect on the actual maximum bending strength, and tests have shown this to be the case for the majority of problems. The only exception to this proposition is conceivable in regions of constant shear where the shear web (or the area of elastic stress distribution) may be subjected to shearing stresses near the yield value. Loading condition Ring IV, 2.3.0, may be cited as an example of this situation.

3.3.0 Progressive Deformations under Varying Loads*

The problem of progressive deformations under varying loads may be divided into two separate categories, which are:

1.) Alternating Plasticity

2.) Deflection Stability ("Shakedown")

1.) The phenomenon of alternating plasticity may be considered best from the illustration shown in Figure 3.3.1. The curves represent the moment curvature relationship for a cantilever beam laden with a concentrated load at the free end. It is customarily assured that the action of alternating plasticity

*See reference 5, section 9.5

induces a premature failure when the wall section (at the built-in end) is subjected to repeated cycles of loads that induce further yielding at each successive cycle. This condition assimilates the elastic phenomenon of fatigue of the material, but is actually a plastic fatigue.

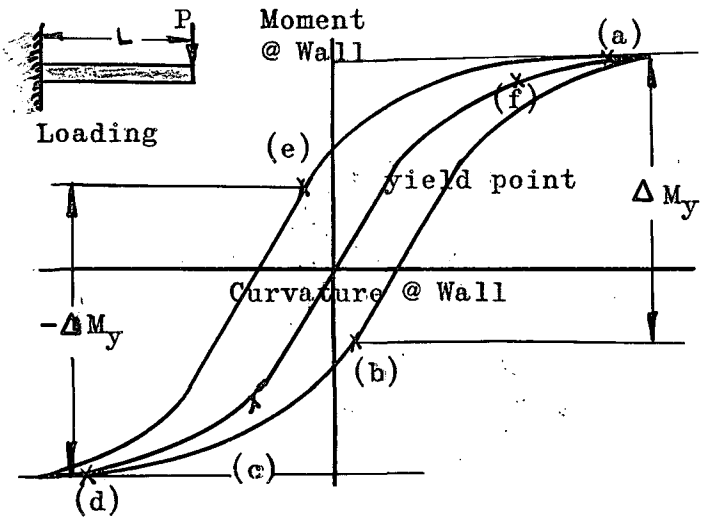

FIGURE 3.3.1-Moment Curvature Relation for a Cantilever Beam

Suppose that the load P is first applied downward, and beyond the yield point of the material (position "a" of Figure 3.3.1). Suppose, further, that the load is released and then reversed to a negative value (position "b" of Figure 3.3.1). The linear distance from "a" to "b" is represented by the dimension ΔM_y. Further application of load in the reversed direction causes more yielding but in an opposite sense. Eventually point "d" is reached corresponding to a negative value of moment $-\Delta M_y$. The complete cycle is realized by finishing the remaining trajectory d - e - f - a.

As long as the load does not exceed a limiting value corresponding to the moments at ("a" or "d" the structure is still capable of sustaining loads. Hence, the obvious conclusion is that there exists some range of P or M values for which a structure behaves elastically regardless of its previous loading history.

The necessary condition to insure against the possibility of failure due to alternating plasticity is

$$(M_i)_{max.} - (M_i)_{min.} \leq \triangle M_y \qquad \text{.....(3.3.1)}$$

where M_i denotes the moment values of any section "i" being considered.

Hence, as long as the loads are increased in the same proportion, they may be applied indefinitely as long as they do not violate the alternating plasticity condition (equation 3.3.1).

2.) Suppose now that the loads are not increased proportionately. Then, the structure behaves differently, and the result of this behavior is known as "progressive deformations due to varying loads" or "shakedown".

The quandary of progressive deformations under varying loads has already been discussed in the introduction on pages 38 and 39. At that point in the discussion, it was asserted that progressive deformations under varying loads do not appear to present a serious problem. Accordingly, for most structures (and rings are included in this category) encountered in practice, the difference between the true ultimate load considering the effect of repeated variable loading and the load based on simple plastic theory is usually insignificant. On the other hand, the analyst should be familiar with the problem such that, when it is important, a solution can be made for the case in hand.

Essentially, the problem of shakedown is one which arises when a structure is subjected to several loads, each of which may vary between certain prescribed maximum and minimum limits regard-

less of the size of the other loads being applied. Once the structure has yielded at some point because the load has exceeded the elastic limit value it is possible for the structure to stabilize itself for further cycles of loading of residual stress. The load then would be supported in a purely elastic manner. The converse of this is also true. Above a given loading, deflections will not stabilize but will rather increase at each cycle of loading.

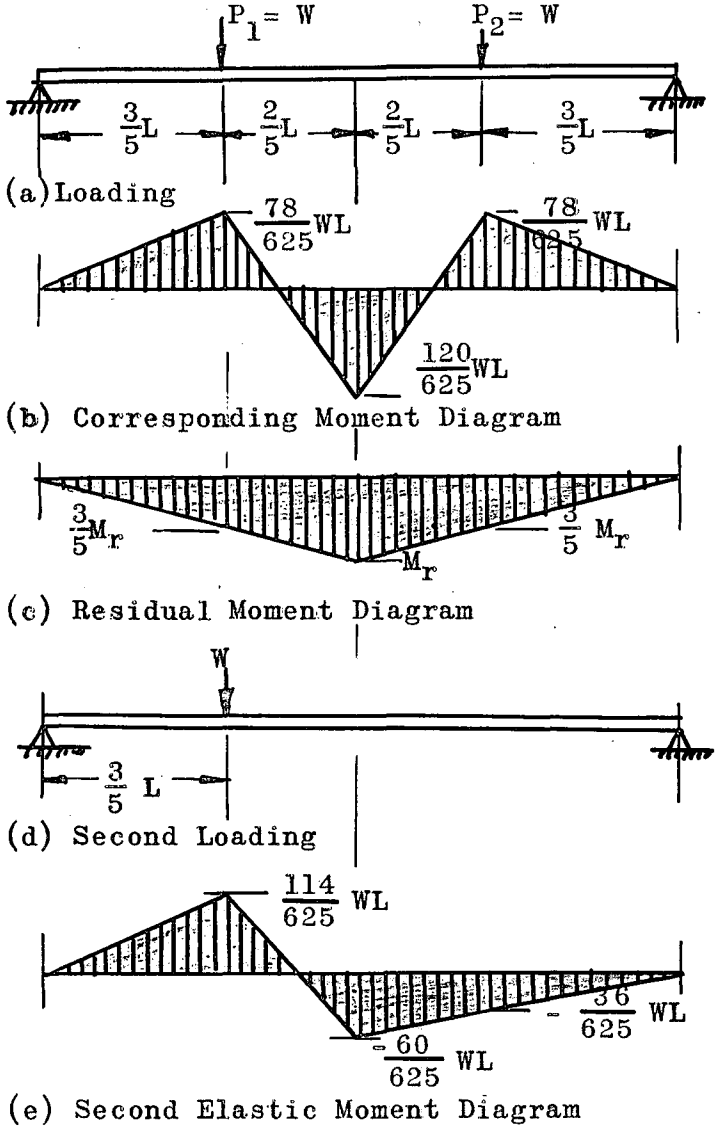

FIGURE 3.3.2 Shakedown Phenomenon

To illustrate this phenomenon, Figure 3.3.2 was constructed. As an instance suppose a continuous beam of two equal spans is laden with W loads as shown in Figure 3.3.2(a). If the loads are imposed beyond the yield load, the maximum moment for the elastic diagram is at the center support $\frac{120}{625}$ WL

in Figure 3.3.2(b), if the loads are withdrawn there is a residual moment, M_r, induced at the center support because the load has progressed beyond its elastic capacity. There is a respective moment of 3/5 M_r at the locations of the W loads. To continue the discussion, suppose that only one of the loads W is restored as shown in (d). Then its resulting elastic moment diagram is shown in Figure 3.3.2(e).

To satisfy the condition of shakedown (see Page 39) two inequalities must be established. These are:

$$m_i + (M_i)\ \max \leqslant M_{pi}$$

$$m + (M_i)\ \min \leqslant -M_{pi} \qquad \text{.....(3.2)}$$

where the i denotes the section under consideration. (Note the moments on the left hand side of the inequalities are elastic moments).

For the problem at hand (see Figure 3.3.2), the inequalities become equalities

$$m_1 = M_p - (M_1^e)_{max} = M_p - 114/625WL$$

$$m_2 = -M_p - (M_2^e)_{max} = -M_p + 120/625WL$$

$$m_3 = M_p - (M_3^e)_{max} = M_p - 114/625WL$$

Give the continuous beam a virtual rotation θ at the left hand end (see Figure 3.3.3).

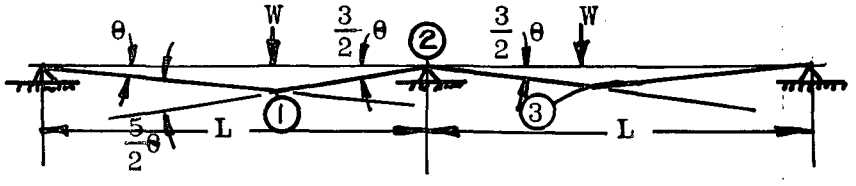

FIGURE 3.3.3 Virtual Rotations of Two Span Beam

Then $\sum m_1 \theta_1 = 0$

$$(M_p - 114/625 WL) \frac{5}{2} \theta + (-M_p + \frac{120}{625} WL) (-\frac{3}{2} \theta) = 0$$

$$M_p = .1862 \text{ WL or } W_s = 5.38 \frac{M_p}{L}$$

If shakedown is not considered the maximum moment obtained is

$$P\theta (\frac{3}{5}) L = 4 M_p \theta$$

$$M_p = .1500 \text{ WL or } W_s = 6.67 \frac{M_p}{L}$$

Thus, the structure can carry 19.5 percent less load. This is a significant difference. However, it is noticed that the structure is less stiff when only one load is imposed at a time, since a load on the adjacent span would cause much smaller deflections and moments. This is not necessarily true for rings, since, if only one load is imposed on a structure as contrasted to two loads imposed at the same time, the structure is not significantly weaker (or the difference in moment diagram is not significantly defferent).

For this reason an example problem of deflection stability has not been considered.

SECTION 4.0.0

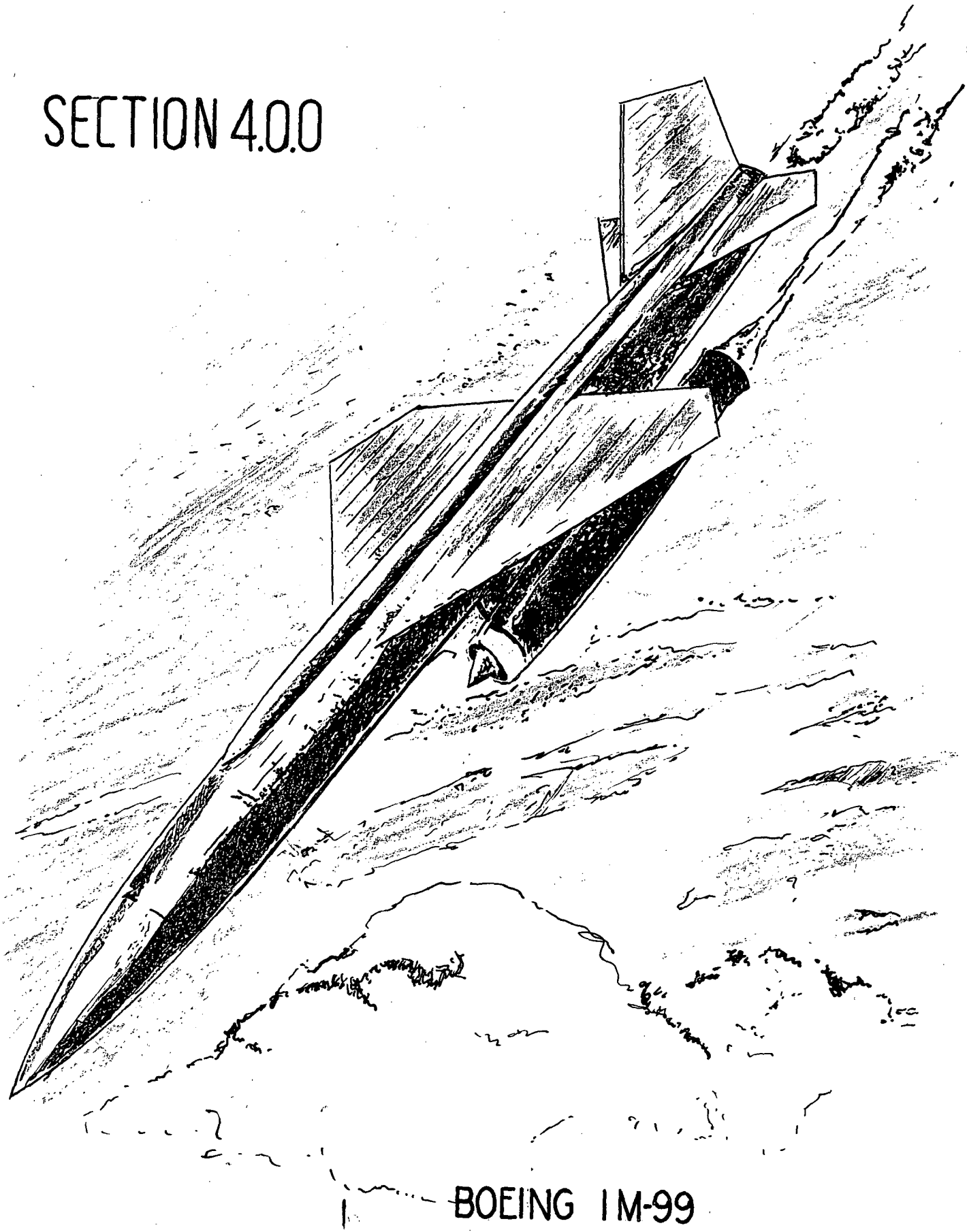

BOEING IM-99

IV Conclusions and Recommendations

4.0.0 Recommended Systematic Procedure

It was stated on page 42 that the primary object of this dissertation is to present a straight forward methodical procedure for analyzing continuous rings by means of a plastic theory. It is hoped that this ambition has been realized in the preceding text.

It is believed that any circular ring may be analyzed plastically by going through, step by step, the method proposed in any of the rings analyzed. Nevertheless, the method will be outlined, presently, to feature some of the highlights encountered in the foregoing text.

If the analyst wishes to analyze a continuous circular frame by the recommended method, he should employ this procedure. First of all, the magnitude of the applied loads and the manner in which these loads are externally reacted must be established before entering into a solution.

1.) Without a doubt, the first step in the procedure is to determine the hinge pattern, or the arrangement of the points of maximum moment around the ring. The whole crux of the problem lies in the competency of the analyst to ascertain the configuration of the hinges. Consequently, once a few general rules are imbued in his mind, he is ready to undertake any circular ring problem and arrive at a solution.

By definition maximum moments occur at the locations of zero shear. Thus, a hinge may form in any of the following places.

a.) at the position of a concentrated load. (This is not necessarily a point of zero shear, but may be the place where the shear translates from a negative to a positive value.

b.) at equal angles to an axis of symmetry by virtue of geometrical symmetry and symmetry of loading.

c.) at an abrupt change of direction of a member. (This condition may be induced by geommetrical limitations, wherein the inner mold line is fixed and a plastic hinge would be compelled to form at an abrupt change of stiffness. This condition assimilates the geometrical fixity of the base of a fixed-ended rigid frame.)

Any other condition which fixes the point of zero shear is also a valid guide. Actually, the analyst should not be discouraged if he has difficulty in ascertaining the locations of the hinges at first. If all of the hinges are left in terms of four general unknowns, the ensuing solution could be maximized with respect to each angle successively to obtain the general solution. In such a case implicit differentiation will prove to be more workable. Obviously, symmetry and other conducive means help to simplify the process.

2.) Secondly, the next step requires a little inherent ingenuity on the part of the analyst. In order to relate the various distortions of the ring, some point or segment of the frame must be fixed in space. A wise choice concerning this quandary will save much time and avoid tedious,complicated mathematical manipulations. Howbeit, if the analyst

does not make a prudent choice the first time, the geometry and mathematical work expressions become so involved that he is obliged to give up this pursuit and start all over by fixing another point or segment of the structure in space. Prudent selections of structural fixity develop from experience, and should not dismay the analyst right away.

3.) The structure is given a virtual (imaginary) rotation at one of the hinges or the instantaneous center, and the corresponding relationships between the virtual rotations of the different segments of the ring are evaluated.

4.) Whether this next step is to be included in the procedure or not is considered the analyst's prerogative. The next suggested step is to resolve the external shear flows into their equivalent components, in order to expedite the computation of the external work of the shear flow. This step is optional since some analysts may wish to deal with the shear flow directly, that is, without breaking it up into components. The selection of the center of the ring for this resolution is also arbitrary because any other point may have been chosen just as well.

Step 4.) could have been recommended to precede step 2.);however, it is felt that some time and effort is saved, if the ring is fixed first and then the components of the shear flow are resolved afterwards. In this manner, some of the components are eliminated because the shear components on the fixed portion do no work.

5.) Consistent with the imparted virtual rotations,

the internal and external work is evaluated.

The internal work is simply the addition of the products of the hinge moments and their corresponding virtual movements. Note: The internal work performed by the individual virtual rotations always adds, regardless of the direction of the rotations. Therefore, the sign of the work performed by the internal plastic hinge rotation is automatically defined.

The external work is ascertained by computing the work done by all external forces and moments(i.e. P,X,Y,M) about their individual instantaneous centers. The sign convention is designated such that positive work is determined by the sign of the moment of the components. In other words, positive moment is that moment which assists the rotation of the failure mode.

The execution of the principle of virtuals displacements is accomplished by equating external to internal work. The result is the expression for maximum moment, M_p, in terms of the load P and the geometry of the ring.

6.) The exact solution of the problem is the determination of the exact angles which furnish the maximum moment. These angles are evaluated by maximizing the moment expression with respect to each unknown angle defining the locations of the hinges.

7.) The last step in the procedure is to perform the plasticity check. This consists of constructing the collapse mechanism and then plotting the moment diagram from expressions derived from internal forces and moments. If the condition $M \leq M_p$ is

satisfied, then this is the correct or ultimate solution.

Thus, the complete procedure may be summarized in the seven following steps:

1.) Determine the hinge pattern.

2.) Choose a point or segment of the structure to be fixed in space. (Caution, a hinge can not be contained inside the limits of the fixity)

3.) Determine the relative virtual rotations of the various segments of the ring.

4.) Resolve shear flows into their equivalent components.

5.) Apply the principle of virtual rotations

$$W_{int} = W_{ext}$$

6.) Maximize the resulting moment expression.

7.) Perform the plasticity check.

Now, that the procedure has been presented, the primary purpose of the thesis has been acheived.

4.1.0 Discussion of the Proposed Method in Conjunction with Design Procedures

It has already been acknowledged on page 8 that the problem of ring analysis is not approached from the design aspect in this thesis. Nevertheless, a design comparison would be an effective manner in which to compare an elastic to a plastic solution of a problem.

Since a plastic design has already been performed (see Figure 3.1.9) this would be a convenient example for an elastic to plastic comparison. To acheive an elastic design some bending rigidity, EI, must be assumed. In order to simplify the deter-

mination of an elastic design, assume that the ring has a constant stiffness all of the way around the circle. Thus, the resulting solution to the problem would be of the nature of the elastic curves at the end of loadings 2.0.0, 2.1.0, and 2.2.0. Superposition of loading is compatible for an elastic solution, however, the resulting designs are most certainly not suitable for the proposition of superposition. Consequently, not only is the ensuing design dependent on the maximum moment within the ring for a particular loading, but the final design is based upon the maximum moment of the governing loading.

The governing loading appears to be condition 2.2.0, and the maximum moment for the elastic solution occurs at the applied vertical loading. Referring to Figure 3.1.9, the prevailing loading is P_t = 30,000 lb. If the cross section is to be designed consistent with this loading, the ultimate moment and thrust combination occurs under the load just above the hinge. Transferring the moment to the centerline of the section $M = .264PR + .152\left(\frac{d}{2}\right)P$

$$\sigma_y = \frac{P}{A} + \frac{M}{-} = \frac{.152(30,000)}{bd} + \frac{.264(30,000)(4)+.152\frac{d}{2}(30,000)\ 4}{bd^2}$$

$$\text{where } z = \frac{bd^2}{4}$$

Let b=.8 in. and σ_y = 40,000psi(24ST bar aluminum)

$$d = \sqrt{\frac{5700(d) + 594,000 + 11,400(d)}{40,000}}$$

d = 4.07 inches .....(4.1.1)

Note: The above calculation assumes that the cross section

at the applied load (and that section only) is fully plasticized at failure.

The total wieght of the ring for the preceding computations then becomes a simple calculation.

The volume is

$2(15-2.035)(\pi)(4.07)(.8) = 266$ cubic inches.

Since the material employed is aluminum, its total weight is

$W_e = 266(.100 \text{ lb/in}^3) = 26.6 \text{ lb}.$

An approximation to the weight of the ring of Figure 3.1.9 may be obtained by assuming straight lines between the known depths of the designed frame at 10^o intervals around the ring.

The volume is approximated

$2(\text{average depth})(\text{average radius})\ \frac{10}{180}\ (3.1416)(18)(.8) =$

$2(2.97)(13.51)(3.142)(.8) = 201.7$ cubic inches

The total weight

$W_p = 201.7\ (.100 \text{ lb/in}^3) = 20.2 \text{ lb}.$

Percentage of weight saving

$$\frac{W_e - W_p}{W_e} = \frac{26.6-20.2}{26.6} = 24.6\%$$

This truly is a remarkable saving in weight. It is realized that the approximation of the illustration is crude, because an elastic solution would actually be performed by a trial and error process. First a constant bending rigidity, EI, would be assumed, and a solution would be obtained. With this trial stiffness another trial solution could be performed, resulting in a new stiffness. The analyst could proceed with this

method until he felt he had an optimum design, but it is questionable if he will ever reach the plastic design.

It is noticed that no mention has been given the subject 'factor of safety' or 'margin of safety'. The reason for the deliberate disregard of the subject is the variance between the arbitrary factors or margins employed in different types of industrial designing. Actually a factor of safety (or margin of safety) is incorporated in the design by virtue of the fact that the load and strength used was a limit load and yield stress and not an ultimate loading or ultimate strength. Thus, the factor of safety was really concealed in the comparison of the two methods, being equal for each case. For an actual design one would first increase his loads by the desired margin of safety and then proceed to design the structure to fail at this increased load.

4.2.0 The Effects of Stability on Plastic Analysis

Structural Stability is always a significant problem whether designing elastically or plastically. It appears, however, that the problem of buckling is more severe for plastic design, and consequently, there are more extreme limitations placed on the cross sectional shape than for conventional elastic design.

It was already asserted that continuous circular rings for almost all practical cases are inherently stable laterally, since the ring is normally contained within a semi-monocoque type structure. (Diversified examples would be, aircraft fuselages, submarine shells, ship stiffening frames, penstocks for dams, cylindrical tanks stiffened by intermitent frames, etc.)

Therefore, the only form of stability which presents a problem is the dilemma of local instability (commonly referred to as crippling or local buckling). Notwithstanding, crippling by no means is a minor problem as may be interpreted from the subtleness of the previous statement. As a matter of fact, much could be presented in treating this subject properly. A treatise of this subject is not an intention of this thesis. Thus, only a few recommendations concerning crippling will be advocated.

Fundamentally, the question of local buckling reduces to two considerations.

1. First, it must be determined how much rotation is necessary to develop the assumed hinges.

2. Second, the geometric proportions or limitations of the cross sectional shape, which provide the ability of the shape to attain this much rotation without inducing local flange buckling, must be defined.

With respect to the first consideration, the essential rotation capacities of the hinges varies with each particular structure and each loading condition. In general, if the flange can be strained to strain hardening before local buckling occurs, the section is proportioned satisfactorily for a plastic hinge type action. This fact is based on the observation that most typical cases require a rotation capacity less than $\epsilon_{st.}/\epsilon_{y}$. The aptness of this course of action relies on the assumption that material properties in the strain-hardening range are again linear as in the elastic range.

The second consideration demands much more involved eluci-

dation than the previous solution for the first problem. An excellent reference on this subject is contained in reference 15 of section VI. Mr. Haaijer points out the fact that the structure will attain its full ultimate load, only, if those parts where yielding starts first, can undergo sufficiently large deformation. At these locations the flanges of the section must then be able to sustain strains considerably larger than the yield strain. Accordingly, the flanges should be proportioned such that local (plate) buckling does not occur before the ultimate load is acheived.

The above statement implies that the correlation between the increments of stresses and strains due to the deflection of the plate out of its plane must be known. The critical buckling load may be predicted in good agreement with test results within the elastic range, if the material is presumed to be isotropic and homogeneous. A satisfactory transition curve between the elastic limit and the yield point can be determined by applying Bleich's semi-rational theory to an effective stress-strain curve (see Bleich, F. "Buckling Strength of Metal Structures", McGraw-Hill, New York, 1950).

Rather than become too involved in the subject, it suffices to state that certain recommendations can be made at this time, and the reader must seek information elsewhere. It was found for WF structural shapes* of mild steel (ASTMA A-7) that if ϵ_{cr}, the critical buckling strain, is equal to ϵ_{st}, then $\frac{b}{t} \leq 17$ (for an outstanding flange) will provide sufficient hinge rotation

*See reference 5, page 9.24

capacity. Thus, a recommended $\frac{b}{t}$, where t is the thickness and b the width of the outstanding flange, of less than 17 is proposed.

4.3.0 Recommendation for Deflection Calculations*

Although the subject of deflections has not been mentioned before, the analyst may be very interested in computing deflections. Rather than go through an actual calculation for a particular ring problem the equations will be presented and a procedure will be outlined using as an example a fixed-ended beam.

Before any method of analysis may be formulated the fundamental assumptions and conditions necessary for a simplified solution must be specified. Therefore, the assumptions made relative to determining deflections within the plastic range are specified below.

a) Idealized moment-curvature relationship (see page 9).

b) Each segment retains its flexual rigidity, EI, for the whole length outside of yield areas between hinges.

c) Unlimited rotation is possible at hinge sections.

It is obvious that deflections are dependent upon the structural stiffness of the frame regardless if elastic or plastic deflections are preferred. Thus, a design must be accomplished before applying the equations.

Just as there are several methods of solution for simple plastic analysis, so there are various methods of computing plastic deflections. As a matter of fact, most of the elastic methods with appropriate modifications would be satisfactory for

*See reference, page 8.6

calculating plastic deflections. For purposes of this thesis, slope-deflection equations will be used throughout.

In order to apply the proposition of slope deflection a sign convention must be established. If clockwise moment and rotation are considered positive, the equation for slope at end A is expressed as (see Figure 4.3.1)

$$\theta_a = \theta_a' + \frac{\Delta}{l} + \frac{l}{3EI}\left(M_{ab} - \frac{M_{ab}}{2}\right) \qquad \text{.....(4.3.1)}$$

where the nomenclature is defined in Figure 4.3.1

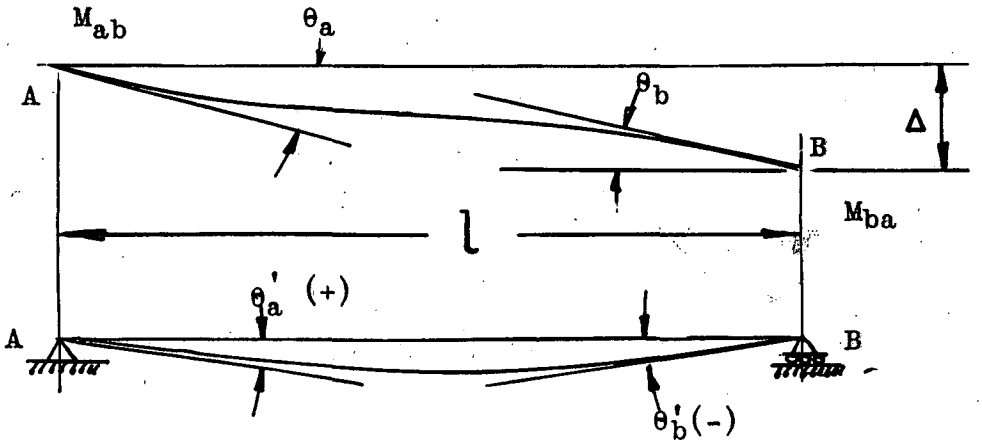

FIGURE 4.3.1 Definition of Slope Deflection Conventions

An important principle in connection with deflection computations will be specified at this point*.

"Although 'kinks' form at the other hinge sections, just as the structure attains the computed ultimate load there is continuity at that section at which the last plastic hinge forms."

Note: Before any calculation may be determined, it must be understood that certain information are now available which make computations possible. The information is

*See reference 5, page 8.3

(a) the ultimate load and moment diagram from a plastic analysis

(b) the slope-deflection equations (equation 4.3.1)

(c) the principle of compatibility at the last hinge to form (The cycle of hinge formation has already been discussed for the various cases)

The correct deflection at ultimate load is the maximum value obtained when the last hinge is formed. If the elastic solution is available, the last hinge will always form at the least value of the maximum moments of the elastic moment diagram. If the elastic solution is not available, then the analyst must resort to a trial and error process to determine the last hinge.

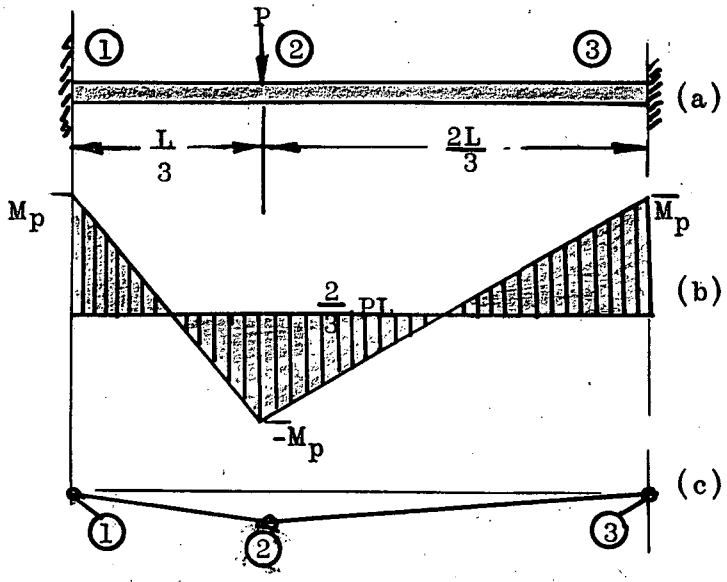

FIGURE 4.3.2 Example Deflection Study

As an example, if the structure shown in Figure 4.3.2 is to be analyzed by a slope deflection procedure, the resulting moment diagram and mechanism are shown in Figure 4.3.2(b) and (c). The first trial undertaken may be attempted at section ①.

Trial at hinge ①

From the slope deflection equation

$$\theta_1 = \theta_1' + \frac{\Delta}{l}1 + \frac{l}{3EI}(M_{12} - \frac{M_{21}}{2})$$

$$0 = 0 + \frac{\Delta_1}{\frac{L}{3}} + \frac{\frac{L}{3}}{3EI}\left(-M_p + \frac{M_p}{2}\right)$$

$$\Delta_1 = + \frac{M_p L^2}{54EI}$$

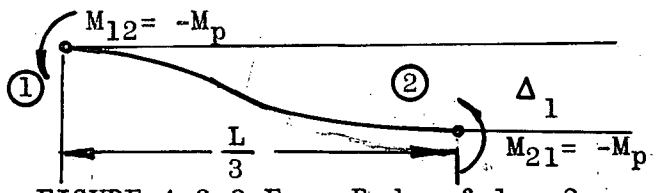

FIGURE 4.3.3 Free Body of 1 - 2

Trial at hinge (2)

$$\theta_{21} = \frac{\Delta_2}{\frac{L}{3}} + \frac{\frac{L}{3}}{3EI}\left(-M_p + \frac{M_p}{2}\right)$$

$$\theta_{21} = \frac{3\Delta_2}{L} - \frac{M_p L}{18EI}$$

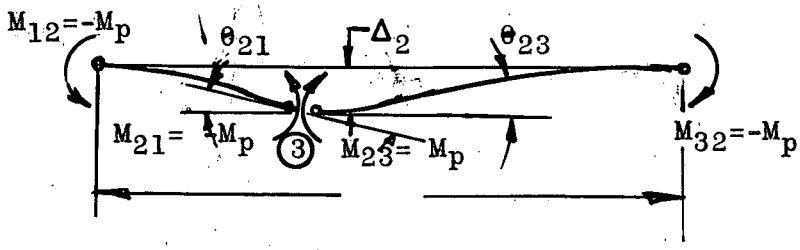

FIGURE 4.3.4 Free Body of (1) - (3)

From the principle of continuity of the last hinge,

$$\theta_{21} = \theta_{23}$$

$$\Delta_2 = \frac{M_p L^2}{27EI}$$

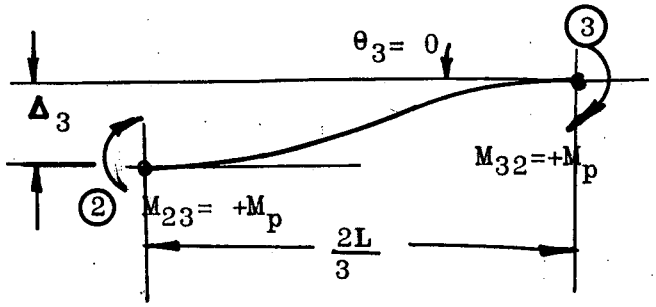

FIGURE 4.3.5 Free Body of (2) - (3)

Trial at hinge (3)

$$(\theta_3 = 0)$$

$$\theta_3 = \frac{\Delta_3}{L} + \frac{\Delta}{3EI}\left(M_{32} - \frac{M_{23}}{2}\right)$$

$$0 = -\frac{\Delta}{\frac{2L}{3}} + \frac{\frac{2L}{3}}{3EI}\left(M_p - \frac{M_p}{2}\right)$$

$$\Delta_3 = \frac{2}{27}\frac{M_p L^2}{EI} \qquad \text{(This is the maximum deflection)}$$

The last hinge forms at (3). All other trials yielded smaller deflections and resulted in "negative kinks" which are impossible by comparison to the correct trial.

Although the method needs refinements, this same trial and error procedure may be employed in ring analysis.

4.4.0 Limitations of Plastic Analysis.

In all sincerity, it is difficult to declare that simple plastic analysis has any more limitations than simple elastic analysis for ring analysis. On the other hand, one of the drawbacks in the use of a plastic type analysis is the sizeable deflections encountered in certain instances. It is believed that, in the category of practical ring problems, deflections will not govern design. This does not mean that deflections should not be investigated. On the contrary, it is conceivable that a study of deflections concerning a certain ring design may reveal excessive deflections, which impose overloads on adjacent structure. Furthermore, extreme rigidity may be a governing factor, which compels the analyst to incorporate more stiffness into the structure.

Another objection to plastic analysis, which should soon be corrected, is the inadequacy of large scale structural tests. Much concerning the subject of plastic analysis is yet to be brought to light. Treatises similar to this one only starts a trend. Before plastic methods can be employed in ring analysis, scaled model tests must be performed, and other problems investigated.

This thesis only 'brushed over the surface' on many subjects, such as local stability, deflections, rotation capacity, length of hinge, alternating plasticity and shake down, and derivation of external loads. Hence, it is hoped that the proposed arguments and methods of this thesis will be accepted and further investigations made on the subject of plastic analysis

for stiffening rings.

4.5.0 Advantages of Simple Plastic Analysis over Elastic Analysis

One of the most promising advantages of simple plastic analysis over a comparable (that is for the same problem) elastic analysis is its rational approach. It was mentioned on page 43 that just because a structure is adequate or useful does not imply that it is efficiently designed. Many times in civil engineering structures, where stiffness or rigidity and deflections are controlling factors, economy and efficiency must be sacrificed for weight. Although rigidity and deflections may be limiting factors in aircraft and submarine structures, weight is a much more critical factor and a moot point for these type structures.

It is sincerely believed by many people that plastic analysis assumes a more rational consideration of the problem. Most of all it approaches the problem from the failure or collapse mechanism point of view, whereas an elastic analysis approaches the objective by basing "failure" on an arbitrary limiting stress. Because of this assumption, an elastic analysis is incapable of predicting structural failure which means that the real margin of safety is unknown. In other words elastic analysis is predicating usefullness on the basis of limiting stresses, whereas plastic analysis bases it on acutal load carrying capacity.

Another advantage of simple plastic analysis is the extreme simplicity. Fortunately, it is easier, or at least as easy, to apply as an elastic method.

Last but not least, the economy, straight forwardness and sometimes infallibility of plastic analysis make it superior to elastic analyses. As an instance, observe the saving in weight and also the certitude of the interaction curve procedure when the two methods were contrasted in section 4.1.0. It is obvious, that regardless of how many trial and errors are perforemd, an elastic design could at best equal the plastic design.

On the other hand, the author does not mean to imply to repudiate elastic analysis because of the advent of plastic analysis. On the contrary, a comprehensive background in elastic analysis could be a very helpfull tool in grasping the implications and deduction of plastic analysis. As J. A. Van Den Broek* suggests, "The entire mathematical theory of Elasticity is but a supplementary theory". Elastic analysis can be usefull for deflection studies, shakedown investigations and the determination of hinge locations. Furthermore, it must be kept in mind that there are limitations on plastic analysis just as there are limitations on any form of analysis. This brings us to the concluding remark that plastic analysis must be employed discriminately.

*See reference 7

SECTION 5.0.0

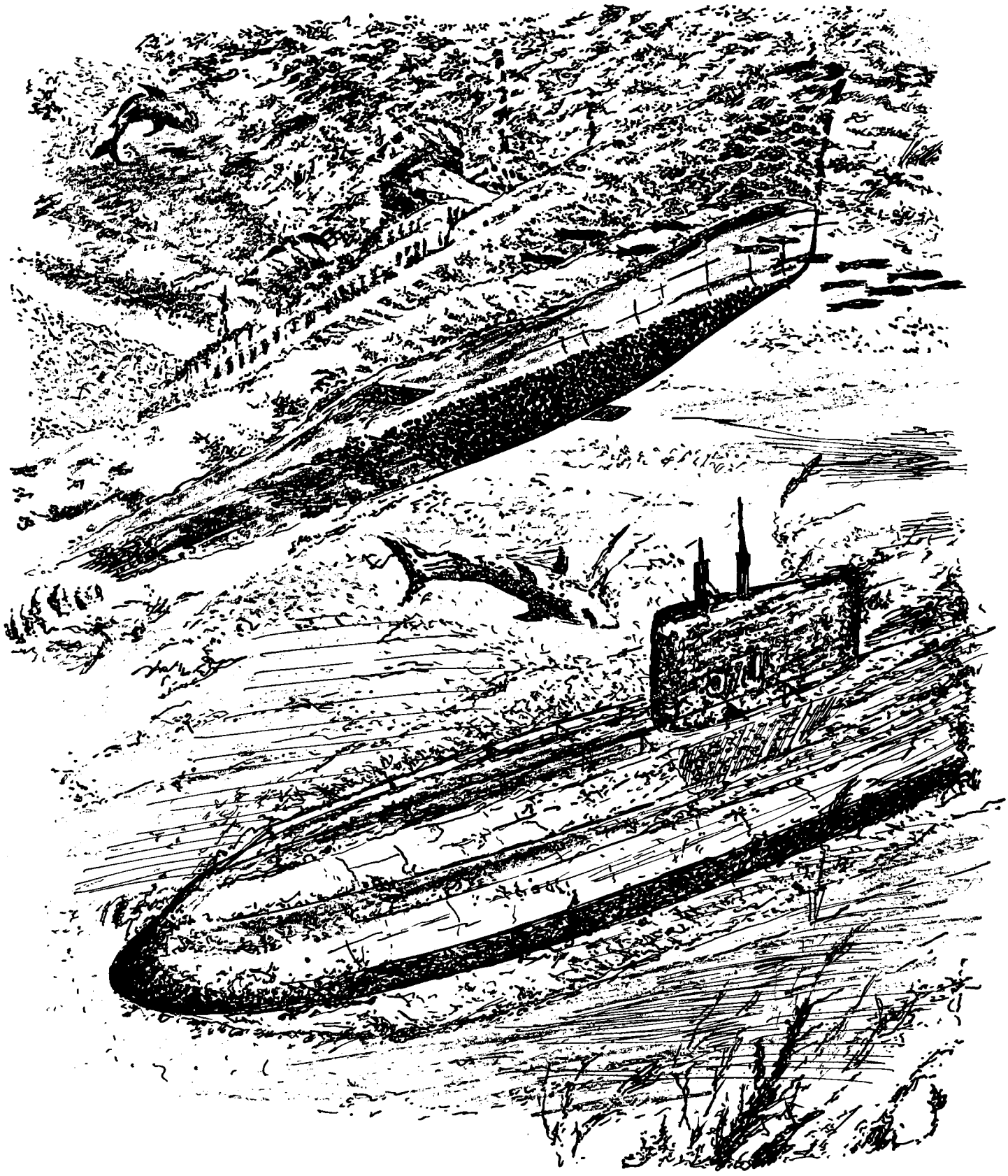

V - 5.0.0 REFERENCES

1. Wise, J.A., "ANALYSIS OF CIRCULAR RINGS FOR MONOCOQUE FUSELAGES", Journal of the Aeronautical Sciences, p. 460, September 1959.

2. Miller, R.A. and Wood C.D., "FORMULAS FOR THE STRESS ANALYSIS OF CIRCULAR RINGS IN A MONOCOQUE FUSELAGE", N.A.C.A Technical Note 462.

3. Miller, R.A., "ASOLUTION OF THE CIRCULAR RING", Airway Age, May 1931, p. 465-468.

4. Stieda, W., "STATICS OF CIRCULAR RING STIFFNERS FOR MONOCOQUE FUSELAGES", N.A.C.A. Technical Memorandum No. 1004.

5. Beedle, L.S., Thürlimann, B., and Ketter, R.L., "PLASTIC DESIGN IN STRUCTURAL STEEL - Lecture Notes of a Summer Course", Lehigh University - American Institute of Steel Construction.

6. Symonds, P.S., and Neal, B.G., "RECENT PROGRESS IN THE PLASTIC METHODS OF STRUCTURAL ANALYSIS", Journal of Franklin Institute, 252(5), p.383-407, November, 1951, and 252(6), p. 469-492, December, 1951.

7. Van den Broek, J.A., "THEORY OF LIMIT DESIGN", John Wiley and Sons, Inc., New York, 1948.

8. Neal, B.G., "PLASTIC COLLAPSE AND SHAKEDOWN THEOREMS FOR STRUCTURES OF STRAIN-HARDENING MATERIAL" - Journal of Aeronautical Sciences, Vol. 17, No. 5, May, 1950.

9. Euler Leonhard, "SUR LA FORCE DES COLONNES", Académie des Sciences des Berlin, 1757, p. 252, For English translation with comments, see American Journal of Physics, July 1947.

10. "THE COLLAPSE METHOD OF DESIGN", prepared by the British Constructional Steelwork Association.

11. Horne, M.R., "A MOMENT DISTRIBUTION METHOD FOR THE ANALYSIS AND DESIGN OF STRUCTURES BY THE PLASTIC THEORY", Proceedings of the Institution of Civil Engineers, 3 (part 3), 51, (1954).

12. Neal, B.G., and Symonds, P.S. "THE COLLAPSE LOAD OF FRAME STRUCTURES", Journal of the Institution of Civil Engineers, No. 1, November 1950, p. 31.

13. Ketter, R.L. "PLASTIC DESIGN OF MULTI-SPAN RIGID FRAMES", Welded Continuous Frames and Their Components, Fritz Laboratory Interim Report No. 31, June, 1956.

14. Niles, A.S. and Newell, J.S., "AIRPLANE STRUCTURES", John Wiley and Sons, Volume II, third edition.

15. Haaijer, G., "BUCKLING OF UNIFORMLY COMPRESSED STEEL PLATES IN THE STRAIN-HARDENING RANGE", Welded Continuous Frames and Their Components, Fritz Laboratory, Progress Report 20.

VI NOMENCLATURE

A = cross sectional area of a structural component

= dimension defined in hinge pattern geometry (loading cases 2.0.0, 2.3.0, 7.0.0)

B = dimension defined in hinge pattern geometry (loading cases 2.0.0, 2.3.0, 7.0.0)

b = width of flange or rectangular cross section

C = dimension defined in hinge pattern geometry (loading cases 2.0.0, 2.3.0, 7.0.0)

c = distance from the neutral axis to the extreme fibre

D = dimension defined in hinge pattern geometry (loading case 2.3.0)

d = depth of cross section

E = Young's modulus of elasticity

E_{st} = strain-hardening modulus = $\left.\frac{d\sigma}{d\epsilon}\right|_{st.}$

f = shape factor = $\frac{M_p}{M_y}$ =

h = difference to first approximation and the next approximation to the taylor's series

I = second moment of area (moment of inertia)

I_e = moment of inertia of elastic part of cross-section

I_p = moment of inertia of plastic part of cross-section

L = length of span

ΔL = length of plastic hinge

l = distance between hinges for deflection calculations

M = moment (M_a = internal moment at some random section)

M_p = plastic moment

M_r = residual moment

M_y = moment at which the yield point is reached in flexure

P = externally applied concentrated load

P_u = ultimate load corresponding to failure

P_y = external load corresponding to yield stress level

q = external shear flow around the ring

q_m = dimensionless coefficient for moment in the inter-action curve

q_n = dimensionless coefficient for normal load in the inter-action curve

R = radius of circular ring

S = elastic section modulus

S_a = internal shear at some random section of the ring

S_e = section modulus of elastic part of cross-section

t = flange thickness

t_e = effective skin thickness of semi-monocoque structure

V = vertical shear on a beam

W_{ext} = external work due to a virtual displacement

W_{int} = internal work due to a virtual displacement

X = redundancies of an indeterminate frame

= vertical component of external shear flow

x = roots to the function $F = f(x)$

x_o = first approximation to the x roots

Y = horizontal component of external shear flow

y = distance from the neutral axis to a random point in the cross section

Z = plastic section modulus, $z = M_p$

Z_e = plastic modulus of elastic portion of a cross section

Z_p = plastic modulus of plastic portion of a cross section

α = angle with respect to the vertical axis of symmetry designating the angular distance to the lower hinges

β = angle with respect to the vertical axis of symmetry designating the angular distance to the upper hinges

Δ = absolute deflection

δ = vertical deflection

ϵ = strain

ϵ_{cr} = critical buckling strain

$\epsilon_{st.}$ = strain at strain-hardening

ϵ_y = strain corresponding to first attainment of yield stress levels

γ = specific angle with respect to the vertical axis of symmetry denoting the angular distance to a concentrated load

θ = virtual angle change

= slope deflection angle

ρ = radius of curvature of a bent structural component

π = Greek letter to denote the absolute value 3.1416

φ = angle with respect to the bottom point of the circular ring at the vertical axis designating the angular distance to a random section "a"

σ = normal stress

σ_u = ultimate tensile strength of a material

σ_y = yield stress level

τ = shear stress

ϕ = rotation per unit length, or average unite rotation, curvature of moment-curvature (M-ϕ) relationship

= curvature corresponding to first yield in flexure

φ = angle with respect to the bottom point of the circular ring at the vertical axis designating the angular distance to a random section "a"

VII. APPENDIX - Limiting Cases

7.0.0 Loading Condition-Ring V-Opposing Radial Forces

Probably the simplest loading condition that comes to mind is the case of a circular ring with two radial forces imposed upon it, (the limiting case of Ring I).

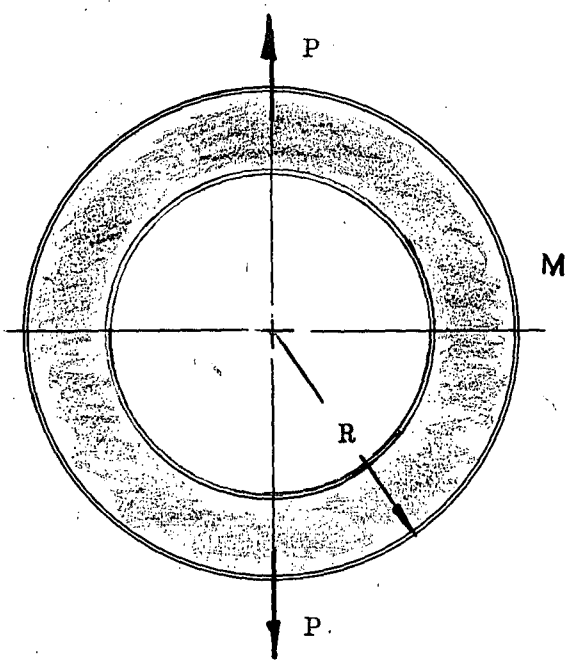

FIGURE 7.0.0-Loading Condition V

Note: There are no external shears applied to the ring. That is, the ring equilibrium is maintained by opposing forces.

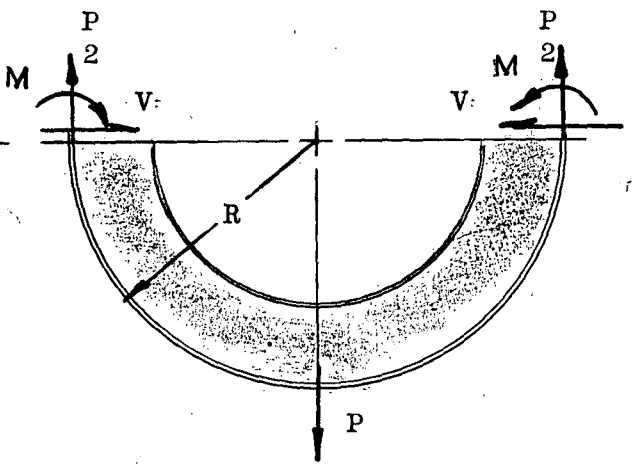

FIGURE 7.0.0(b)

As outlined in the procedure of section 4.0.0, the first step in the method is to determine the location of the hinges around the ring. Because of the simplicity of this loading, they are fairly obvious. According to the rules for determining the hinge locations, (page 49), two hinges are constrained to form at the concentrated loads. The remaining two hinge positions may be deduced by considering rule (b) on the same page. The analyst knows that four hinges are necessary to create a failure mechanism, and also, that two of the hinges are defined by location of the concentrated loads. Hence, the other two hinges must form between these two and symmetrically about the

vertical axis. The remaining two hinge positions are ultimately established by virtue of the fact that both the upper half and lower half are identically (or symmetrically) loaded. Consequently, symmetry of loading and symmetry of geometry place the hinges half way between the two radial forces.

It is feasible to readily select hinge ① (or ③) of Figure 7.0.1 as the point of fixity in space rather than pick ② or ④. Since either choice of ① or ③ yields the same collapse configuration, point ① will be selected and the following geometry results.

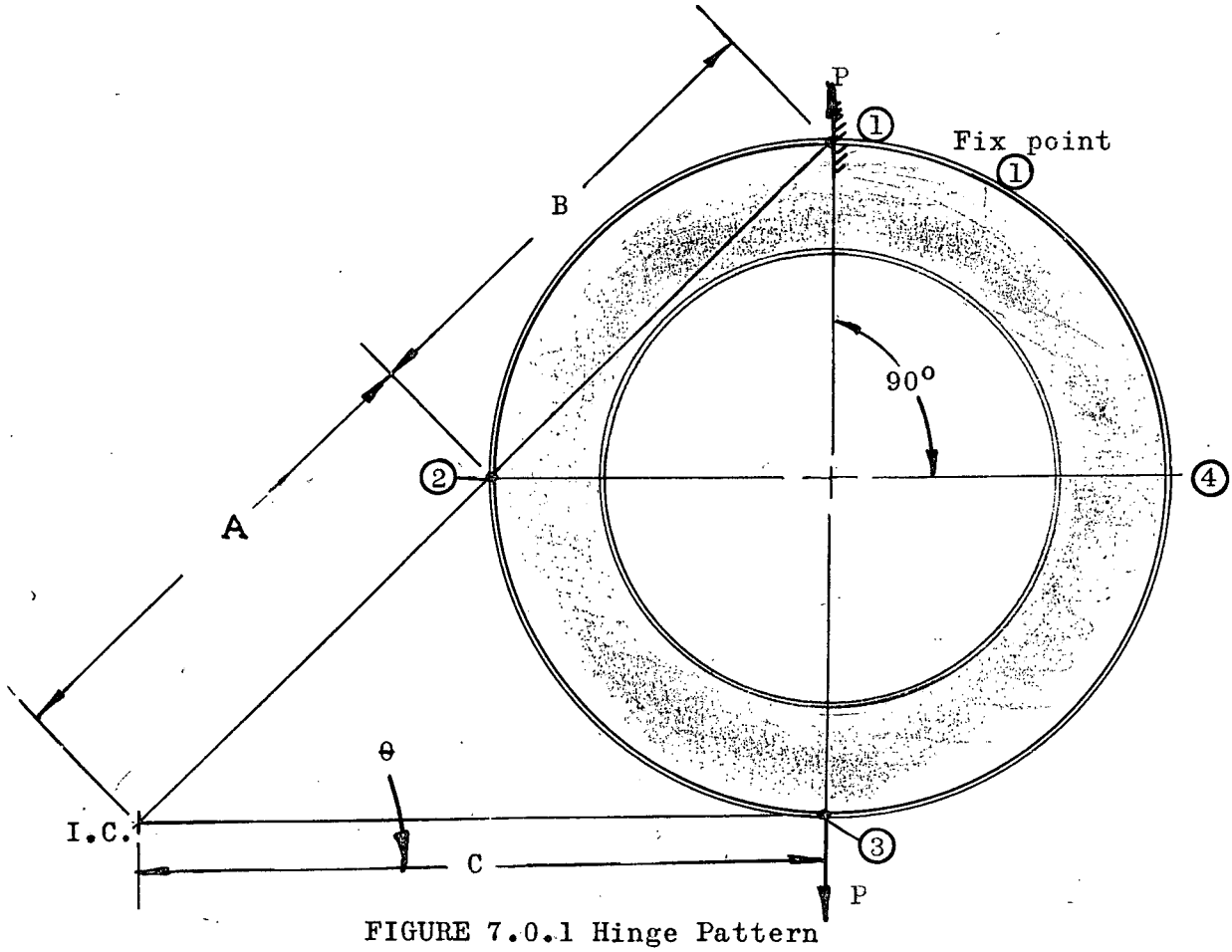

FIGURE 7.0.1 Hinge Pattern

Referring to Figure 7.0.1, if point ① is fixed in space, the ring assumes the same failure made as ring I on page .

Because of geometrical symmetry point ③ is restrained to move vertically down an amount equal to the distance C times the virtual rotation θ. Working with the left half of the ring, the geometry is resolved by observing the simple geometrical proportions of Figure 7.0.2.

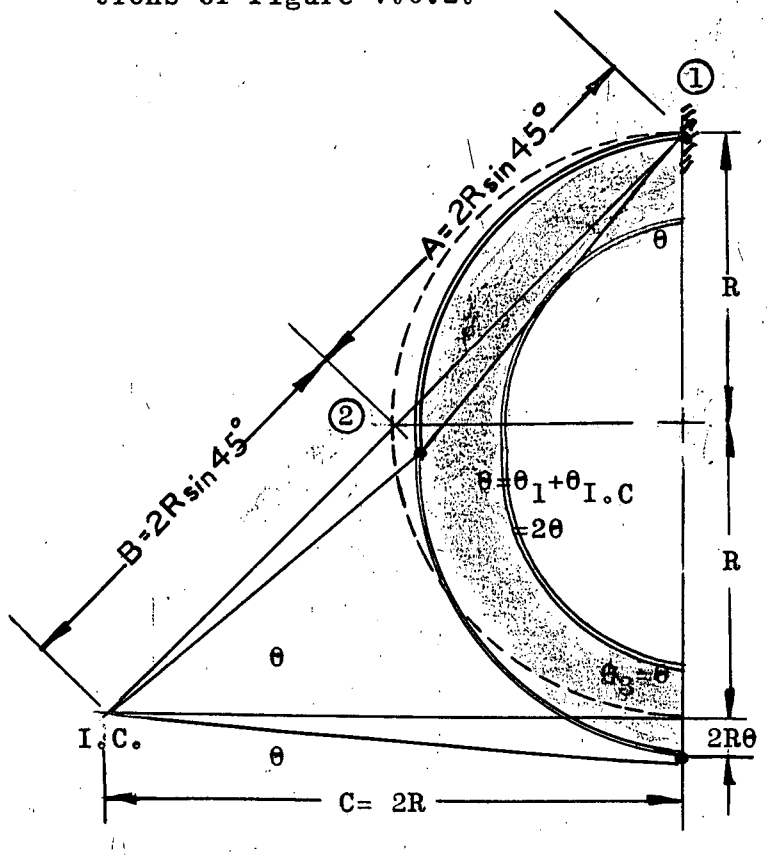

FIGURE 7.0.2
Virtual Rotation Relations

The instantaneous center of rotation of segment ②-③ is ascertained by noting that point ③ is restricted to move vertically down. Thus, segment ②-③ is constrained to rotate about a point horizontally opposite hinge ③. Since segment ①-② is restrained to rotate about the fixed point ① its radius of rotation is constructed through plastic hinges ① and ②. Where the two radius's intersect is the instantaneous center of rotation.

The dimensions A, B, and C are found very simply by referring to Figure 7.0.2.

$A = 2R \sin 45^{o}$ .....(7.0.1)

$B = A\ 2R \sin 45^{o}$ .....(7.0.2)

$C = 2R$ .....(7.0.3)

If the structure is given a virtual of θ about the instantaneous center then the following trigonometric relations between the angular rotations ensue.

If $\theta_{I.C.} = \theta$, ...(7.0.4)

then,

$$\theta_1 = \frac{2R \sin 45^\circ \theta_{I.C.}}{2R \sin 45^\circ} = \theta \quad \text{.....(7.0.5)}$$

$$\theta_3 = \theta_{I.C.} = \theta \quad \text{.....(7.0.6)}$$

$$\theta_2 = \theta_{I.C.} + \theta_1 = 2\theta \quad \text{.....(7.0.7)}$$

7.0.1 Application of Principle of Virtual Displacements

The internal work is merely the sum of all of the virtual rotations at each hinge multiplied by their respective moment capacities.

$$M_p (\theta_1+\theta_2+\theta_3) = M_p(\theta+2\theta+\theta) = 4M_p\theta \quad \text{.....(7.0.8)}$$

The evaluation of the external work is even easier. From Figure 7.0.2

$$\theta \; C \frac{P}{2} = \theta 2R \frac{P}{2} = PR\theta \quad \text{.....(7.0.9)}$$

Equating equations 7.0.8 to 7.0.9,

$$4M_p \theta = PR\theta$$

$$M_p = \frac{PR}{4} \quad \text{.....(7.0.10)}$$

Since the exact location of all hinges were known prior to determining the value of M_p, the problem is completely solved, and all that remains is to perform the plasticity check.

If the collapse mechanism is constructed as illustrated in Figure 7.0.3, a quarter section of the ring can be isolated from the remainder of the structure. (Figure 7.0.3(b))

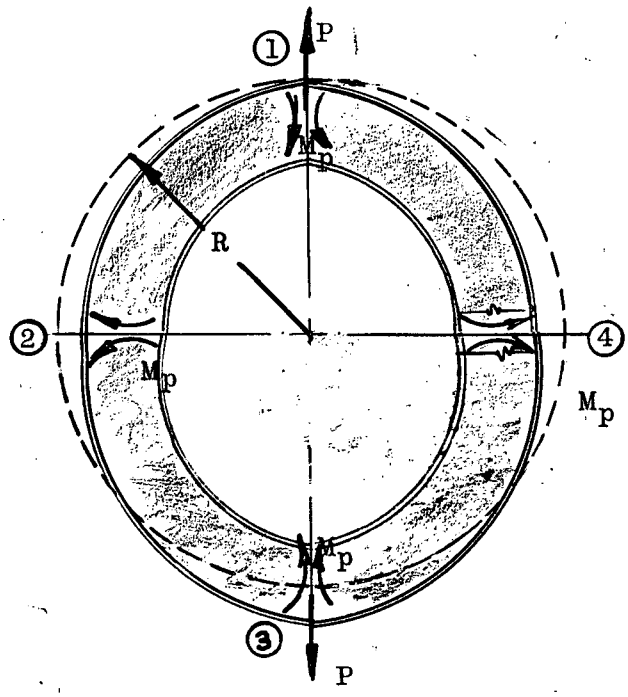

7.0.3 Collapse Mechanism

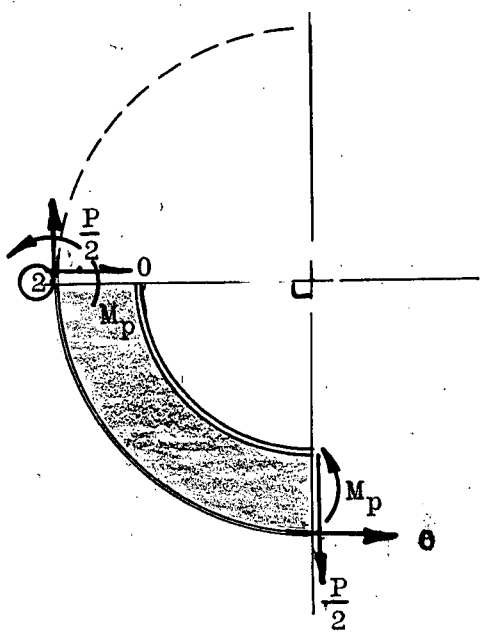

7.0.3(b) Segregation of One Quarter of the Ring

The complete solution of the plasticity check is accomplished by determining the internal forces in terms of the general angle φ .

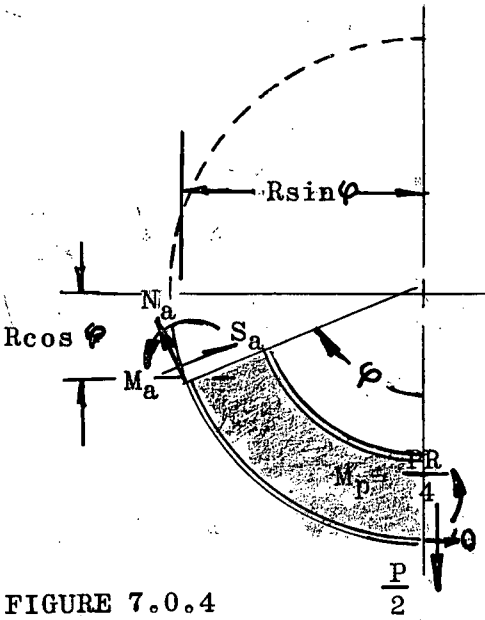

FIGURE 7.0.4

From Figure 7.0.4,

$$M_a = M_p - \frac{P}{2} R\sin\varphi$$

$$= \frac{PR}{4} - \frac{PR}{2}\sin\varphi \qquad \ldots\ldots(7.0.11)$$

$$N_a = \frac{P}{2}\sin\varphi \qquad \ldots\ldots(7.0.12)$$

$$S_a = \frac{P}{2}\cos\varphi \qquad \ldots\ldots(7.0.13)$$

If values of φ for every 5^o are substituted into equations 7.0.11,

OPPOSING RADIAL P FORCES ON A TANGENTIALLY SUPPORTED CIRCULAR RING

TABLE 7.0.1

Comparison of Plastic to Elastic Moment, Shear and Axial Load Coefficients						
Angle From Vertical	Plastic Moment Coeff.	Elastic Moment Coeff.*	Plastic Axial Load Coeff.	Elastic Axial Load Coeff.*	Plastic Shear Coeff.	Elastic Shear Coeff.*
0^{o}	.25000	.31831	0	0	.50000	.50000
5^{o}	.20642	.27473	.04358	.04358	.49809	.49809
10^{o}	.163175	.231485	.086825	.086825	.49240	.49240
15^{o}	.12059	.18890	.12941	.12941	.48296	.48296
20^{o}	.07899	.14730	.17101	.17101	.46984	.46984
25^{o}	.03869	.10700	.21131	.21131	.45315	.45315
30^{o}	0	.06831	.25000	.25000	.43301	.43301
35^{o}	-.03679	.03152	.28679	.28679	.40957	.40957
40^{o}	-.071395	-.003085	.321395	.32139	.38302	.38302
45^{o}	-.103555	-.035245	.353555	.35355	.35355	.35355
50^{o}	-.13302	-.06471	.38302	.38302	.32139	.32139
55^{o}	-.159575	-.091265	.409575	.409575	.28679	.28679
60^{o}	-.183015	-.114705	.433015	.433015	.25000	.25000
65^{o}	-.203155	-.134845	.453155	.453155	.21131	.21131
70^{o}	-.219845	-.151535	.469845	.469845	.17101	.17101
75^{o}	-.232965	-.164655	.482965	.482965	.12941	.12941
80^{o}	-.242405	-.174095	.492405	.492405	.08682	.08682
85^{o}	-.248095	-.179785	.498095	.49809	.04358	.04358
90^{o}	-.250000	-.18169	.500000	.50000	0	0

*Values obtained from Equations of Reference 2, Table 3, Case V

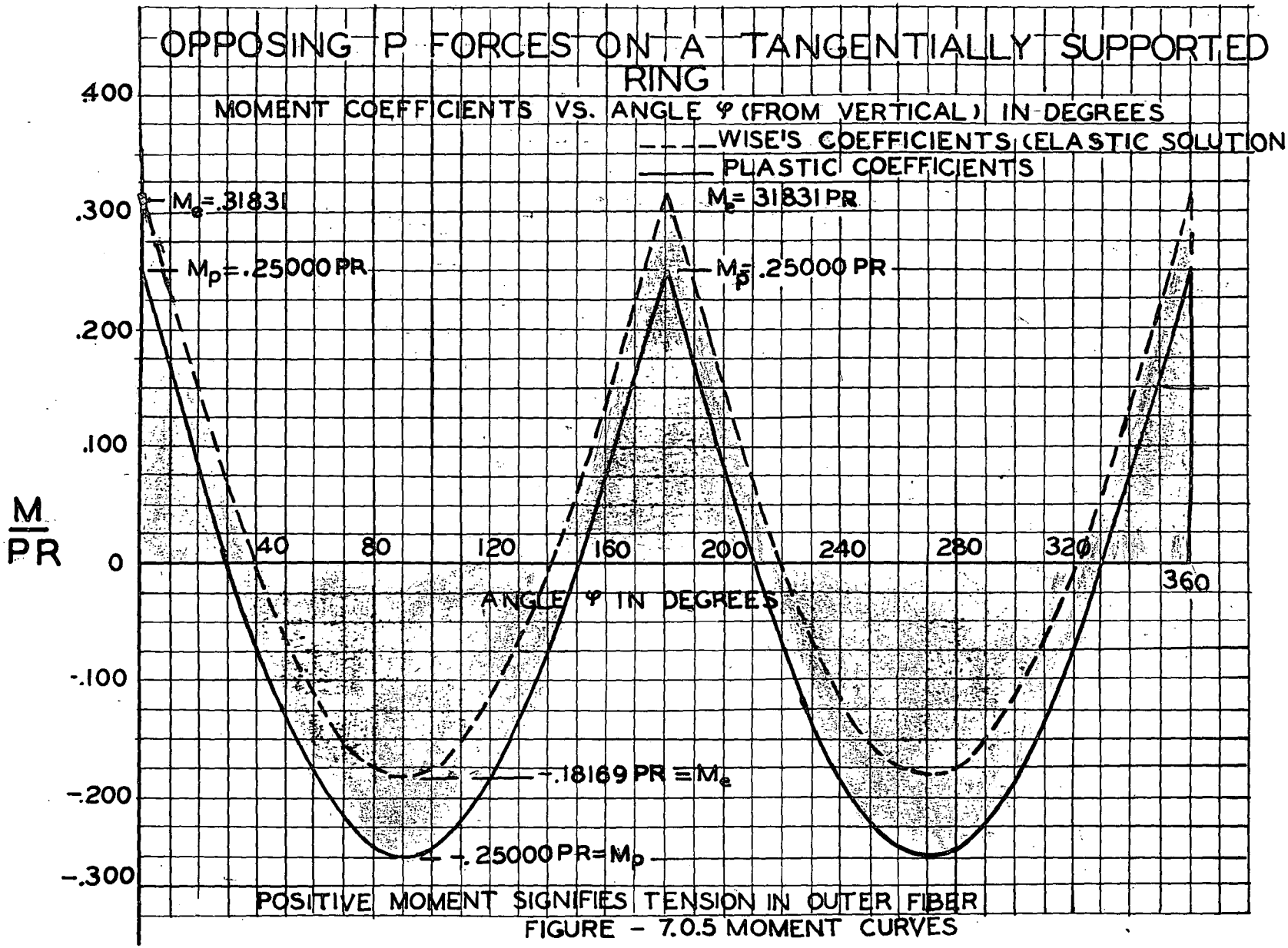

FIGURE - 7.0.5 MOMENT CURVES

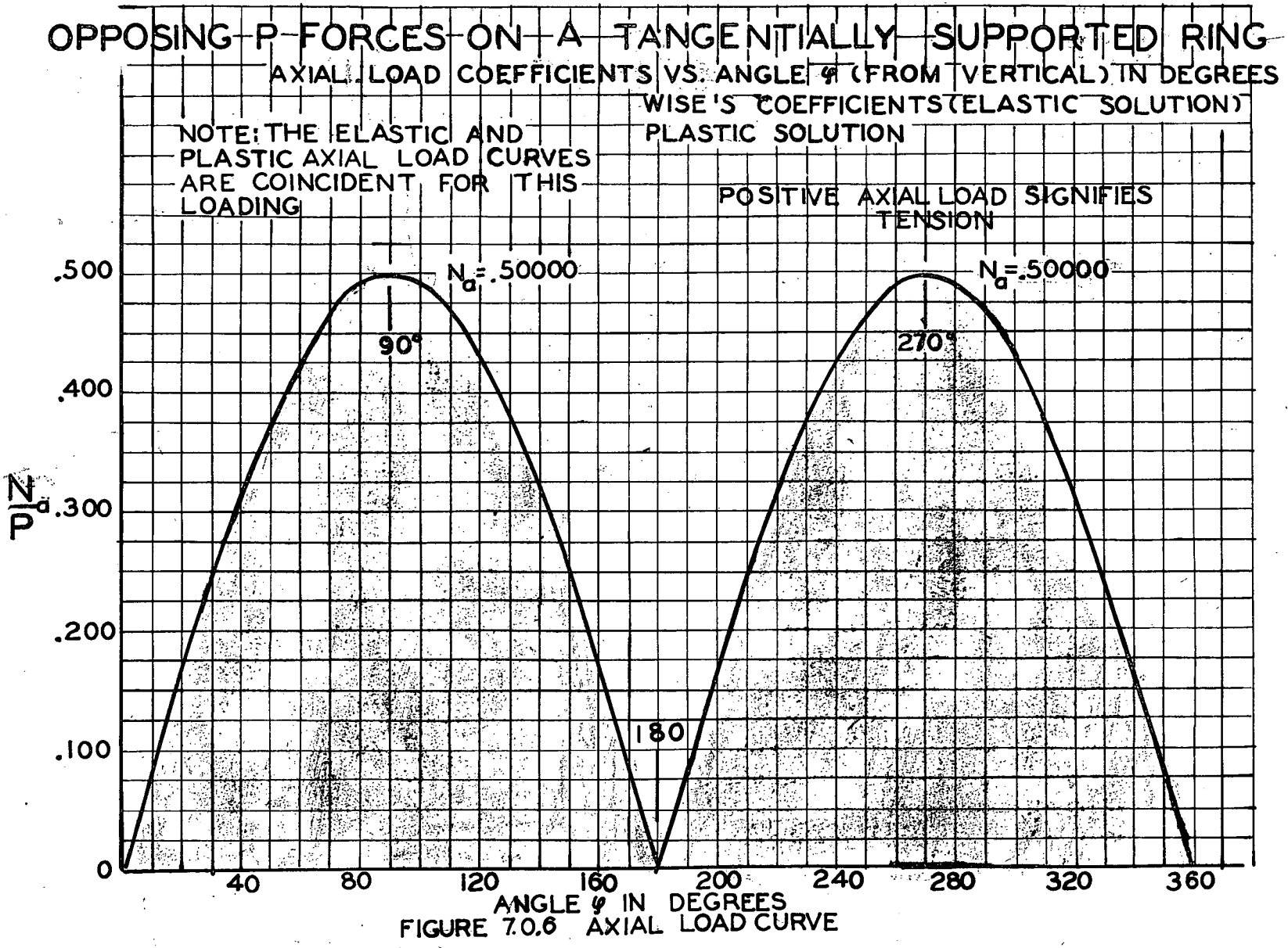

FIGURE 7.0.6 AXIAL LOAD CURVE

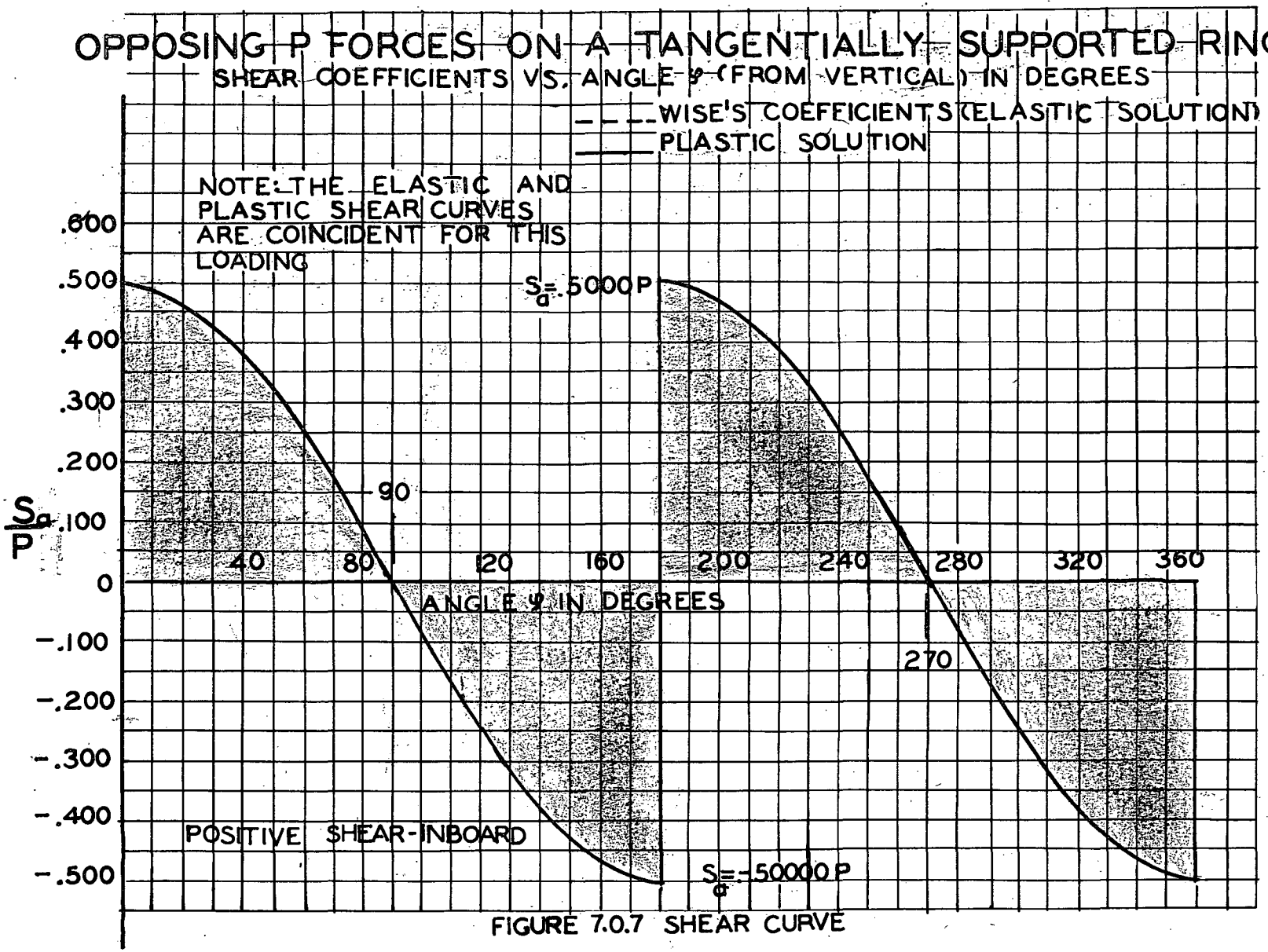

FIGURE 7.0.7 SHEAR CURVE

7.0.12, and 7.0.13, table 7.0.1 and graphs, Figures 7.0.5, 7.0.6, and 7.0.7 evolve.

It is interesting to note that the shear and axial load curves are coincident for both the plastic and the elastic solutions, whereas the moment curves show a distinct variation between the two solutions. Furthermore, because the moment distribution is the only variable of the three functions, it may again be emphasized that the plastic solution shows a much better distribution of moment.

The consideration which may confuse the analyst is not so much the fact that the point of maximum moment does not shift towards the concentration of the load (as in Ring I), but the fact that there actually is a variation in the moment curve at all. Normally if the maximum moments of an elastic solution are located completely symmetrical about the ring, and of equal moment the plastic solution yields the same solution as an elastic analysis. In other words, when a solution yields a completely symmetrical hinge pattern, as the load is increased beyond the yield load there is no difference in the moment diagram. In fact, the next loading condition, Ring VI, section 7.1.0, illustrates this very fact. However, for condition V the reason the moment curve augments at the point of maximum moment is because there are no external shears on the ring to influence the distribution of moment above the yield point. Thus, as the radial loads reach the yield load, P_y, hinges form simultaneously at ① and ③. When the radial loads are increased above P_y, the points of maximum moment do not shift away from ② and ④ because there are

no external shears to develop such a shift. Nevertheless, there is an increase of moment at these points and the magnitude of moment does increase. At a certain value of radial load the moment at ②and ④reaches the full plastic moment value simultaneously, and the structure collapses.

LIMITING CASE

7.1.0 Loading Condition-Ring VI-Tangential Twist PR on a Tangentially Supported Circular Ring.

This ring loading may be considered the limiting case of either Ring II, section 2.1.0, or Ring III, section 2.2.0.

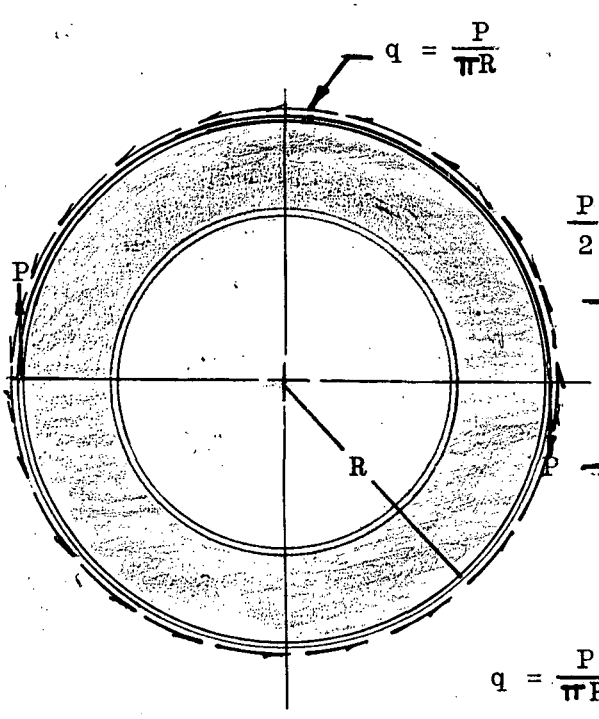

7.1.0 External Loading
Ring VI Tangential Twist

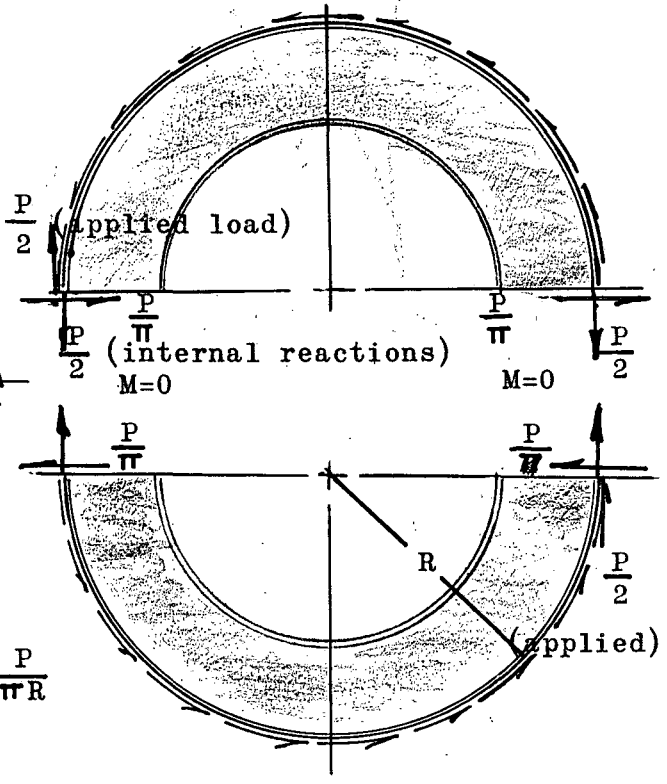

7.1.0(b) Isolating
Bottom Half of Ring

Proceeding as before, the determination of the composition of the hinge pattern is the first step in the investigation. The arrangement of the hinges, in this case, is easily obtainable. If the ring is split into two portions (see Figure 7.1.0(b)), it may be discernible that the ring appears very similar to the addition of Figures 2.0.1 and 2.0.3. The hinge pattern for Ring II is symmetrical about the vertical axis (horizontal axis in Figure 7.1.0). Here, too, the hinge pattern is symmetrical about

the axes of symmetry, where α and β are equal for this limiting loading condition. Hence, only one variable angle need be considered as seen in Figure 7.1.1.

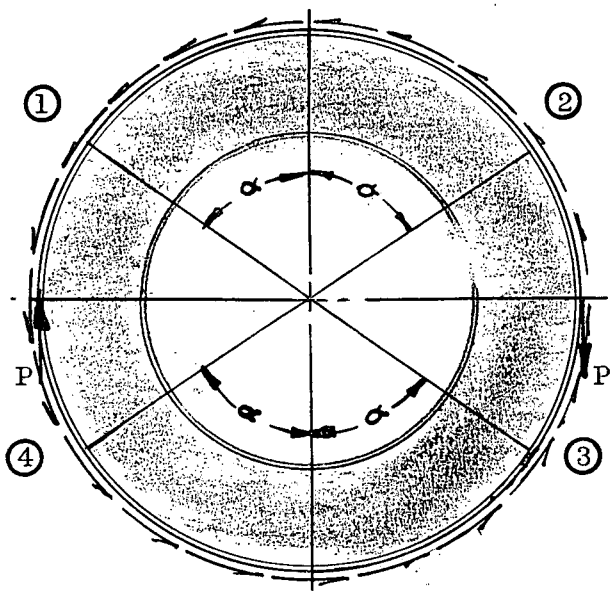

FIGURE 7.1.1 Hinge Pattern

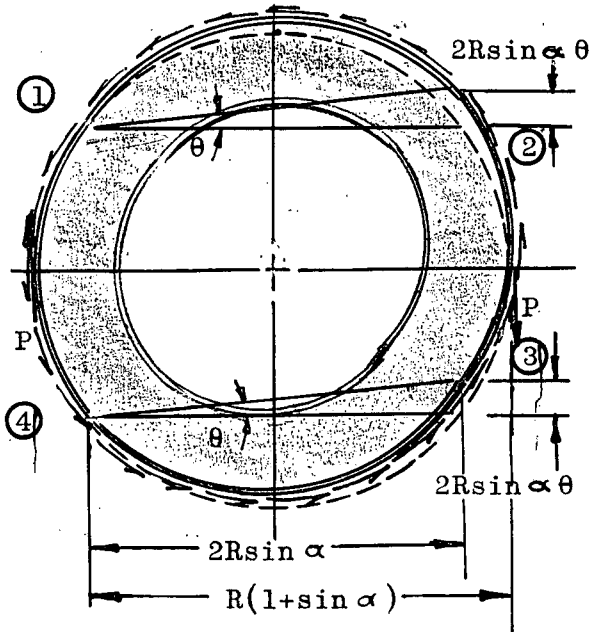

Note: Deformations were purposely assumed in the wrong direction in order to note the change in sign of the solution.

FIGURE 7.1.2 Assumed Failure Mode

It appears that the best selection of ring fixity for symmetrical hinge patterns is a failure mode resembling a panel mechanism for a rectangular rigid frame. For this particular instance, fixing segment ①-④ (or ②-③) results in a collapse mechanism simulating the sidesway panel mechanism of a rectangular rigid frame. Referring to Figure 7.1.2, it is perceivable that segment ①-② must hinge about point ① which fixes its instantneous radius through points ① and ②. The same reasoning is evident from Figure 7.1.2 for hinges ③ and ④. Thus if segment ①-② is given a virtual rotation θ, the segment ③-④ must also revolve through the same angle.

The interjection of the expedient resolution of ring shears, at this point, is efficient. Figure 7.1.3 illustrates the resolution of the shear forces into an axial load, moment, and shear components about the center of the ring.

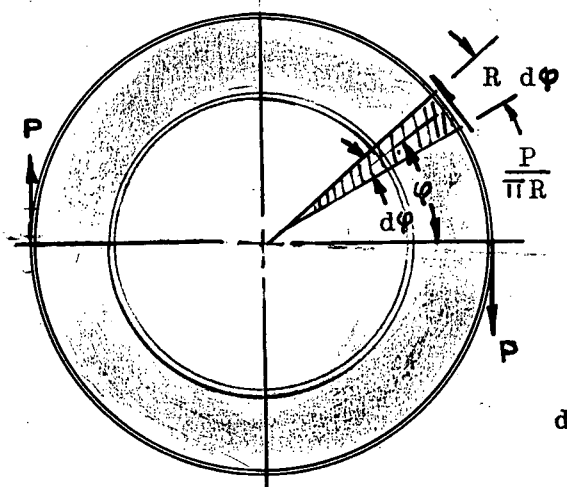

FIGURE 7.1.3(a) Resolution of Shear Flows

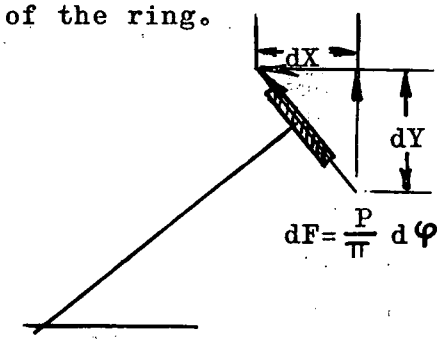

FIGURE 7.1.3(b)

$$dX = \frac{P}{\pi} \sin\varphi \, d\varphi \quad .....(7.1.1)$$

$$dY = \frac{P}{\pi} \cos\varphi \, d\varphi \quad .....(7.1.2)$$

$$dM = \frac{P}{\pi} R d\varphi \quad .....(7.1.3)$$

Commencing the procedure as performed in previous examples, the components are evaluated from the following integrals

$$X = \int \frac{P}{\pi} \sin\varphi \, d\varphi = \frac{P}{\pi} \Big[-\cos\varphi \Big] \begin{matrix} \text{upper limit} \\ \text{lower limit} \end{matrix} \quad ....(7.1.4)$$

$$Y = \int \frac{P}{\pi} \cos\varphi \, d\varphi = \frac{P}{\pi} \Big[\sin\varphi \Big] \begin{matrix} \text{upper limit} \\ \text{lower limit} \end{matrix} \quad ....(7.1.5)$$

$$M = \int \frac{PR}{\pi} \, d\varphi = \frac{PR}{\pi} \Big[\varphi \Big] \begin{matrix} \text{upper limit} \\ \text{lower limit} \end{matrix} \quad .....(7.1.6)$$

FIGURE 7.1.4 Sign Convention

Between hinges ① and ②

$$X = \frac{P}{\pi} \Big[-\cos\varphi \Big]_{\frac{\pi}{2}-\alpha}^{\frac{\pi}{2}+\alpha} = \frac{P}{\pi} \Big[-\cos\left(\frac{\pi}{2}+\alpha\right) + \cos\left(\frac{\pi}{2}-\alpha\right) \Big] = \frac{2P}{\pi} \sin\alpha$$

$$Y^{1-2} = 0 \quad \text{(From observation)}$$

$$M^{1-2} = \frac{PR}{\pi} \Big[\varphi \Big]_{\frac{\pi}{2}-\alpha}^{\frac{\pi}{2}+\alpha} = \frac{PR}{\pi} (2\alpha)$$

Between hinges ② - ③

$$X^{2-3} = \frac{P}{\pi}\left[-\cos\varphi\right]_{\alpha-\frac{\pi}{2}}^{\frac{\pi}{2}-\alpha}$$ There is no rotation of segment ② - ③, and there will be no work done during a virtual displacement

$$Y^{2-3} = \frac{P}{\pi}\left[\sin\varphi\right]_{\alpha-\frac{\pi}{2}}^{\frac{\pi}{2}-\alpha} = \frac{P}{\pi}\left[\sin\left(\frac{\pi}{2}-\alpha\right)-\sin\left(\alpha-\frac{\pi}{2}\right)\right] = \frac{2P}{\pi}\cos\alpha$$

$$M^{2-3} = \frac{PR}{\pi}\left[\varphi\right]_{\alpha-\frac{\pi}{2}}^{\frac{\pi}{2}-\alpha}$$ This moment does no work for the same reason X^{2-3} does no work

Between hinges ③ and ④

$$X^{3-4} = \frac{P}{\pi}\left[-\cos\varphi\right]_{-(\frac{\pi}{2}+\alpha)}^{\alpha-\frac{\pi}{2}} = \frac{P}{\pi}\left[-\cos\left(\alpha-\frac{\pi}{2}\right)+\cos-\left(\alpha+\frac{\pi}{2}\right)\right] = -\frac{2P}{\pi}\sin\alpha$$

$Y^{3-4} = 0$ (From observation)

$$M^{3-4} = \frac{PR}{\pi}\left[\varphi\right]_{-(\frac{\pi}{2}+\alpha)}^{\alpha-\frac{\pi}{2}} = \frac{PR}{\pi}\left[-\frac{\pi}{2}+\alpha+\frac{\pi}{2}+\alpha\right] = \frac{2PR}{\pi}\alpha$$

Summarizing the results of the integrations in Figures 7.1.4 (a), (b), and (c), the work done by the shear flow components and the applied load may be visualized.

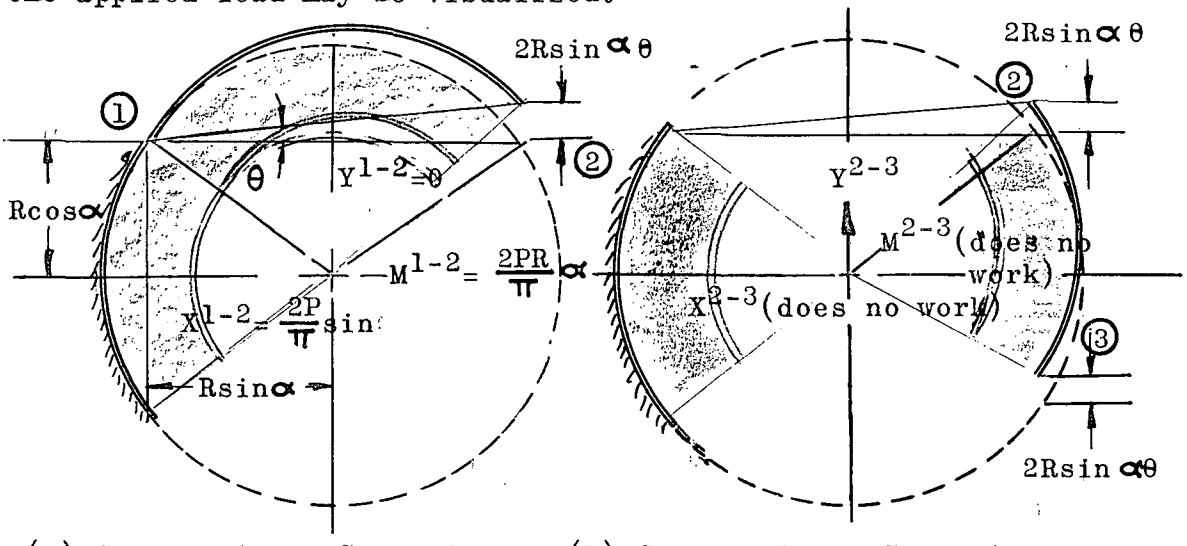

(a) Components on Segment ① - ②

(b) Components on Segment ② - ③

Note: The failure deformation is deliberately assumed in the wrong direction in order to note the change in the sign of the solution for M_p.

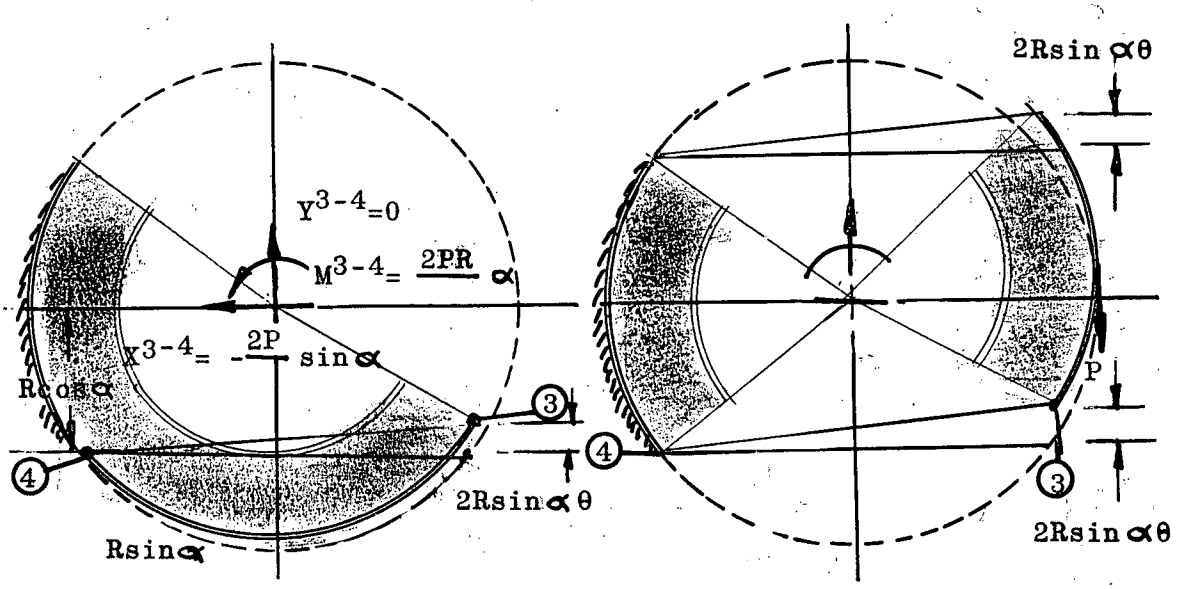

(c) Components on Segment ③ - ④ (d) Work done by the Applied Loads

FIGURE 7.1.4 Summary of Shear Flow Components

It is apparent that, if segment ① - ② is given a virtual rotation of θ about point ①, the segment ③ - ④ also rotates through a corresponding angle θ and segment ② - ③ just translates vertically. Hence, the hinge rotations at each hinge may be stated as below.

$$\left.\begin{aligned} \theta_1 &= \theta \\ \theta_2 &= \theta \\ \theta_3 &= \theta \\ \theta_4 &= \theta \end{aligned}\right\} \quad \ldots\ldots\ldots\ldots\ldots\ldots (7.1.7)$$

7.1.1 Derivation of External and Internal Work Expressions

The internal work is simply the sum of the rotation of each hinge times the magnitude of its corresponding maximum moment, or

$$M_p \quad \theta_1 + \theta_2 + \theta_3 + \theta_4 \quad = 4M_p\theta \quad \ldots\ldots\ldots\ldots (7.1.8)$$

The external work is obtained by summing the products of the external forces and their corresponding differential or virtual movements. Expression 7.1.8 follows as a result of this summation. Referring to Figures 7.1.4(a), (b), (c), (d)

$$4M_p=-P(2R\sin\alpha)\theta-X^{1-2}\theta(R\cos\alpha)+Y^{1-2}\theta(R\sin\alpha)+M^{1-2}\theta+Y^{2-3}\theta(2R\sin\alpha)$$
$$+X^{3-4}\theta(R\cos\alpha)+Y^{3-4}\theta(R\sin\alpha)+M^{3-4}\theta$$

$$4M_p= -2PR\sin\alpha-(R\cos\alpha)\left[\frac{2P}{\pi}\sin\alpha\right]+(R\sin\alpha)(\theta)+\frac{2PR}{\pi}+$$
$$(2R\sin\alpha)\left[\frac{2P}{\pi}\cos\alpha\right]+(R\cos\alpha)\left[-\frac{2P}{\pi}\sin\alpha\right]+(R\sin\alpha)\theta+\frac{2PR}{\pi}$$

$$4M_p = 2PR\sin\alpha\left(-1+\frac{2\cos\alpha}{\pi}-\frac{\cos\alpha}{\pi}-\frac{\cos}{\pi}\right)+\frac{4PR}{\pi}\alpha$$

$$M_p = \frac{2PR}{4}\left[\frac{2\alpha}{\pi}-\sin\alpha\right]$$

$$M_p = \frac{PR}{2\pi}\left[2\alpha-\pi\sin\alpha\right] \qquad \text{.....(7.1.9)}$$

The complete solution to the problem is attained by solving for the unknown angle α. This is accomplished by differentiating the maximum moment (M_p) expression with respect to α.

Thus,

$$\frac{dM_p}{d\alpha} = 0$$

$$\frac{d}{d\alpha}\left[2\alpha-\pi\sin\alpha\right] = 0$$

$$2\pi \quad \cos\alpha = 0$$

$$\cos\alpha = \frac{2}{\pi}$$

$$\alpha = .6366 \text{ rad.} \qquad \text{.....(7.1.10)}$$

The angle which satisfies equation 7.1.10 is

$$\alpha = 50^{\circ}\ 27'$$

Thus, when this value of α is substituted into expression 7.1.9,

$$M_p = \frac{PR}{2}\ (1.76126 - \pi \sin 50^{\circ}\ 27')$$

$$= \frac{PR}{6.283185}\ (.661379)$$

$$M_p = .10526\ PR \qquad \text{.....(7.1.11)}$$

7.1.2 Plasticity Check

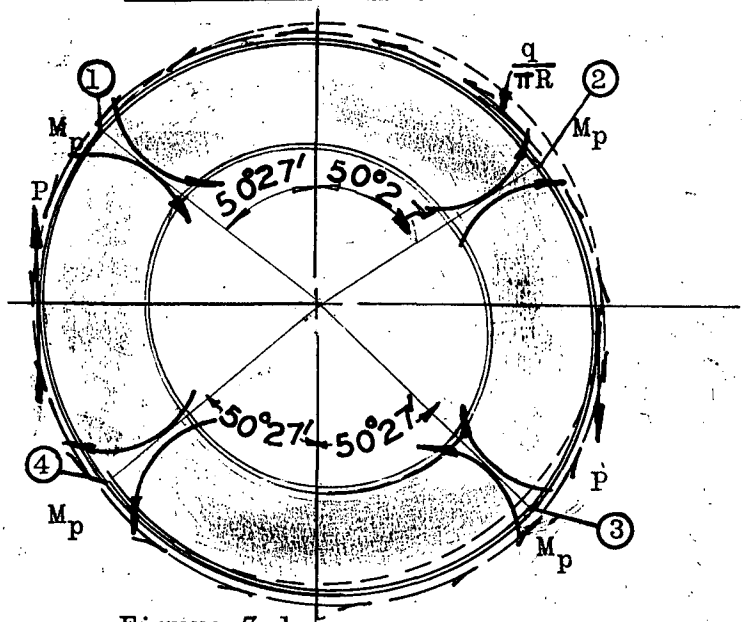

Figure 7.1.5
Failure Configuration

Note: The direction of the maximum moments, M_p, is always such as to restore the deformed structure to its original shape or position.

The completeness of the plasticity check is insured when the moment curve is plotted and the limitation $M \leq M_p$ is satisfied. In order to satisfy this latter condition, Figures 7.1.5 and 7.1.6 were constructed, and the resulting expressions 7.1.12, 7.1.13, 7.1.14, develop.

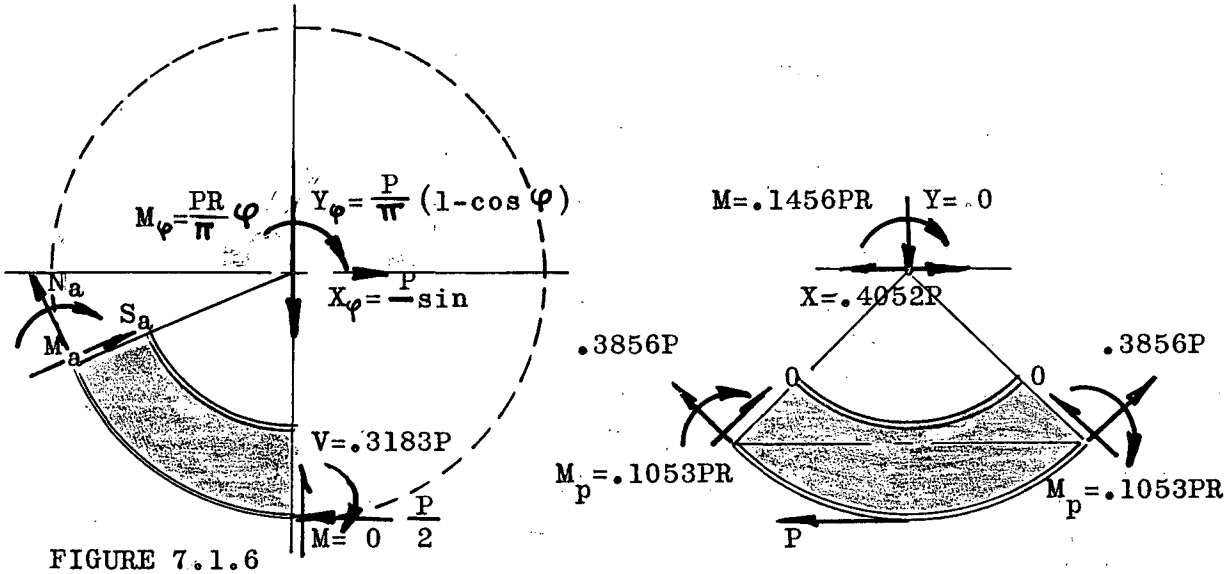

FIGURE 7.1.6

$$M_a = \frac{PR}{2}(1-\cos\varphi)+\frac{P}{\pi}\left[(1-\cos\varphi)-.3183\pi\right]R\sin\varphi+\frac{P}{\pi}(\sin\varphi)R\cos\varphi-\frac{PR}{\pi}\varphi$$

$$M_a = \frac{PR}{\pi}\left[\frac{\pi}{2}(1-\cos\varphi)-\varphi\right] \qquad \text{.....(7.1.12)}$$

$$N_a = \left[\frac{P}{2}-\frac{P}{\pi}\sin\varphi\right]\cos\varphi+\left[-\frac{P}{\pi}(1-\cos\varphi)+.3183P\right]\sin\varphi$$

$$N_a = \frac{P}{\pi}\left[\frac{\pi}{2}\cos\varphi+\sin\varphi(.3183\pi-1)\right] = \frac{P}{2}\cos\varphi \qquad \text{.....(7.1.13)}$$

$$S_a = \left[\frac{P}{2}-\frac{P}{\pi}\sin\varphi\right]\sin\varphi-\left[.3183\pi P-(1-\cos\alpha)\frac{P}{\pi}\right]\cos\varphi$$

$$S_a = \frac{P}{\pi}\left[\sin\varphi\left(\frac{\pi}{2}-1\right)\right] \qquad \text{.....(7.1.14)}$$

An elastic solution to this problem can be obtained by referring to the equations of reference 2, Table 4, Case no. X, or by superimposing the loading condition-Ring II-of section 2.1.0 upon itself with the tangential loads 180^0 apart. If either one of the suggested methods are used, it will be discovered that both the elastic and the plastic analysis yield identical solutions.

TANGENTIAL TWIST PR ON A TANGENTIALLY SUPPORTED CIRCULAR RING

TABLE 7.1.1

Comparison of Plastic to Elastic Moment, Shear and Axial Load Coefficients

Angle φ From Vertical	Plastic Moment Coeff.	Elastic* Moment Coeff.	Plastic Shear Coeff.	Elastic* Shear Coeff.	Plastic Axial Load Coeff.	Elastic* Axial Load Coeff.
0	0	0	-.31834	-.31834	.50000	.50000
5	-.02587	-.02587	-.27475	-.27475	.49810	.49810
10	-.04796	-.04796	-.23150	-.23150	.49240	.49240
15	-.06629	-.06629	-.18891	-.18891	.48297	.48297
20	-.08095	-.08095	-.14731	-.14731	.46985	.46985
25	-.09204	-.09204	-.10701	-.10701	.45316	.45316
30	-.09968	-.09968	-.06831	-.06831	.43302	.43302
35	-.10402	-.10402	-.03152	-.03152	.40958	.40958
39 32'	-.10525	-.10525	0	0	.38559	.38559
40	-.10524	-.10524	.00308	.00308	.38302	.38302
45	-.10355	-.10355	.03524	.03524	.35356	.35356
50	-.09917	-.09917	.06471	.06471	.32140	.32140
55	-.09234	-.09234	.09127	.09127	.28679	.28679
60	-.08333	-.08333	.11471	.11471	.25000	.25000
65	-.07242	-.07242	.13485	.13485	.21131	.21131
70	-.05989	-.05989	.15155	.15155	.17101	.17101
75	-.04607	-.04607	.16467	.16467	.12941	.12941
80	-.01580	-.01580	.17411	.17411	.08683	.08683
85	-.01580	-.01580	.17980	.17980	.04358	.04358
90	0	0	.18170	.18170	0	0

*See reference 2, Table IV, Case No. X for elastic equations

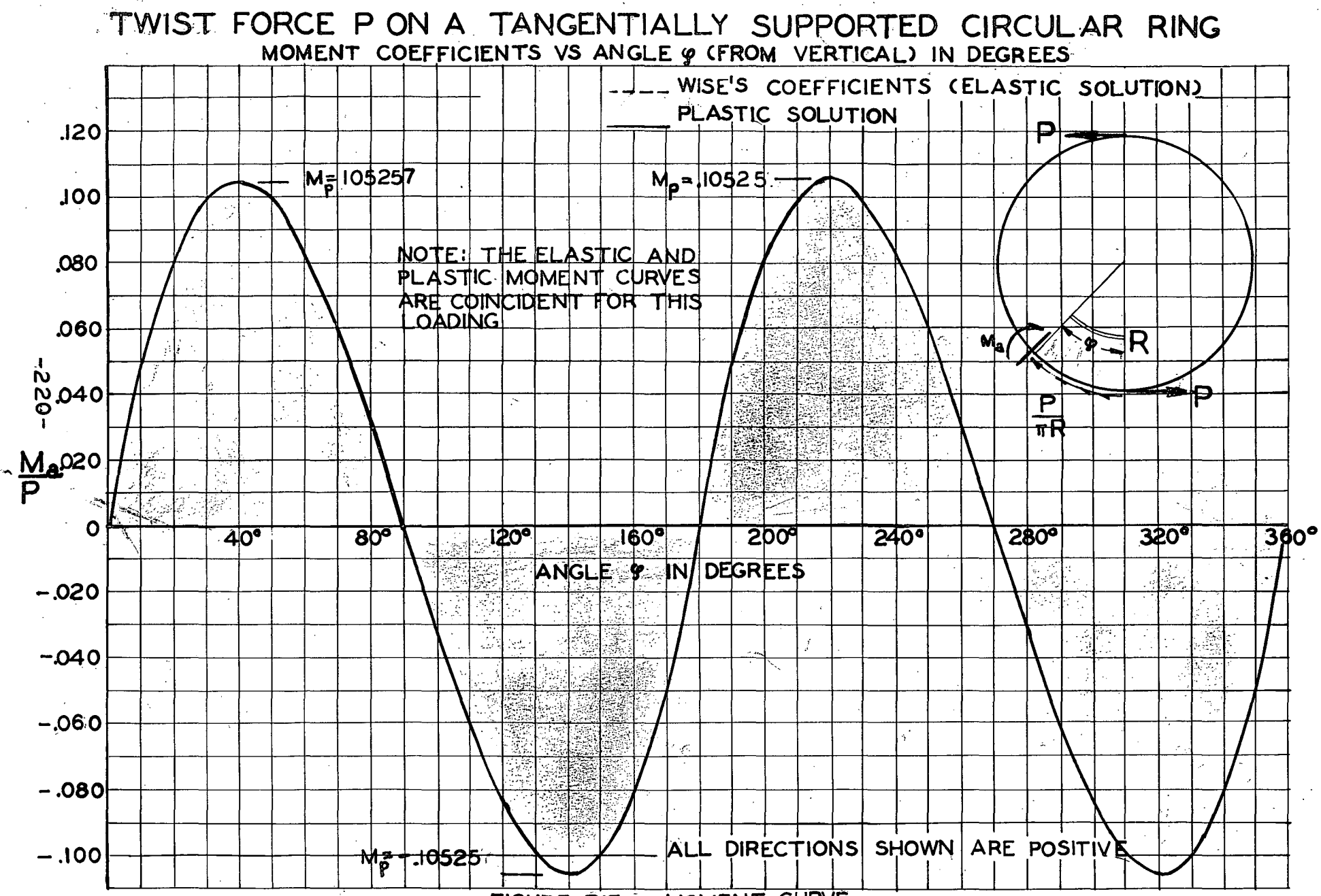

FIGURE 7.1.7 MOMENT CURVE

TANGENTIAL TWIST P ON A TANGENTIALLY SUPPORTED CIRCULAR RING

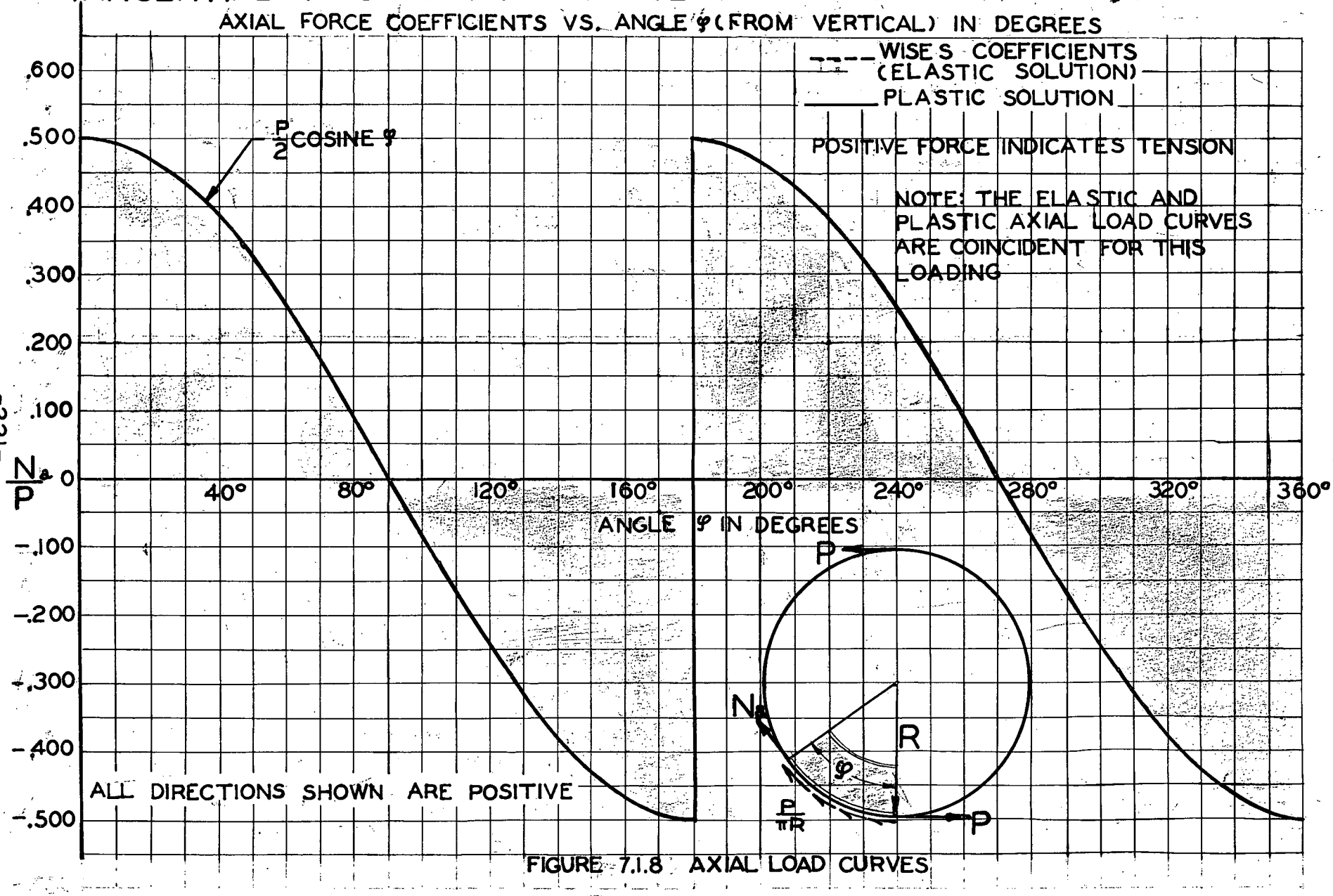

FIGURE 7.1.8 AXIAL LOAD CURVES

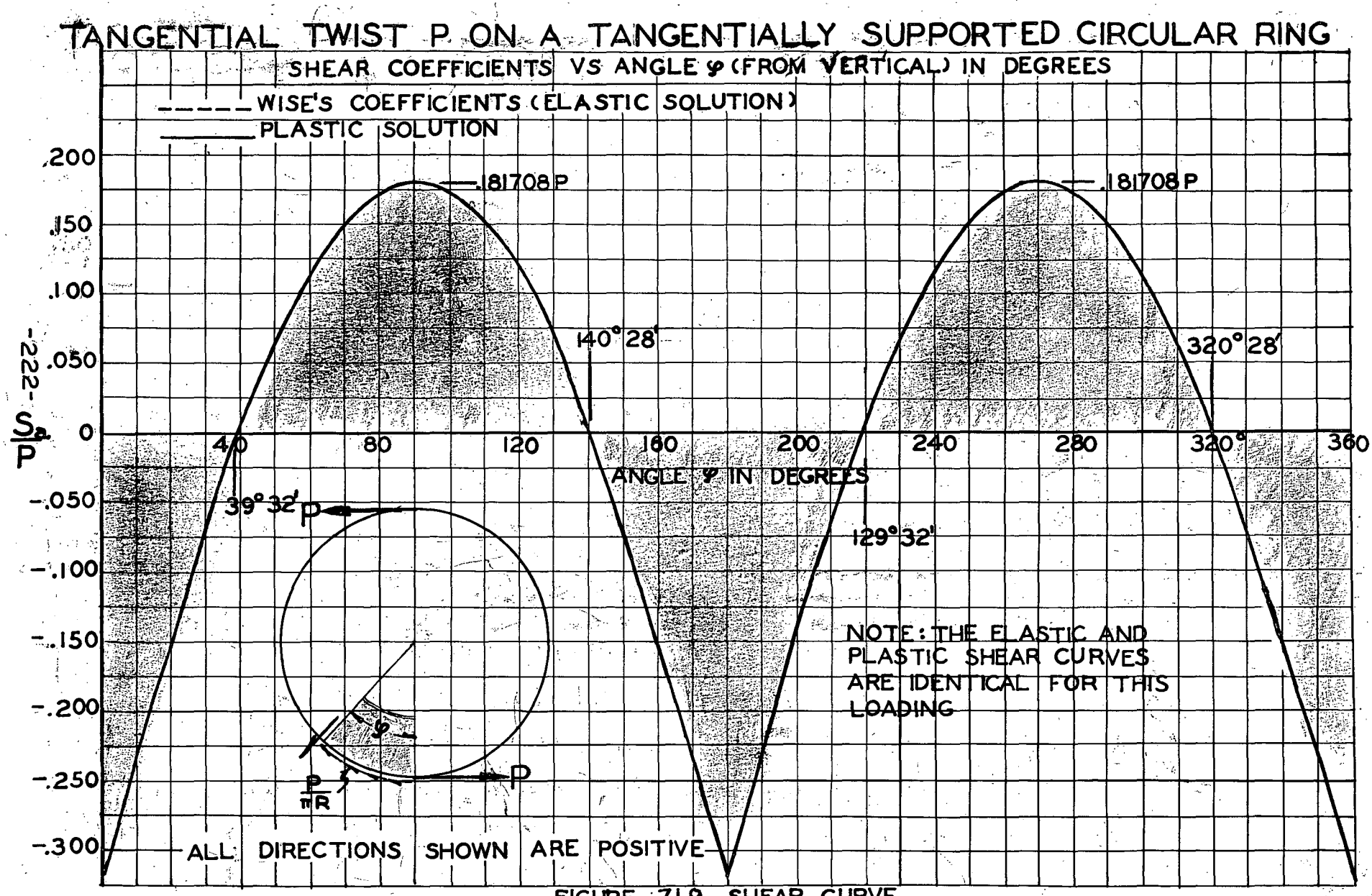

FIGURE 7.1.9 SHEAR CURVE

If values of φ every 5^{o} are substituted in to the equations (7.1.12, 7.1.13, and 7.1.14) for internal moments and forces, the substitution renders the table 7.1.0 and graphs Figures 7.1.7, 7.1.8, 7.1.9.

The reason this ring loading was selected for presentation was asserted on page 209 under the discussion for Ring V. It was decided to present one loading condition where there is no redistribution of moment, so that the reader will not be perplexed if such a case arises. If the reader refers to the moment curve Figure 7.1.7, it is noticed that the moment function is periodic resembling a sine curve with its crest shifted a few degrees. That is why the values of table 7.1.0 only cover a quadrant, being repititious for the succeeding quandrants. All four hinges are reached at the same time, and it is obvious from the elastic solution that all of the maximum moments are of the same magnitude. Furthermore, when the yield load is attained, since the maximum moments are the same at each hinge, the structure experiences the hinging action but there is no redistribution of moment. Instead the structure just keeps on yielding, and nothing other than the plastification of the cross-section is merited by a plastic solution as contrasted to an elastic solution.

7.2.0 Loading Condition-Ring VII-Moment Applied Externally at a Single Point

The purpose of this section is not to complement the rest of the text, but merely to establish the fact that three plastic hinges around a circular ring can not generate a failure mode. Referring to Figure 7.2.0, it can be seen from the moment diagram, superimposed on the ring, that there are only three points of maximum moment. Thus, there could be just three possible plastic hinge locations. There is no feasible manner in which a ring loaded in this manner could fail as a kinematic mechanism. Hence, plastic analysis offers no beneficial redistribution of moments.

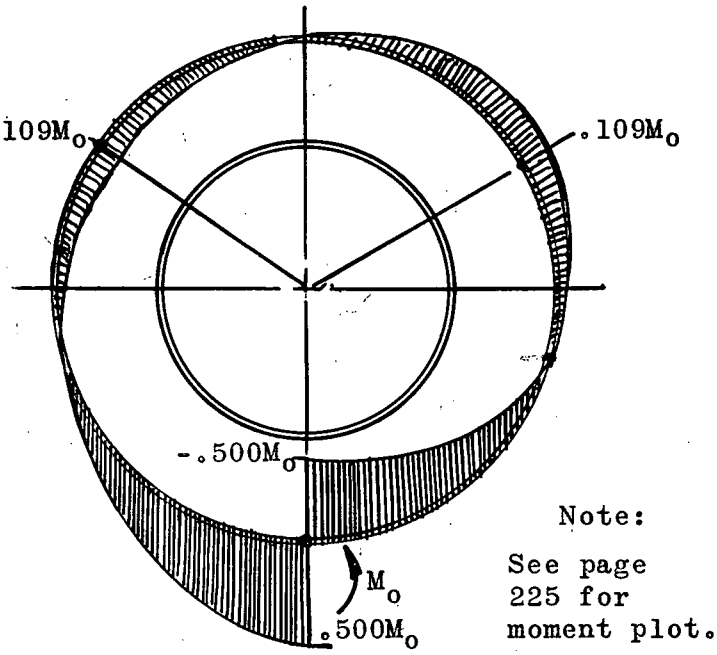

Note: See page 225 for moment plot.

FIGURE 7.2.0 Loading Case VII

The manner in which the ring fails is evidently going to be a local failure. As the load is magnified the three points of maximum moment just progressively increase in magnitude until there is a failure of local buckling or some other stability type failure. Perhaps the collapse of adjacent structure due to excessive deformations would constitute a failure in this case.

This case concludes the study of the different possible fail-

MOMENT APPLIED EXTERNALLY AT A SINGLE POINT

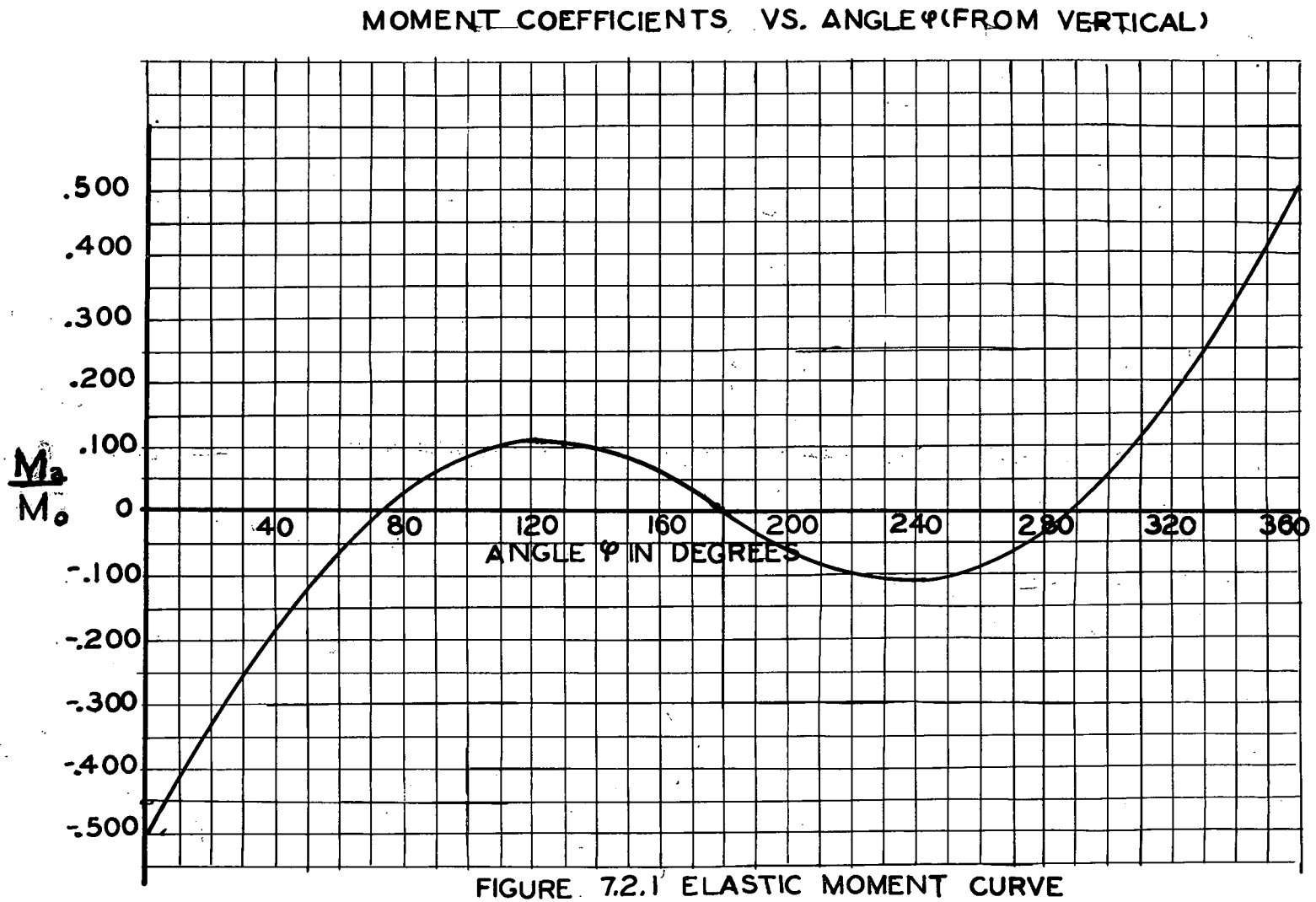

FIGURE 7.2.1 ELASTIC MOMENT CURVE

ure mechanisms. Loading 7.0.0 was chosen to illustrate the fact that a ring loading can induce a kinematic mechanism without shifting the plastic hinges and yet benefit by a redistribution of moment. Ring Loading 7.1.0 was chosen to point out the possibility of creating a failure mechanism without a redistribution in moment. Thus, no advantage is acheived by analyzing plastically since both elastic and plastic methods yield the same solution. This case, Loading 7.2.0, was selected to establish the fact that three points of possible hinges cannot possibly produce a kinematic failure. Lastly, Case IV, Loading 2.3.0, was selected to emphasize the possible necessity of more than four hinges to create a kinematic mechanism.

VITA

The author was born in St. Louis, Missouri on February 27, 1930. He is the second child of Wilbur H. and Evelyn Emma Stuhlman. He attended the elementary and High schools of St. Louis. In September of 1946 he entered George Washington University of St. Louis as a pre-medical student. In Septermber 1948 he transferred to the engineering school of that university, and in June 1951 he received the degree of Bachelor of Science in Civil Engineering.

Upon graduating he accepted the position of stress engineer with McDonnell Aircraft Corporation of St. Louis. In May 1953 he requested active duty in the U.S. Navy Reserve. After serving two years in the Navy Air Force, he returned to McDonnell Aircraft for the summer of 1955.

In September of 1955, he accepted a position of research assistant in the Prestressed Concrete Division at Fritz Laboratory, Lehigh University. Desiring employment closer to his interests he accepted a position assisting Professor F.P. Beer, of the Applied Mechanics Department, in consulting work for Boeing Aircraft in October 1956.